SEPTEMBER 2023

Ph.D. in Civil Engineering

ZHVAN BAQI QADIR

REPUBLIC OF TÜRKİYE

GAZİANTEP UNIVERSITY

GRADUATE SCHOOL OF NATURAL & APPLIED SCIENCES

ANALYZING GEOTECHNICAL CHARACTERISTICS OF ERBIL SOILS VIA GIS

Ph.D. THESIS
IN
CIVIL ENGINEERING

BY

ZHVAN BAQI QADIR

SEPTEMBER 2023

ANALYZING GEOTECHNICAL CHARACTERISTICS OF ERBIL SOILS VIA GIS

Ph.D. Thesis

in

Civil Engineering

Gaziantep University

Supervisors

Prof. Dr. Ali Firat ÇABALAR

Co-Supervisor

Dr. Zuheir KARABASH

by

Zhvan Baqi QADIR

September 2023

©2023[Gaziantep University]

I hereby declare that all information in this document has been obtained and presented in accordance with academic rules and ethical conduct. I also declare that, as required by these rules and conduct, I have fully cited and referenced all material and results that are not original to this work.

Zhvan Baqi Qadir

ABSTRACT

ANALYZING GEOTECHNICAL CHARACTERISTICS OF ERBIL SOILS VIA GIS

QADIR, Zhvan Baqi
Ph.D. in Civil Engineering
Supervisors: Prof. Dr. Ali Firat ÇABALAR
Co-Supervisor: Dr. Zuheir KARABASH
September 2023
200 pages

The objective of this research is to investigate the geotechnical characteristics of soils in Erbil city using a combination of Geographic Information Systems (GIS) and Artificial Neural Networks (ANNs). The study collected data from 102 boreholes at three different depth levels (1.5 m–3.5 m, 3.5 m–6.5 m and 6.5 m–9.5 m) to analyze soil properties such as fines content, moisture content, soil plasticity, shear strength parameters, compressibility, Standard Penetration Test (SPT), and bearing capacity. GIS was used to visualize and analyze the geotechnical characteristics of the soils. The study showed that the predominant soil type in the study area was silty clay with a small amount of sandy gravel (CL) based on the results analyzed via GIS. Most of the soils in Erbil City had SPT–N values ranging from 33 to 50, indicating denser and stronger soil. The average internal friction angle of the soil layers was found to be 10°, and the predominant cohesion was approximately 100 kPa. The compression index of soils ranged between 0.11 to 0.31. To predict the SPT-N value and bearing capacity of the soil, the research applied ANN techniques based on geotechnical properties and made correlations between SPT values and shear strength parameters with the bearing capacity of the soil. The results showed that the ANN models were able to accurately predict the geotechnical parameters of the soil types in the study area. The use of GIS and ANN techniques allowed for a comprehensive analysis of the geotechnical characteristics of the soils in Erbil, providing valuable information for future construction and development projects. Also, the results of this study can be used to design safe and cost-effective foundations for buildings, bridges, and other infrastructure projects in Erbil City. Overall, this study highlights the importance of combining GIS and ANN techniques to analyze and model the geotechnical characteristics of soils in urban areas. The findings of this research can contribute to the development of sustainable and safe infrastructure projects in Erbil and other cities with similar soil properties.

Key Words: Erbil, Geotechnical Characterization, GIS, ANN

ÖZET

ERBİL ZEMİNLERİNİN GEOTEKNİK ÖZELLİKLERİNİN CBS İLE ANALİZİ

QADIR, Zhvan Baqi
Doktora Tezi, İnşaat Mühendisliği
Danışman: Prof. Dr. Ali Firat CABALAR
İkinci Danışman: Dr. Zuheir KARABASH
Eylül 2023
200 sayfa

Bu araştırmanın amacı, Erbil şehrindeki zeminlerin geoteknik özelliklerini, Coğrafi Bilgi Sistemleri (CBS) ve Yapay Sinir Ağlarının (ANN) bir kombinasyonunu kullanarak araştırmaktır. Çalışmada, ince dane içeriği, nem içeriği, zemin plastisitesi, kayma mukavemeti parametreleri, sıkışabilirlik, Standart Penetrasyon Testi (SPT) ve taşıma kapasitesi gibi zemin özelliklerini analiz etmek için üç farklı derinlik seviyesinde (1,5 m–3,5 m, 3,5 m–6,5 m ve 6,5 m–9,5 m) 102 sondaj deliğinden elde edilen veriler kullanılmıştır. Zeminlerin geoteknik özelliklerini görselleştirmek ve analiz etmek için CBS kullanılmıştır. Hakim zemin tipinin, CBS ile analiz edilen sonuçlara göre, az miktarda kum–silt içeren düşük plastisiteli kil (CL) olduğu gösterılmiştir. Erbil şehrindeki zeminlerin çoğu, daha sıkı ve daha güçlü zeminlere işaret eden 33 ila 50 arasında değişen SPT-N değerlerine sahiptir. Zemin tabakalarının ortalama içsel sürtünme açısı 10° olarak bulunmuş ve hakim kohezyon yaklaşık 100 kPa olmuştur. Zeminlerin sıkışma indeksi 0.11 ile 0.31 arasında değişmiştir. Zeminlerin SPT-N değerini ve taşıma kapasitesini tahmin etmek için, geoteknik özelliklere dayalı ANN teknikleri uygulanmış ve SPT değerleri ile kayma mukavemeti parametreleri arasında zeminin taşıma kapasitesi ile korelasyonlar yapmıştır. Sonuçlar, ANN modellerinin çalışma alanındaki zemin tiplerinin geoteknik parametrelerini doğru bir şekilde tahmin edebildiğini göstermiştir. CBS ve ANN tekniklerinin kullanılması, Erbil'deki zeminlerin geoteknik özelliklerinin kapsamlı bir analizine izin vererek, gelecekteki inşaat ve geliştirme projeleri için değerli bilgiler sağlamıştır. Ayrıca, bu çalışmanın sonuçları Erbil'deki binalar, köprüler ve diğer altyapı projeleri için güvenli ve uygun maliyetli temeller tasarlamak için kullanılabilecektir. Genel olarak, bu çalışma, kentsel alanlardaki zeminlerin geoteknik özelliklerini analiz etmek ve modellemek için CBS ve ANN tekniklerini birleştirmenin önemini vurgulamaktadır. Bu araştırmanın bulguları, Erbil ve benzer zemin özelliklerine sahip diğer şehirlerde sürdürülebilir ve güvenli altyapı projelerinin geliştirilmesine katkıda bulunabilir.

Anahtar Kelimeler: Erbil, Geoteknik Özellikler, CBS, ANN

"Dedicated to my family"

ACKNOWLEDGEMENTS

In the name of Allah, the Most Compassionate, the Most Merciful. I would like to begin by expressing my profound gratitude and thanks to the Almighty God, who is the Creator, the Ruler, and the Nourisher of the universe and all that exists within it. It is solely through His mercy and assistance that this task has been accomplished, and I sincerely hope that this humble endeavor is deemed worthy in His sight.

TABLE OF CONTENTS

Page

ABSTRACT ..... **v**

ÖZET ..... **vi**

ACKNOWLEDGEMENTS ..... **viii**

TABLE OF CONTENTS ..... **ix**

LIST OF TABLES ..... **xii**

LIST OF FIGURES ..... **xv**

LIST OF SYMBOLS AND ABBREVIATIONS ..... **xxi**

CHAPTER 1:INTRODUCTION **1**

1.1 Background 1

1.2 Statement of the problem 4

1.3 Objective of the study 5

1.4 Scope of research 5

1.5 Organization of thesis 6

CHAPTER 2:LITERATURE REVIEW **7**

2.1 Introduction 7

2.2 Data collection in geotechnical engineering 7

2.2.1 Investigation boreholes 8

2.2.2 Laboratory soil tests 19

2.3 Geotechnical data reporting and archiving 21

2.3.1 Geotechnical databases 21

2.3.2 Hard copies 22

2.3.3 Electronic image formats 23

2.3.4 GIS-based archiving of geotechnical data 23

2.4 Geographic information systems 25

2.5 Statistical analysis of geotechnical data 28

2.6 Artificial neural network 29

2.6.1 Artificial intelligence in geotechnical engineering 30

2.6.2 Use of neural networks for predict the geotechnical properties of soils 31

2.7 Development of artificial neural network models 36

2.7.1 Determination of model inputs. 36
2.7.2 Division of data 37
2.7.3 Data pre-processing 39
2.7.4 Determination of model architecture 39
2.7.5 Model optimization (Training) 42
2.7.6 Model validation 42
CHPTER 3:METHODOLOGY 44
3.1 Introduction 44
3.2 The study area 45
3.2.1 Geology of study area 47
3.3 Geotechnical properties of soils in area study 48
3.3.1 In situ testing 49
3.3.2 Laboratory experimental testing. 51
3.3.3 Bearing capacity analysis 52
3.4 Identification of spatial data 53
3.4.1 GIS software 54
3.4.2 Data integration 57
3.4.3 Data visualization 58
3.4.4 Data presentation 59
3.5 Statistical Analysis 60
3.6 Artificial neural networks 61
3.6.1 Definition of Artificial neural networks (ANN) 61
3.6.2 Main components of ANN 64
3.6.3 Neural network types 65
3.6.4 Description of the proposed models 68
CHAPTER 4:RESULTS AND DISCUSSION 79
4.1 Introduction 79
4.2 GIS Models for soil characterizes in study area 79
4.2.1. Validation of interpolations based on semi-variograms 79
4.2.2 Fines content 82
4.2.3 Atterberg limits 85
4.2.4 Natural water content 90
4.2.5 Shear strength parameters 93
4.2.6 Consolidation parameters 98
4.2.7 SPT-N value 102

4.2.8 Bearing capacity 106
4.3 Artificial neural network 111
4.3.1 Prediction for SPT-N value.....112
4.3.2 Prediction of Q-ultimate bearing capacity 122
4.3.3 Prediction to Q-ultimate bearing capacity II (included SPT-N).....135
4.3.4 Percentage error of ANNs models 144
4.3.5 Analysis of models.....146
CHAPTER 5:CONCLUSIONS.....149
REFERENCES.....153
APPENDIX A 175
APPENDIX B 192
CURRICULUM VITAE.....200

LIST OF TABLES

Page

Table 2.1 Common borehole types in geotechnical engineering investigations (Look, 2007).....10
Table 2.2 Common sample types in geotechnical engineering investigations (Look, 2007).....11
Table 2.3. List of common field tests in geotechnical engineering investigations (Look, 2007).....12
Table 2.4 List of common geophysical tests in geotechnical engineering (Hunt, 2005).....18
Table 2.5 List of some of the most common laboratory tests in geotechnical engineering (Hunt, 2005). 20
Table 2.6 Partial list of geotechnical engineering database programs (GGSD, 2021) 22
Table 2.7 Some of the Web-based geotechnical data management and archiving systems (Chang and Park, 2004).....24
Table 2.8 Models structure used in the study of Günaydın (2009) 31
Table 3.1 Investigations for study area 49
Table 3.2 The soil properties and SPT data were measured using hammer systems for BH (1-5).....50
Table 3.3 The biological nervous system shares similar features with ANNs as reported by Sagiroglu et al. (2003).....64
Table 3.4 Description of the ANN models.....70
Table 4.1 Accuracy of coefficient determination (Chin, 1998).....112
Table 4.2 ANN models for SPT-N prediction.....132
Table 4.3 ANN models for Q-Ultimate prediction.....133
Table 4.4 ANN models for Q-Ultimate II prediction.....134
Table 4.5. Analysis of models and effect each parameter on the output of prediction. 147

Table A1 The soil properties and SPT data were measured using hammer systems for BH (1-5).....175
Table A2 The soil properties and SPT data were measured using hammer systems for BH (6-10).....176
Table A3 The soil properties and SPT data were measured using hammer systems for BH (11-15).....177
Table A4 The soil properties and SPT data were measured using hammer systems for BH (16-20).....178
Table A5 The soil properties and SPT data were measured using hammer systems for BH (21-26).....179
Table A6 The soil properties and SPT data were measured using hammer systems for BH (27-33).....180
Table A7 The soil properties and SPT data were measured using hammer systems for BH (34-40).....181
Table A8 The soil properties and SPT data were measured using hammer systems for BH (41-47).....182
Table A9 The soil properties and SPT data were measured using hammer systems for BH (48-53).....183
Table A10 The soil properties and SPT data were measured using hammer systems for BH (54-60).....184
Table A11 The soil properties and SPT data were measured using hammer systems for BH (61-66).....185
Table A12 The soil properties and SPT data were measured using hammer systems for BH (67-72).....186
Table A13 The soil properties and SPT data were measured using hammer systems for BH (73-78).....187
Table A14 The soil properties and SPT data were measured using hammer systems for BH (79-84).....188
Table A15 The soil properties and SPT data were measured using hammer systems for BH (85-90).....189
Table A16 The soil properties and SPT data were measured using hammer systems for BH (90-96).....190
Table A17 The soil properties and SPT data were measured using hammer systems for BH (97-102).....191

Table B1. Full data of all boreholes of study area. 192

LIST OF FIGURES

Page

Figure 2.1 Geotechnical data sources included soil borings, field tests and laboratory tests, this data used in various discipline.....8
Figure 2.2 Standard penetration test/split spoon sampler (ASTM d1586).....14
Figure 2.3 Picture shows a simple drilling conducting SPT (original picture to collation data from Erbil, 2019).....15
Figure 2.4 Example of mechanical cone penetrometer tip (Dutch mantle cone). (ASTM D3441, 2016).....16
Figure 2.5 A laboratory data from direct shear test.....19
Figure 2.6 Map making (Azad, 2009).....25
Figure 2.7 Overlay Analysis (GEOL-260, 2021).....26
Figure 2.8 Show the raster, vector and real world (Spiller and Agudelo, 2011).....27
Figure 2.9 Residual analysis of Model 1 in predicting fcs. (Moghaddam, 2010).....29
Figure 2.10 Simple linear regression analysis results; a) LL versus OMC, b) PL versus OMC, c) LL versus MD, d) PL versus MDD (Günaydın, 2009).32
Figure 2.11 Comparison between measured values, and the estimated MMD by Model II (Günaydın, 2009).....32
Figure 2.12 Comparison between the predicted values of soil type and the measured values from Hassannejad et al. (2015) study.....33
Figure 2.13 Observed OMC vs Predicted OMC values during a) Training, b) Testing, and c) Simulation (Tenpe and Kaur, 2015).....34
Figure 2.14 Observed OMC vs Predicted MDD values during a) Training, b) Testing, and c) Simulation (Tenpe and Kaur, 2015).....34
Figure 2.15 a) Experimental LL versus predicted LL, b) Experimental MDD versus predicted MDD, and c) Experimental OMC versus predicted OMC (Bahmed et al., 2017).....35
Figure 2.16 a) Measured FC versus predicted FC, b) Measured LL versus predicted LL, c) Measured PI versus predicted PI (Reale et al., 2018).....36
Figure 2.17 ANN architecture with Cascade-Correlation (Fahlman et al, 1990). 42

Figure 3.1. Flow chart showing in a simple way the methodology adopted in the present study.....45
Figure 3.2 Location of Erbil City, of Iraq 46
Figure 3.3 Erbil city photographic 47
Figure 3.4 Boreholes location in the study area 48
Figure 3.5 Attribute data for soil types 58
Figure 3.6 Symbols and styles of ArcGIS software 59
Figure 3.7 Mapping of selecting lawyers represented an example of SPT-N value .60
Figure 3.8 A simplified model of a biological neuron (Özbay, 2007). 62
Figure 3.9 Adaptive resonance theory (ART) network structure (Miljkovic, 2010) 62
Figure 3.10 General architecture of a Backpropagation Neural Network (Tarsauliya et al., 2011).....65
Figure 3.11 RBF network structure (Kaynar et al., 2016).....66
Figure 3.12 Kohonen network architecture (Amine et al., 2008) 66
Figure 3.13 Topology of Hopfield networks, here with 3 neurons as an example. Linear transfer functions of its neurons characterize the linear Hopfield network (Lendaris et al., 1999). 66
Figure 3.14 Recurrent neural network (RNN) (Mishra et al., 2018).....67
Figure 3.15 Forward strategy for selecting NN architecture and model (Zekić et al., 2005).....67
Figure 3.16 Structure of neural network model A-Group A 71
Figure 3.17 Structure of neural network model A1-Group A 71
Figure 3.18 Structure of neural network model A2-Group A 71
Figure 3.19 Structure of neural network model A3-Group A 72
Figure 3.20 Structure of neural network model A4-Group A 72
Figure 3.21 Structure of neural network model A5-Group A 72
Figure 3.22 Structure of neural network model A6-Group A 73
Figure 3.23 Structure of neural network model A7-Group A 73
Figure 3.24 Structure of neural network model B-Group B 73
Figure 3.25 Structure of neural network model B1-Group B 74
Figure 3.26 Structure of neural network model B2-Group B 74
Figure 3.27 Structure of neural network model B3-Group B 74
Figure 3.28 Structure of neural network model B4-Group B 75
Figure 3.29 Structure of neural network model B5-Group B 75

Figure 3.30 Structure of neural network model B6-Group B 75
Figure 3.31 Structure of neural network model B7-Group B 76
Figure 3.32 Structure of neural network model C-Group C 76
Figure 3.33 Structure of neural network model C1-Group C 76
Figure 3.34 Structure of neural network model C2-Group C 77
Figure 3.35 Structure of neural network model C3-Group C 77
Figure 3.36 Structure of neural network model C4-Group C 77
Figure 3.37 Structure of neural network model C5-Group C 78
Figure 3.38 Structure of neural network model C6-Group C 78
Figure 3.39 Structure of neural network model C7-Group C 78
Figure 4.1 Semivariograms/Covariance Modeling. 80
81
Figure 4.2 Searching Neighborhood Dialog Box of Ordinary Kriging.....81
Figure 4.3-a Fines content model for soil layer at depth, 1.5-3.5m 83
Figure 4.3 -b Fines content model for soil layer at depth, 3.5-6.5m.....84
Figure 4.3-c Fines content model for soil layer at depth, 6.5-9.5m. 84
Figure 4.4-a Liquid limit for soil at depth, 1.5-3.5m 86
Figure 4.4-b Liquid limit model for soil layer at depth, 6.5-9.5m 87
Figure 4.4-c Liquid limit model for soil layer at depth, 6.5-9.5m. 87
Figure 4.5-a Plastic limit model for soil layer at depth, 1.5-3.5m 89
Figure 4.5-b Plastic limit model for soil layer at depth, 6.5-9.5m 89
Figure 4.5-c Plastic limit model for soil layer at depth, 6.5-9.5m 90
Figure 4.6-a Water content variation model for soil layer at depth, 1.5-3.5m.....91
Figure 4.6-b Water content model for soil layer at depth, 3.5-6.5m.....92
Figure 4.6-c Water content model for soil layer at depth, 6.5-9.5m 92
Figure 4.7-a Cohesion model for soil layer at depth, 1.5-3.5mb ($kN/m^{2)}$.....95
Figure 4.7-b Cohesion model for soil layer at depth, 3.5-6.5m (kN/m^2).....96
Figure 4.7-c Cohesion model for soil layer at depth, 6.5-9.5m (kN/m^2) 96
Figure 4.8-a Angle of internal friction distribution model for soils at depth, 1.5-3.5m (degree).....97
Figure 4.8-b Angle of internal friction distribution model for soils at depth, 3.5-6.5m (degree) 97
Figure 4.8-c Angle of internal friction distribution model for soils at depth, 6.5-9.5m (degree).....98

Figure 4.9-a Compression index for soil layer at depth, 1.5-3.5m 99
Figure 4.9-b Compression index for soil layer at depth, 3.5-3.5m 100
Figure 4.9-c Compression index for soil layer at depth, 6.5-9.5m.....100
Figure 4.10-a Rebound index for soil layer at depth, 1.5-3.5m 101
Figure 4.10-b Rebound index for soil layer at depth, 3.5-6.5m.....102
Figure 4.10-c Rebound index for soil layer at depth, 6.5-9.5m 102
Figure 4.11-a SPT-N Value model for soil layer at depth, 1.5-3.5m.....103
Figure 4.11-b SPT-N Value model for soil layer at depth, 3.5-3.5m 103
Figure 4.11-c SPT-N Value model for soil layer at depth, 6.5-9.5m.....104
Figure 4.12 Correlation of SPT-N values with cohesion of soils in the study area.105
Figure 4.13 Correlation of SPT-N values with angle of internal friction (ϕ) of soils in the study. 105
Figure 4.14-a Ultimate bearing capacity model for soil layer according to Meyerhof's equation at depth, 1.5-3.5m (kN/m^2) 106
Figure 4.14-b Ultimate bearing capacity model for soil layer according to Meyerhof's equation at depth, 3.5-6.5m (kN/m^2) 107
Figure 4.14-c Ultimate bearing capacity model for soil layer according to Meyerhof's equation at depth, 6.5-9.5m (kN/m^2) 107
Figure 4.15-a Ultimate bearing capacity model from SPT-N value at depth, 1.5-3.5m (kN/m^2).....108
Figure 4.15-b Ultimate bearing capacity model from SPT-N value at depth, 3.5-6.5m (kN/m^2).....109
Figure 4.15-c Ultimate bearing capacity model from SPT-N value at depth, 3.5-6.5m (kN/m^2).....109
Figure 4.16 Correlation of ultimate bearing capacity (Meyerhof) with SPT-N values of soils in study area.....110
Figure 4.17 Correlation of ultimate bearing capacity (SPT-N) with soil cohesion of soils in study area. 111
Figure 4.18 Model A relations between (LL, PL, PI, WC, c, ϕ, Fine cont) and SPT-N 114
Figure 4.19 Model A1 relations between (LL, PL, PI, WC, c, ϕ) and SPT-N.....115
Figure 4.20 Model A2 relations between (LL, PL, PI, WC, ϕ) and SPT-N.....116
Figure 4.21 Model A3 relations between (LL, PL, PI, WC, c) and SPT-N 117
Figure 4.22 Model A4 relations between (LL, PL, PI, c, ϕ, Fine cont) and SPT-N118

Figure 4.23 Model A5 relations between (LL, PL, WC, c, ϕ, Fine cont) and SPT-N 119
Figure 4.24 Model A6 relations between (LL, PI, WC, c, ϕ, Fine cont) and SPT-N 120
Figure 4.25 Model A7 relations between (PL, PI, WC, c, ϕ, Fine cont) and SPT-N 121
Figure 4.26 Model B relations between (LL, PL, PI, WC, c, ϕ, Fine cont) and Q ultimate.....123
Figure 4.27 Model B1 relations between (LL, PL, PI, WC, c, ϕ) and Q ultimate ..124
Figure 4.28 Model B2 relations between (LL, PL, PI, WC, ϕ) and Q ultimate 125
Figure 4.29 Model B3 relations between (LL, PL, PI, WC, c) and Q ultimate 126
Figure 4.30 Model B4 relations between (LL, PL, PI, c, ϕ, Fine cont) and Q ultimate 127
Figure 4.31 Model B5 relations between (LL, PL, WC, c, ϕ, Fine cont) and Q ultimate.....128
Figure 4.32 Model B6 relations between (LL, PI, WC, c, ϕ, Fine cont) and Q ultimate.....129
Figure 4.33 Model B7 relations between (PL, PI, WC, c, ϕ, Fine cont) and Q ultimate.....130
Figure 4.34 Model C relations between (LL, PL, PI, WC, c, ϕ, Fine cont., SPT-N) and Q ultimate 135
Figure 4.35 Model C1 relations between (LL, PL, PI, WC, c, ϕ, SPT-N) and Q ultimate.....136
Figure 4.36 Model C2 relations between (LL, PL, PI, WC, ϕ, SPT-N) and Q ultimate.....137
Figure 4.37 Model C3 relations between (LL, PL, PI, WC, c, SPT-N) and Q ultimate 138
Figure 4.38 Model C4 relations between (LL, PL, PI, c, ϕ, Fine cont., SPT-N) and Q ultimate.....139
Figure 4.39 Model C5 relations between (LL, PL, WC, c, ϕ, Fine cont., SPT-N) and Q ultimate.....140
Figure 4.40 Model C6 relations between (LL, PI, WC, c, ϕ, Fine cont., SPT-N) and Q ultimate.....141
Figure 4.41 Model C7 relations between SPT-N and Q ultimate 142

Figure 4.42 Comparison ANN models for predict SPT-N.....143
Figure 4.43 Comparison ANN models for predict Q-ultimate.....143
Figure 4.44 Comparison ANN models for predict Q-ultimate II.....144

LIST OF SYMBOLS AND ABBREVIATIONS

ANNs	Artificial Neural Networks
ART	Adaptive Resonance Theory Networks
ASMOD	Adaptive spline modeling of observation data
ASTM	Stands for the American Society for Testing and Materials
B	Bulk disturbed sample
B	Width of the footing (in meters or feet)
C	Core sample
c	Soil cohesion
CAD	Stands for Computer-Aided Design
Cc	Compression index
CPT	Cone Penetration Test
Cs	Swelling index
Cv	Soefficient of consolidation
D	Disturbed sample
DCP	Dynamic cone penetrometer
DMT	Dilatometer test
D_r	Relative density
EPB TBM	Earth pressure balance tunnel boring machine
FC	Fines content
GIS	Geographical Information System
GPS	Global Positioning System
IDW	Inverse Distance Weighting
LL	Liquid limit

LPT	Light Penetration Test
MAE	Mean Absolute Error
MDD	Maximum dry density
MINITAB 17	Statistical software package used for data analysis and quality improvement
Nc, Nq, and Nγ	Bearing capacity factors that depend on the soil's properties and the geometry of the foundation
N-value	Blow count
OMC	Optimum moisture content
Pc	Preconsolidation pressure
PDF	Stands for Portable Document Format
PI	Plastic index
PL	Plastic limit
PLT	Plate loading test
PT	Pressure meter test
QC	Cone resistance
qult	Ultimate bearing capacity of the soil
R^2	R-squared (Training and Testing)
RBFN	Radial Basis Function Network
R_c	Rebound index
RMSE	Root Mean Square Error
RNN	Recurrent Neural Networks
s-f	Shape factor that accounts for the shape of the foundation.
SPT N-V	Standard penetration test
U (0)	Undisturbed sample (50mm diameter tube)
U (100)	Undisturbed sample (100mm diameter tube)
U (75)	Undisturbed sample (75mm diameter tube)
USCS	Unified Soil Classification System
W	Water sample

WC	Water content
y-mea, y-pre, and y-m	Average of existing output, predicted output, and actual output, respectively
γ	Unit weight of the soil (in kN/m^3 or lbs/ft^3)
λ	Is a dimensionless parameter used to characterize the shape of the soil-water retention curve
ϕ	internal friction angle
CPTu	Cone penetration test with con resistance
LM	Levenberg Marquardt
TP	Test pit sample

CHAPTER 1
INTRODUCTION

1.1 Background

One of the important primary steps before the construction of infrastructure is geotechnical site investigation. It provides information regarding site suitability for design criteria and possible construction problems such as time and costs (Clayton et al., 1982). Conducting a soil survey is vital when undertaking the construction of various structures like multi-story buildings, highways, bridges, and industrial facilities. It is imperative to assess important factors such as soil type, consistency, relative density, and groundwater to ensure the soundness of the project (Roy and Bhalla, 2017). All constructions depend on the soils they are built upon for stability, therefore it is important to consider both the weight of the structure and external loads. They are also influenced by events like earthquakes, settlements, and groundwater that exist under the ground. Structural engineers need to know about the soil characteristics to analysis and design the construction. Geotechnical data can be applied to various constructions and civil engineering projects, as well as to infrastructure. In the engineering field, geotechnical data is often used in the areas of infrastructure, environmental and risk assessments (Winter et al., 2015). Additional data related to geotechnical is increasingly being utilized in these types of assessments, where more sophisticated and realistic analyses take into account consistent input characteristics (Whitman, 2000).

Understanding the bearing capacity of soil layers is imperative in designing the appropriate foundation type and depth for any superstructure (Roy and Bhalla, 2017; Skempton, 1984 and Lupiezowiec, 2013). In order to strengthen infrastructure a suitable geotechnical investigation must be conducted of safe and long-term engineering structures. In order to calculate soil bearing capacity and settlement accurately, an effective method for obtaining geotechnical parameters is through in situ testing. This approach involves the extraction of both disturbed and undisturbed specimens from various depths beneath the ground surface, followed by conducting a series of geotechnical experiments on these samples. The purpose of these experiments

is to determine different parameters that are commonly employed in the design of foundations (Patel, 2019). The investigation of soil properties is considered as a significant tool for the design of projects. Currently soil filed tests such as the Standard Penetration Test (SPT) test is utilized profusely to evaluate bearing capacity in order to design the foundations at the structure (Al-Mamun and Ansary, 2018; Zakaria, 2011). Also, there are many other methods implemented for site investigation, such as pressure meter tests, dilatometer tests, cone penetration tests (CPT), and a plate load test (Clayton et al., 1982).

Over the years, thousands of pieces of board equipment have been used in various types of engineering projects, each with its own distinct focus and purpose. Several construction projects in Iraq have been completed without drilling earth borings in the last few decades. Hard-copy boring logs were used to archive geotechnical data. Hard copies are an inaccurate form of long-term archiving since they are a cumbersome process, weak to lose and degradation, and difficult to access. They have similar difficulties that are connected with using hard copies. Because of these obstacles, huge quantities of lost, missing, or unavailable geotechnical data have been incurred. Computer-aided drawing software and personal computers brought on a whole new way to deal with logs since they allowed for electronic format logging. Although storage techniques have improved geotechnical data archives, the accessibility and distribution of geotechnical data has not seen much improvement over time. Geotechnical engineering has been slow to adopt new information technology and geographic information systems. However, in recent years, there has been a significant increase in geotechnical data stored in databases and delivered over the Internet (Satyanayarana and Stetson, 2000).

A Geographic Information System offers an analytical tool that simplifies the time-consuming process of developing model entry data across various spatial scales (Wan-Mohamad and Abdul-Ghani, 2011; Ahmed et al., 2020). The utilization of GIS empowers individuals to combine, analyze, and present data in a manner that facilitates the identification of relationships, patterns, trends, and the resolution of complex issues. By organizing data interactively, GIS allows for the early recognition of potential challenges in the project's design process, ultimately saving time in construction projects. Acting as a useful tool, GIS aids in supporting geotechnical site

assessments, guiding land preparation, and seamlessly integrating field data with existing datasets (Arnous, 2013).

Due to data collection mistake some of the properties or parameters could be correlated with other data to use it for design and analysis of soil properties. Artificial intelligence tools are becoming ever more widely used since it is being shown to handle challenging issues and has shown great efficiency and accuracy (Nilsson, 2009). A new type of tools applying artificial intelligence has evolved, offering an alternative approach for regression analysis. In order to generate neural network models, the first step is to identify important parameters governing the total characteristics. Different methodologies have been adopted by researchers to predict the parameters. As may be noted, these methodologies may suffer from such factors as subjective analysis of the problem at hand and/or lack of experience (Oberlender and Trost 2001).

Artificial Neural Networks (ANN) usually simply named neural networks (NNs) or neural nets are computing systems motivated by the biological neural networks that include human brains. Research on both software and hardware levels for ANNs is still ongoing. ANNs are currently used in various fields such as industrial engineering, intelligence issues, and object recognition. (Abiodun et al., 2018; Awodele and Jegede, 2009). ANNs have found successful applications in geotechnical and construction engineering. These techniques have been used for slope stability analysis, prediction of soil properties, and estimation of rock mass parameters, among others. By consuming ANNs, geotechnical engineers and construction professionals can efficiently analyze and process large amounts of data, leading to more accurate predictions and cost-effective solutions. Ongoing research in ANNs is expected to further enhance their capabilities and broaden their application in the field of geotechnical and construction engineering. (Jeremiah et al., 2021; Liu et al., 2021). Randomly distributed input parameters cause the ANN's structure and weight of the neurons to vary during its training and testing. In the same way as a live organism's nervous system, it has a structure that can adjust itself (Basheer and Hajmeer, 2000). In another way, it may change its structure and learn based on internal and external stimulation at this point, the connection weights are activated, allowing them to come up with a solution on their identifiable. As a result, it is impossible to predict how the system will behave in a given scenario. This is the factor that creates a virtual feature to the system. Outlined below are the objectives of the study and the approaches

undertaken to achieve them. The dissertation is also organized into various sections, each of which provides a concise summary of the subsequent sections.

1.2 Statement of the Problem

The production of a set of maps for the city of Erbil via, using Geographic Information System (GIS), has provided valuable tools for engineers in the construction design and infrastructure projects. These maps offer insights into various aspects of the city's geography, such as topography, land use, and infrastructure networks, which can aid in the planning and decision-making processes. However, despite the availability of GIS-based maps, there is currently a gap in the geotechnical data for Erbil city. In the past, there has been a lack of utilization of comprehensive data analysis to cover all the geotechnical characteristics of soil in a given region. This includes detailed information on the physical and mechanical properties of soil. This lack of data poses challenges to engineers in accurately assessing the geotechnical behavior of soil, which is critical for designing safe and reliable construction and infrastructure projects. To address this gap, this thesis proposes an innovative approach that utilizes neural networks to investigate the feasibility of replicating different geotechnical engineering models. Neural networks, as a type of machine learning technique, have shown great potential in capturing complex patterns and relationships within large datasets, including geotechnical data. The use of neural networks in this research aims to leverage big data on physical and mechanical properties of soil to develop analytical models that can accurately estimate geotechnical parameters, such as shear strength, consolidation characteristics, and permeability, for Erbil city.

The outcomes of this research are expected to contribute to the understanding of the geotechnical behavior of soil in Erbil city and provide valuable insights for engineers in the design and construction of infrastructure projects. Moreover, the approach developed in this research has the potential to be extended to cover all soil properties in northern Iraq, facilitating engineers in treating and analyzing soil data more effectively. This, in turn, can simplify the design and scheduling of engineering projects, by providing reliable and comprehensive geotechnical information for decision-making processes. Overall, this research aims to bridge the gap in geotechnical data for Erbil city and northern Iraq, and contribute to improved geotechnical engineering practices in the region

1.3 Objective of the Study

Subsequently, a wide range of civil engineering projects have investigated numerous boreholes. It is uncommon for a construction project in Erbil, Iraq, to be undertaken without using soil investigation. From these facts, it can be assumed that a quantity of data about subsurface soil layers' record over the last few years. As a result, data was traditionally produced and archived in boring logs on the document. Archiving hard copies is problematic since they are large, difficult to retrieve, and susceptible to loss and degradation. This resulted in amounts of geotechnical data being misplaced or unapproachable. On the other hand, the Erbil government engineers have not established a uniform approach. In major geotechnical engineering projects, this is still an issue, but it has a more significant effect on big studies using data from many disciplines, including geotechnical data. It is common for geotechnical engineering applications to use huge amounts of data and few times to analyze and condition individual data pieces; thus, these investigations require a larger amount of data.

The study concludes that the accessibility and utilization of geotechnical data can be improved by implementing modern technological solutions and evaluating their effectiveness. This involves adapting existing technologies used in other industries for geotechnical engineering applications. While geotechnical engineers are leading this effort, the integration of geotechnical information with other data sources could also benefit research and engineering disciplines beyond geotechnical engineering.

1.4 Scope of Research

The objective of this thesis is to investigate the discrepancies in geotechnical data pertaining to the soil layers in specific regions of Erbil City, employing:

- Through the application of GIS techniques and available parameters, it is possible to determine the ultimate bearing capacity of soil. While numerous researchers have conducted investigations on various soil properties in other regions of Iraq, there is a dearth of such research and data for Erbil City. Therefore, this study will serve as a foundation for researchers in the city to develop a comprehensive geo-database for the entire Erbil governorate. As the database expands, it will become simpler to visualize the soil properties and behaviour in the study area.

- Designing or construct models to predict the SPT N-Value, shear strength parameters, bearing capacity, and compression index of Erbil soils
- Assess the performance of the models developed in comparison to ANNs models using statistical assessment tools, including R^2, MAE, and RMSE.

1.5 Organization of Thesis

The thesis is structured into five chapters, and a summary of each chapter is presented below:

Chapter 1: Introduction.

Chapter 2: literature review.

Chapter 3: Methodology and ANN Models for Geotechnical Data.

Chapter 4: Results and Discussion.

Chapter 5 Conclusion.

Appendix A

CHAPTER 2
LITERATURE REVIEW

2.1 Introduction

This chapter focuses on the different kinds of data that are commonly encountered in geotechnical engineering, with a specific emphasis on evaluating various aspects of geotechnical data. Such aspects include the size of the data, their sources, as well as the methods employed to gather, store, and analyze them. The chapter concludes by reviewing current approaches and highlighting their limitations. The influence of computer technology on geotechnical engineering is substantial, extending beyond the realm of analysis and mathematical modeling, but also in how engineers record, store, retrieve, process, visualize, and present important geotechnical data. This includes the use of a wide range of information technology tools, from ubiquitous spreadsheet packages to specialized database software and advanced graphics visualization tools. Also, ANN have been increasingly used in geotechnical engineering for a range of applications, including slope stability analysis, settlement prediction, soil classification, and earthquake engineering. ANNs are advantageous in dealing with complex nonlinear problems and handling large datasets in this field.

2.2 Data Collection in Geotechnical Engineering

There are four major sources of geotechnical data as follow:

(a) in-situ tests, including geophysical tests.

(b) boreholes, test pits and trenches.

(c) samples obtained from boreholes were evaluated to laboratory tests.

(d) data-gathering as part of geotechnical analysis and the development of site characterization models.

A part of geotechnical data gathered from excavations, surface observations or test pits; Consequently, they constitute a considerable portion of the data when compared to borehole data and are usually processed in a similar way (Stokoe et. al., 2004; Zhang et al., 2018).

In Figure 2.1, the basic data types in geotechnical engineering are demonstrated, as well as the various fields that make use of this data. The collection and processing of data are crucial in the development of spatial geotechnical data. The chapter goes on to explore several techniques for acquiring geotechnical data, such as borehole sampling, in-situ testing, and laboratory analysis.

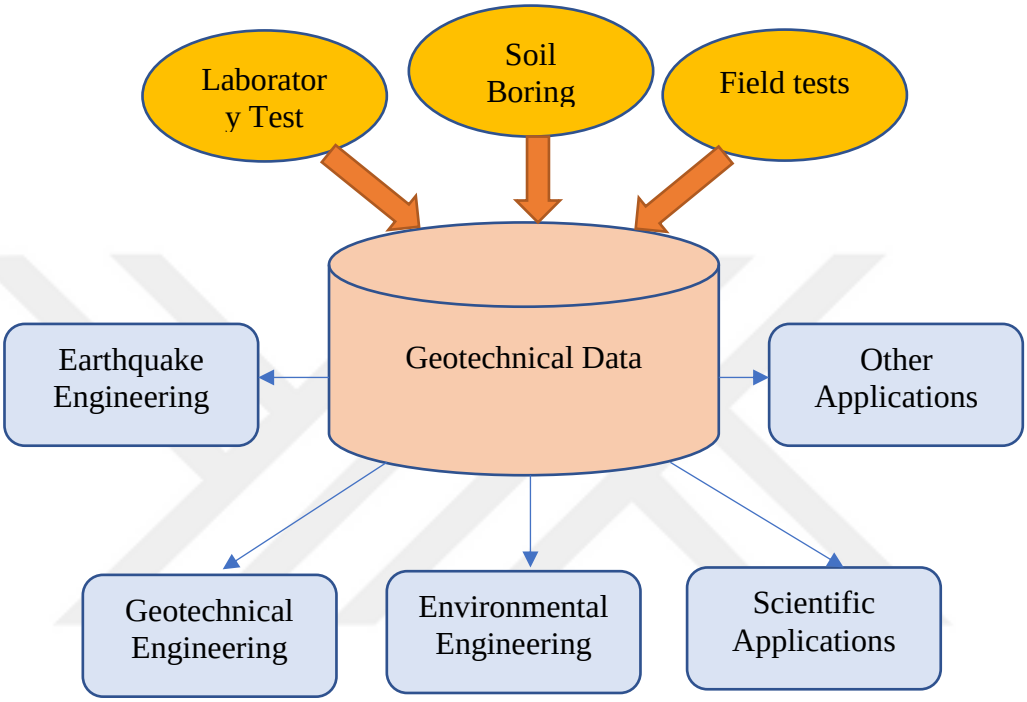


Figure 2.1 Geotechnical data sources included soil borings, field tests and laboratory tests, this data used in various discipline

2.2.1 Investigation Boreholes

A borehole refers to any excavation made into the ground, irrespective of its orientation, such as vertical, inclined, horizontal, or curved holes. The primary purpose of drilling such holes is to collect information and samples from various soil layers, enabling a better understanding of their properties (Look, 2007). Investigation boreholes are drilled to obtain samples on the variety, lateral distribution, thickness, geo-environmental and geotechnical characteristics of underground soil and rock material (Reiffsteck et. al., 2018; Rowe, 2012). Moreover, boreholes are commonly employed for in-situ investigations, soil and rock samples are obtained for laboratory

testing, often by excluding soil and rock cuttings/cores that are taken directly from the borehole (Zand, 2011).

Boreholes can be implemented through a variety of techniques, and the corresponding geotechnical investigation services should be performed. Numerous factors, such as the type and size of the structure and the expected ground conditions, significantly impact the extent and mode of investigation. Site characterization, laboratory testing, and expert data analysis are Geotechnical testing is employed to finalize the design and construction of site improvements. Table 2.1 enumerates the most commonly used types of geotechnical boreholes (Look, 2007). The drilling method is a crucial factor that can significantly affect the accuracy of in-situ test results and samples (Liber et. al., 2007). Table 2.2 displays the different soil and rock sample methods utilized in geotechnical engineering investigations. Sampling is typically carried out at intervals of 1 to 3 meters, with two samples collected continuously at the same depth. This approach is adopted to facilitate the utilization of different sample types for various tests. Additionally, standard boreholes are driven into the ground, and additional borings are used in geotechnical investigations (Fang, 2013).

Table 2.1 Common borehole types in geotechnical engineering investigations (Look, 2007).

Boring Type	Uses
Solid stem auger	Used in dry holes in competent materials. May need to use casing for collapsing material
Hollow stem auger	Similar to solid stem (continuous flight) auger drilling, except hollow stem is screwed into the ground and acts as casing. Sampling and testing from inside of auger. Penetration in strong soils/gravel layers difficult.
Wash boring	Used to advance the borehole and keep the hole open below the water table. Fluid may be mud (polymer) or water depending on the soil conditions. Maintains hydrostatic head.
Rock coring	Hardened cutting bit with a core barrel used to obtain intact rock samples
Air track probes	Provides a rapid determination of rock quality/depth to rock based on the time to advance the hole. Rock assessment is difficult as rock chippings only obtained.

Table 2.2 Common sample types in geotechnical engineering investigations (Look, 2007).

Symbol	Sample or Test
TP	Test pit sample
W	Water sample
D	Disturbed sample
B	Bulk disturbed sample
SPT	Standard penetration test sample
C	Core sample
U (50)	Undisturbed sample (50mm diameter tube)
U (75)	Undisturbed sample (75mm diameter tube)
U (100)	Undisturbed sample (100mm diameter tube)

In-situ Tests

In-situ testing involves conducting tests directly on the soil in the field, as opposed to laboratory tests that are carried out on samples brought to the lab. Geophysical tests are also classified as in-situ testing within this definition (Monnet, 2015). Table 2.3 lists the more common in-situ tests in geotechnical engineering, excluding geophysical testing. The significant advantage of in-situ experiments is that they allow the examination of soils in their natural environment, such as in-situ density and moisture content (Radan, 2015). Sampling can alter soil characteristics in several ways. It can be challenging to obtain samples from sandy soils with low cohesion since the soil density changes due to the disturbance caused by sampling. However, fine-grained soils are sensitive to moisture content and disturbance, despite being often thorough described by laboratory samples. Several sampling techniques, such as thin-walled tubes, give relatively undisturbed samples (Gilbert, 1992).

Table 2.3. List of common field tests in geotechnical engineering investigations (Look, 2007).

Symbol	Test	Measurement
DCP	Dynamic cone penetrometer	Blows/100mm
SPT	Standard penetration test	Blows/300mm
CPT	Cone penetration test	Cone resistance qc (MPa); friction ratio (%)
CPTu	Cone penetration test with cone resistance	Cone resistance qc (MPa); friction ratio (%); pore pressure measurement pressure (kPa). time for pore pressure (Piezocone); dissipation t (sec)
PT	Pressure meter test	Lift-off and limit pressures (kPa); volume change (cm^3)
PLT	Plate loading test	Load (kN); deflection (mm)
DMT	Dilatometer test	Lift-off and expansion pressures (kPa)
PP	Pocket penetrometer test	kPa
VST	Vane shear test	Nm, kPa
WPT	Water pressure (packer) test	Lugeons

Engineers rely significantly on the results of in-situ tests to determine characteristics such as soil density and shear strength. In current practice, numerous design parameters in geotechnical engineering are based on SPT correlations. Various design methods employing the SPT blow count are used for geotechnical structures to address diverse issues such as bearing capacity, settlement, liquefaction, piles, and drilled shafts (Schnaid, 2005).

In recent years, design techniques that use CPT findings rather than SPT blow counts have been developed. Therefore, it seems that these two tests will continue to be the most often used in-situ tests for geotechnical applications in the possible future and that they will play a significant role in any geotechnical investigation. These two tests

are described in more detail in the following sections due to their relevance (Coduto, 2014).

Standard Penetration Test SPT

In geotechnical investigations, the standard penetration test (SPT) is the most used in-situ test (Clayton, 1995; Sancio and Bray, 2005; Wazoh and Mallo, 2014). The American Society for testing materials conducted the standard penetration test in 1958, with periodical evaluations since then (ASTM D1586/D1586M-18). With the most recent modification in 1999, the approach was further standardized. In 1975, the test "Determination of penetration resistance using a spatula splitting tool" was submitted to the British Standard (BS 1377).

The ASTM standard is widely used, although different countries have their own standards. According to ASTM (D1586) guidelines (refer to Figure 2.2), The conventional Split Spoon Sampler (SPT) typically has an outer diameter of 51mm, an inner diameter of 35mm, and a length ranging from 45cm to 65cm. The sampler is attached to a series of drill rods and inserted into a previously drilled and cleaned borehole. The sampler is driven into the soil by a slide hammer weighing 63.5kg with a free fall length of 760mm, which is repeated in three successive 15cm increments. Each increment involves a total of 150mm of blows, with the first 150 mm known as the seating drive. The total of strokes required for the second and third lifts of 150 mm is utilized as the SPT-N value for penetration. The SPT is typically completed when the total number of strokes required to drive any portion surpasses 150 mm by 50 blows or when no more depth can be achieved with ten consecutive blows. The repeat test is carried out every 1.5 meters or even when the soil layers change. The sampling tube is withdrawn and dismantled at the end of each SPT operation to gather representative disrupted samples for further laboratory testing (Bowles, 1997).

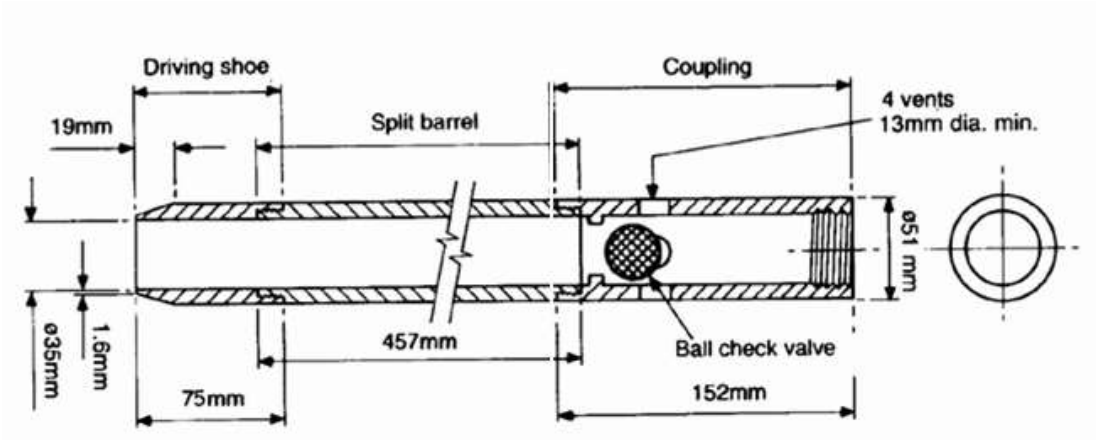


Figure 2.2 Standard penetration test/split spoon sampler (ASTM d1586).

The drilling rig shown in Figure 2.3 is equipped with SPT apparatus. These rigs usually switch between the SPT sampler and a larger diameter sampler, such as the Modified California Sampler, to obtain both SPT N-Value and a relatively undisturbed sample of larger diameter from the same borehole. One of the most significant differences is the use of a sampler with a larger diameter than the SPT sampler. A larger diameter sampler is preferred because it can retain a stack of rings and gather reasonably undisturbed samples. These tests are sometimes referred to as significant penetration tests or Light Penetration Tests (LPT). Another deviation is the use of large hammers that deliver more energy to the sampler. This makes sampler driving easier and is sometimes necessary to obtain usable samples in stiffer soils. However, the energy supplied by a particular arrangement may differ from the results of typical experiments when using conventional hammers and samplers. This is a well-known issue with SPT tests, and combining these deviations often requires some form of blow count modification. Considerable research has been conducted on making this correction, and the findings are available (Aggour and Radding, 2001 and Daniel et al., 2003).



Figure 2.3 Picture shows a simple drilling conducting SPT (original picture to collation data from Erbil, 2019).

Cone Penetration Test, CPT

The cone penetrometer test (CPT) involves inserting a cone-shaped device into the ground, which is accomplished using a hydraulic jack. These days, modern cone penetrometers are typically used in conjunction with the jack, and they may be installed on a variety of vehicles, including trucks, railroads, barges, and drilling ships (ASTM D3441, 2016). CPT cones of various diameters are shown in Figure 2.4. The cone's tip resistance and skin friction are measured using strain gauges and load cells. The pore water pressure may also be measured using modern cones. Typically, measurements are taken every five centimetres interval and are automatically recorded in electronic format.

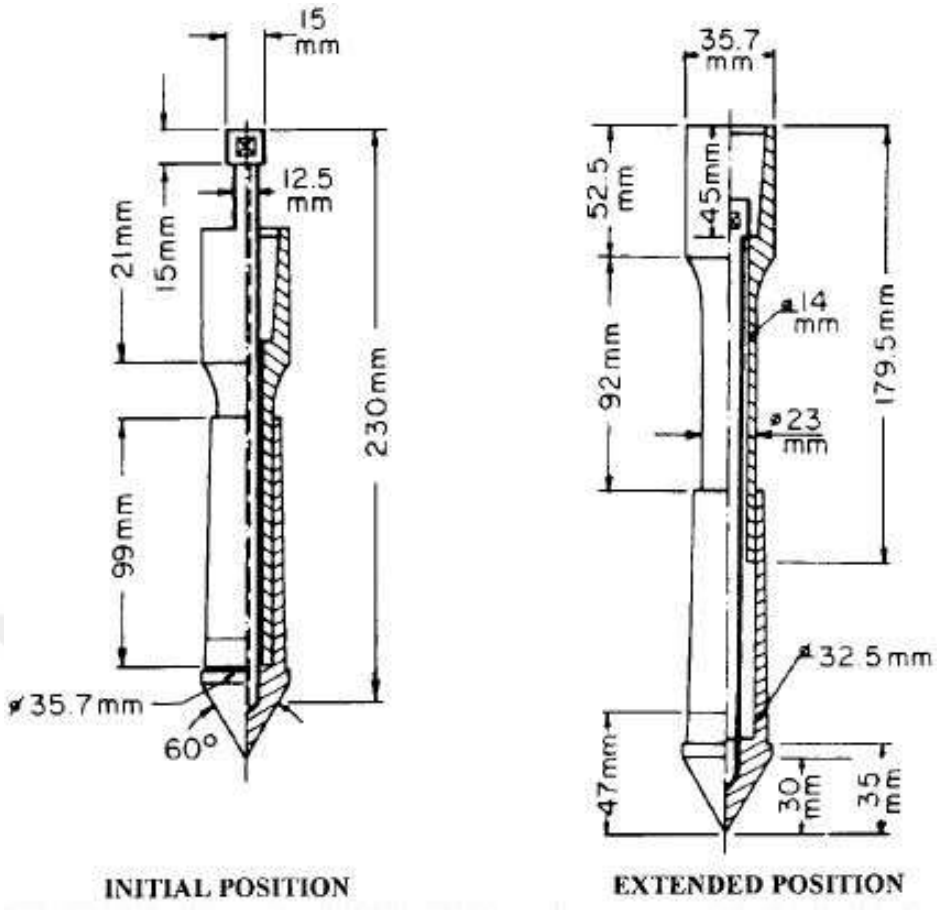


Figure 2.4 Example of mechanical cone penetrometer tip (Dutch mantle cone). (ASTM D3441, 2016).

CPT is a technique of study that is both quick and cost-effective (Lokesh el. al., 2014; Robertson, 2016). A standardized testing method is applied, and the measurements obtained do not require user interpretation. The cone penetrometer test (CPT) can be performed on soils and weathered bedrock, but not on soils that have large boulders or hard rock. However, a limitation of the test is that there is no direct visualization of subsurface soils during the test. While obtaining samples from CPT is allowed, it is not commonly practiced as it undermines one of the test's primary benefits, which is its efficiency and cost-effectiveness (Eslami et al., 2019). Another significant benefit of CPT is that the results may analyze soil parameters. On the other hand, Material variations between two consecutive Split Spoon Sampler (SPT) samples may not be directly identifiable and must be interpreted by humans, as the samples are collected at discrete intervals. Furthermore, CPT measurements standard and continuous character make it simple to include into automated analysis and design methods. As an illustration, CPT data may be used directly for liquefaction analysis, and the

analysis requires much less human interpretation than SPT-based approaches (Kayen, 1992; Chen and Juang, 2000; Lenz and Baise, 2007).

Geophysical Tests

Geophysical tests are used to gather data about soil and rock arrangements indirectly. They are regularly consumed to gather rapid economic data over large regions (Coutinho and Mayne, 2012). The information gathered from these tests is universal and representative on a enormous scale. They are especially beneficial in regions with light rock structures (Kanta et al., 2013). Seismic refraction survey is the most common geophysical test (Schuster, 2017). Table 2.4 shows a record of standard geophysical tests and the benefits and drawbacks of each approach.

Table 2.4 List of common geophysical tests in geotechnical engineering (Hunt, 2005).

Method	Application	Comments
Seismic refraction from surface	Obtain stratum depths and velocities, land or water. Geologic sections interpreted	Most suitable if velocities increase with depth and rock surface regular
Seismic direct (crosshole, downhole)	velocities for particular strata; dynamic properties; rock mass quality	Requires drill holes. Crosshole yields best results. Costly
Seismic reflection	General subsurface section depicted. Water bodies yield clearest sections	Land results difficult to interpret. Velocities not obtained. Stratum depths comps require other data
Electrical resistivity	Locate saltwater boundaries, clean granular and clay strata, rock depth, and underground mines by measured anomalies	Difficult to interpret. Subject to wide variations. No engineering properties obtained. Probe configurations vary
Gravimeter	Detect faults, domes, intrusions, cavities, buried valleys by measured anomalies	Precise surface elevations needed. Not commonly used, measures density differences
Magnetometer	Mineral prospecting, location of large igneous masses	Normally not used in engineering or groundwater studies
Ground-probing radar	General subsurface section depicted. Most useful to shows buried pipe, bedrock, voids, boulders	Interpretation difficult. Limited to shallow depths. No engineering properties
Thermography	Shallow subsurface section depicted. Useful for water pipeline leaks	Interpretation difficult. Limited to shallow depths. No engineering properties

2.2.2 Laboratory Soil Tests

After collection in the field, soil samples are typically transported to the laboratory for sorting and analyzing (Kalinski, 2011). The most familiar laboratory tests include density (using a relatively undisturbed sample), moisture content, sieve analysis, soil classification and geotechnical or mechanical tests. The geotechnical engineers assign various other soil tests following the project's requirements. The soil laboratory testing in the Erbil government established according to American Society for Testing and Materials (ASTM) (Germaine and Germaine, 2009).

Some of the most universal laboratory soil tests are included in Table 2.5. To provide test results, most soil laboratories utilize Excel spreadsheets. In most cases, the results are organized by borehole name, sample ID, and depth from the top of the borehole. Users may determine the original site of the test sample by using the borehole name and depth from the outward. A lab test form for a direct shear test is shown in Figure 2.5. The results of such tests may be supplied in hard copy, PDF, or worksheet format.

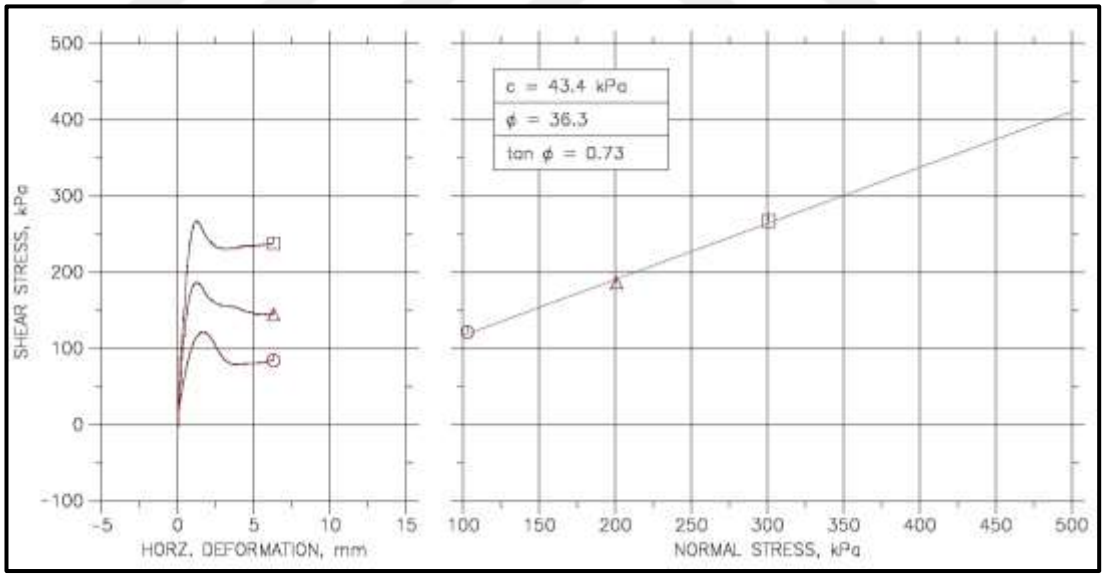


Figure 2.5 A laboratory data from direct shear test

Table 2.5 List of some of the most common laboratory tests in geotechnical engineering (Hunt, 2005).

Test Name	Comments
Moisture Content	Determine moisture content of the sample
Density	Determine density of the sample
Specific Gravity	Determine specific gravity of the sample
Sieve Analysis	Determine grain size distribution for coarse grains
Hydrometer	Determine grain size distribution for fine grains
Atterberg Limits	Determine liquid limit and plastic limit
Soil Classification	Determine soil classification per one of the classification methods
Compaction	Determine maximum dry unit weight and optimum moisture content
R-Value	Measures the response of a compacted sample of soil or aggregate to a vertically applied pressure under specific conditions
Direct Shear	Measures the shear strength of soils under direct shear
Unconfined Compression	Measures the unconfined compressive strength of cohesive soils
Triaxial Test	Measures the shear strength of soils under triaxial loading condition
Consolidation	Measures the compressibility of fine-grained soils

2.3 Geotechnical Data Reporting and Archiving

Geotechnical data is converted to various forms depending on project requirements when fieldwork and laboratory tests are completed. Traditional hard copies, PDF and picture formats, spreadsheet and database formats are all illustrations of these forms, as explained in the following sections (Payne and Bell, 2021).

2.3.1 Geotechnical Databases

Geotechnical engineering has been utilizing database programs for over two decades. These programs have been widely used in industries such as mining and oil, which typically involve larger investigations than geotechnical engineering (Hopkins et al., 2005). The Geotechnical and Geoenvironmental Engineering Software Directory website provides a list of geotechnical database programs in Table 2.6 (GGSD 2021).

A relational database is essentially these programmes, which also have a reasonably basic borehole schema as a built-in (Nemoto, 2015). The outline is retractable, and users may add new data fields to active tables or create new tables built on their specific requirements.

Table 2.6 Partial list of geotechnical engineering database programs (GGSD, 2021)

Program	Operating system
BLDM	DOS, Intergraph Microstation
GDM	Win95/98, WinNT, Win2000
GeoBASE	Win95/98
GEODASY	Win95/98, WinNT
GEO-LOG 2	Win3x, Win95/98, WinNT
GEO-LOG 3	Win95/98, WinNT, Win2000
gINT Logs Plus	Win2000, WinXP
gINT Professional	Win2000, WinXP
GIS-Key Winlogs	Win95/98, WinNT
HoleBASE III	Win95/98, WinNT, Win2000, WinXP
HoleBASE Wizard	Win95/98, Excel
Hydro GeoLogger	Win2000, WinXP, WinVista
SID	DOS, Win3x, Win95/98, WinNT
TECHBASE	DOS, Win95/98, WinNT, UNIX, LINUX, Open VMS

2.3.2 Hard Copies

Boring logs and laboratory forms in hard copy format have traditionally been used to prepare geotechnical data. Hand drawing was conducted to create the hard prints. After that, the physical copies were prepared using computer software (LogPlot, AutoCAD and Micro Station) (Deaton, 2013). On the other hand, consultants often implemented

the program internally to generate hard copies during the changeover time, while electronic-format data was left unsubmitted to the data holder and so lost.

For example, Caltrans has a significant library of soil data in hard copy setup. This type is bulky, difficult to recover, and prone to loss and degeneration due to physical harm (Manual, 2008). When these documents were transferred to microfilm, they had the identical difficulty to a minor degree.

2.3.3 Electronic Image Formats

Data has been stored and reported using the image and CAD software for several years. Several organizations demand that consultants present boring records and test outcomes in PDF or CAD format (McPhail, 2001). For example, Erbil government laboratories have required drilling logs to be supplied in PDF and Microsoft format for the past few years. However, many organizations have switched their paper archives to digital format (usually scanned to PDF or image format). Furthermore, some data is often lost during this transfer due to lost original hard copies or scanning resolution and legibility issues.

2.3.4 GIS-Based Archiving of Geotechnical Data

Web-based database systems with geographic information system (GIS) interfaces are becoming more popular in geotechnical data transmission (Chung and Rogers, 2010). Some agencies have applied this strategy in recent years to designate their geotechnical data repository accessible over the Net (Tsangaratos, 2010).

Here are two kinds of Web-based geotechnical records available; the first kind includes metadata for searching, but the primary data (boring log) is stored as an image (PDF or jpg). The customer uses criteria to query the information, and the record returns a list of boreholes that satisfy the requirements, as well as a link to download each borehole log's image file. The second method uses a geotechnical database schema to store the real data from the borehole in a database (Graettinger, 2011).

According to (Kunapo et al., 2005), the first technique is more suitable for legacy data, as it is readily accessible or can be easily transferred to an image format. This approach allows for the database to be generated within a reasonable timeframe and at a reasonable cost (Cheung et al., 2004) have established a model for evaluating positional uncertainty in a shortened line, which can be utilized for programmed line

simplification algorithms. By utilizing this model, it is possible to determine the acceptance for line simplification built on a predefined standard level of accuracy. Because it enables exploration and suspect techniques on a varied variety of data, the second approach gives significantly more utility for new borehole data (Graettinger, 2011). Web-based geotechnical data management and archiving systems are included in Table 2.7. Due to the large number of projects available in the region, the list provided may not be comprehensive, and it was not practical to include all of them in the table. A model of this type of geotechnical archive is the COSMOS/PEER-LL Geotechnical Virtual Data Center (Chang and Park, 2004). The next section outlines several of the web-based database systems for geotechnical data.

Table 2.7 Some of the Web-based geotechnical data management and archiving systems (Chang and Park, 2004)

Name	Description	Owner/Developer	URL
GeoDOG	Caltrans Geotechnical Services electronic database that houses geotechnical information and Documents produced during the course of project development	Caltrans	N/A Caltrans employee access only
COSMOS/ PEER-LL GVDC	A distributed system for archiving and dissemination of geotechnical data. Provides access to several data providers' geotechnical data using a common data format.	COSMOS/PEER-LL	http://geodata2.usc.edu/
Kobe Jibankun	Geotechnical database and GIS system for Kobe City	Kobe City	N/A
National Geotechnical Database	Holds geotechnical information extracted from site investigation records provided by clients, consultants and contractors and from field and laboratory testing carried out by the British Geological Survey. Uses AGS format.	British Geological Survey	N/A

2.4 Geographic Information Systems

GIS allows selection of a numerical map to display various prospects of geographic entities at different sizes and levels of detail applying a zoom in and zoom out tool. Site inspection works and laboratory testing are often used to collect geotechnical data for site planning and development. Site and laboratory studies obtain detailed information on soil type and strength. Information is essential in design of infrastructure and structures that are both cost-effective and safe. After the projects are completed, in the offices of the concerned project, important information is often left dispersed in its original form (Wan-Mohamad et al., 2011). A framework that can effectively store, analyze, and update data and provide various types of information such as map and tables may help decision-makers and designers operate more efficiently (First et. al., 1996). Engineers and planners in the land development business will find these systems to be useful (Chandio et al., 2013). It is well recognized that geographic information systems (GIS) can supply these characteristics, such as storing information in a multi-layered database (Bolstad, 2016). Furthermore, it may be used to manage information in spatial records; as a result, geographic information systems are being used in many engineering applications, including geotechnical, environmental, human resources, construction, and transportation. Figures 2.6, 2.7 and 2.8 shown the Overlay Analysis, raster, vector and real world of GIS.

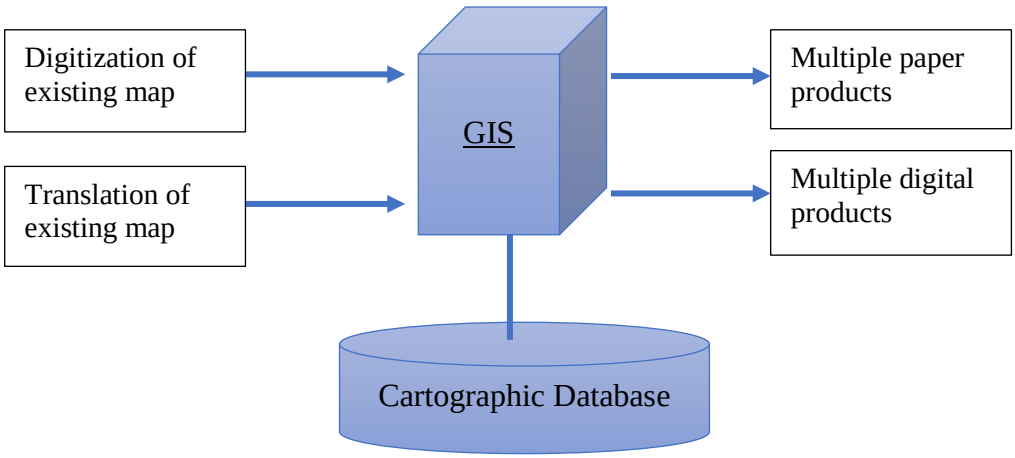


Figure 2.6 Map making (Azad, 2009).

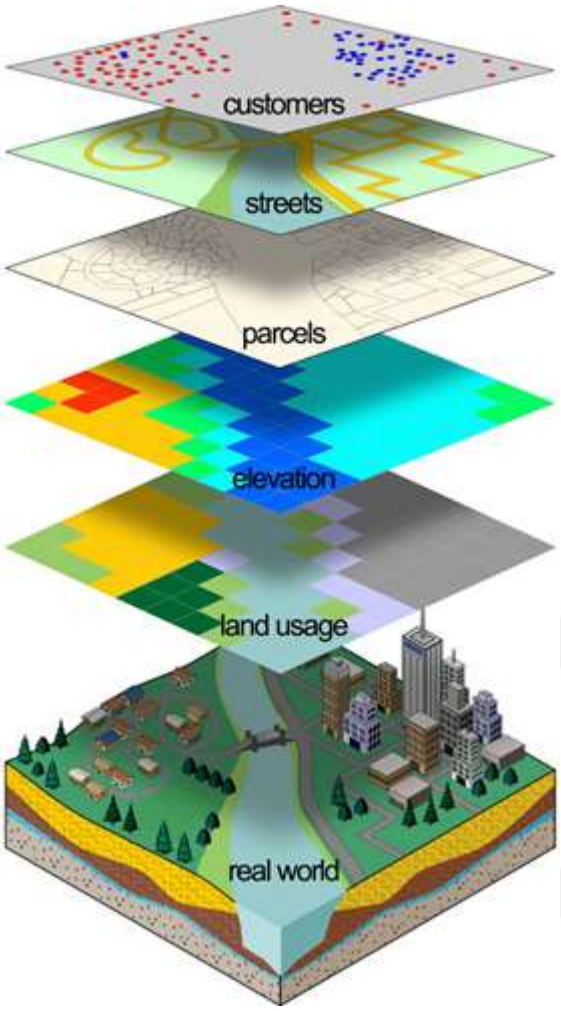


Figure 2.7 Overlay Analysis (GEOL-260, 2021)

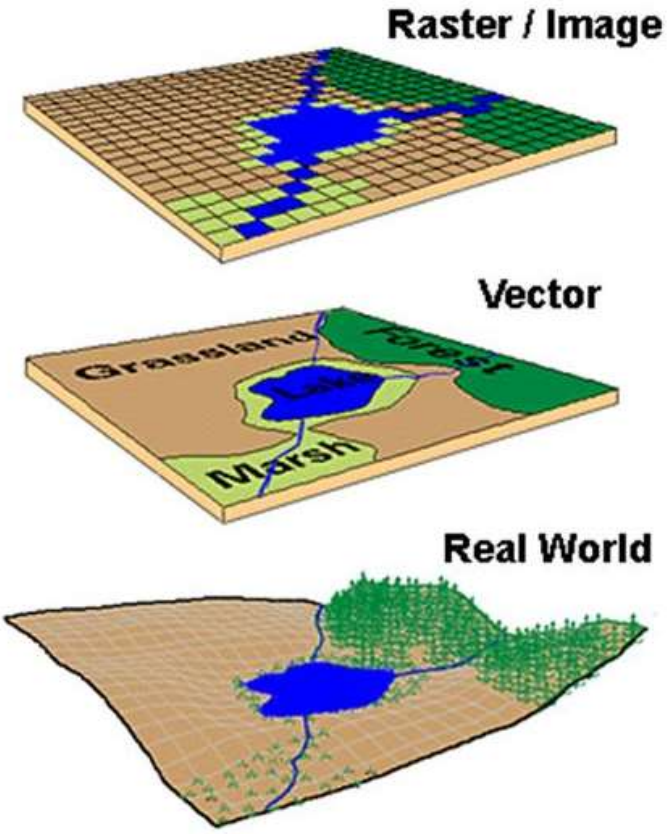


Figure 2.8 Show the raster, vector and real world (Spiller and Agudelo, 2011).

The use of geographic information systems in geotechnical engineering to establish the locations of boreholes allows engineers or planners to perform a new inquiry, specifically for the location of a new site (Oloufa A.A., 1995). At the same time, for environmental engineering, the choice of many waste sites using this software is difficult to recover, production facilities and highways in a large area. The geographic information systems are used for the initial stage to determine the site layout and the location of the temporary facilities (Innes and Simpson, 1993).

The Global Positioning System (GPS) makes it easier to determine the layout of a site and the location of temporary facilities (Hofmann et al., 2012). GIS has gained popularity in transportation engineering. For instance, it is used in traffic planning to display origin-destination densities, noise complaints, trip generation, inter-destination routes, and transportation access (Oloufa A.A., 1995). GIS refers to a set of universally applicable tools for describing, converting, managing, analyzing, and presenting data, particularly in spatial data. The use of GIS technology in analysis and

explanation systems enables data visualization, which enhances users' understanding compared to analytical and statistical products or reports (Yu et al., 2005).

Rashed and Hussein (2020) employed GIS as a instrument to identify expansive soil in Sulaymaniyah city. They used the Inverse Distance Weighting (IDW) interpolation tool inside the GIS program to generate maps. Their primary aim was to generate digital soil maps for the study area and identify areas with high expansive soil. There have been numerous studies on the purpose of GIS in geotechnical engineering. " GIS as a tool in geotechnical engineering " by Hellawell (2001) provides a comprehensive overview of GIS applications in geotechnical engineering.

2.5 Statistical Analysis of Geotechnical Data

- Geotechnical engineers rely on testing data to obtain parameters for characterizing and designing projects. However, the available information is often incomplete, uncertain, or not specific enough. A competent engineer must consider this variability and uncertainty while parameterizing and modeling the physical system. The degree of detail required depends on the chosen approach (Uzielli, 2008). In this context, the following methods are used:

- Define the sources of geotechnical uncertainty and identify the primary factors contributing to alterability in geotechnical testing data.

- Explain the application domains of statistical analyses in geotechnical engineering.

Some relevant examples from the geotechnical literature to support the discussion. Zhang (2018) conducted a study in which they utilized the R statistical program to implement statistical corresponding and dependability analysis for geotechnical engineering problems. The study focused on characterizing the dependence structures among variables by fitting parameterized models to the division of respected samples. The study also employed various analysis methods, such as the first- and second-order consistency and random sampling simulation methods. Avunduk and Copur (2018) used the Minitab statistics software for predicting the excavation performance of an earth tension balance tunnel boring machine (EPB TBM) based on soil properties. The study was conducted to determine the impacts of soil properties on the excavation

performance of used EPB TBM in the Istanbul Ayvali Waste Water Tunnel Project to develop observed performance prediction models. Obianyo et al. (2020) employed single and linear multivariable regression methods to conduct data analysis. Their study aimed to investigate multivariable regression models that could predict the compressive strength of bone ash stabilized lateritic soil for sustainable building. The study utilized both multivariate and non-linear models to predict the compressive strength of the lateritic bricks. The resulting model has practical applications in predicting the compressive strength of stabilized lateritic soil for sustainable housing construction in Nigeria. The residual analysis of the model selection is shown in Figure 2.9.

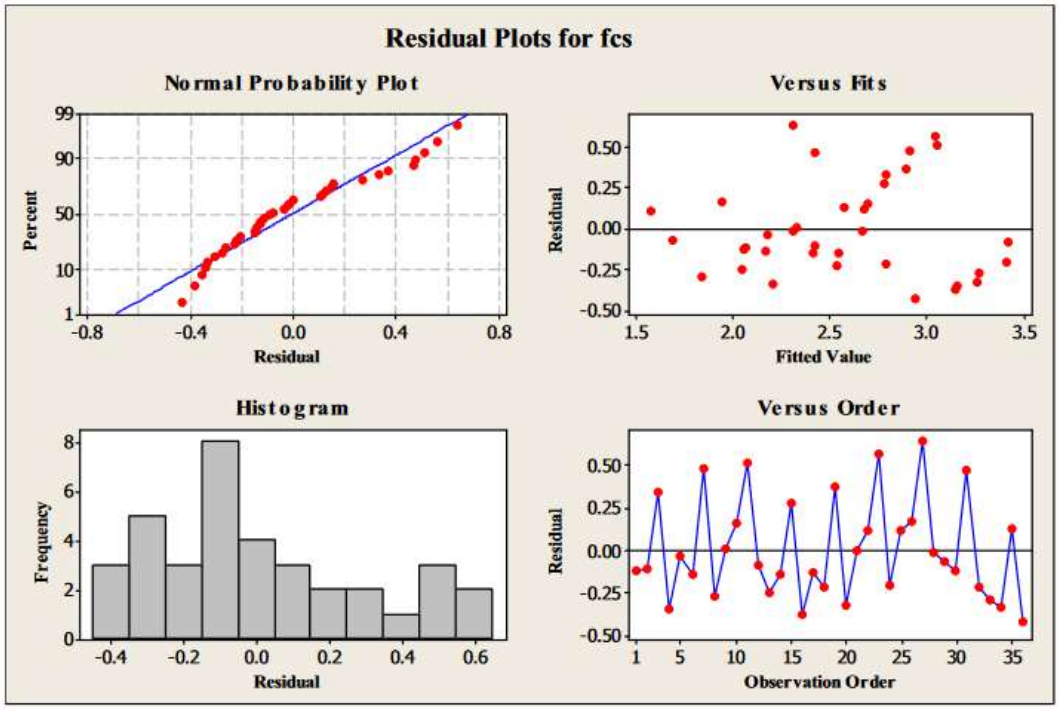


Figure 2.9 Residual analysis of Model 1 in predicting fcs. (Moghaddam, 2010)

2.6 Artificial Neural Network

ANNs continue to evolve in both software and hardware (Yegnanarayana, 2009). ANNs have a broad range of applications across various fields, including finance, manufacturing engineering, automation, electronic circuit design, electronic engineering, computer programming, medicine, academic research, computer vision, object recognition, and more (Basheer and Hajmeer, 2000). Due to advancements in computational science and increased processing power, ANNs have also found

successful applications in the areas of geotechnical and construction engineering (Shahin et al., 2008).

2.6.1 Artificial Intelligence in Geotechnical Engineering

ANN have gained extensive usage in civil and geotechnical engineering research, Since the early 1990s (Najjar et al., 1996; Yuanyou et al., 1997; Yang and Zhang, 1998; Hurtado et al., 2001; Rafiq et al., 2001; Lee et al., 2003; Basma and Kallas, 2004). It has been demonstrated in previous studies that ANN is a useful tool in predicting various geotechnical parameters such as compaction and uplift of pile foundations, axial and lateral load capacities (Teh et al., 1997; Nawari et al., 1999; Rahman et al., 2001; Hanna et al., 2004; Das and Basudhar, 2006; Ahmad et al., 2007; Shahin and Jaksa, 2009), drilled shafts (Goh et al., 2005; Shahin and Jaksa, 2009), foundation settlements (Sivakugan et al., 1998), and anchor embedment (Shahin et al., 2004, 2005; Shahin and Jaksa, 2006). The application of ANN can also be observed in various other earth science fields, including but not limited to retaining walls (Ozturk, 2014; Ghaleini et al., 2019), dams (Ranković et al., 2014; Stojanovic et al., 2016), earthquake analysis (Dindar et al., 2017), geographic information systems, and mining (Afram et al., 2017), geoenvironmental engineering (Shang et al., 2004), and petroleum engineering (Kulga et al., 2018).

The study examined the use of relative density (Dr) and average effective stress as inputs in an ANN model applied to both typically loaded and over-consolidated sands. The model outputted cone penetration test (CPT) and cone resistance (QC). To train the model, 93 data points were used, with an additional 74 data points utilized for testing. The correlation analysis revealed a strong nonlinear relationship, with a coefficient of 0.97 for training and 0.91 for testing. However, predicting foundation settlements, like other complex geotechnical issues, is subject to uncertainty. To address this challenge, several researchers have utilized ANN for settlement prediction. Sivakugan et al. (1998) used ANN to estimate shallow foundation settling on coarse-grained soils. To develop the ANN tool, a total of 79 data sets were utilized, with 69 of them designated for training and the remaining ten for testing. The tool employed five factors as input values, which included applied net pressure, average SPT values, foundation width, foundation shape, and foundation depth. The predictions obtained from the ANN model were then compared against those from two conventional methods.

Due to the interactions between variables, traditional statistical approaches may be inadequate. It is difficult to predict the physical attributes of soil by using statistical approaches, the Mineralogy, porosity, water content and particle size (Yang and Rosenbaum, 2002). It is possible to utilize ANN algorithms to estimate/determine various soil parameters, including soil categorization (Cal, 1995).

2.6.2 Use of Neural Networks for Predict the Geotechnical Properties of Soils

In earlier studies, researchers have already utilized the ANN approach to estimate soil characteristics and classify soils. ANN and classical regression analysis approaches have been compared in the preceding works. Günaydın (2009) used different approaches to predict OMC and maximum dry density (MDD) values. A total of 126 samples were utilized in the study, with various fine-grained, sand and gravel, LL, and PL combinations (Table 2.8). The techniques of Simple-Multiple Analysis and ANN were competed in this research. For multiple linear regression analysis, R^2 values were determined to be in the range of 0.77 to 0.78 (Equation 2.1), 0.74 to 0.82 for simple linear regression analysis (Figure 2.10), and 0.67 to 0.89 for ANN analysis (Figure 2.11).

$$\mathrm{OMC} = 0.3802 w_L + 2.4513 \qquad R^2 = 0.82 \qquad (2.1)$$

where OMC is the optimum water content (%) and w_L is the liquid limit (%)

Table 2.8 Models structure used in the study of Günaydın (2009)

Model	Inputs	Structure	Transfer function
I	FG, *S*, *G*, *Gs*, w_L, w_P, ST	7-3-3	Tag sig-log sig
II	FG, *S*, *G*, *wL*, *w*	5-3-2	Tag sig-log sig
III	FG, *S*, *G*	3-3-2	Tag sig-log sig
IV	w_L, w_P	2-6-2	Tag sig-log sig
V	w_L, w_P	2-3-1	Tag sig-log sig

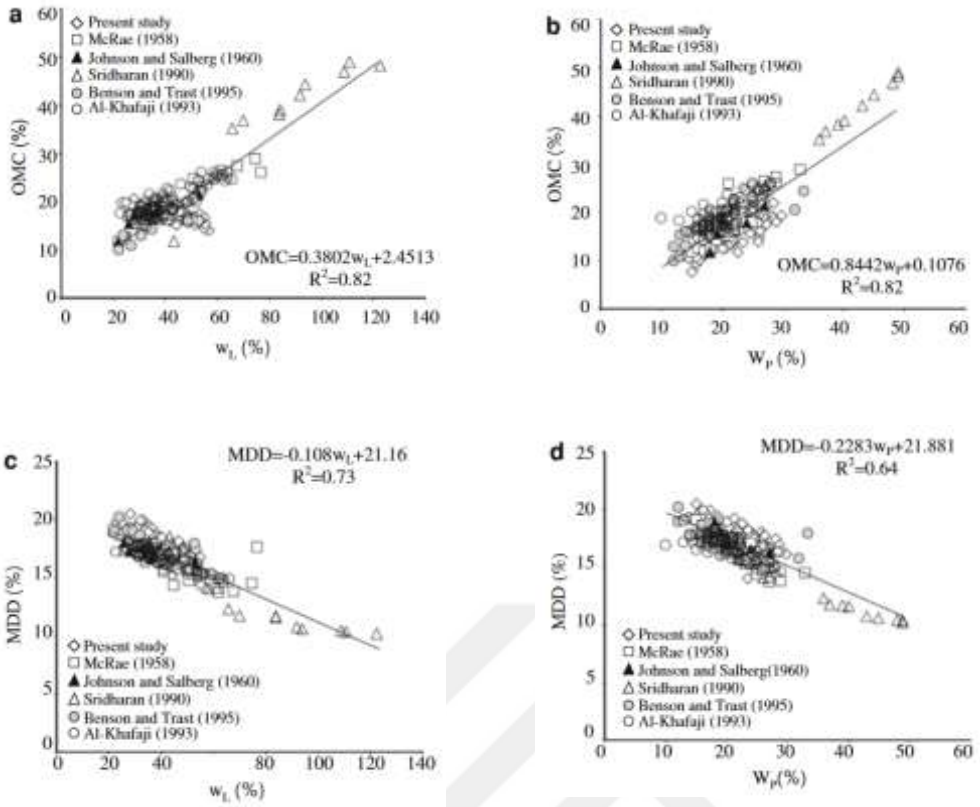


Figure 2.10 Simple linear regression analysis results; a) LL versus OMC, b) PL versus OMC, c) LL versus MD, d) PL versus MDD (Günaydın, 2009)

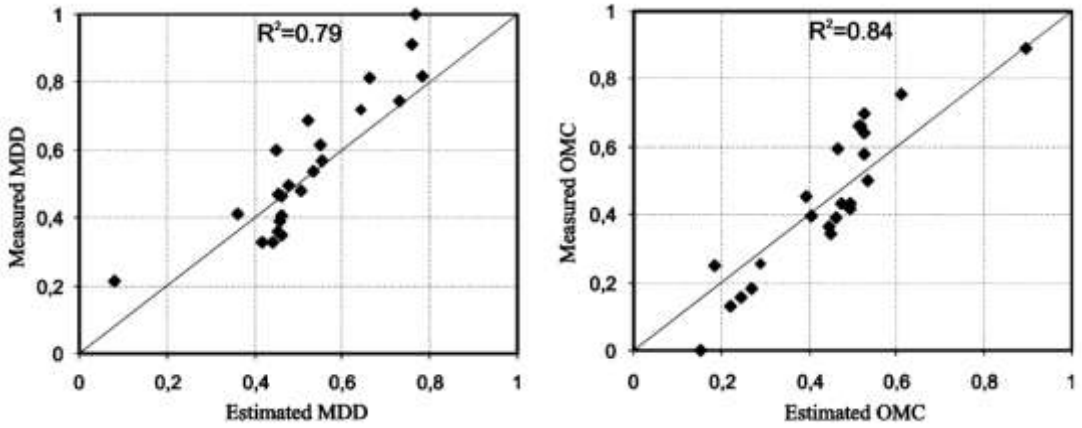


Figure 2.11 Comparison between measured values, and the estimated MMD by Model II (Günaydın, 2009)

Hassannejad et al., (2015) used 120 samples to classify soil using several ANN techniques for moisture content, LL, PL, and SPT values. Specifically, they stated based on the Levenberg-Marquardt method is the most accurate approach for estimating soil categorization. Figure 2.12 show the modelling of the study. The OMC and MDD were estimated by using ANN approaches with utilized 210 samples of LL, PL, and sieve analysis data. According to the findings of the ANN model, R^2 values for OMC values were 0.85 in training, 0.76 in the test, and 0.95 in the simulation, respectively (Figure 2.13 a, b, and c). In addition, the R2 for MDD was 0.88 in training, 0.81 in testing, and 0.95 in simulation. (Figure 2.14 a, b, and c).

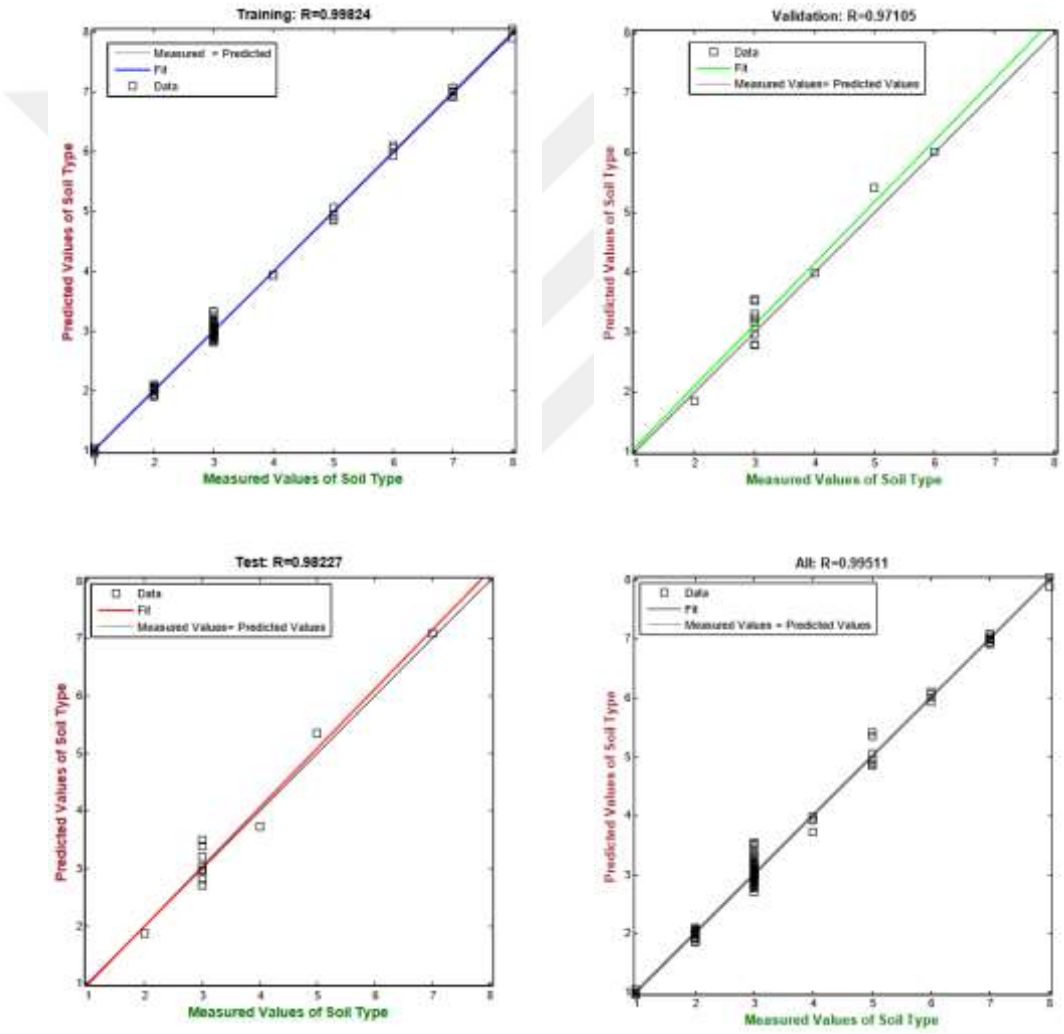
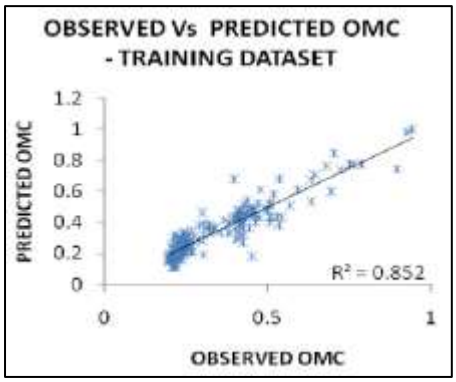
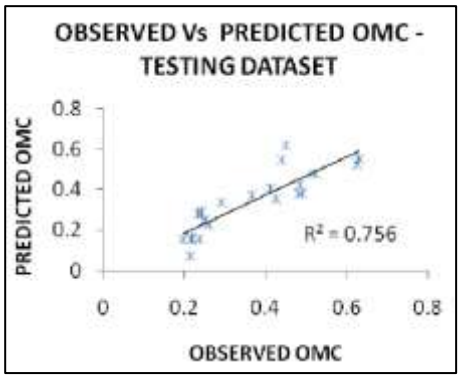


Figure 2.12 Comparison between the predicted values of soil type and the measured values from (Hassannejad et al., 2015).

a)



b)



c)

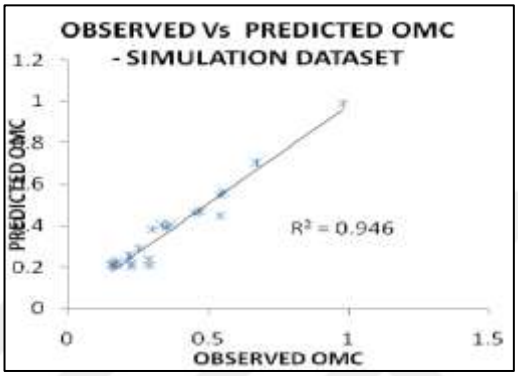
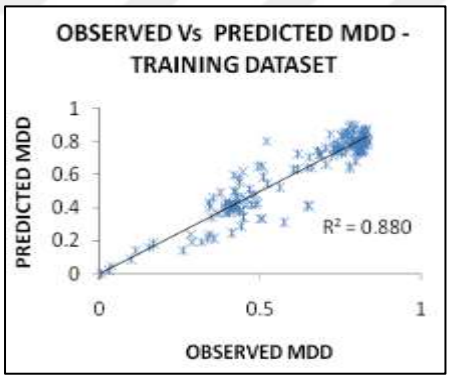
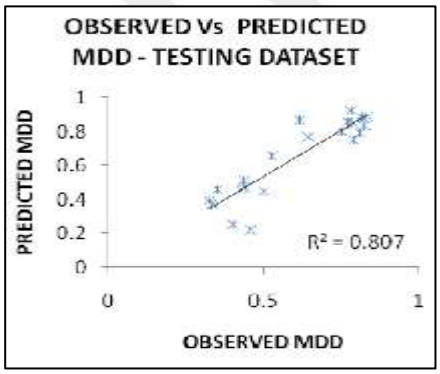


Figure 2.13 Observed OMC vs Predicted OMC values during a) Training, b) Testing, and c) Simulation (Tenpe and Kaur, 2015).

a)



b)



c)

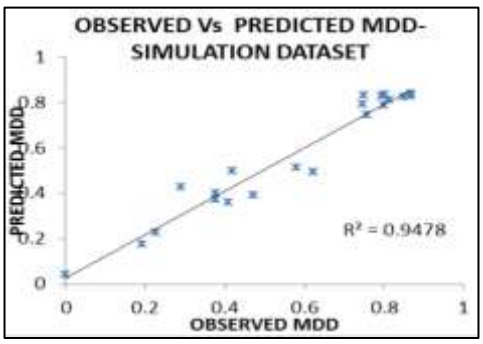


Figure 2.14 Observed OMC vs Predicted MDD values during a) Training, b) Testing, and c) Simulation (Tenpe and Kaur, 2015).

In their study, Bahmed et al. (2017) utilized an Artificial Neural Network (ANN) to predict the values of PI, MDD, and OMC based on input parameters such as LL, PL, and Lime content. The researchers analyzed 280 data points from previous studies for their analysis. The R^2 value for the PI was 0.91 and 0.83 for MDD and OMC, as shown in Figure 2.15 a, b, and c. Reale et al. (2018) employed CPT values to estimate soil categorization using artificial neural networks (ANN). As a result, they used the 216 data set. Furthermore, they created two separate ANN networks. The first network was created to estimate fines content (FC), while the second network prediction LL and PI. The R^2 of correlations values for FC were 0.79, 0.85 for LL, and 0.78 for PI, respectively. (Figure 2.16 a, b and c).

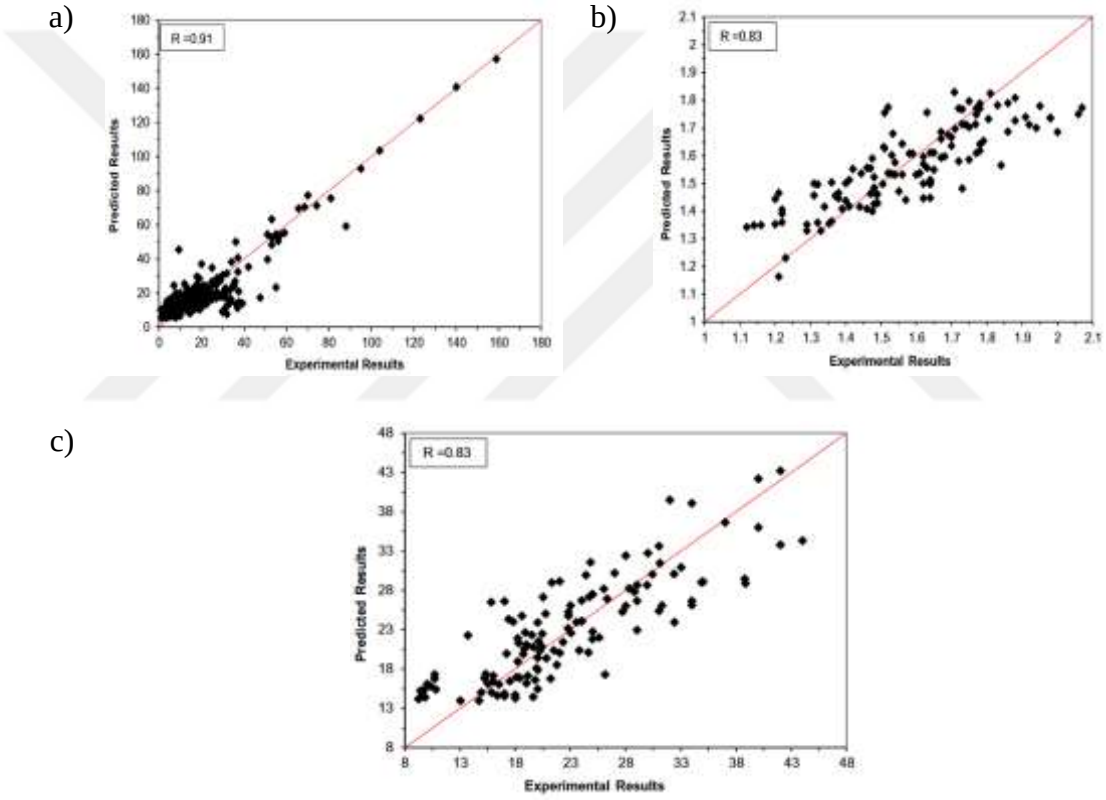


Figure 2.15 a) Experimental LL versus predicted LL, b) Experimental MDD versus predicted MDD, and c) Experimental OMC versus predicted OMC (Bahmed et al., 2017).

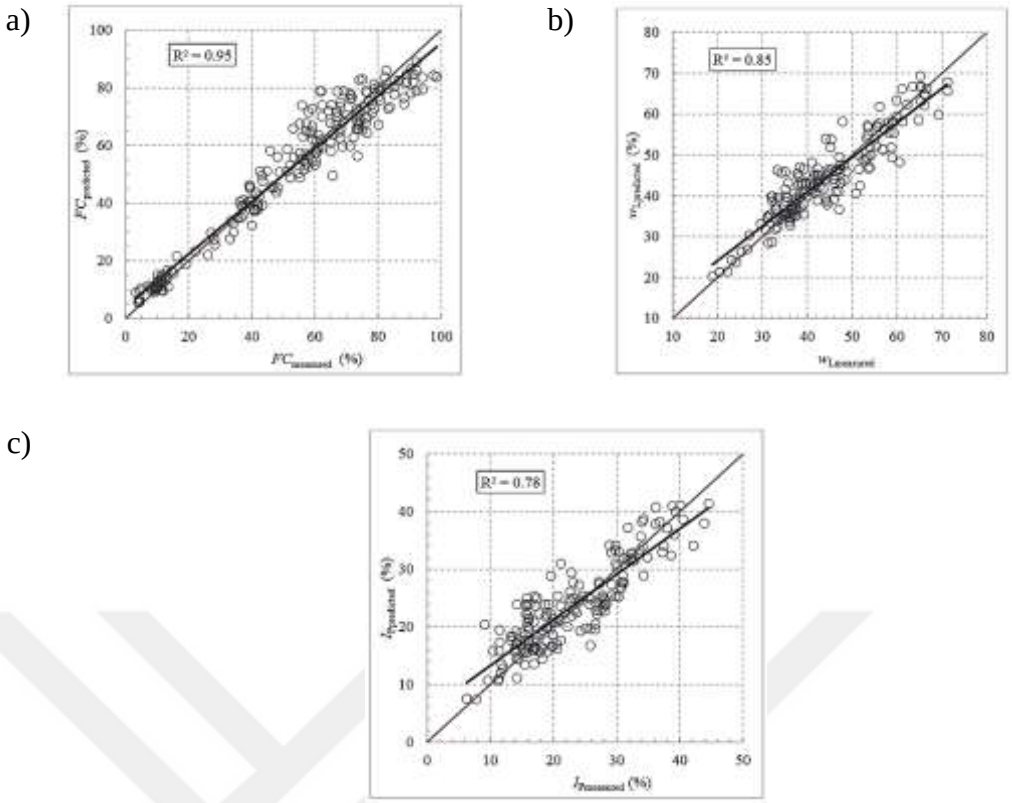


Figure 2.16 a) Measured FC versus predicted FC, b) Measured LL versus predicted LL, c) Measured PI versus predicted PI (Reale et al., 2018)

2.7 Development of Artificial Neural Network Models

A systematic approach is required for the development of ANN models to improve their efficiency. This strategy could take into account significant aspects, such as identifying appropriate model inputs, data pre-processing and division, selecting an appropriate network architecture, and cautiously choosing internal parameters that regulate the optimization process, along with the stopping criteria and model validation (Maier and Dandy 2000). The following sections elaborate on these factors.

2.7.1 Determination of Model Inputs.

Identifying the input variables that have the most significant impact on model performance is a crucial step in the development of ANN models. Choosing a well-defined subset of input variables can significantly improve model performance. However, providing a large number of input variables to ANN models often results in an increase in network size, reducing processing speed and network efficiency (Lachtermacher and Fuller, 1994). Various techniques have been suggested in literature to facilitate input variable selection. In geotechnical engineering, a prevalent

method involves preselecting a fixed number of input variables believed to be the most effective in relation to the model output variables. This technique will be employed in developing the ANN models for this study. Conversely, some researchers (Najjar et al. 1996; Ural and Saka 1998) adopt an alternate approach where multiple neural networks are trained using different input variable combinations, and the network with the best performance is selected.

Maier and Dandy (2000) proposed a step-wise technique in which individual networks are trained using only one available variable as a model input. The best-performing network is retained, and the variable that produces the best performance is combined with each of the remaining variables. This process is repeated for an increasing number of input variables until the addition of any further variable does not improve model performance. Another effective method is to utilize a genetic algorithm to search for the best set of input variables (NeuralWare 1999). For each potential set of input variables chosen by the genetic algorithm, a neural network is trained, and subsets of potential inputs are ranked using the model error obtained with those variables. A set of input variables is deemed fit based on the model error produced using those variables. The adaptive spline modeling of observation data (ASMOD) algorithm proposed by Kavli (1993) is also a useful technique for developing parsimonious neuro-fuzzy networks by automatically selecting combinations of model input variables with the most significant impact on the outputs.

2.7.2 Division of Data

ANNs operate similarly to traditional statistical models during the calibration phase, in that they adjust model parameters, such as connection weights, to minimize the error between the model's outputs and the corresponding measured values for a specific dataset, which is typically the training set. However, When ANNs are not required to extrapolate beyond the calibration data range, they have an advantage as they tend to perform better under these circumstances (Flood and Kartam, 1994; Minns and Hall, 1996; Tokar and Johnson, 1999). The primary goal of ANNs is to conduct nonlinear interpolation or generalization in high-dimensional space between the calibrated data points. ANNs have a large number of model parameters, including connection weights, which can lead to overfitting to the training data, particularly when the training data contains noise. This is unlike traditional statistical models.

In other words, when the model's degrees of freedom are high relative to the number of data points used for calibration, the model may fail to capture the general trend. Instead, it may learn the idiosyncrasies of the particular data points used for calibration, resulting in "memorization" rather than "generalization." Therefore, to ensure that the model can generalize within the calibration data range, a separate validation set is required. Usually, the available data is split into two distinct subsets: the training set, which is used to develop the neural network model, and an independent validation set, which is used to evaluate the model's performance in real-world applications (Twomey and Smith, 1997; Maier and Dandy, 2000). It is commonly recommended that two-thirds of the available data be used for model training, which encompasses both the training and testing sets, while the remaining one-third is reserved for validation purposes (Hammerstrom, 1993).

A modification of the previously mentioned data division method is cross-validation, which divides the data into three subsets: training, testing, and validation. The training set is used to adjust the connection weights, and the testing set is used to evaluate the model's performance at different stages of training and to decide when to halt the training process to prevent overfitting. The validation set is used to estimate the model's performance in a real-world environment. At present, there are no standardized guidelines in the literature regarding the optimal proportion of data to be assigned to the training, testing, and validation subsets. In Chapter 4 will investigate the correlation between the ratio of data allocated to the training, testing, and validation subsets and the performance of the ANN model. The aim is to determine an optimal proportion of data that yields the best model performance. There are instances when the available data is scarce, and it may not be feasible to set aside a specific portion of the data for validation purposes. In such cases, the leave-k-out method is a technique used in artificial neural network (ANN) training and validation, as proposed by (Masters, 1993) can be implemented. This method involves reserving a small fraction of the data for validation and utilizing the remaining data for training. Following training, the model's performance is estimated using the validation set. The process of constructing an optimal ANN model involves repeating the data division process multiple times by withholding different subsets of data until the best model is achieved using all available data. Geotechnical engineering applications utilizing ANNs usually divide data into subsets arbitrarily. However, recent research suggests

that the data division process can significantly influence the analysis outcomes (e.g., Tokar and Johnson, 1999). As ANNs face challenges in extrapolating beyond the range of data utilized for calibration, it is critical to incorporate all patterns within the available data into the calibration set to develop the most optimal ANN model. When extreme data points are present in the data but not included in the calibration set, the model's ability to perform well during validation cannot be assumed, as it would be testing the model's extrapolation capabilities instead of its interpolation abilities. The best evaluation of the model's generalization ability is achieved when all patterns, rather than just a subset, are included in the validation data, assuming that all data patterns available are included in the calibration set.

2.7.3 Data Pre-processing

Before feeding the available data into their respective subsets, i.e., training, testing, and validation, it is crucial to pre-process the data in an appropriate format for their application in the ANN. This pre-processing step is essential to ensure that all variables receive equitable treatment during the training process and also facilitates faster learning. Various forms of pre-processing, including data scaling, normalization, and transformation, can be implemented to achieve this goal. (Masters, 1993) It is crucial to scale the output data to ensure they are within the limits of the transfer functions used in the output layer. For instance, the output data must be between -1.0 and 1.0 for the tanh transfer function and between 0.0 and 1.0 for the sigmoid transfer function. On the other hand, scaling the input data is not mandatory, but it is typically advised. (Masters, 1993). In certain instances, it may be advantageous to have input data that follows a normal distribution to achieve optimal results (Fortin et al., 1997). However, Burke and Ignizio (1992) argued that knowledge of the probability distribution of input data is not necessary. They suggested that transforming input data into a known form, such as linear, log, or exponential, could improve the performance of ANNs. Shi (2000) also discovered that converting input data into a uniform distribution enhanced network performance by 50%. However, experimental tests conducted by Faraway and Chatfield (1998) indicated that model fits were unaffected by whether raw or transformed data were used.

2.7.4 Determination of Model Architecture

Determining the architecture of a neural network is a challenging yet crucial task in the development of an artificial neural network (ANN) model (Maier and Dandy,

2000). It involves selecting the optimal number of layers and nodes in each layer. Unfortunately, there is no single theory to determine the best ANN architecture. Usually, the number of layers in a neural network is predetermined, and the number of nodes in each layer is selected. In all neural networks, two layers represent the input and output variables. Several studies have revealed that a single hidden layer is sufficient to approximate any continuous function, provided there are enough connection weights (Hornik et al., 1989). Moreover, Hecht-Nielsen (1989) showed that a single hidden layer of neurons with a sigmoidal activation function is enough to model any practical solution surface.

On the other hand, Flood (1991) argued that using a sigmoidal network with just one hidden layer can be insufficient to model numerous solution surfaces. Furthermore, several researchers (Flood and Kartam, 1994) suggest that using more than one hidden layer can offer the required flexibility to model complex functions in various scenarios. Chester (1990) suggests that the first hidden layer of a neural network is responsible for capturing the local features of input patterns, while the second hidden layer is better suited for capturing the global features of training patterns. However, Masters (1993) claimed that using more than one hidden layer often results in a dramatically slower training process and an increased risk of getting trapped in local minima. Determining the optimal number of nodes in each hidden layer of a neural network is not a straightforward process. While the number of nodes in the input and output layers is determined by the number of inputs and outputs, respectively, for a given problem, the number of hidden layer nodes requires a trial-and-error approach. In geotechnical engineering, researchers typically experiment with different numbers and connectivity's of hidden nodes to achieve satisfactory performance. However, studies have shown that neural networks with a large number of free parameters (i.e., connection weights) are more prone to overfitting and poor generalization. Therefore, it is generally preferable to minimize the number of hidden nodes while ensuring satisfactory network performance (Masters, 1993).

This approach offers several advantages:

a) it reduces the computational time needed for training;
b) it helps the network achieve better generalization performance;
c) it avoids overfitting, and

d) it enables easier analysis of the trained network.

There are several heuristics to determine the optimal number of hidden nodes in single hidden layer neural networks. One rule of thumb is to assume that the number of hidden nodes should be 75% of the number of input units (Salchenberger et al. 1992). Another method suggests that the ideal number of hidden nodes should fall between the sum and the average of the nodes in the input and output layers (Berke and Hajela 1991). A third strategy involves setting an upper limit for the number of hidden nodes and working within that constraint

Hecht-Nielsen (1989) and Caudill (1988) proposed an upper limit for the number of hidden nodes in a single-layer network as (2I+I), where I represents the number of inputs. Nawari et al. (1999) discovered that the best strategy is to begin with a small number of nodes and gradually increase the number until there is no significant improvement in model performance. Yu (1992) proved that for networks with one hidden layer and (I-1) hidden nodes, the error surface has no local minima. To determine the number of nodes in each layer for networks with two hidden layers, the geometric pyramid rule suggested by Nawari et al. (1999) can be employed. This method postulates that the number of nodes follows a geometric progression resembling a pyramid shape, in which the number of nodes decreases from the input layer towards the output layer. Kudrycki (1988) discovered that the optimal ratio of nodes in the first and second hidden layers is 3:1, even for high-dimensional inputs. The Cascade-Correlation method (Fahlman et al., 1990) is a technique that can automatically determine the optimal architecture of ANNs. This technique involves the following steps. To begin, the neural network is trained using Fahlman's quickprop algorithm (Fahlman et al, 1990) with no hidden nodes and direct connections between the input and output layers. Subsequently, one or a few hidden nodes are added randomly, and these new nodes receive connections from all the previously established hidden nodes and the original inputs. Once new hidden nodes are added, their connections with the inputs are frozen, and only their output connections are trained using the quick prop algorithm. This process continues until there is no further improvement in the model's performance. Consequently, the architecture of ANN networks using Cascade-Correlation comprises input nodes connected to the output nodes, and the hidden nodes connected to the input and output nodes, as well as other previously established hidden nodes, as illustrated in Figure 2.17.

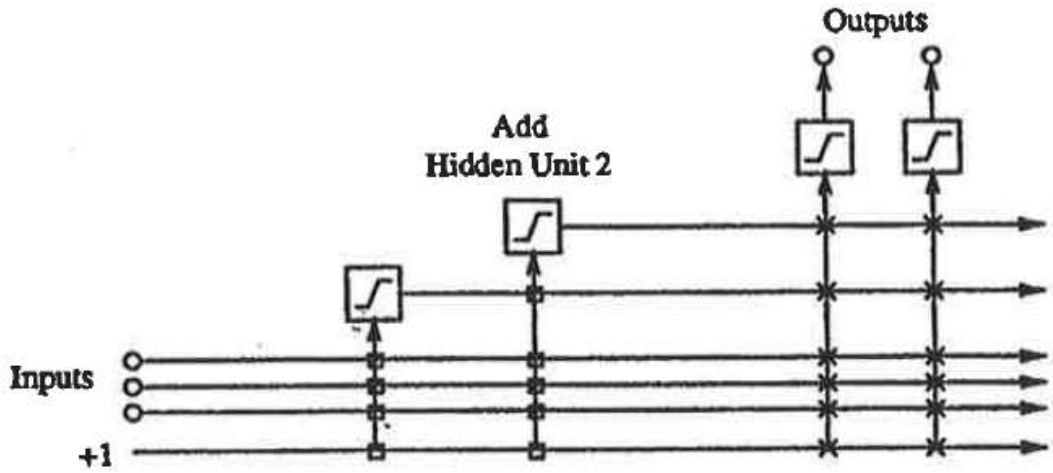


Figure 2.17 ANN architecture with Cascade-Correlation (Fahlman et al., 1990).

2.7.5 Model Optimization (Training)

The process of modifying the connection weights to improve performance is known as 'training' or 'learning', which is akin to the parameter estimation phase in conventional statistical models. The main goal is to find a general solution to a complex non-linear optimization problem. The back-propagation algorithm (Chan and Fallside, 1987), which uses first-order gradient descent, is the most commonly employed technique for finding the optimal weight combination of feed-forward neural networks. Some researchers have also suggested employing global optimization techniques, such as simulated annealing and genetic algorithms (Hassoun, 1995). These techniques offer the advantage of being able to avoid getting trapped in local minima in the error surface, resulting in optimal or nearly optimal solutions. However, they tend to have a slow convergence rate. The choice of training algorithm will ultimately depend on the problem-specific performance criteria. If training speed is not a significant factor, the back-propagation algorithm can be effectively used, as per Breiman (1994).

2.7.6 Model Validation

Once the training phase of the model is successfully completed, it is essential to validate the model's performance. The primary aim of the model validation phase is to verify that the model can reliably generalize within the boundaries set by the training data, rather than simply memorizing the input-output relationships in the training data. To accomplish this, the conventional approach in the literature is to assess the performance of the trained ANNs on an independent validation set that was not utilized

during the model construction phase. If the performance is acceptable, the model is considered to be capable of generalization and is regarded as robust.

CHAPTER 3
METHODOLOGY

3.1 Introduction

The study of geotechnical properties of soil is an important aspect of civil engineering, as it plays a significant role in determining the behaviour of soil under different loading conditions. To comprehend and anticipate the conduct of soil, different models and methods can be used. The use of Geographic Information System (GIS), statistical analysis, and artificial neural network (ANN) models are among the most commonly used methods in this field.

Erbil city, located in the Kurdistan Region of Iraq, was selected as the area study for this project. Erbil is a rapidly growing city, with significant construction activities taking place. The area is also prone to earthquakes, making it important to understand the conduct of the soil in this locality. The creation of GIS, statistical analysis, and ANN models for geotechnical properties of the soil in Erbil can be useful in planning and designing construction projects.

The study methodology encompassed field data collection in Erbil city center, followed by data analysis employing both GIS and ANNs. The collected data was processed and evaluated using these tools to extract insights and draw conclusions regarding the study area. The methodology is visually presented in Figure 3.1, serving as a helpful tool for readers to comprehend the research process employed in this study. A flow chart can show the different steps involved in integrating GIS, ANN, and lab analyses, making it easier for readers to follow and comprehend the study's methodology.

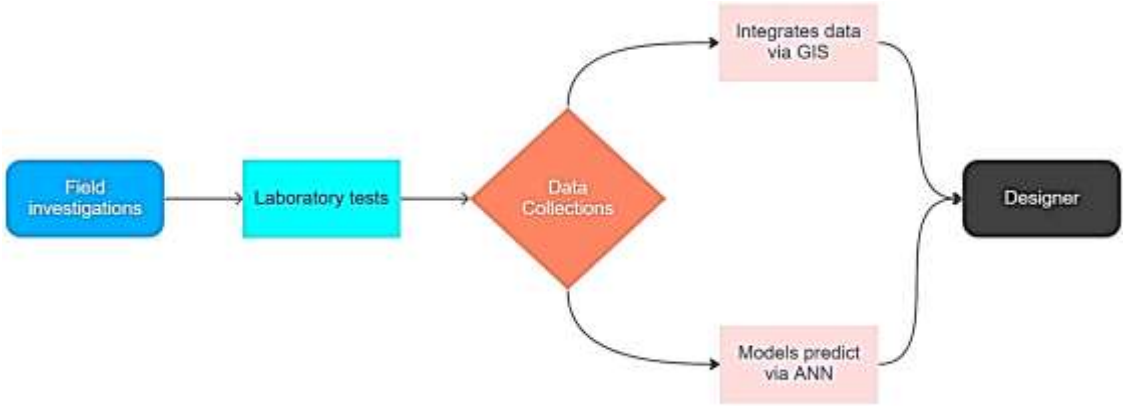


Figure 3.1. Flow chart showing in a simple way the methodology adopted in the present study.

3.2 The Study Area

Erbil is placed in the low folded belt of northern Iraq in the structural through with an NW-SE axial trend, Erbil is positioned in Iraq's structure approach tectonic unit, which includes the foothill area. The area of the city is more than 250 km^2, the GPS coordinates of the city are 36°11'27.4"N 44°00'33.7" as shown in Figure 3.2. Erbil had significant growth in various industries, attracting several international companies and investors who were urged to come to Erbil and establish bases there, Erbil became a market and trade hub for the whole country of Iraq as a result of this development (Hameed, 2013).



Figure 3.2 Location of Erbil City, Iraq

Erbil is one of the world's oldest and most historic cities, with the Erbil Citadel covers back to 6000 B.C., the views of the city are observed in Figure 3.3. Erbil is located approximately 420 meters above sea level on average, and its total land area of government is 40643 km^2, Because the majority of the state is flat, which is advantageous for a variety of agricultural items that depend on groundwater for irrigation ideas. In terms of the city's climate, it is very impassioned in the summer and exceedingly cold in the winter, with temperatures ranging from 2 to 7 degrees Celsius in the winter to upcoming 50 degrees Celsius in the summer. The average annual rainfall is around 400 millimetres per year (Ibrahim et al., 2015).



Figure 3.3 Erbil city photographic

3.2.1 Geology of Study Area

The geology of Erbil soil is characterized by a diverse range of soil types, which are influenced by the region's climate, geology, and topography. A research conducted by Karim et al. (2019) examined the chemical and physical characteristics of soil in Erbil city. It was discovered that the soil mainly consists of clay, silt, and sand, with differing levels of minerals and organic matter. The study also found that the soil is highly susceptible to liquefaction, which is a common hazard in the region due to its seismic activity.

Erbil city is located in a region that is prone to seismic activity, which has led to the development of soils that are highly susceptible to liquefaction. Liquefaction is a phenomenon that occurs when soil loses its strength and stiffness as a result of being saturated with water, usually during an earthquake or other seismic event. This can result in soil liquefying and behaving like a liquid, which can cause significant damage to structures built on top of it.

Sedimentation is made up mainly of soils, gravel, and conglomerates with some sands, clay, and silt, and conglomerate and cover more than 80 % of the study area (Al-Sanjari and Al-Tamimi, 2009). Geomorphologically, the region is flat-lying, with just a few low-lying hills that are unusual. The region is stratigraphically covered by

quaternary and Pleistocene sediments characterized by clays, silt, and sand (Jassim and Goff, 2006.

Overall, the geography of Erbil soil is complex and influenced by a range of factors. Understanding the geotechnical properties of the soil, as well as its relationship with the region's geology, climate, and human activities, is essential for planning and designing construction projects, as well as for assessing the potential risks associated with seismic activity and other natural hazards.

3.3 Geotechnical Properties of Soils in Area Study

The study area was georeferenced with the city center of Erbil; for analysis and modelling purpose soil properties from 102 boreholes were used as shown in Figure 3.4. SPT-N value, physical, and geotechnical properties were considered as the main variables, a whole borehole with a depth of between 1.5 and 9.5 m below the ground.

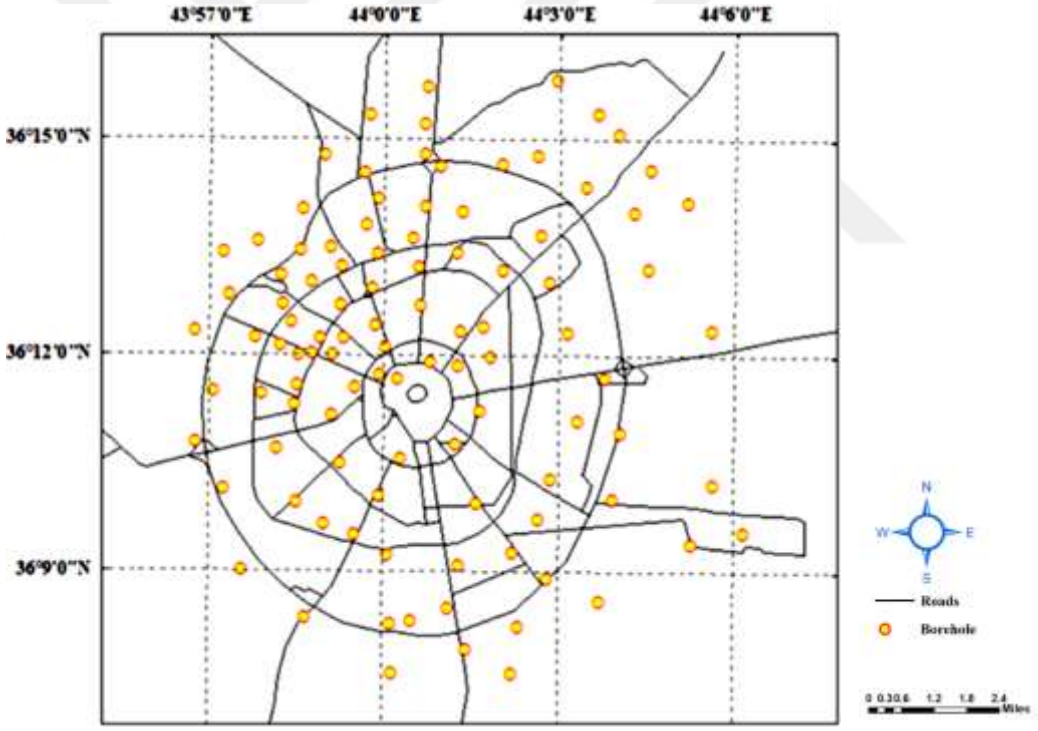


Figure 3.4 Boreholes location in the study area

The geotechnical investigations data have been collected and performed from directory of Erbil construction Lab and Andrea Lab, and procedure of investigations of study area was conducted as two parts of testing as demonstrated in table 3.1.

Table 3.1 Investigations for study area

Investigations area	
Field test	Lab Tests
SPT	1. Visual Classification (ASTM D-2488)
	2. Natural Moisture Content and Unit Weight. (ASTM D-2216)
	3. Specific Gravity. (ASTM D-854)
	4. Grain Size Distribution. (ASTM D-422)
	5. Liquid and Plastic Limits. (ASTM D-4318)
	6. Shear Test: -Direct shear test. -Unconfined Compression Test. (ASTM D2166/D2166m-13)

3.3.1 In Situ Testing

For the collection of undisturbed soil samples from Shelby cylinders, a hydraulic jack, which was specially designed for this purpose, was utilized to create complete boreholes. Presently, the most commonly used and economical method for evaluating the in-situ strength of soil is the SPT. This test measures the resistance of the soil by counting the number of blows (N-value) required to drive a regular sample tube into the ground, from which the bearing capacities of the foundation material can be determined. To perform the test, a free-falling hammer is dropped from a specific height onto the drill rods, which drives the regular sample tube into the soil (Mwajuma, 2015). According to the study description and borehole records; SPT data and soil properties were discovered from the boreholes, as shown in the Table 3.2 which represent BH.1 to BH.5, other boreholes details are following an Appendix.

Table 3.2 The soil properties and SPT data were measured using hammer systems for BH (1-5)

BH ID	DEPTH	SPT- N VALUE	SOIL PROPERTISE
BH-1	1.5-3.5 m	5	fill material is a soft, brownish-gray mixture comprising sandy, lean, and silty clay with numerous broken brick fragments/pieces. Additionally, the material contains black traces of organic matter and white spots of soluble salts.
	3.5-6.5 m	18	Fill materials; soft to medium brown and light brownish-gray sandy, lean, and silty clay. It contains black spots of organic matter and rusty traces of iron oxide compounds, along with some broken brick pieces.
	6.5-9.5 m	12	Fill materials; The material is a medium to stiff brown to brownish-gray sandy, lean, and silty clay with small brick pieces and rusty traces of iron oxide compounds.
BH-2	1.5-3.5 m	53	The material is a very stiff brown to dark brown lean silty clay with black spots of organic matter and white pockets of calcareous materials. Additionally, there is some fine gravel present at the bottom.
	3.5-6.5 m	72	The material is very stiff to hard brown fat silty clay with black spots of organic matter and white pockets of calcareous materials.
	6.5-9.5 m	83	
BH-3	1.5-3.5 m	41	Stiff to very stiff brown fat Silty CLAY with little fine-grained Gravel and black spots of organic matter.
	3.5-6.5 m	70	
	6.5-9.5 m	100	hard brown tolight brown lean silty claywith white spots calcareous materials
BH-4	1.5-3.5 m	65	Dense to very dense brown to grayish brown fine, medium to coarse grained Clayey Sandy GRAVEL with little white spots of carbonate compound.
	3.5-6.5 m	90	Very dense grayish brown fine, medium to coarse grained Silty Sandy GRAVEL.
	6.5-9.5 m	100	
BH-5	1.5-3.5 m	45	Stiff to very stiff brown lean Silty CLAY with little fine to medium grained Gravel and black spots of organic matter.
	3.5-6.5 m	73	Dense to very dense brown to light brown mixture of fine, medium to coarse grained Clayey GRAVEL.
	6.5-9.5 m	92	very stiff brown fat silty clay with white pockets of calcareous materials and black spots of organic matter. Additionally, there is some fine gravel present.

SPT Test Procedure

The SPT is a common geotechnical test used to determine the subsurface soil properties, particularly the soil resistance to penetration and the soil density. The procedure for conducting an SPT test typically involves the following steps:

- Drilling: To achieve the required depth, a drilling rig or equipment is employed to borehole, which usually has a diameter of 2 to 4 inches.
- Installation of the SPT equipment: A standard split-spoon sampler is installed in the borehole. The sampling tool is comprised of a slender steel tube with a cutting shoe at its base and a driving head at the top.
- Driving the sampler: To push the sampler into the soil, a weight of 140 lbs (63.5 kg) is dropped from a height of 30 inches (76.2 cm), and the number of strikes necessary to drive the sampler down by 12 inches (30.5 cm) is noted as the "blow count" or "N-value."
- Recovery of the sampler: After reaching the desired depth or a specified number of blows, the sampler is carefully extracted from the borehole using a sample extractor or a hydraulic jack.
- Sample collection and testing: The soil sample collected in the sampler is carefully removed and preserved for further laboratory testing, such as moisture content, grain size analysis, and shear strength.
- Field observations: While conducting the test, several on-site observations are noted, including the type of soil encountered, the existence of groundwater, and the state of the soil sample.
- Reporting: The test results, including the blow count (N-value) and any field observations, are documented in a report, which is used for geotechnical engineering analysis and design.

It is noteworthy that the SPT test is just one method of soil testing, and the procedure may vary slightly depending on local standards, project requirements, and equipment used. It is typically performed by qualified geotechnical engineers or technicians with experience in conducting and interpreting the results of the SPT test

3.3.2 Laboratory Experimental Testing.

The laboratory testing carried out as soil classification analysis for the soils was utilized to define the type of the soils that were done according to ASTM D 6913

(ASTM, 2009). According to the procedure, soil specimens were examined to liquid limit and plastic limit tests, ASTM D 4318 (ASTM, 2010), and moisture content was taken for all boreholes. The undisturbed soil samples were tested to the Triaxial test ASTM 3080, and Direct Shear test, which was carried out in conformity with ASTM 3080 (ASTM, 1994).

Each test was performed following the applicable standards of ASTM, which are indicated alongside each test.

3.3.3 Bearing Capacity Analysis

Because structural damage may occur as a consequence of both soil failure (collapse) and excessive settlement, the subsequent requirements must constantly be utilized when assessing bearing capacity:

1. An acceptable safety feature against failure.
2. Acceptable allowance for excessive settlement.

The assessment of bearing capacity in this study was carried out using the following method:

To estimate the bearing capacity of soil, the commonly used approach is the Terzaghi equation, which was modified by Meyerhof (1963). The Terzaghi equation computes the ultimate bearing capacity of the soil, which represents the maximum load the soil can withstand without failure. Meyerhof's modification takes into account the shape and depth of the footing, along with the soil's cohesion and angle of internal friction, to produce a more precise estimate of the bearing capacity.

$$q_{ult} = CN_c + qN_q + 0.5\,\gamma\, B_\gamma\, N_\gamma \quad \text{continuous footing} \quad (3.1)$$

$$q_{ult} = 1.3\,CN_c + q\,N_q + 0.4\,\gamma\, B\, N_\gamma \quad \text{square footing} \quad (3.2)$$

$$q_{ult} = 1.3\,CN_c + q\,N_q + 0.6\,\gamma\, B\, N_\gamma \quad \text{round footing} \quad (3.3)$$

$$q_{ult} = CN_c\, S_c\, d_c + q\,N_q\, S_q\, d_q + 0.5\,\gamma\, B\, N_\gamma\, S_\gamma\, d_\gamma \quad (3.4)$$

- qult" refers to the ultimate bearing capacity of the soil, expressed in units of kN/m² or lbs/ft².
- c is the soil cohesion (in kN/m^2 or lbs/ft^2)

- The bearing capacity factors Nc, Nq, and Nγ are influenced by both the soil properties and the footing shape.
- The parameter γ represents the density of the soil, typically measured in units of kN/m^3 or lbs/ft^3.
- B denotes the width of the foundation, usually expressed in units of meters or feet.

$$S_c = 1 + \frac{N_q}{N_c}\frac{B}{L} \quad , \quad S_q = 1 + \frac{B}{L}\tan\phi \, , \quad S_\gamma = 1 - 0.4\frac{B}{L} \tag{3.5}$$

$$d_c = 1 + 0.4\frac{D_f}{B} \, , \quad d_q = 1 + 2\tan\phi(1 - \sin\phi)^2 \frac{D}{B} \tag{3.6}$$

The Terzaghi's equation, modified by Meyerhof, is widely used in geotechnical engineering to evaluate the load-bearing capacity of soils for various types of shallow foundations, such as spread footings and mat foundations. Ensuring the stability and safety of structures constructed on soil is crucial, and one key parameter in the foundation design process. However, it is important to note that other factors, such as settlement, consolidation, and ground water conditions, should also be considered in foundation design in addition to bearing capacity. It is recommended to consult with a qualified geotechnical engineer for accurate and site-specific foundation design. For example, using shear strength parameters for (10 x 10 m).

3.4 Identification of Spatial Data

Geospatial data, or spatial data, refers to data that provides information about the geographic location of a particular entity or feature. The information indicates the location of physical objects or processes in relation to the Earth's surface (OGC, 2021). Spatial objects consist of both theoretical data, such as restrictions and lines of distinction, and real objects, such as structures and roads.

Nowadays, spatial data is considered to be an essential piece of information in modern societies. Various types of geographic data are utilized in making important decisions at the local, regional, national, and international levels. They are used in a variety of applications, including urban governance and land development, company growth, risk mitigation plans, and tragedy recapture development.

Spatial data are found in a variety of engineering disciplines, notably in those that describe geographic characteristics for example rivers, lakes and borders, 3D graphics and virtualization, as well as separated civil infrastructure networks (e.g., pipelines, bridges, and highways). Spatial data are the foundation of current geographic information systems, and they are being progressively incorporated into a wide range of disciplines in engineering, research, and business (Blasby et al., 2003).

3.4.1 GIS Software

A GIS software is a tool utilized for the storage, retrieval, management, display and analysis of various forms of geographic and spatial data. It enables the production of maps and other visualizations of GIS for the purpose of analysis and presentation. Site inspections and laboratory testing are often used to collect geotechnical data for site planning and development. The results of site and laboratory tests provide specific information about the soil's characteristics. In order to develop infrastructure and buildings that are both cost-effective and safe design, information is essential (Arnous, 2013; Khan et al., 2021).

A technology that can rapidly store, analyse, and update data, as well as provide various types of data the same as maps and tables, may help decision-makers and designers work more quickly. Engineers and designers in the land development industry would find these types of technologies very useful. GIS is recognized to be capable of providing these services since it could store data in a multi-layer database. It may also be used to progression information from spatial data. As a result, GIS is operated in a variety of engineering disciplines, such geotechnics, the environment, human resources, building, and transportation. Geographic information systems are used in geotechnical engineering to find borehole locations and thereby assist engineers or planners in conducting new investigations, particularly for new site positions (Oloufa and Ikeda, 1995; Barczewski and Kania, 2004).

In terms of environmental engineering, several locations have been selected for this program since it is hard to recover due to the fact that housing, manufacturing facilities, and roadways cover a large area. Initially, GIS is utilized to identify the site plan as well as the placement of temporary amenities. With the use of a global positioning system (GPS), decision-making for site planning and the placement of temporary facilities becomes more efficient. GIS has become popular in transport

engineering. As an illustration, GIS is used in traffic development to display origin / destination densities, Noise problems, trip creation, and inter-destination routes as well as transit accessibility are all factors to be considered (Bolstad, 2016).

This research focuses at how geographic information systems could be stored, analysed, and presented in a way that planners, architects, and engineers can utilize to make better choices and create safer and more cost-effective solutions. GISs are characterized as "a fundamental and generally usable collection of rate-added technologies for the capture of information, conversion, management, its analysis and presentation, particularly in spatial data. Furthermore, GIS's use of technology to analyze and explain data allows for data visualization. (Yu et al., 2005). In comparison to analytical and statistical products or reports, visualizing data helps researchers to get a better understanding. As a result, three essential GIS applications are explored in this study: data integrity, data visualization, and existing data.

Many techniques for spatial interpolation have been created in many areas, with a variety of terminology to identify them, same interpolating and non-interpolating approaches (Laslett et al., 1987). Spatial interpolation methods are linear spatial interpolation procedures invers distance weighting (IDW), spline and kriging. These approaches were all commonly used in interpolation investigations, and most associated software packages offer their implementation. The techniques of spatial interpolation, which are frequently consumed in soil investigation and environmental research, could be divided into three groups:

- combined methods,
- non-geostatistical methods, and
- geostatistical methods

Approaches that handle secondary information are sometimes termed to as multivariate in egotistic, even though approaches that do not employ secondary data are referred to as "single variable" methods. Observe that the term (multivariate) Guides to more than one response variable, even though it is often applied to more than one explanatory variable, are directed to as "many variables" in specific sources.

The study involved the generation of a digital database for the study area by utilizing data obtained from soil investigations, field surveys, and laboratory tests. The

geotechnical properties collected were used as input values for mapping software. For the analysis and presentation of data, ArcGIS (version 10.7) software was employed. Deterministic methods, specifically inverse distance weighting, were utilized to create spatial data models and maps. These methods rely on predetermined algorithms and rules to develop models and maps, as opposed to geostatistical techniques commonly used for analyzing and modeling spatial data (Wan-Mohamad and Abdul-Ghani, 2011). Deterministic methods are often employed to examine patterns, relationships, and trends within extensive and complex datasets. Some of the commonly used geostatistical methods in ArcGIS include.

Some of the most commonly used deterministic methods in ArcGIS include:

- Interpolation in ArcGIS predicts values at unsampled locations using observed data, employing methods like inverse distance weighting, spline, and triangulated irregular network (TIN).
- Buffering is a technique used to generate a polygon surrounding a specific feature, representing a defined distance. Buffers are commonly employed in spatial analysis to identify areas within a specified distance from a particular feature of interest.
- Overlay is a technique that involves merging multiple maps based on specific conditions or rules. By utilizing this method, a new map can be generated, depicting the spatial relationships and associations between features found in the source maps. It enables the visualization and analysis of how different features interact and overlap in the geographical space.
- Reclassification is a method utilized to modify the values of a raster or vector layer by applying a predefined set of rules or conditions. This technique is commonly employed to simplify complex data or to generate new data layers derived from existing data. By reclassifying the values, the data can be organized, standardized, or transformed to facilitate analysis or create meaningful representations.
- The extraction method is utilized to isolate features from a map by applying specific conditions or rules. This approach enables the creation of new data layers that exclusively contain features that meet particular criteria or conditions. It allows for a focused analysis of specific features that fulfill the

desired requirements, facilitating a more targeted exploration of the data. (Wan-Mohamad and Abdul-Ghani, 2011).

The generated digital maps provide valuable visual representations of the soil formation patterns, distribution, and geotechnical properties at various depths. These maps offer simplified information to aid designers and site engineers in making informed decisions during construction projects. The main objective of creating digital maps using GIS techniques was to assess the bearing capacity of foundations at different depths. This study employed two methods for estimating the bearing capacity. The first method utilized shear strength parameters within a 10 x 10-meter grid using the Meyerhof method (1963). The second method involved estimating the bearing capacity using standard penetration numbers. (Das, 2018).

3.4.2 Data Integration

There is a huge range of data in papers, books, images, etc., and during merging them together, they will provide better results. At the moment that combining data from different sources, data retrieval intention takes less time and data going to be more systematic and organized. Figure 3.5 describes the quality of data that was developed in this study using the ArcGIS, which one of GIS software. As a representative data for soil characteristics and standard penetration test at various depths between 1.5-3.5m, 3.5-6.5m, 6.5-9.5m.

Table

BH 1.5-3.5 m

FID	Shape *	F1	BH_NO	X	Y	DEPTH_M	LL_	PL_	PI_	WC	DD	Gs	UC	C	
0	Point ZM	0		0	0		0	0	0	0	0	0	0	0	
1	Point ZM	1	4-2348	406851.5	4009570	1.5-3.5	45	21	24	28.2	13.7	2.72	33	50	4
2	Point ZM	2	4-a	405972.9	4009284.2	1.5-3.5	46	22	24	28.3	0	0	47	51	3
3	Point ZM	3	7-1883	407487.6	4007947.1	1.5-3.5	49	26	23	17.1	16.8	2.69	0	11	5
4	Point ZM	4	7-a	406121.1	4008204.7	1.5-3.5	40	22	18	15	0	0	0	96	3
5	Point ZM	5	8-2084	407443.2	4008702.7	1.5-3.5	50	27	23	20.8	16.4	2.71	0	10	4
6	Point ZM	6	8-a	407941.4	4009347.7	1.5-3.5	50	28	22	13.9	0	0	0	10	4
7	Point ZM	7	9-2027	408217.9	4008512.23	1.5-3.5	35	20	19	20	0	0	0	96	3
8	Point ZM	8	10-1842	408997.4	4008917.8	1.5-3.5	39	21	18	16.3	16.9	2.7	0	10	4
9	Point ZM	9	11-2039	408743.4	4009398.1	1.5-3.5	47	25	22	18	17.2	2.71	0	99	4
10	Point ZM	10	11-a	408026.1	4010406	1.5-3.5	45	24	21	16.6	0	0	0	96	4
11	Point ZM	11	12-2150	409617.8	4011321.6	1.5-3.5	46	27	19	20.2	16.3	2.68	0	99	4
12	Point ZM	12	12-a	408588.1	4011780.2	1.5-3.5	45	25	20	19	0	0	0	97	4
13	Point ZM	13	12-b	409762.1	4012805.4	1.5-3.5	48	26	22	19.7	0	0	0	94	5
14	Point ZM	14	13-2205	411184.2	4011787.2	1.5-3.5	49	23	26	19.6	15.3	2.7	0	10	4
15	Point ZM	15	13-a	411184.3	4012540.7	1.5-3.5	47	25	22	15.6	0	0	0	10	4
16	Point ZM	16	14-2278	411247.7	4013522.9	1.5-3.5	48	26	22	18.4	15.8	2.69	0	58	3
17	Point ZM	17	16-2234	409969.9	4010643.8	1.5-3.5	58	31	27	20.5	15.6	2.72	0	91	3
18	Point ZM	18	16-a	409662.9	4009977	1.5-3.5	56	30	26	18.8	0	0	0	94	4
19	Point ZM	19	17-2342	409915.1	4009232.2	1.5-3.5	45	24	21	13.6	17.1	2.7	0	77	3
20	Point ZM	20	18-2183	410862.1	4009607.35	1.5-3.5	44	25	19	18.3	16.3	2.7	0	69	4
21	Point ZM	21	18-a	411994.6	4009216.9	1.5-3.5	42	23	19	19.2	0	0	0	70	4
22	Point ZM	22	19-1983	411166.1	4010438.9	1.5-3.5	50	26	24	17.9	16.8	0	0	95	4

Figure 3.5 Attribute data for soil types

3.4.3 Data Visualization

Integrated geotechnical data can be readily understood by users as it is presented on a map. Generally, the site form would be built from the integrated data and the model displayed in the map-view and then used to visualize and evaluate the site model. Different layers are responsible for the execution and application of the model. Consequently, the built-in data layers could be turned on and off as needed. Furthermore, symbols may be used to represent data in order to perform relationships with features etc. From Figure 3.6, at 9.5 m depth, SPT dominates the majority of the boreholes. The soil characteristics represented in all the maps were categorized into six main legends, with each legend assigned a distinct color representation.

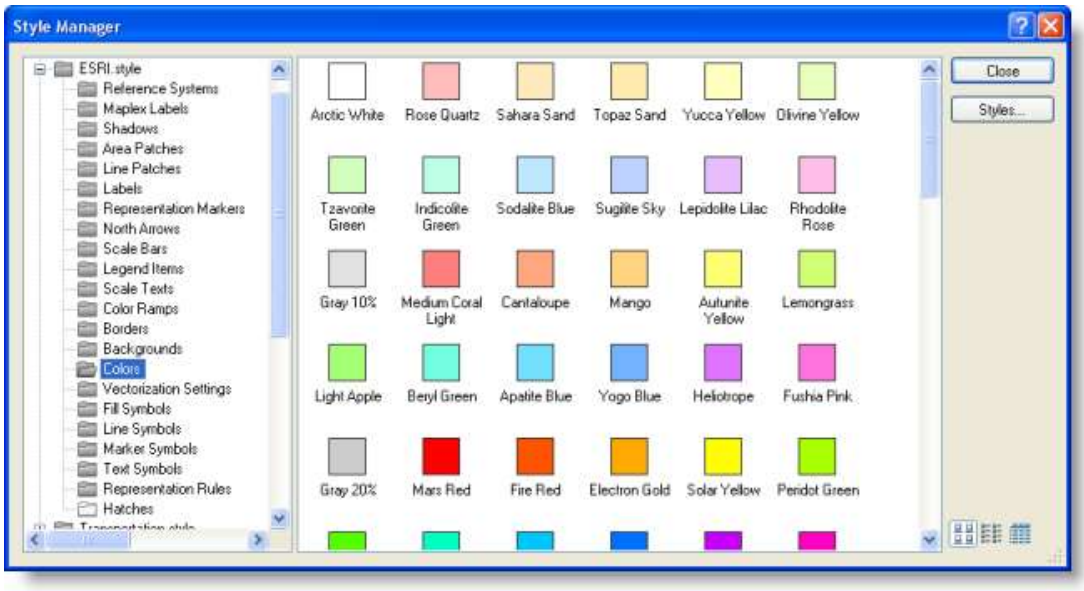


Figure 3.6 Symbols and styles of ArcGIS software

3.4.4 Data Presentation

Once data is stored in GIS format, the final step is to display it. Typically, the information represented in the layout and might be prepared for use in reports, papers, posters, and other types of publications. Information same to scales, labels, icons, northern text and, arrows may all be used to create more relevant maps and data. Customer and consultant both expressed satisfaction with the completed data presentation, which included useful information and well-printed maps.

Following the creation of the database and mapping, the next stage was to provide the information to the client or consultant. Since many layouts, sizes and designs could be created from in this program, data throw out to display in posters, reports etc., Figure 3.7 display an example of mapping.

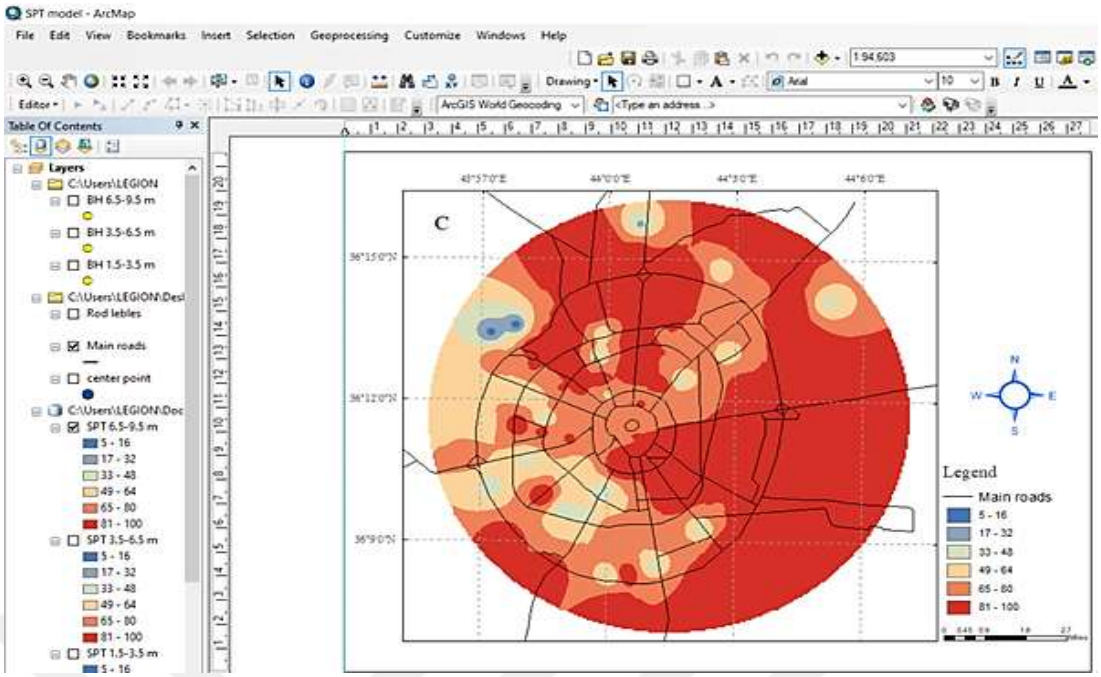


Figure 3.7 Mapping of selecting lawyers represented an example of SPT-N value

3.5 Statistical Analysis

Creating a highly correlated statistical model is a critical step in geotechnical engineering to predict the properties of the soil accurately. The process involves analysing the data in accordance with statistical methodology and making a correlation between various geotechnical properties. The data collected from soil investigations conducted in the study area were analyzed using MINITAB 17 software. This analysis aimed to identify the key factors that have a significant influence on the geotechnical properties of the soil (Lesik, 2018).

MINITAB 17 is a software package widely used in statistical analysis. It is used to perform various statistical, numerical, and graphical calculations, making it a valuable tool in geotechnical engineering. Regression analysis was performed to establish correlations between the SPT values of soil strata, shear strength parameters of soils, and the ultimate bearing capacity. This widely employed approach in analyzing multifactor data helps identify the relationship between the response variable (Y) and predictor variable (X), facilitating the understanding of how different factors influence the variables of interest. By using this approach, geotechnical engineers can identify the key factors that affect the properties of the soil and develop a highly correlated statistical model to predict these properties accurately. The resulting model can be used to optimize site improvements and reduce costs associated with construction.

Therefore, this approach is essential in geotechnical engineering and is widely used in various industries that involve soil analysis, including construction, mining, and environmental engineering.

3.6 Artificial Neural Networks

ANNs inspired by the structure and functioning of the human brain, making them a type of computational model. ANNs are used in machine learning and artificial intelligence to process and analyze complex data, recognize patterns, and make decisions. Neural networks are comprised of layers of interconnected nodes or neurons, where the connections between the neurons are assigned weights based on the learning process. Tasks like image and speech recognition, natural language processing, recommendation systems, and a variety of other applications often utilize ANNs for their implementation. They can be trained on large datasets to learn from examples and improve their performance over time, making them capable of handling a wide range of tasks and solving complex problems. ANNs have been widely employed for various applications in numerous fields, including computer vision, speech recognition, finance, healthcare, and many others. They are also increasingly used in geotechnical engineering and soil mechanics to model and predict the behaviour of soil.

3.6.1 Definition of Artificial Neural Networks (ANN)

ANNs is a cultured network comprised of numerous basic neurons that work in combination with each other (Lippmann, 1987). The original cell model provided by McCulloch and Pitts in 1942 served as the foundation for the ANNs. The ability to solve nonlinear problems, as well as distributed parallel structure, learning, error tolerance, and generalization are all significant traits of importance ANNs. These characteristics are used in a variety of situations; learning and generalization are two fundamental characteristics of ANNs. By analysing the relationship between the inputs and outputs that are presented to it, the network is capable of producing satisfactory results even with unfamiliar data (Garip, 2011).

The construction of ANN is based on how a live nervous system works. As realised in Figure 3.8 and 3.9, nerve cells in the living nervous system receive signals and transmit signals in response to the signals they receive. The signals that have been received are transferred to the center of the cell-body. Whenever the gathered signals reach a

certain level, the signal is conveyed to the other nerve cells through the axons of the nerve cells (Yegnanarayana, 2009).

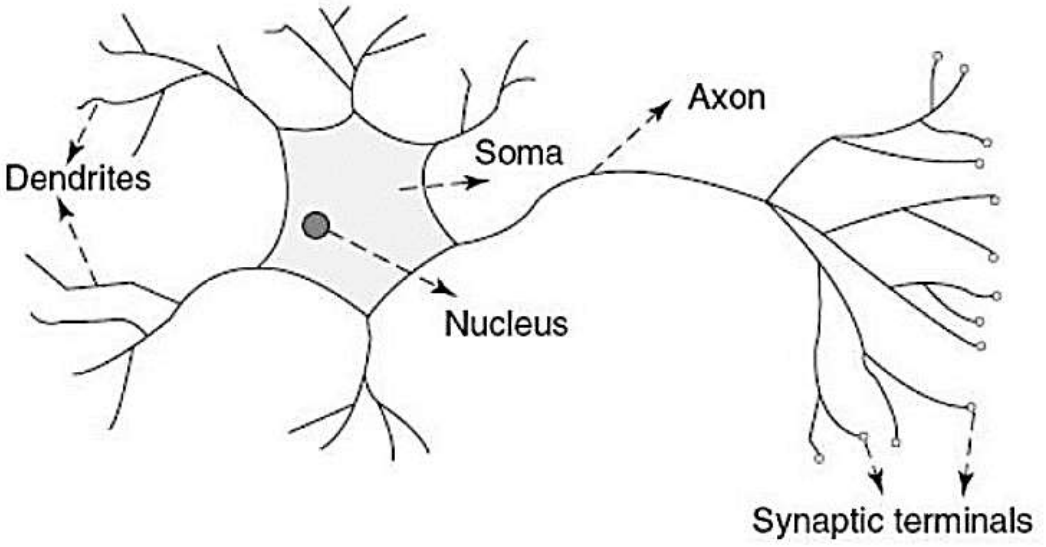


Figure 3.8 A simplified model of a biological neuron (Özbay, 2007).

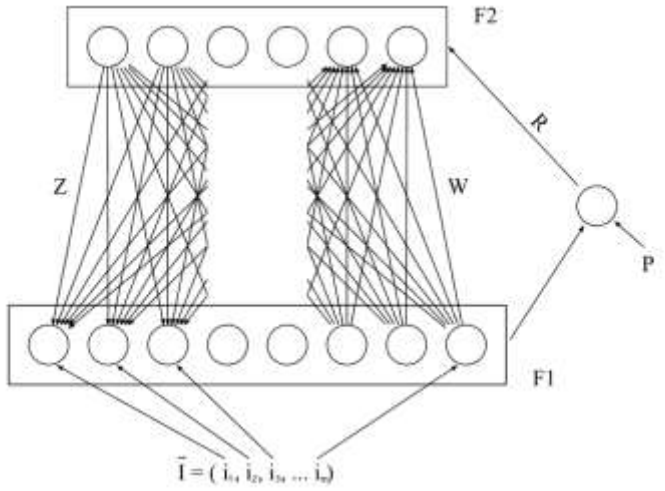


Figure 3.9 Adaptive resonance theory (ART) network structure (Miljkovic, 2010)

The neural network is a computerized model used for software-based modelling. It is an information processing technique that is designed based on neurons, which consist of three key parameters: weights, bias, and an activation function (Hecht-Nielsen, 1989).

- R^2 Training
- R^2 Testing
- MSE= Mean squared error

To assess performance, the Mean Squared Error computes the mean of the squared discrepancies between the predicted outputs and the actual targets. A smaller value indicates superior performance, while zero signifies no errors. During training, the network received supervised instruction, as input/target training patterns were presented to it along with their corresponding measured outputs. This enabled the network to learn through explicit instruction. The backpropagation method was utilized for training, which involved minimizing the difference between the predicted and desired outputs. A Levenberg Marquardt (LM) learning algorithm was used, along with a tangent sigmoid transfer function described by equation 3.7. The weighted sum of input components was calculated as shown in the equation:

$$F_j = \sum_{i=1}^{n} w_{ij} * x_i + b \qquad (3.7)$$

In the proposed NN models, the weight coefficient between the i^{th} and j^{th} neurons is represented by w_{ij}. The parameter n is the total number of input neurons that contribute to a cell, while b is the bias that models the threshold. Various activation functions have been proposed for processing the net input obtained from a sum function, which then determines the cell output. In this thesis, the proposed ANN models develop the tangent-sigmoid transfer function.

The ability of an artificial neuron to learn is accomplished by modifying the weights in accordance with the selected learning algorithm (Abraham, 2001). The proportion in which data is divided for training and testing depends on the specific task and dataset at hand, and there is no fixed rule such as a requirement for 70% of data to be used for training. For instance, with a simple dataset like Reuters, training on 50% of the data and testing on the remaining 50% will yield different precision compared to training on 90%. Generally, in Machine Learning, larger datasets are preferred for training. For more information on precision values based on dataset size, refer to (Divya).

ANNs are constructed by combining numerous artificial nerve cells in a layered, rather than random, manner (Yegnanarayana, 2009). There are three distinct learning techniques that have been utilized in ANNs:

- Supervised Learning: The approach of this machine learning technique involves using considered training data to generate a function that can map input data to corresponding output data. This essentially means that the algorithm learns from the labelled data to develop a function that can appropriately link inputs to outputs. (Hinton et al., 1999).
- Unsupervised Learning: This machine learning approach is based on observations of a situation and aims to learn solely from input data without the aid of output data. This technique is particularly useful in data clustering and dimensionality reduction (Hinton et al., 1999).
- Reinforcement Learning: This type of machine learning shows how an autonomous agent observes its surroundings and learns to take actions that maximize a reward signal. The goal is to make the best decisions to achieve the desired objective (Sutton and Barto, 2018).

3.6.2 Main Components of ANN

The artificial neuron, which is also referred to as the processing unit, is the basic building block of ANN. A processing unit consists of five essential components: inputs, weights, a summing function, a transfer function, and an output. Table 3.3 shows the parallels among the organic nervous arrangement and the ANN (Sagiroglu et al., 2003).

Table 3.3 The biological nervous system shares similar features with ANNs as reported by Sagiroglu et al. (2003).

Biological Nervous System	Artificial Neural Network
Dendrite	Summing Function
Cell Body	Artificial Neuron (Processing Element)
Axons	Transfer Function
Neurons	Artificial Neuron Output
Synapses	Weights

3.6.3 Neural Network Types

There are numerous different varieties of ANNs, including the following:

- Adaptive Resonance Theory (ART) Network
- Back propagation networks- has been make use of in the modelling of this study.
- Kohonen Network
- Recurrent Neural Networks (RNN)
- Hopfield Network
- Radial Basis Function Network (RBFN)

The research employed nftool, a soft computing tool in MATLAB V. R2016b, for constructing neural network models. Neural networks are widely employed in fitting problems to create a connection between a data set of numerical inputs and a data set of numerical targets. The nftool assists in the creation and training of networks, as well as the evaluation of their presentation using mean square error and regression analysis.

The MATLAB program starts with the simplest NN design, one hidden node for the hidden layer, and ends up with the best NN architecture. Figures 3.10 to 3.15 depicts a flowchart of the whole operation. This algorithm has been successfully applied to a wide range of neural network implementation. There has been significant success in applying this technique to a broad variety of neural network applications.

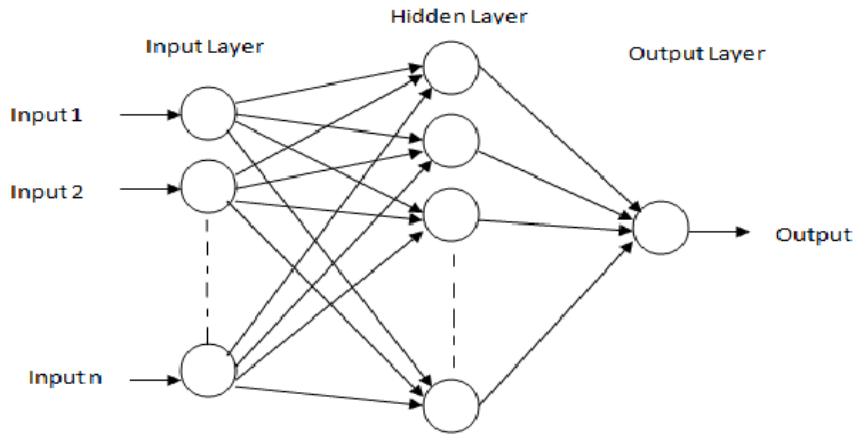


Figure 3.10 General architecture of a Backpropagation Neural Network (Tarsauliya et al., 2011)

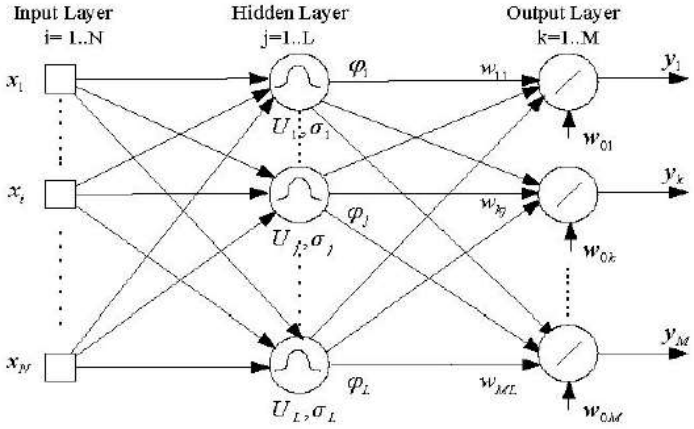


Figure 3.11 RBF network structure (Kaynar et al., 2016)

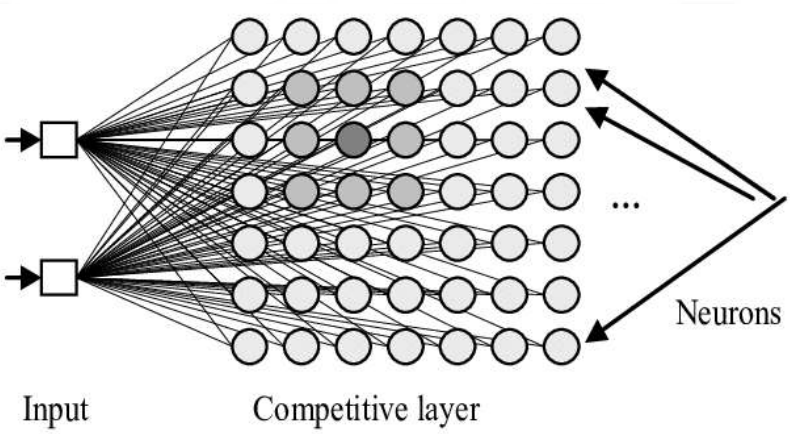


Figure 3.12 Kohonen network architecture (Amine et al., 2008)

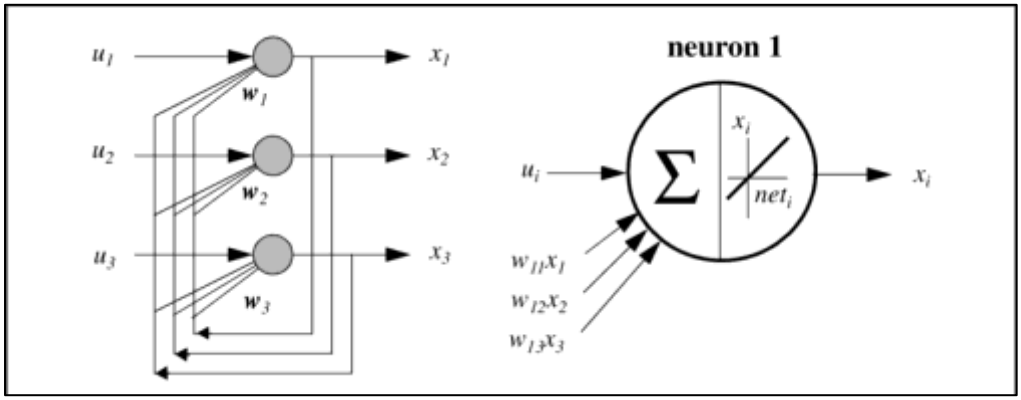


Figure 3.13 Topology of Hopfield networks, here with 3 neurons as an example. Linear transfer functions of its neurons characterize the linear Hopfield network (Lendaris et al., 1999).

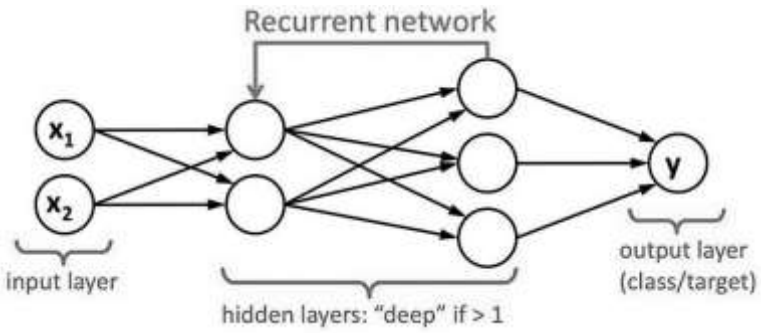


Figure 3.14 Recurrent neural network (RNN) (Mishra et al., 2018).

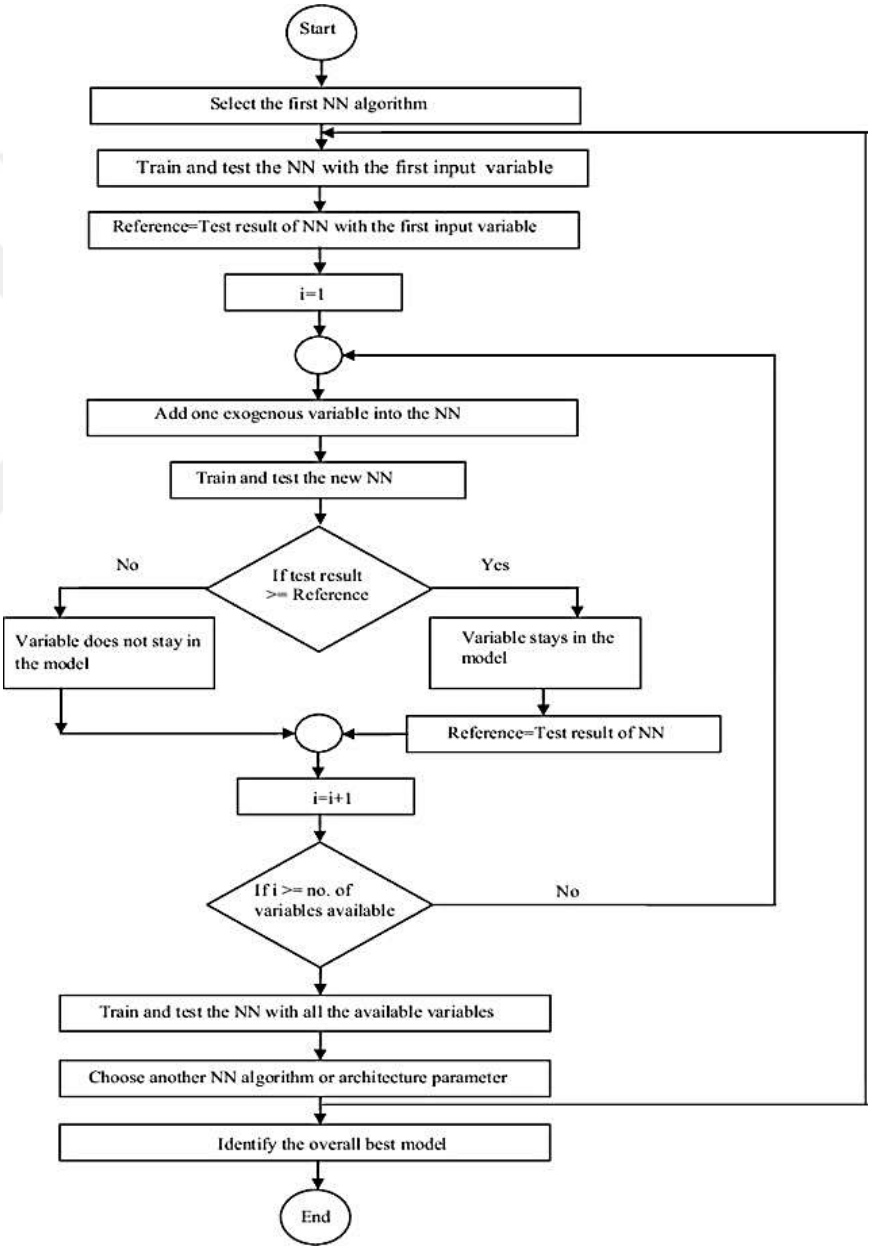


Figure 3.15 Forward strategy for selecting NN architecture and model (Zekić et al., 2005)

3.6.4 Description of the Proposed Models

The MATLAB application was employed to create an ANN in this study. The primary objective was to develop models using the ANN based on data collected on geotechnical properties of soils in the study area. The ANN analysis aimed to predict the SPT N-value and bearing capacity using the Back-propagation algorithm and the same activation function. The network architecture was determined by varying the number of neurons in the hidden layer, with previous research suggesting that the optimal range is between 15 and 18 hidden layers. (Fernando et al., 2019). R^2, known as R-squared or coefficient of determination, is a common performance metric used in artificial neural networks and other regression models the model's ability to explain the variance in the target variable is determined by the R^2 value, which ranges from 0 to 1. A higher R^2 value indicates superior performance. In the evaluation of ANN models, the Root Mean Square Error (RMSE) is a widely used metric that quantifies the discrepancy between predicted and actual values. The RMSE value shares the same unit of measurement as the target variable. A lower RMSE value indicates that the predictions closely align with the actual values, while a higher RMSE value signifies a greater disparity between the predictions and the actual values. In ANN models, RMSE is employed to assess the model's performance and ascertain the accuracy of its predictions. A lower RMSE value indicates a better fit between the predictions and the actual values, suggesting a more precise and reliable model. Additionally, the Mean Absolute Error (MAE) is another commonly used performance metric in ANN models and other machine learning techniques. The mean absolute difference between predicted and actual values in a dataset is determined using a metric known as MAE. In this study, the performance of regression models is evaluated by computing R^2, RMSE, and MAE values for both estimated and actual target parameters. These metrics are expressed mathematically as equations (3.8), (3.9), and (3.10):

$$R^2 = 1 - \frac{\sum_{I=1}^{N}(y_{mea} - y_{pre})^2}{\sum_{I=1}^{N}(y_{mea} - y_m)^2} \tag{3.8}$$

$$RMSE = \sqrt{\frac{\sum_{I=1}^{N}(y_{mea} - y_{pre})^2}{N}} \tag{3.9}$$

$$MAE = \frac{1}{N}\sum_{I=1}^{N}|y_mea - y_pre| \quad (3.10)$$

The variables ymea, ypre, and ym represent the average of existing output, predicted output, and actual output, respectively. N represents the total number of data points. A perfect fit is achieved when R^2 immediately reaches 100%. The model's predictive ability is evaluated using RMSE and MAE. Smaller values for RMSE and MAE indicate a more precise prediction model with higher accuracy.

Figure 3.16 illustrates the neural network models for predicting the SPT N value. Model (a) employs input parameters including liquid limit (LL%), plastic limit (PL%), plasticity index (PI%), water content (WC), cohesion, angle of internal friction (ϕ), and fine content. Model (b) uses the same inputs as model (a) but excludes cohesion. Figure 3.24 presents the neural network models for predicting the ultimate bearing capacity. Model (c) utilizes input parameters of liquid limit (LL%), plastic limit (PL%), plasticity index (PI%), water content (WC), cohesion, angle of internal friction (ϕ), and fine content. Model (d) shares the same inputs as model (c), excluding cohesion.

Table 3.4 categorizes the chosen suggested NN models of the research into three groups, with each group consisting of eight models. The groups' (SPT N-value and Q ultimate) were predicted using numerous inputs such as (LL %, PL %, PI %, WC, c, Fine content). On the other hand, the differences between models were explored in order to get a better outcome in terms of outputs and their consequences.

For all groups, the topologies of suggested models comprise of three layers (input layer, hidden layer, and output layer) as shown in Figures 3.16 to 3.39.

Table 3.4 Description of the ANN models

No	Model No.		Input	Output
1	GROUP A	Mod A	LL%, PL%, PI%, WC, c, ϕ, Fine cont.	SPT-N
2		Mod A1	LL%, PL%, PI%, WC, c, ϕ	
3		Mod A2	LL%, PL%, PI%, WC, ϕ, Fine cont	
4		Mod A3	LL%, PL%, PI%, WC, c, Fine cont	
5		Mod A4	LL%, PL%, PI%, c, ϕ, Fine cont	
6		Mod A5	LL%, PL%, WC, c, ϕ, Fine cont	
7		Mod A6	LL%, PI%, WC, c, ϕ, Fine cont	
8		Mod A7	PL%, PI%, WC, c, ϕ, Fine cont	
9	GROUP B	Mod B	LL%, PL%, PI%, WC, c, ϕ, Fine cont.	Q ultimate
10		Mod B1	LL%, PL%, PI%, WC, c, ϕ	
11		Mod B2	LL%, PL%, PI%, WC, ϕ, Fine cont	
12		Mod B3	LL%, PL%, PI%, WC, c, Fine cont	
13		Mod B4	LL%, PL%, PI%, c, ϕ, Fine cont	
14		Mod B5	LL%, PL%, WC, c, ϕ, Fine cont	
15		Mod B6	LL%, PI%, WC, c, ϕ, Fine cont	
16		Mod B7	PL%, PI%, WC, c, ϕ, Fine cont	
17	GROUP C	Mod C	LL%, PL%, PI%, WC, c, ϕ, Fine cont., SPT	Q ultimate II
18		Mod C1	LL%, PL%, PI%, WC, c, ϕ, SPT	
19		Mod C2	LL%, PL%, PI%, WC, ϕ, Fine cont, SPT	
20		Mod C3	LL%, PL%, PI%, WC, c, Fine cont, SPT	
21		Mod C4	LL%, PL%, PI%, c, ϕ, Fine cont, SPT	
22		Mod C5	LL%, PL%, WC, c, ϕ, Fine cont, SPT	
23		Mod C6	LL%, PI%, WC, c, ϕ, Fine cont, SPT	
24		Mod C7	SPT	

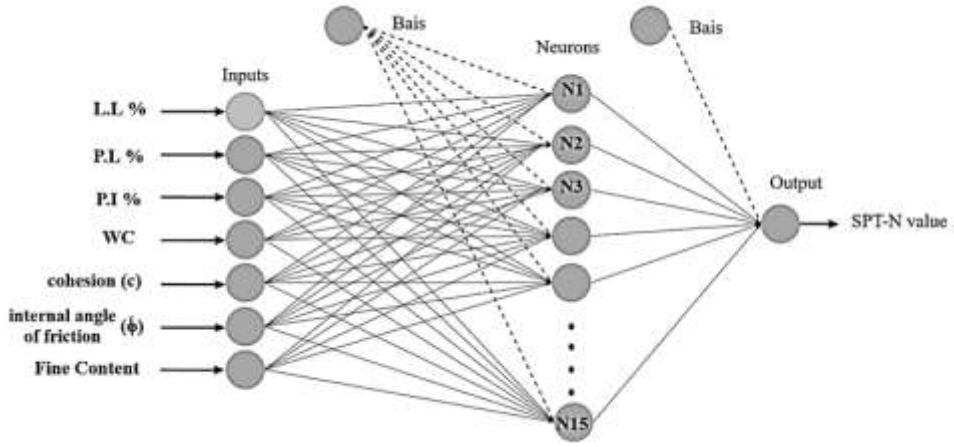


Figure 3.16 Structure of neural network model A-Group A

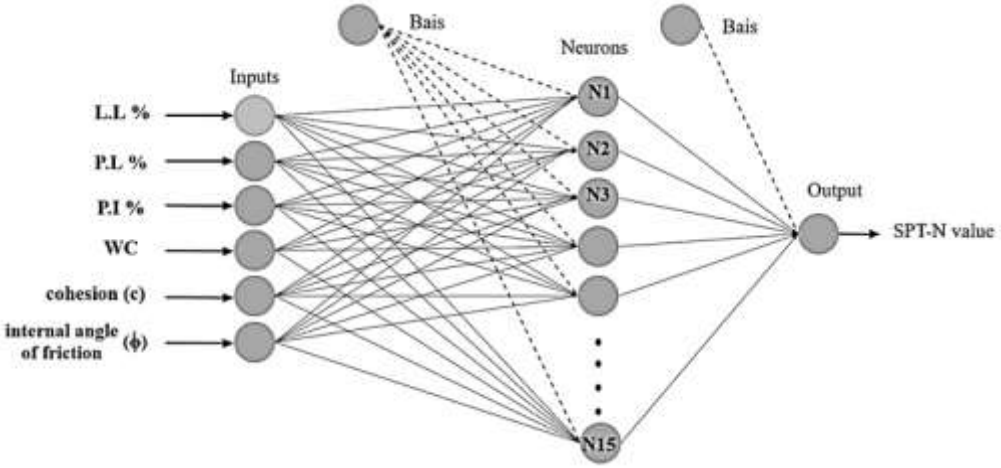


Figure 3.17 Structure of neural network model A1-Group A

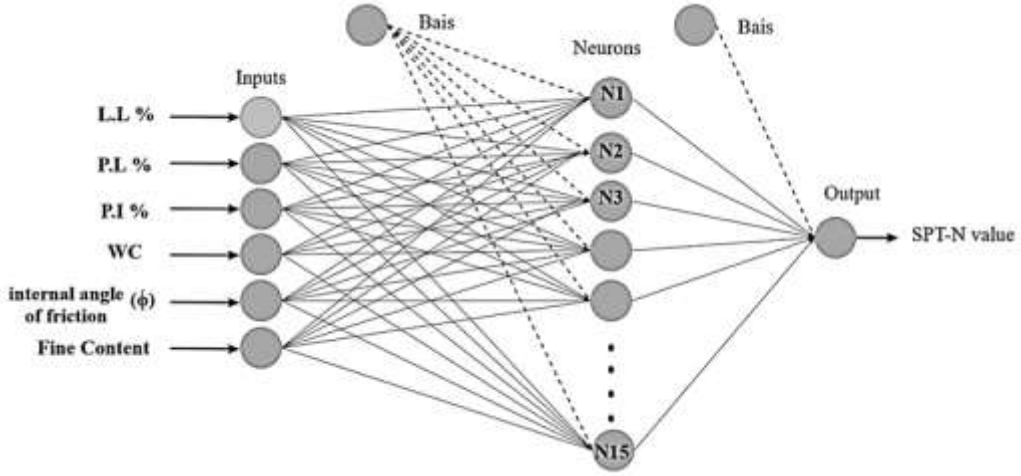


Figure 3.18 Structure of neural network model A2-Group A

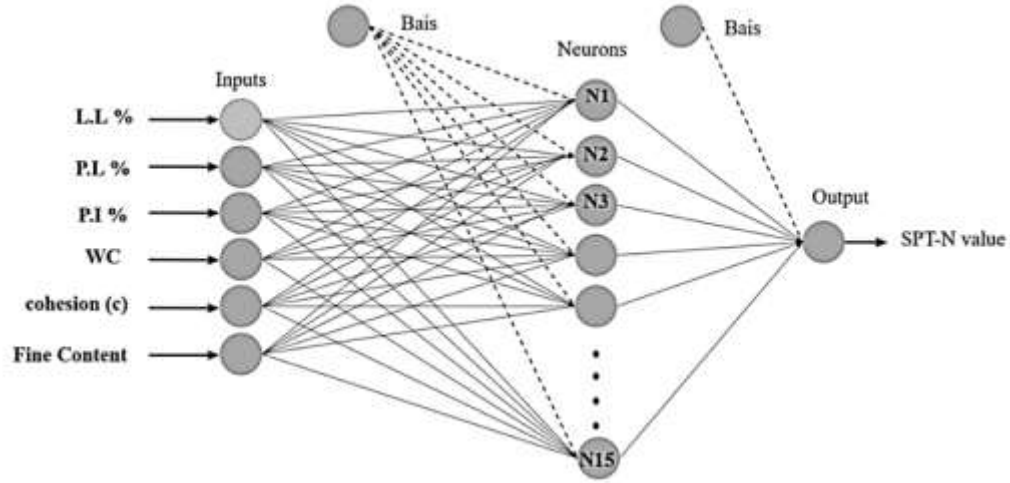


Figure 3.19 Structure of neural network model A3-Group A

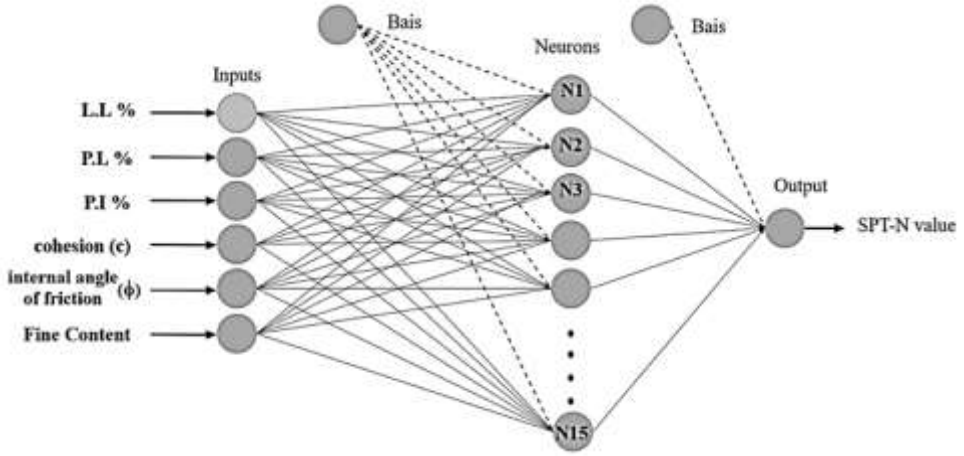


Figure 3.20 Structure of neural network model A4-Group A

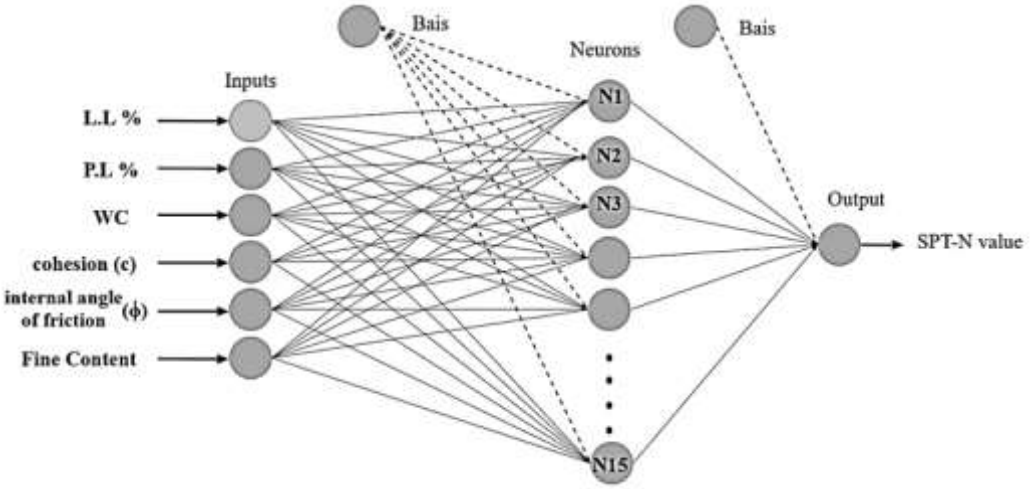


Figure 3.21 Structure of neural network model A5-Group A

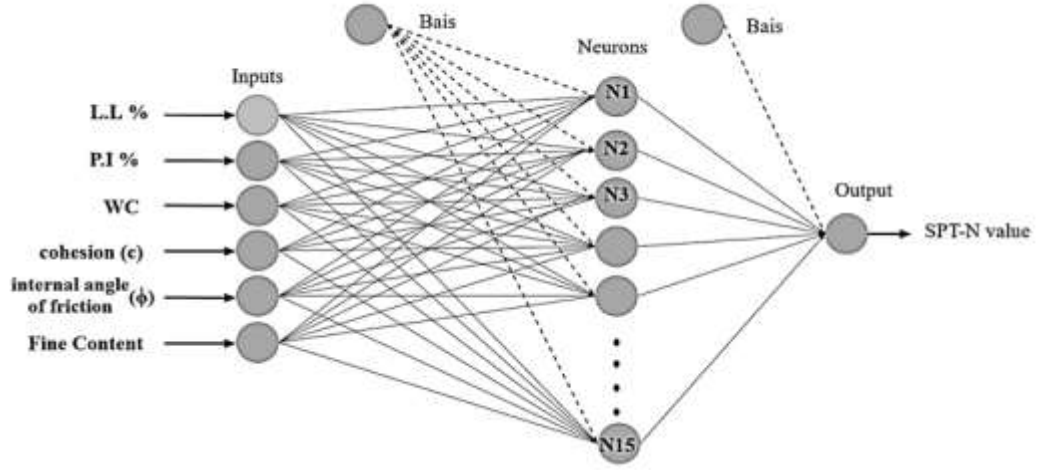


Figure 3.22 Structure of neural network model A6-Group A

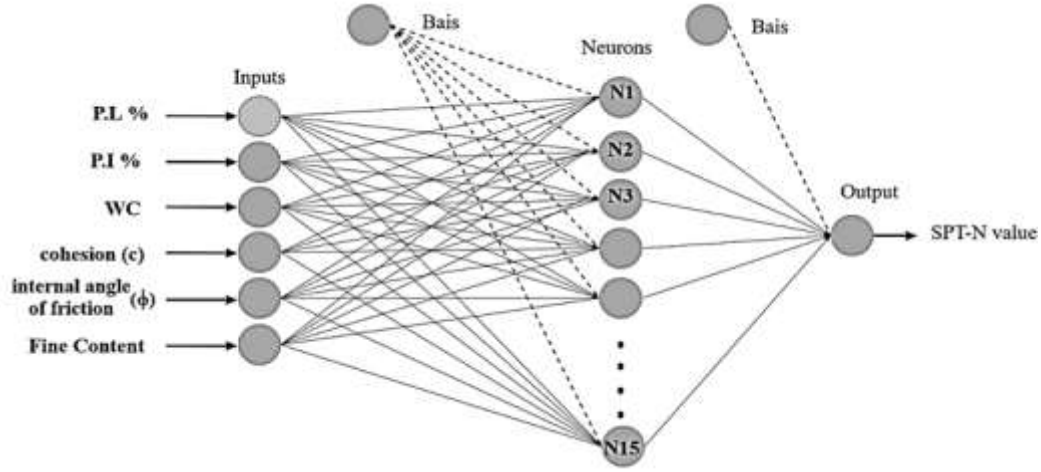


Figure 3.23 Structure of neural network model A7-Group A

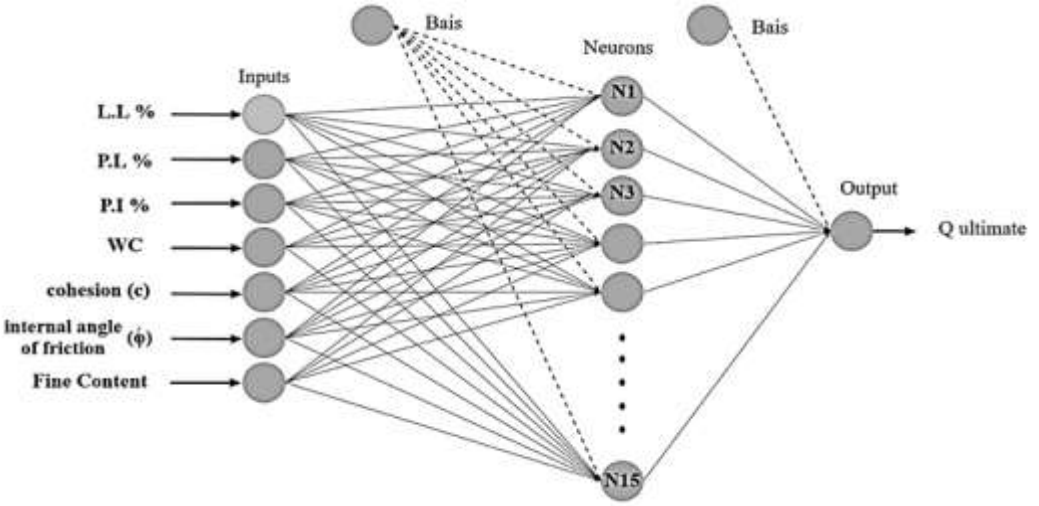


Figure 3.24 Structure of neural network model B-Group B

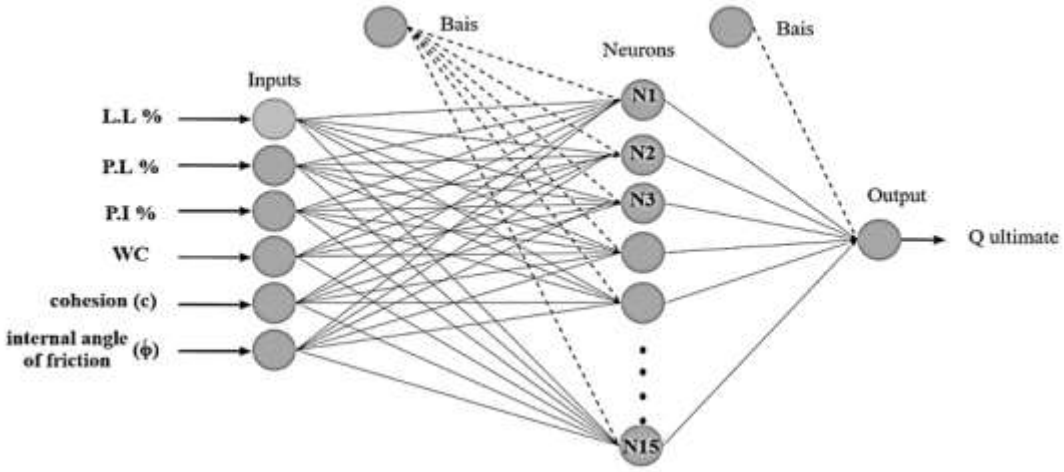


Figure 3.25 Structure of neural network model B1-Group B

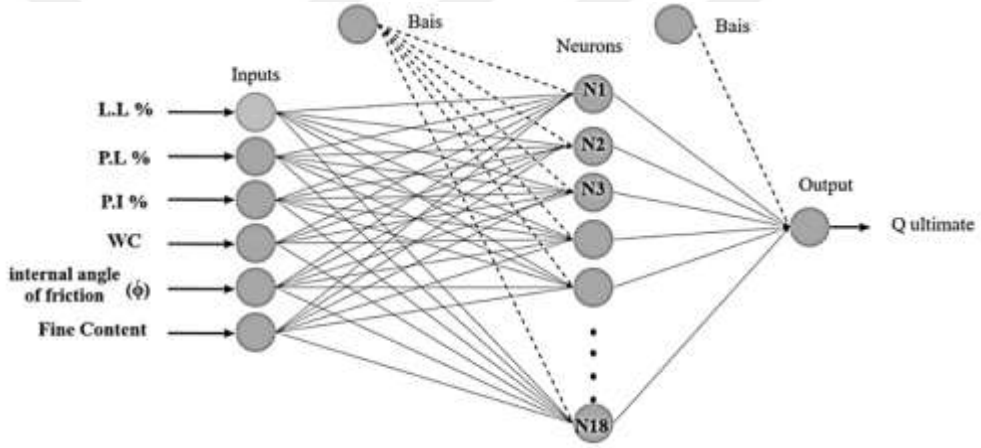


Figure 3.26 Structure of neural network model B2-Group B

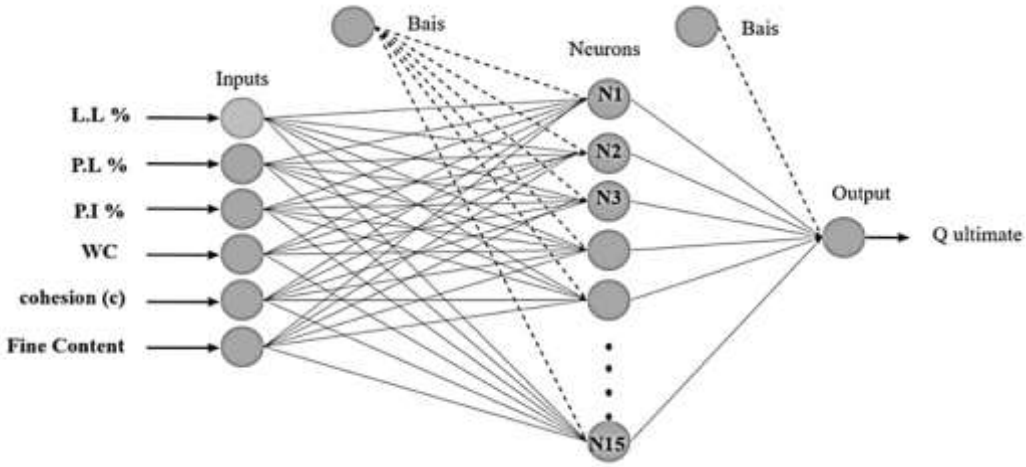


Figure 3.27 Structure of neural network model B3-Group B

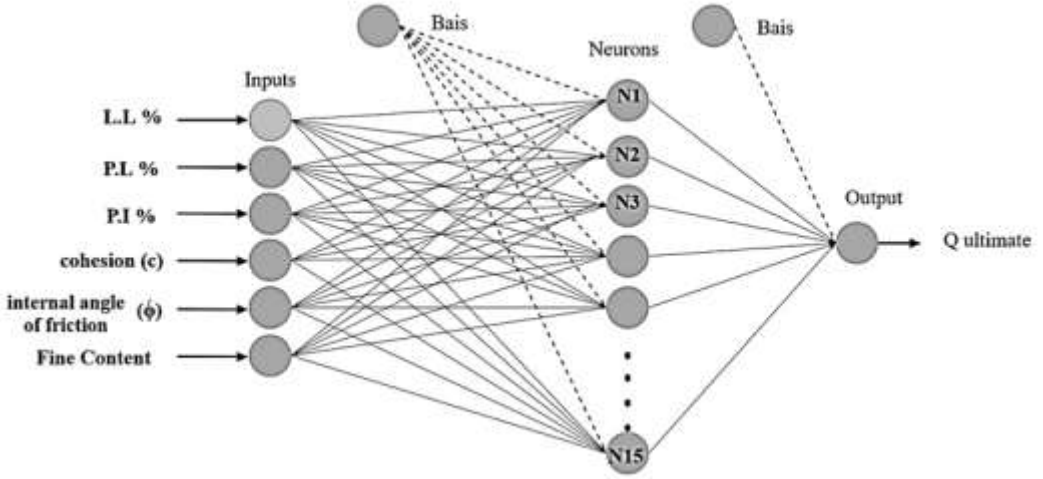


Figure 3.28 Structure of neural network model B4-Group B

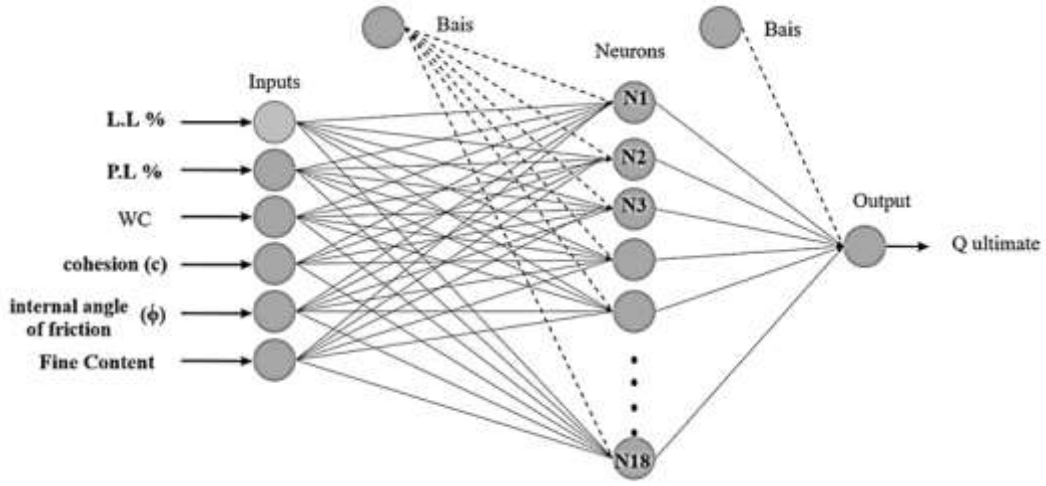


Figure 3.29 Structure of neural network model B5-Group B

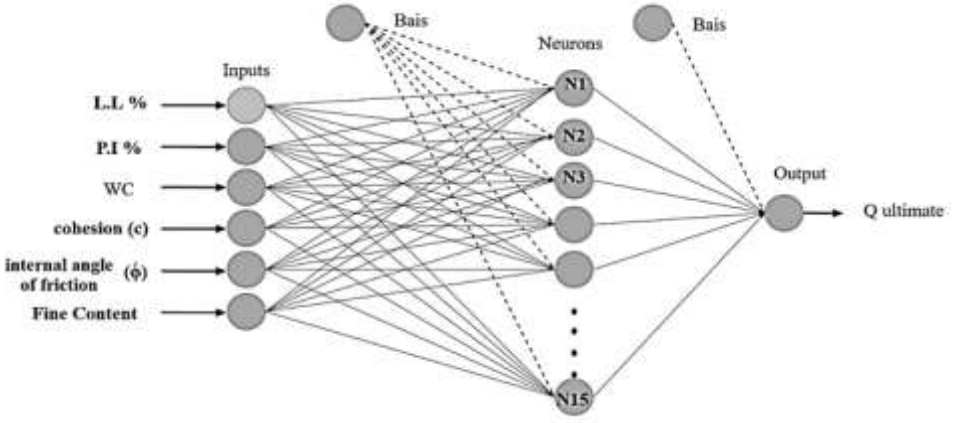


Figure 3.30 Structure of neural network model B6-Group B

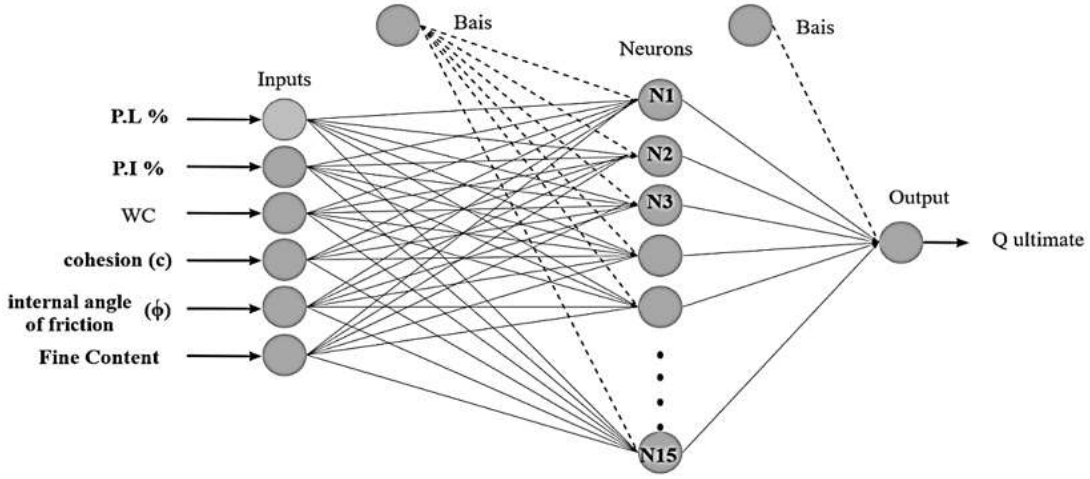


Figure 3.31 Structure of neural network model B7-Group B

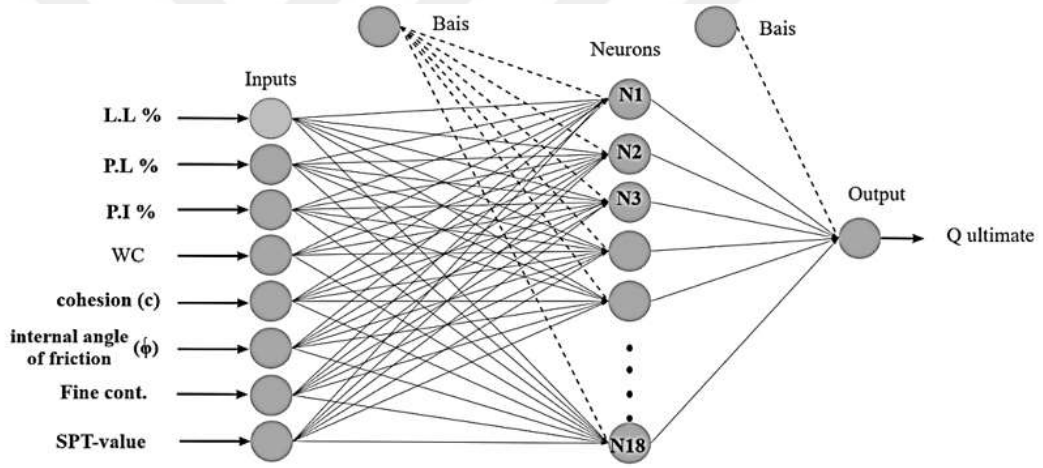


Figure 3.32 Structure of neural network model C-Group C

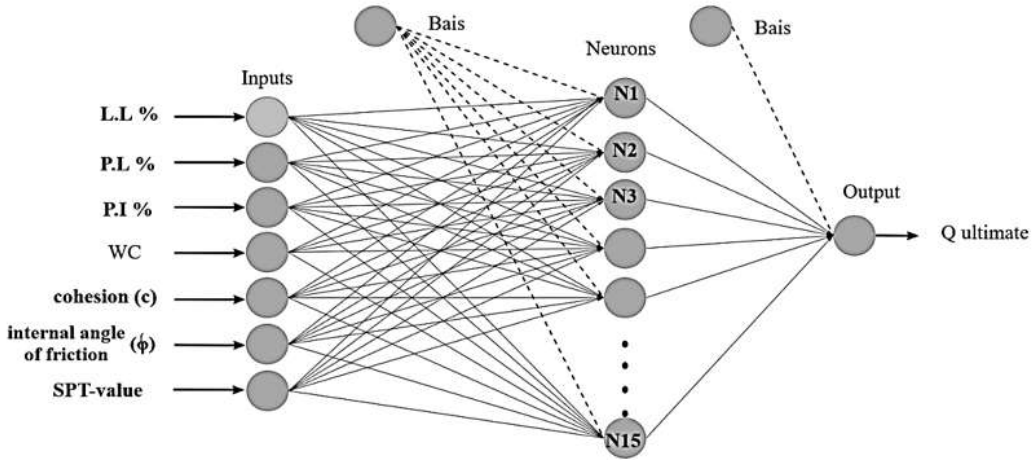


Figure 3.33 Structure of neural network model C1-Group C

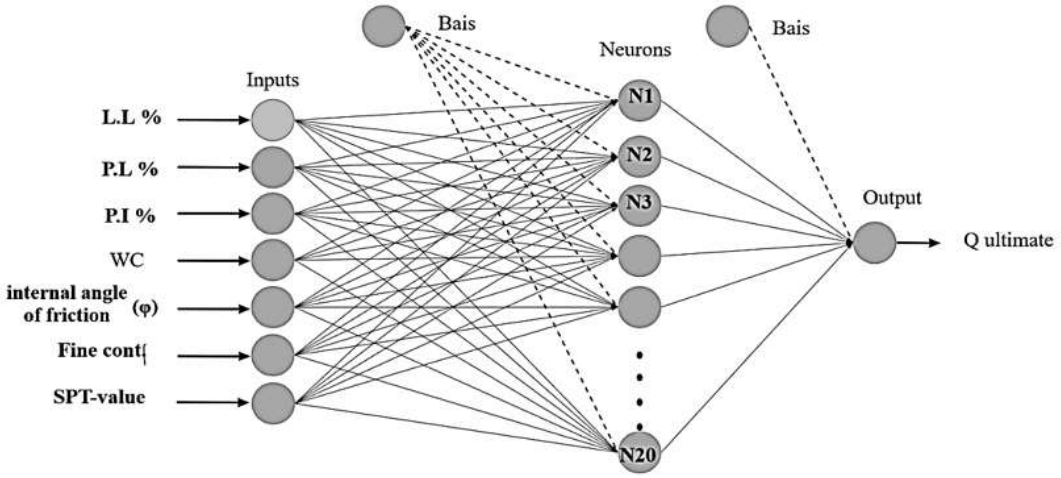


Figure 3.34 Structure of neural network model C2-Group C

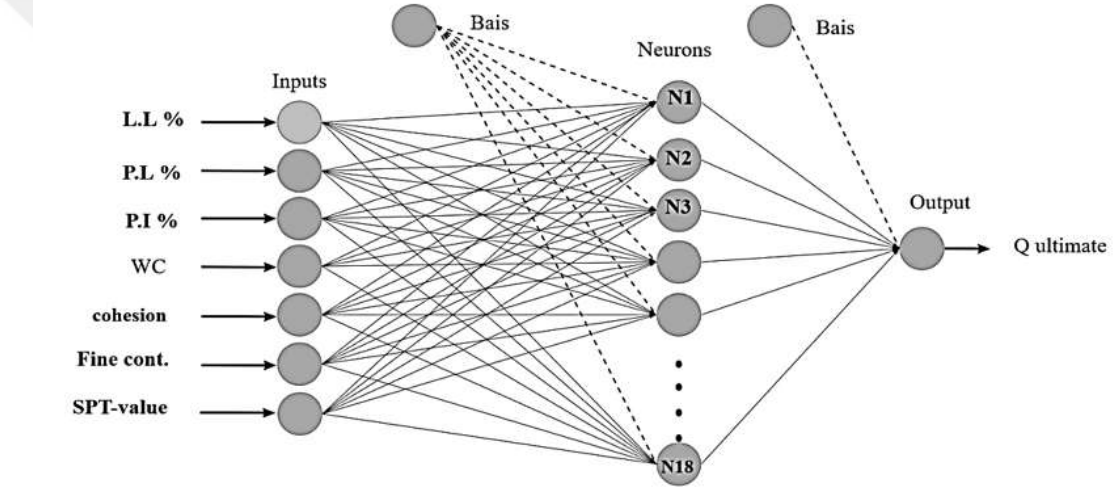


Figure 3.35 Structure of neural network model C3-Group C

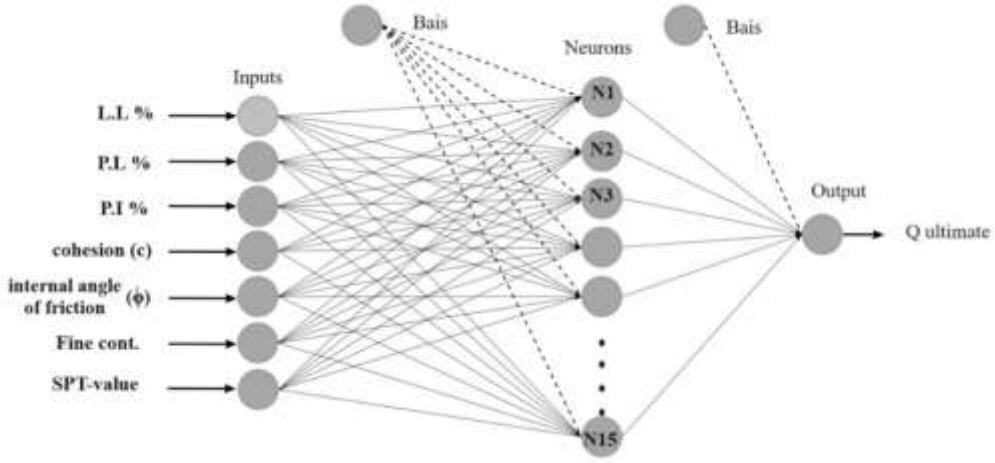


Figure 3.36 Structure of neural network model C4-Group C

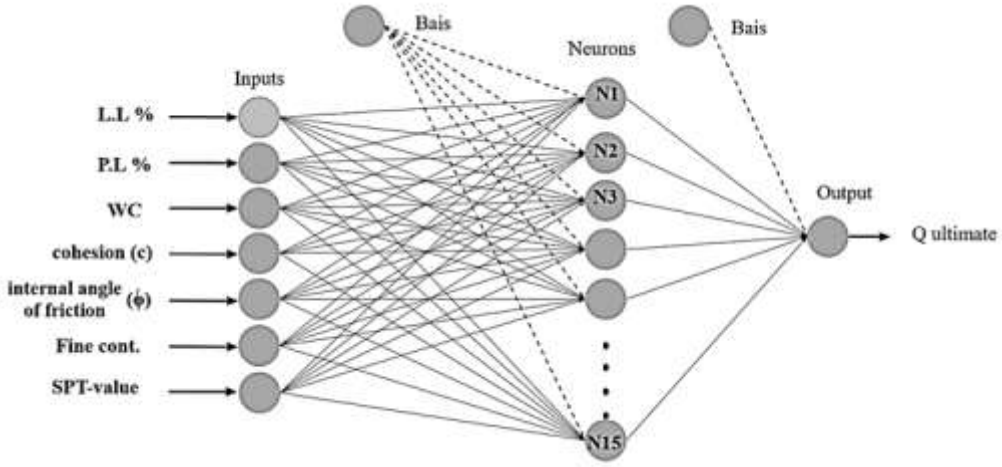


Figure 3.37 Structure of neural network model C5-Group C

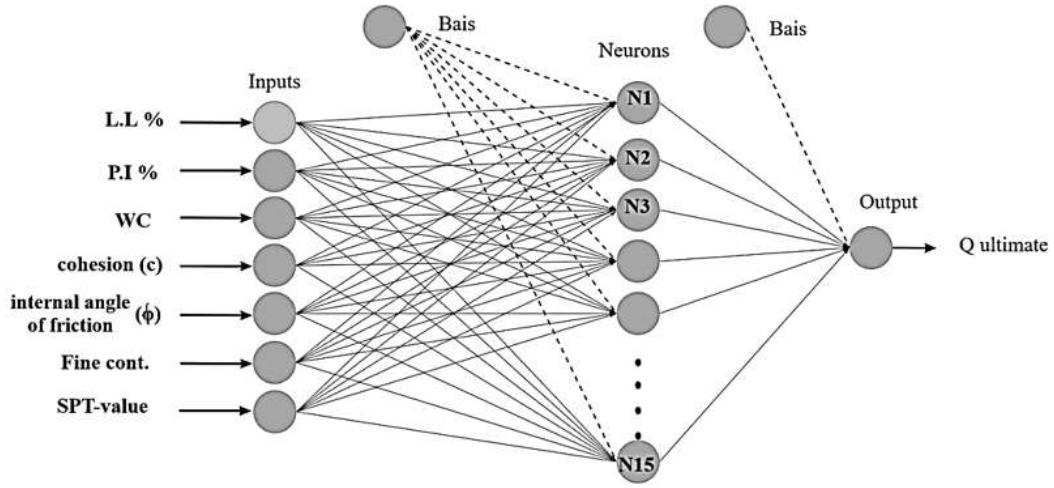


Figure 3.38 Structure of neural network model C6-Group C

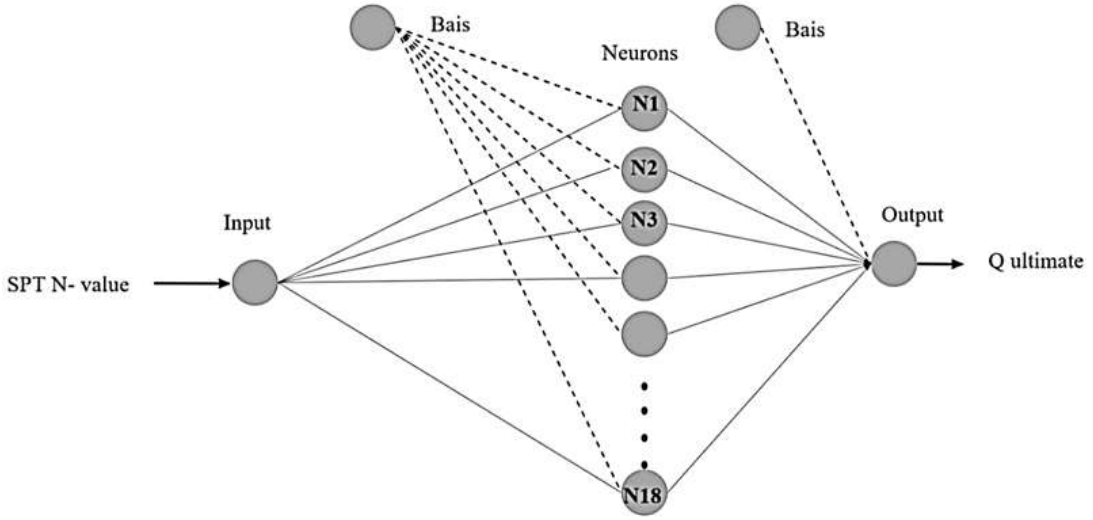


Figure 3.39 Structure of neural network model C7-Group C

CHAPTER 4
RESULTS AND DISCUSSION

4.1 Introduction

The geotechnical characteristics of soils in Erbil, a city in Iraq, play a crucial role in various engineering and construction projects. Analyzing these characteristics is vital for ensuring the stability and safety of structures built on or in the soil. In recent years, the integration of GIS and ANNs has appeared as a hopeful approach for analyzing geotechnical data. In this discussion, would be explore how GIS and ANNs can be used to analyze the geotechnical characteristics of Erbil soils. The benefits of using GIS for spatial data analysis and visualization, and the capabilities of ANNs for predicting soil behavior. Furthermore, discuss the potential interactions and challenges in integrating GIS and ANNs for geotechnical analysis, and how this approach can contribute to improved understanding and management of Erbil soils.

4.2 GIS Models for Soil Characterizes in Study Area

Soil property maps were created for the study area, using GIS. These maps showcased various soil attributes, including soil fines content, natural water content, liquid limit, plastic limit, cohesion, angle of internal friction, compression index, rebound index, SPT–N values, and bearing capacity of foundations at three distinct depth ranges (1.5 m–3.5 m, 3.5 m–6.5 m, and 6.5 m–9.5 m). The soil properties at different depths were interpolated to provide a clear depiction of their distribution across the survey area. To enhance clarity, the soil characteristics were categorized into six main legends, with each legend being assigned a unique color.

4.2.1. Validation of Interpolations Based on Semi-variograms

The semi-variogram covariance modeling was used to model the spatial autocorrelation of the transformed data for SPT-N values at depths of 1.5-3.5m. The semi-variogram analysis is a geostatistical method that examines as the distance between data points increases, the dissimilarity or divergence between them also grows. It is a useful tool for analyzing the spatial dependence of geotechnical data and can help in understanding the spatial patterns of the data.

The semi-variogram covariance modeling was applied to the transformed data to determine the degree of similarity between SPT-N values at different depths. By examining the semi-variogram, it was possible to determine the range of similarity between data points and the degree to which the similarity decreases with distance. This information is essential in geotechnical engineering, as it helps to understand the behavior of the soil at different depths and to identify potential anomalies in the data

At h=0, the semi-variogram should be equal to 0. However, in practice, at very small separation distances, a nugget effect may be observed in the semi-variogram, which results in a non-zero value. In this case, the presence of a nugget effect is observed, which has a value of zero. The range corresponds to the distance where the model reaches a plateau, which is determined to be 5750.634 units. Locations within the range exhibit spatial autocorrelation, while those beyond the range do not exhibit such correlation. The partial sill is calculated as the difference between the sill and the nugget, resulting in a value of 462. 1716.The lag size refers to the size of the distance class, which is measured as 674.7548 units with a total of 12 lags. Figure 4.1 displays the semi-variogram values, with higher values depicted in orange/red and lower values represented in blue/green.

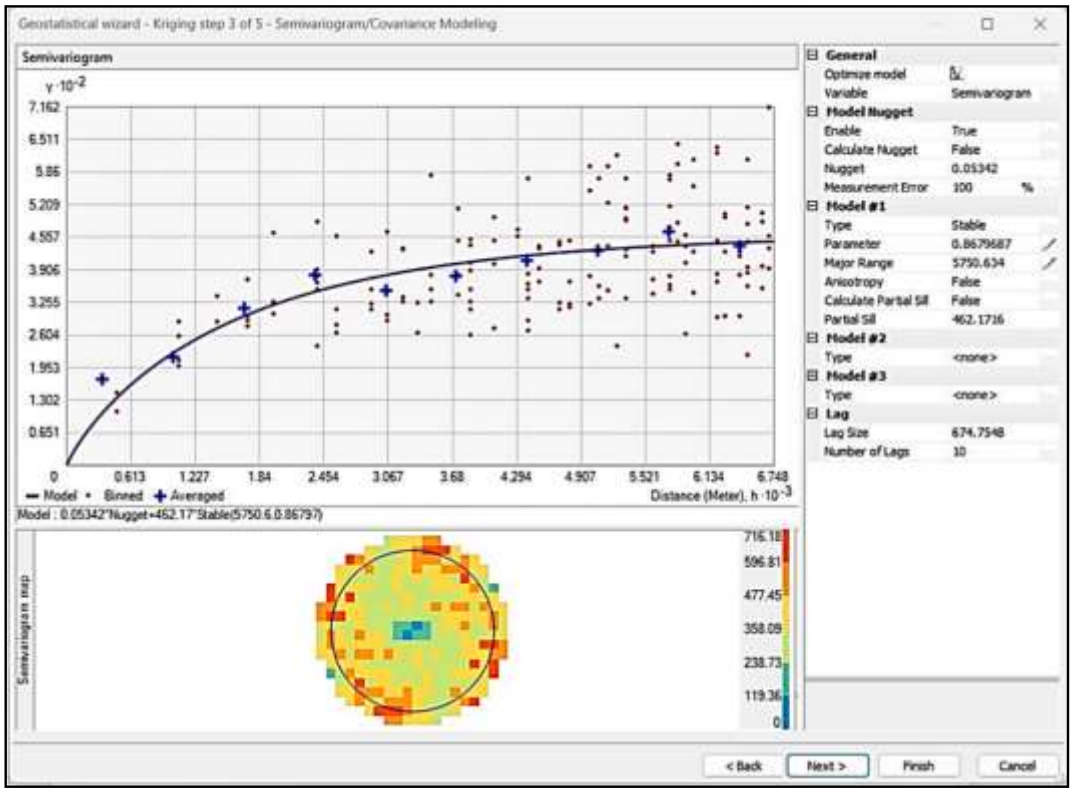


Figure 4.1 Semivariograms/Covariance Modeling.

Kriging is a method employed to estimate spatial values in areas where data is lacking. The process involves determining a search neighborhood, which consists of selecting nearby data points that hold significant influence over the prediction location based on spatial auto-correlation. By eliminating irrelevant points and assigning weights to the nearby points within the search neighborhood, values at the unknown location can be estimated. The search neighborhood is determined by considering factors such as adjacent points, radius, and the number of sectors. The accurate identification and selection of the appropriate nearby points within the search neighborhood are vital for the successful implementation of kriging. Properly defining the search neighborhood ensures more accurate and reliable predictions ocation, which is at the center of the crosshair. Figure 4.2 demonstrates the selection of five neighboring points and the creation of a circle with four sectors. The highlighted points within the dataset represent the assigned weights for each point. These weights play a crucial role in estimating the value at an unknown location situated at the center of the crosshair (Li and Heap, 2008).

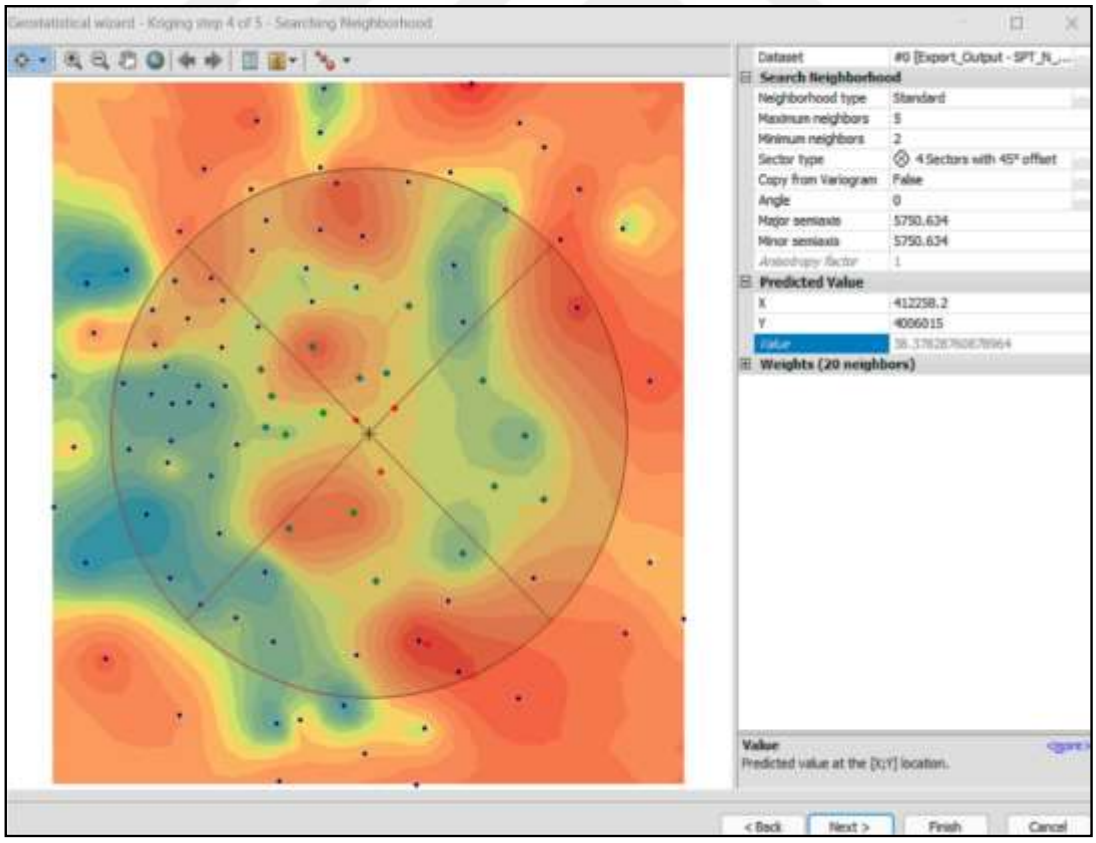


Figure 4.2 Searching Neighborhood Dialog Box of Ordinary Kriging.

4.2.2 Fines Content

Soil is a complex material with various physical and mechanical properties that are critical to the stability of structures built on it. The fines content of soil is considered one of the most influential parameters that impact its behavior. Fines content denotes the proportion of soil particles with a diameter smaller than 0.075 mm, expressed as a percentage. These particles, also known as clay and silt, have a significant impact on soil behavior because of their unique physical and mechanical properties. For instance, clay particles have a high surface area-to-volume ratio, which allows them to attract and hold water molecules. This makes clay soils highly cohesive and adhesive, which can lead to high shear strength and bearing capacity. On the other hand, silt particles have a relatively lower surface area-to-volume ratio than clay particles. This means that they do not have the same high cohesiveness and shear strength as clay. However, silt particles can still significantly affect soil behavior because they are susceptible to compaction, resulting in reduced porosity and increased soil stiffness. The impact of fines content on soil behavior can be seen in several ways. For example, high fines content soils are generally more compressible and less permeable than soils with lower fines content. This is because clay and silt particles can clog up the pore spaces between larger soil particles, reducing the ability of water to flow through the soil. As a result, high fines content soils are more susceptible to settlement and consolidation. Fines content also affects the plasticity of soil, which is its ability to undergo deformation without cracking or breaking. Clay soils are known for their high plasticity because of their high cohesiveness and water-holding capacity (Duong, 2013).

The findings presented in figure 4.3 reveal that the majority of the study area within Erbil city center exhibits a high fines content. As depicted in the figure, the fines content surpasses 81% in most parts of the area, indicating a significant presence of soil particles with a diameter smaller than 0.075 mm. This abundance of fine particles is expected to exert notable influences on various engineering properties of the soil, including shear strength, compressibility, and plasticity. Given the impact of soil properties on load-bearing capacity, resistance to deformation, and load transmission, it is crucial to consider these factors meticulously in future construction and development endeavors in the region. The results derived from figure 4.3 provide engineers and planners in Erbil city center with essential insights, emphasizing the

necessity of incorporating fines content analysis into decision-making processes for development projects. The significance of soil compression levels becomes particularly relevant when coarse particles are displaced by fine particles, and the effect of fines content is most pronounced when the soil is close to saturation. These observations align with prior research conducted by other scholars in the field (Duong, 2013; Ebrahimi, 2011; Kim et al., 2005).

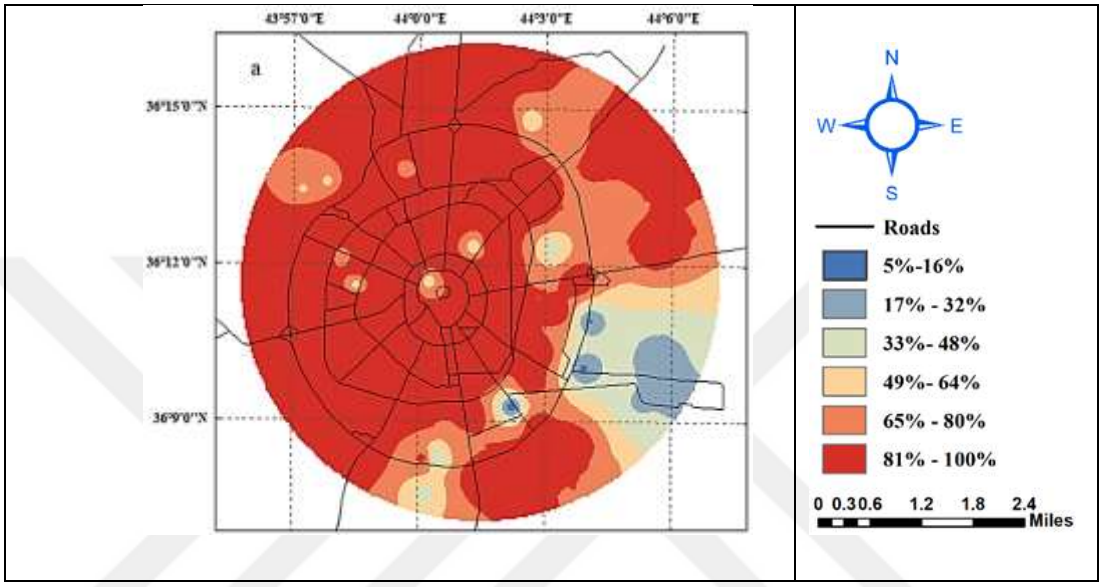


Figure 4.3-a Fines content model for soil layer at depth, 1.5-3.5m.

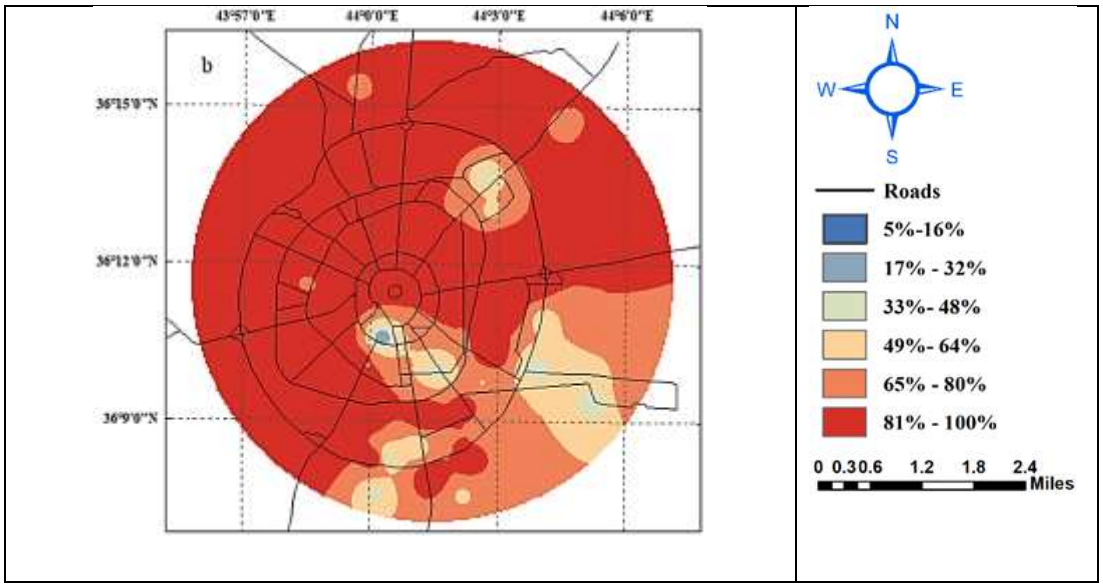


Figure 4.3 -b Fines content model for soil layer at depth, 3.5-6.5m.

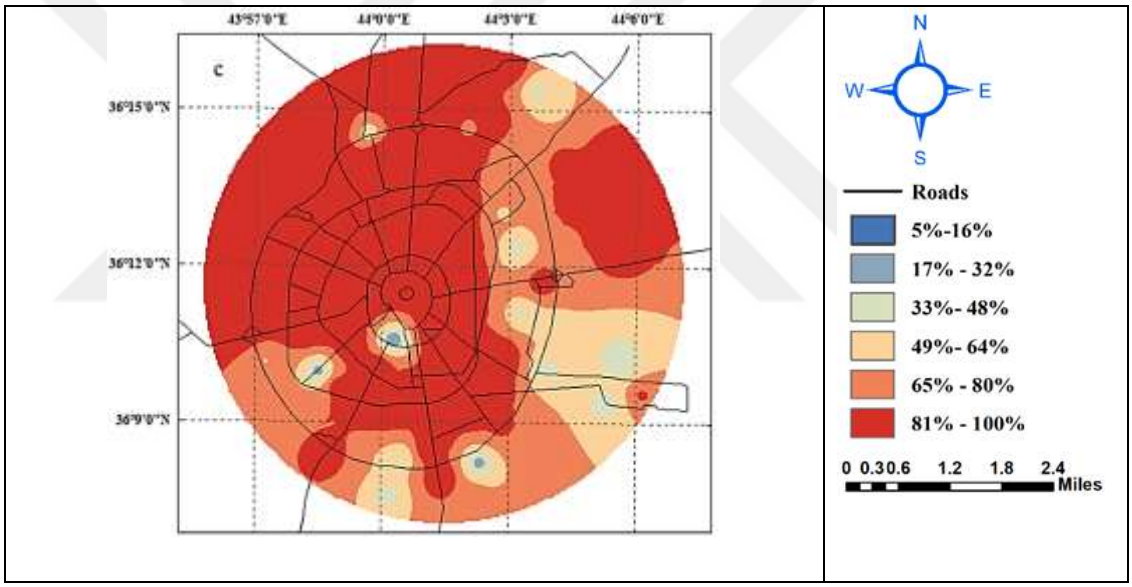


Figure 4.3-c Fines content model for soil layer at depth, 6.5-9.5m.

The relationship between natural water content and fines content is interconnected and cannot be assessed independently. The impact of fines content on soil shear strength can be influenced by changes in natural water content. Enhancing the natural water content sometimes mitigates the effect of fines content on soil shear strength, as fines are highly sensitive to variations in natural water content. Conversely, in dry conditions, fines have minimal influence on soil behavior, largely due to the influence of suction. (Inam et al., 2012; Wang et al., 2013). In conclusion, fines content plays a pivotal role in influencing soil behavior across multiple aspects such as shear strength, compressibility, plasticity, and indirectly, the bearing capacity of foundations. It is

imperative for engineers and geotechnical professionals to comprehend the impact of fines content on soil behavior in order to design structures that are safe and dependable, regardless of the soil type encountered.

4.2.3 Atterberg Limits

Atterberg limits are a set of tests that are commonly used to measure the consistency and plasticity of soils. The tests are named after the Swedish soil scientist Albert Atterberg, who developed them in the early 20th century. Atterberg limits serve as valuable tools for characterizing soil behavior and classification, particularly in assessing the swelling potential of expansive soils. From Atterberg limits, two essential index properties can be derived: the plasticity index (PI) and the liquidity index (LI). These properties can be calculated using the natural water content, liquid limit, and plastic limit of the soil. The liquid limit denotes the water content at which the soil transforms from a plastic state to a liquid state, whereas the plastic limit signifies the water content at which the soil converts from a plastic state to a semi-solid state. The difference between the liquid limit and plastic limit is known as the plasticity index, which characterizes the range of water content in which the soil displays plastic behavior. Soils with a high PI are highly plastic and can display plastic behavior over a broader range of water content. In contrast, soils with a low PI are less plastic and can only exhibit plastic behavior over a narrower range of water content.

The plasticity index and the liquidity index are important for the classification of soils. The Unified Soil Classification System (USCS) uses these indices to classify soils into different categories. Soils with a high PI and a low LI are classified as clay soils, while soils with a low PI and a high LI are classified as silt soils. Soils with a PI and a LI within a certain range are classified as clayey soils or silty soils, depending on their proportions of clay and silt.

Atterberg limits are also important for the design of foundations and earthworks. Expansive soils, which have a high potential for swelling, can cause significant damage to structures if not properly accounted for in the design. Atterberg limits can be used to identify expansive soils and to estimate their potential for swelling. This information is critical for the proper design of foundations and earthworks to ensure their stability and durability over time (Koester, 1992). The consistency of soil is influenced by its water content. When clay soil has a high-water content, it tends to

exhibit liquid-like behaviour because the excess water between the clay particles reduces the attraction among them (Mitchell and Soga, 2005). The liquid limit is employed to assess the consistency of fine-grained soil. This measurement of soil consistency is valuable for estimating soil consolidation properties, as well as determining the acceptable bearing capacity and settlement of foundations (Bogati, 2019)

Figure 4.4 provides an overview of the variations in soil liquid limit across the study area at three different depths. The analysis of liquid limit values reveals that a significant portion of the soils in the area falls within a range of 40% to 52%. This range indicates the presence of low plastic clay, which is characterized by low resistance to deformation under stress and a propensity for collapse. The abundance of low plastic clay in the study area is a crucial factor to consider in construction and development projects, as it can have implications for the stability and structural integrity of built environments.

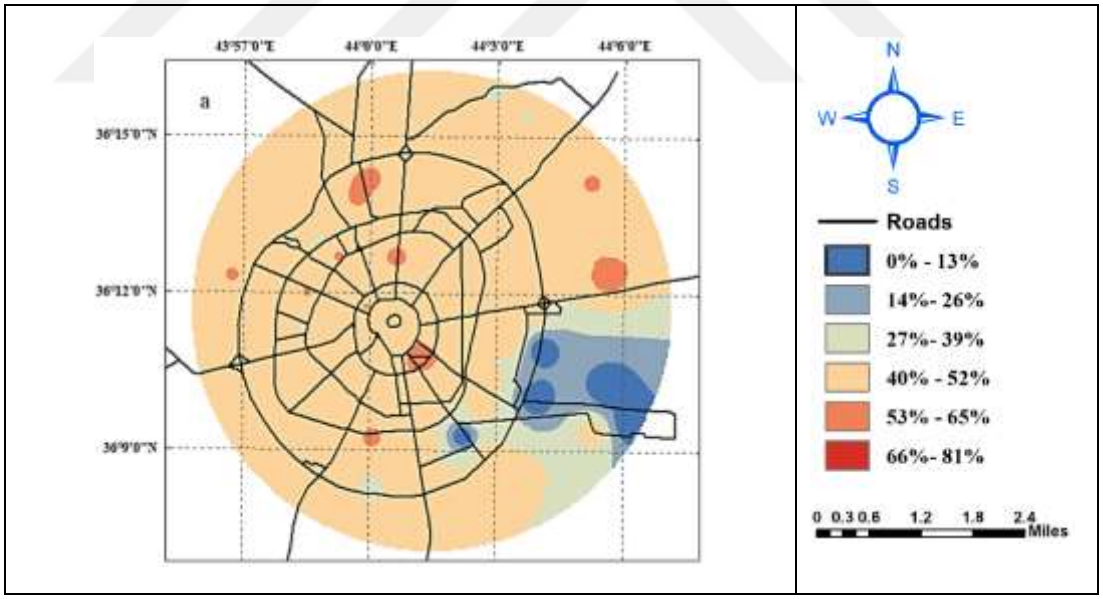


Figure 4.4-a Liquid limit for soil at depth, 1.5-3.5m.

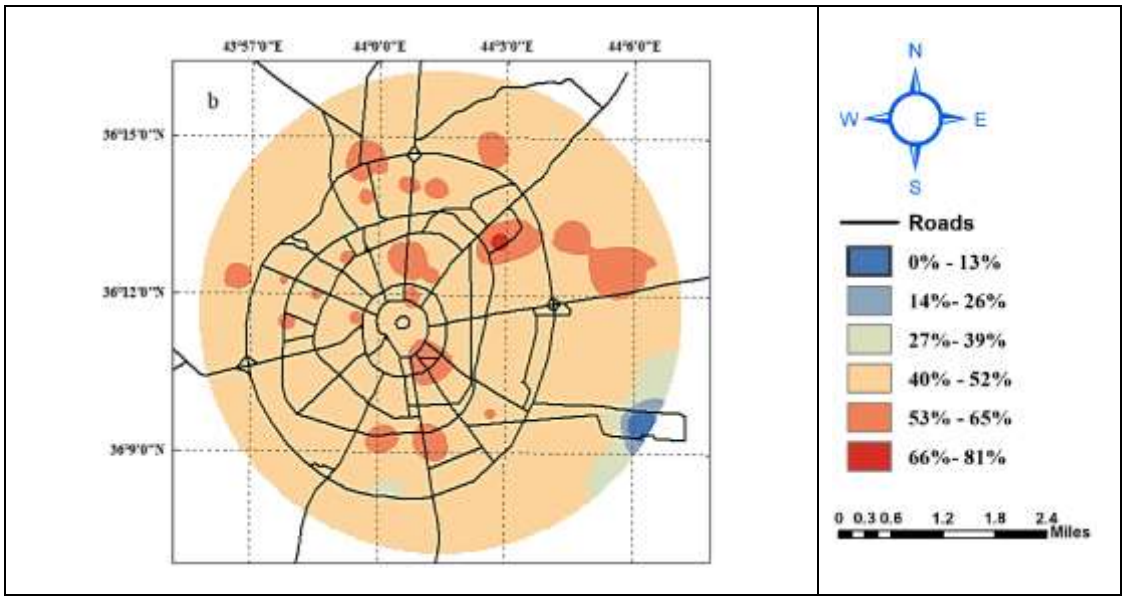


Figure 4.4-b Liquid limit model for soil layer at depth, 6.5-9.5m.

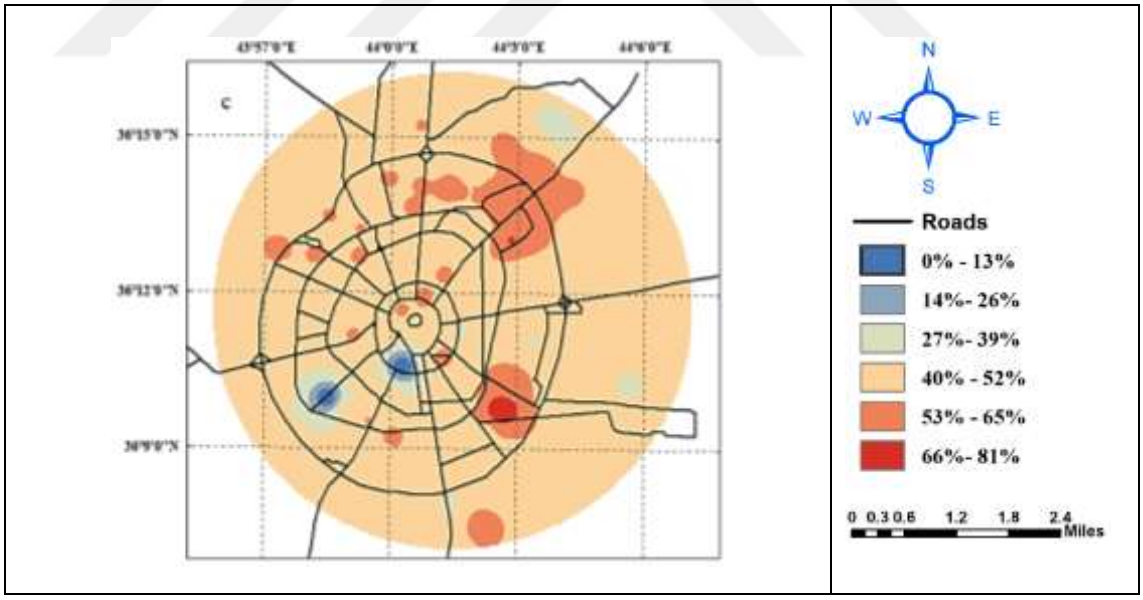


Figure 4.4-c Liquid limit model for soil layer at depth, 6.5-9.5m.

Additionally, noteworthy observations include the identification of soils with high liquid limit values exceeding 53% in central regions. These central zones are deemed critical points within the study area, as soils with high liquid limit values are more susceptible to deformation and instability. The presence of such soils in these areas

further emphasizes the need for careful consideration and mitigation strategies in construction and development. It is crucial to thoroughly evaluate and address these critical points in any future construction and development projects within the area to ensure the stability and integrity of structures built on these soils. Extensive research has been conducted to investigate the correlation between the liquid limit of soils and their swelling potential. Certain clay minerals characterized by a high cation exchange capacity are susceptible to expansion and an increase in the volume of available water (Bogati, 2019; Carter and Bentley, 1991; Spagnoli and Feinendegen, 2017). Plasticity is a significant characteristic of clay, and it primarily arises from the crystallinity of clay minerals. These studies contribute to our understanding of the relationship between the liquid limit of soils and their behaviour, specifically in terms of swelling potential. Such insights are instrumental in informing engineering practices and decision-making processes to effectively manage and mitigate the challenges posed by clayey soils (Carter and Bentley, 1991; Spagnoli and Feinendegen, 2017).

Soil demonstrates plastic characteristics when its moisture content falls between the liquid and plastic limits. The plasticity index quantifies this behavior by measuring the disparity between these two limits, signifying the range of moisture content within which the soil can exhibit plasticity (Casagrande, 1958). The plastic limit serves as an indirect indicator for geotechnical engineers to assess the activity, toughness index, and optimum moisture content of soils. In Figure 4.5, the variation of the plastic limit is depicted at different depths within the study area. Upon analysing the figure, it becomes apparent that half of the study area exhibits a plastic limit range between 19% and 24%, while the other half falls within the range of 25% and 30%. This disparity indicates varying levels of soil plasticity, which measures the ability of soil to undergo shape changes without fracturing under stress. An important observation is the presence of localized zones in the southeast direction characterized by soils with low plastic limits (Figure 4.5-a).

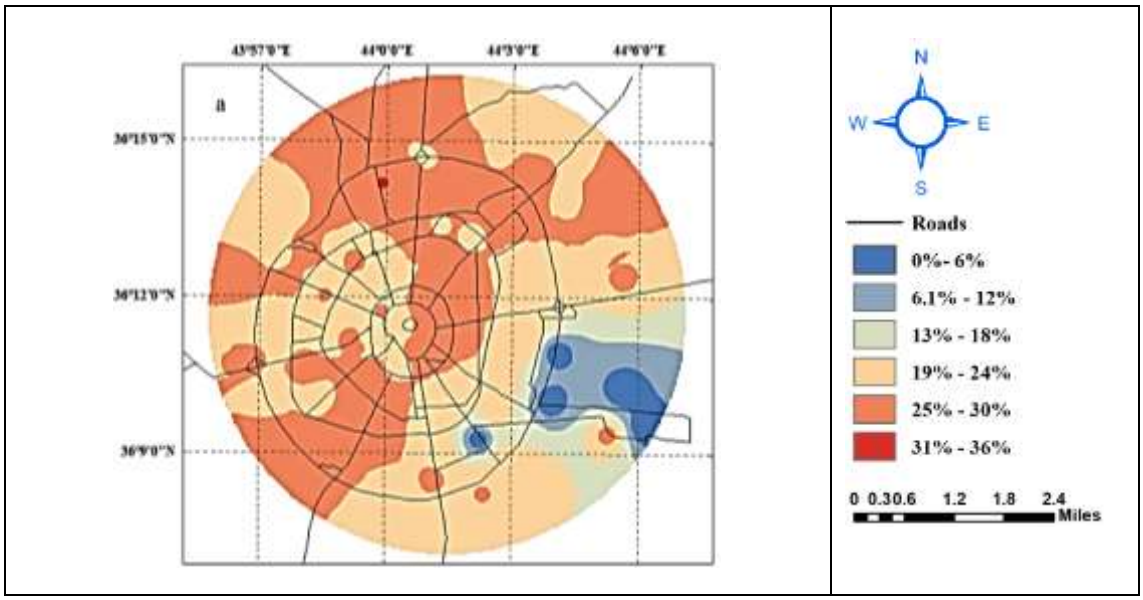


Figure 4.5-a Plastic limit model for soil layer at depth, 1.5-3.5m.

Soils with low plastic limits possess reduced plasticity and increased brittleness, making them susceptible to cracking and failure when subjected to stress. It is crucial to carefully evaluate and address these areas in future construction projects within the region to ensure the stability and reliability of structures built on such soils. Atterberg limits serve as valuable tools for characterizing soil behaviour and classification. The plasticity index and liquidity index offer significant insights into the consistency, plasticity, and swelling potential of soils. This information is essential for accurate foundation design, earthworks planning, and the identification of potentially problematic soils that may cause substantial damage to structures over time.

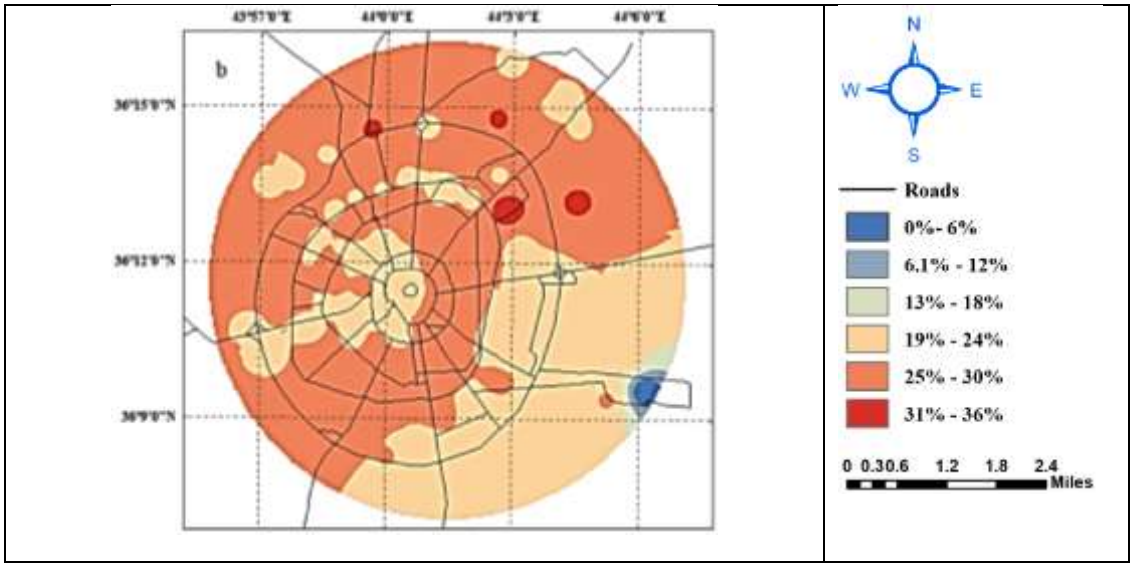


Figure 4.5-b Plastic limit model for soil layer at depth, 6.5-9.5m.

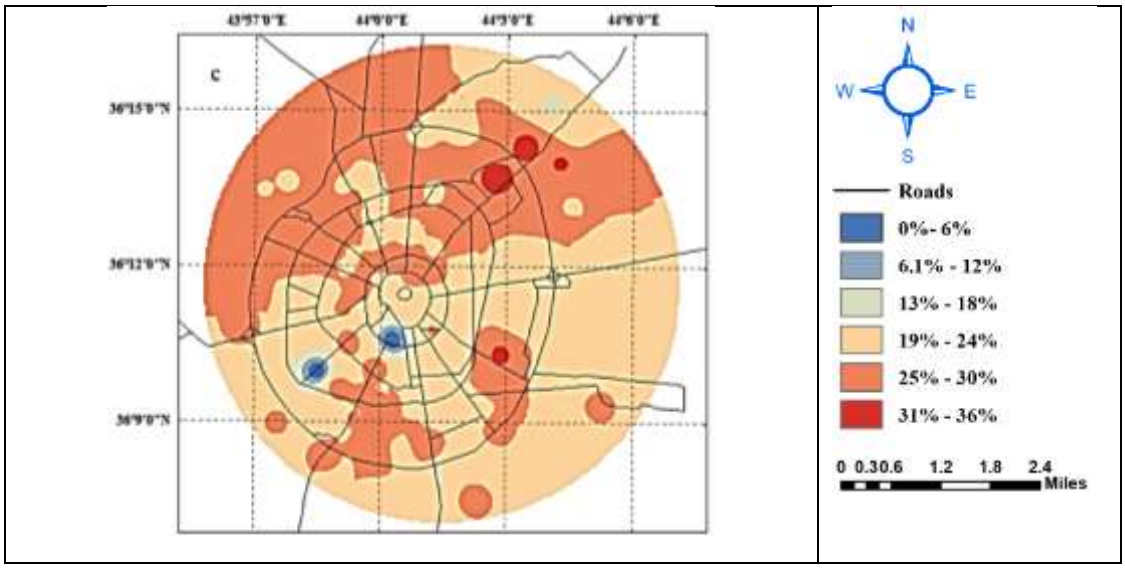


Figure 4.5-c Plastic limit model for soil layer at depth, 6.5-9.5m.

4.2.4 Natural Water Content

The natural water content, also known as the moisture content, is an essential parameter that profoundly affects the geotechnical properties of soil. It refers to the amount of water contained in soil at its natural state, before any external forces or changes are applied. The natural water content of soil is a critical parameter because it affects several key geotechnical properties, including soil strength, compressibility, permeability, and shear strength. Soil strength is a critical parameter in the design of foundations, retaining walls, and other geotechnical structures. The natural water content affects soil strength by influencing the interparticle forces between soil particles. When soil is saturated with water, the interparticle forces weaken, resulting in reduced soil strength. On the other hand, if soil is too dry, the particles may not be able to stick together, leading to a weak soil structure. Compressibility is another important parameter that is influenced by the natural water content.

The compressibility of soil refers to its ability to settle or deform when a load is applied. Soil with high natural water content tends to be more compressible than soil with low natural water content. This is because the water in the soil fills the pore spaces between the particles, reducing the soil's ability to resist compression (Walker, 2012). On the other hand, soil with low natural water content tends to be less compressible because the pore spaces between the particles are not filled with water, allowing the soil to resist compression. Permeability is another critical geotechnical property that

is affected by the natural water content. Permeability refers to the ability of soil to allow water to pass through it. Soil with high natural water content tends to be less permeable because the pore spaces are filled with water, reducing the ability of water to flow through the soil. On the other hand, soil with low natural water content tends to be more permeable because the pore spaces between the particles are not filled with water, allowing water to flow more easily through the soil. The natural water content also affects the shear strength of soil. Shear strength refers to the ability of soil to resist sliding along a plane. Soil with high natural water content tends to have lower shear strength because the water in the soil lubricates the particles, making it easier for them to slide (Gardner et al., 2000; Das, 2008).

Figure 4.6 illustrates the variations in natural water content within Erbil City. The figure depicts the water content at three different depths (1.5 m - 3.5 m, 3.5 m - 6.5 m, and 6.5 m - 9.5 m). The findings reveal that, across these depth ranges, the natural water content in the study area predominantly falls between 16% and 20%. The natural water content of soils holds significant importance in construction and development endeavours, as it directly impacts soil stability, bearing capacity, and compressibility. Soils with high natural water content are more vulnerable to instability, while those with low natural water content are prone to drying and cracking. Consequently, understanding and considering the natural water content of soils is crucial for ensuring the long-term durability and performance of construction projects in the area.

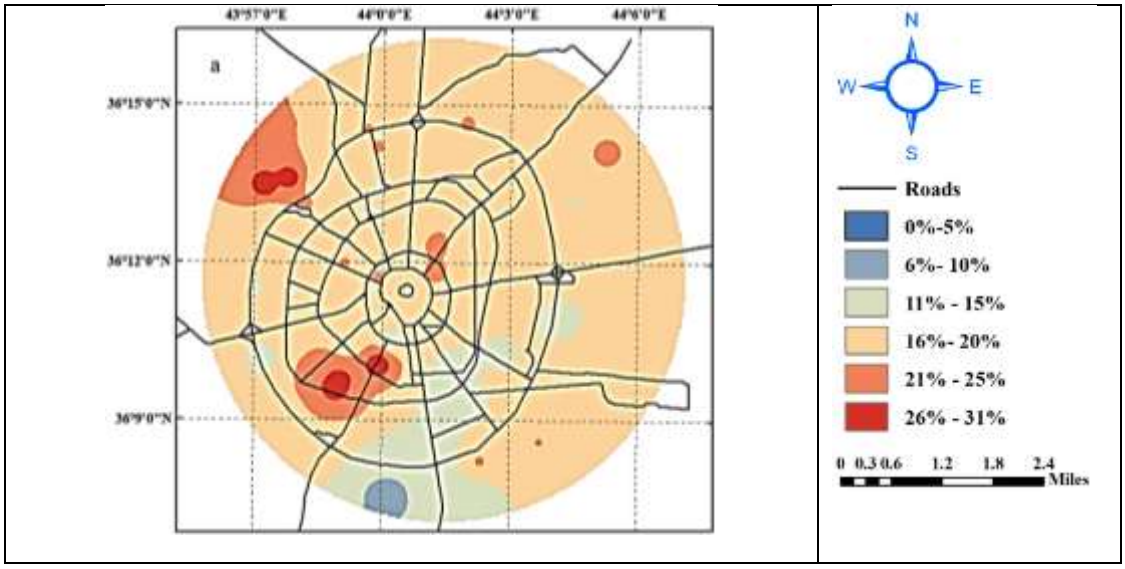


Figure 4.6-a Water content variation model for soil layer at depth, 1.5-3.5m.

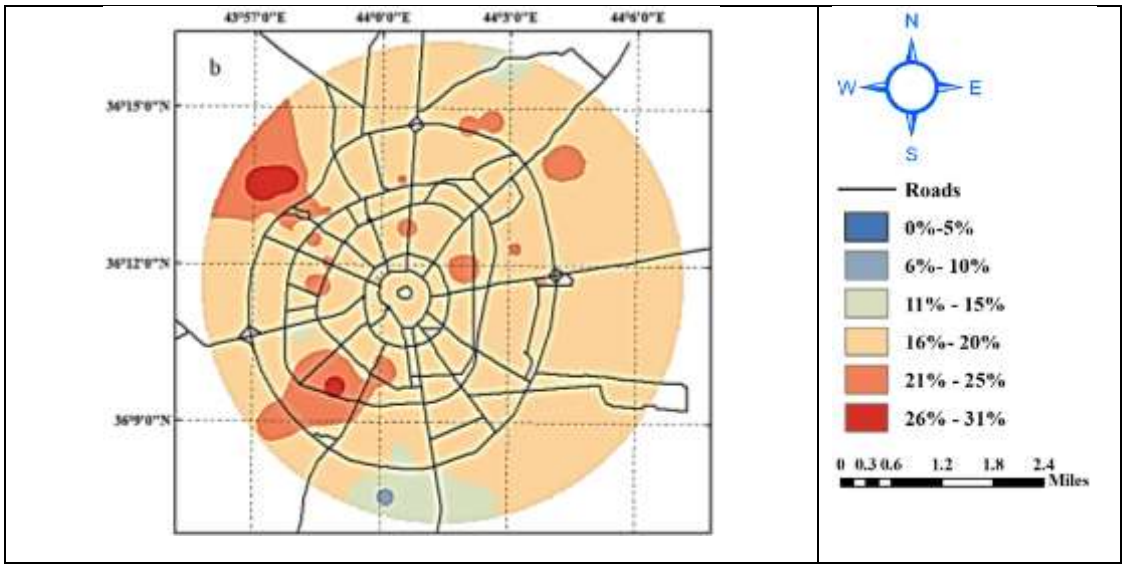


Figure 4.6-b Water content model for soil layer at depth, 3.5-6.5m.

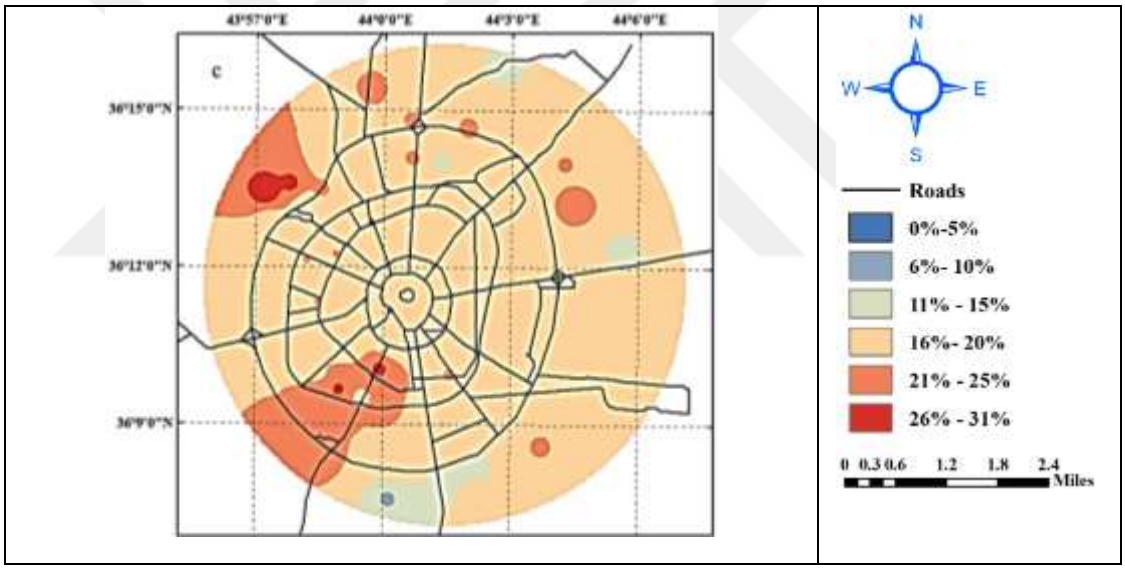


Figure 4.6-c Water content model for soil layer at depth, 6.5-9.5m.

The findings align with previous studies conducted in this region (Gardner et al., 2000; Das, 2008). During the exploration period, the water table was located at considerable depths beneath the natural ground level (NGL), indicating relatively shallow groundwater. The water table experiences seasonal fluctuations, with a rise observed during the spring season. The soil above the water table significantly influences its strength and compressibility. Increased moisture content in the soil leads to reduced strength and heightened compressibility. Below the water table, saturated soil presents settling challenges as the consolidation process decreases the natural water content

under stable loading conditions. This settling phenomenon can have implications for the stability and performance of structures built on such saturated soil layers.

4.2.5 Shear Strength Parameters

The shear strength of soils plays a crucial role in the design of foundations and structures that interact with the soil. It denotes the soil's capacity to withstand forces that induce slipping or sliding along a plane within the soil. This parameter is vital in ensuring the stability and integrity of construction projects built on or in contact with soil. This parameter plays a critical role in the stability and safety of structures that are built on or within the soil. The bearing capacity of shallow and deep foundations is dependent on the shear strength of soils. The shear strength determines the maximum load that the soil can support without undergoing failure or excessive deformation. Inadequate shear strength of soil can lead to settlement, which can cause damage to the foundation and the structure built upon it. Therefore, the design of the foundation must take into account the shear strength of soil to ensure that it can withstand the loads it will experience over its service life.

The shear strength of soils is also essential in the analysis stability of slopes. Slope stability analysis involves evaluating the forces acting on the slope and comparing them with the shear strength of soil. If the forces exceed the shear strength, the slope will fail, leading to landslides and other hazards. Therefore, understanding the shear strength of soils is critical in designing stable slopes, preventing landslides, and ensuring the safety of people and property. Tunnels are another example where the shear strength of soils plays a vital role in their design. The shear strength of soil determines the stability of the tunnel walls and the amount of support needed to prevent collapse. Adequate support must be provided to prevent deformation or collapse of the tunnel walls, which can lead to significant damage and loss of life. Finally, the lateral pressure on structures also depends on the shear strength of soil. When structures are built below the ground level, they experience lateral pressure from the surrounding soil. The shear strength of soil determines the magnitude of the lateral pressure and, consequently, the design of retaining walls or other support systems to prevent excessive deformation or collapse (Das, 2018).

Soil's shear strength arises from cohesive strength (c) and frictional strength, characterized by the angle of internal friction (ϕ). Cohesive strength results from

bonding forces between soil grains and binding material, while frictional strength emerges from interlocking, rolling, and friction among soil grains. These factors determine soil's ability to resist shear forces, influencing foundation and structure design. (Das, 2008; Aldefae et al., 2020). he strength of soil diminishes as shear strain increases and expansion or contraction varies in relation to soil density caused by applied loads. Shear strength parameters are extensively employed in foundation design, particularly in empirical equations, to determine the appropriate strength characteristics of the soil (Nam et al., 2011).

Figures 4.7 and 4.8 exhibit the variations in cohesion and angle of internal friction, respectively. These two parameters collectively determine the shear strength of the soil and demonstrate its variations across the study area and soil depth. At shallow depths (1.5 m - 3.5 m), the majority of soils in the study area displayed cohesion values ranging between 76 kPa and 100 kPa. However, there were smaller regions with cohesion values exceeding 100 kPa or falling below 50 kPa. As depth increased, the area covered by soils with cohesion values surpassing 100 kPa expanded. These findings align with the distribution of fines content observed in the study area. In most parts of the study area, the soil exhibited fines content exceeding 80%, which likely contributes to the higher cohesion values observed. Soils with elevated fines content tend to exhibit increased cohesion values (Bapeer, 2011).

The angle of internal friction is a key parameter in determining soil shear strength and is used in estimating bearing capacity, analyzing slope stability, and evaluating soil lateral earth pressures. In the study area, the soils exhibited an effective angle of internal friction ranging from 2° to 6°, which remained consistent across all three investigation depths. However, in the eastern-southern part of the study area, soils had an angle of internal friction ranging from 7° to 12°. These results indicate that the angle of friction values observed in the study area align with those reported in similar studies conducted in the region. The angle of internal friction is a significant parameter for assessing soil shear strength, and these findings suggest that the soils in the study area possess moderate to low shear strength values. The information obtained from the figures can aid in identifying regions with high or low shear strength, which is crucial for evaluating the suitability of the soil for various types of structures.

The data can be utilized to design and construct structures that are compatible with the prevailing soil conditions in the region (Aldefae et al., 2020; Nareeman and Fattah 2012). In summary, the shear strength of soils holds crucial importance in various foundation engineering designs. It plays a significant role in determining the bearing capacity of both shallow and deep foundations, slope stability, tunnel construction, and lateral pressure exerted on structures. Consequently, comprehending the shear strength of soils is essential to ensure the safety and stability of structures constructed on or within the soil.

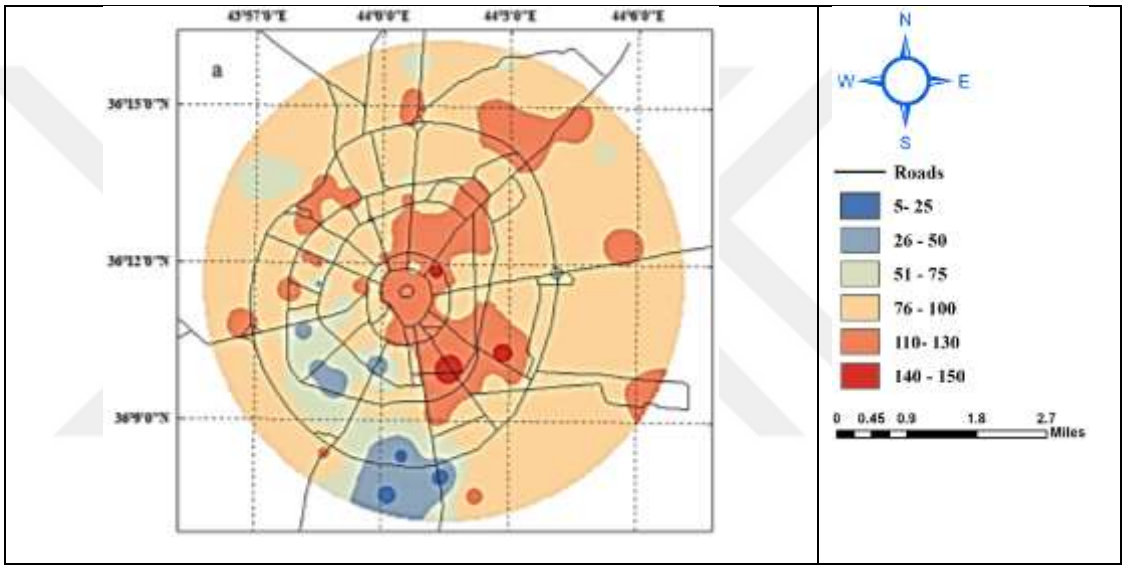


Figure 4.7-a Cohesion model (kN/m^2) for soil layer at depth, 1.5-3.5m.

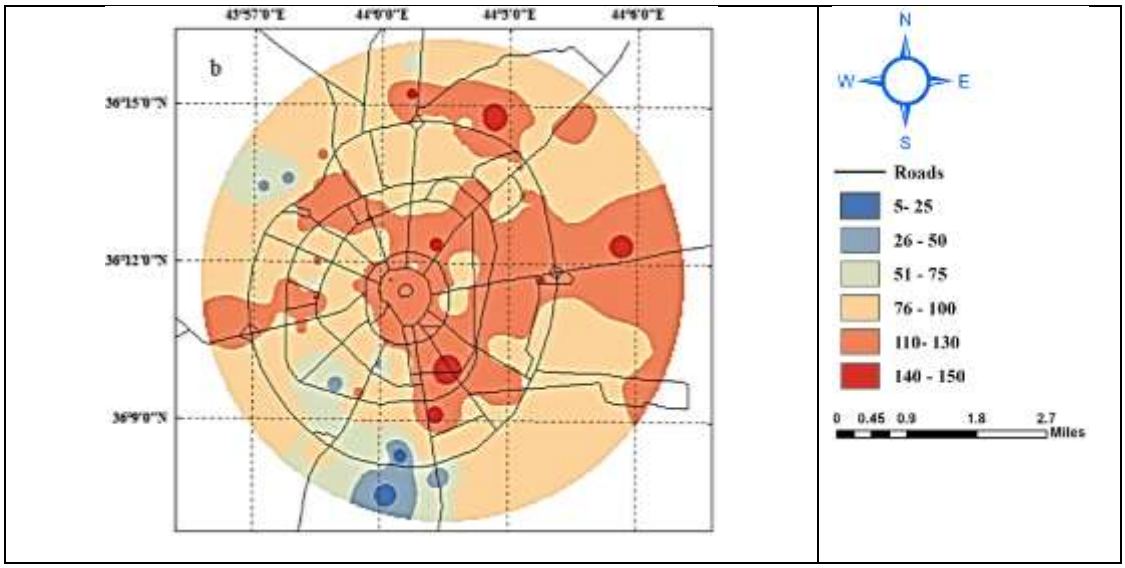


Figure 4.7-b Cohesion model (kN/m^2) for soil layer at depth, 3.5-6.5m.

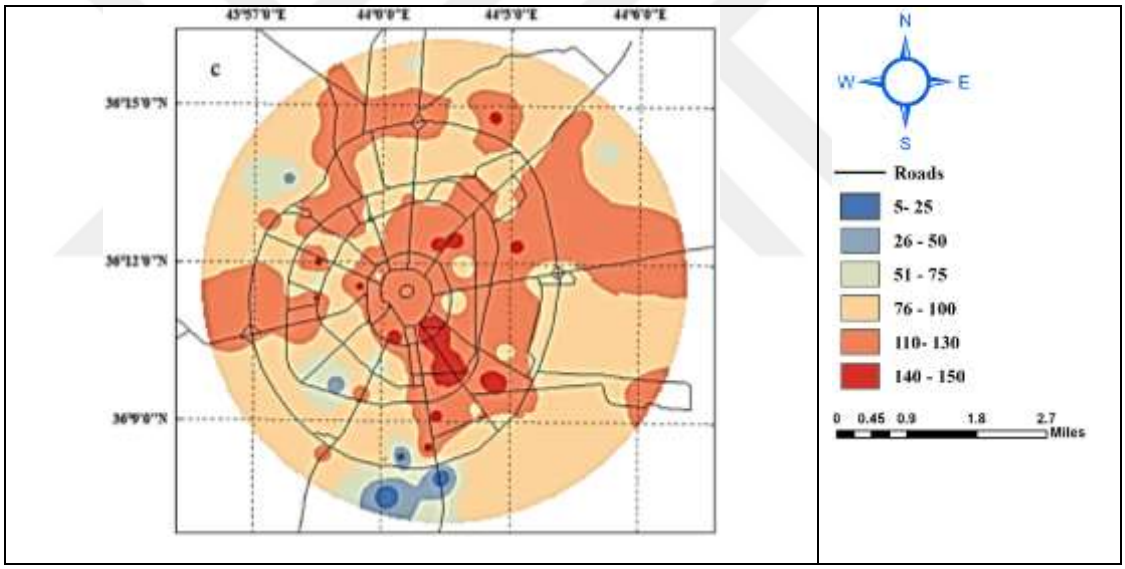


Figure 4.7-c Cohesion model (kN/m^2) for soil layer at depth, 6.5-9.5m.

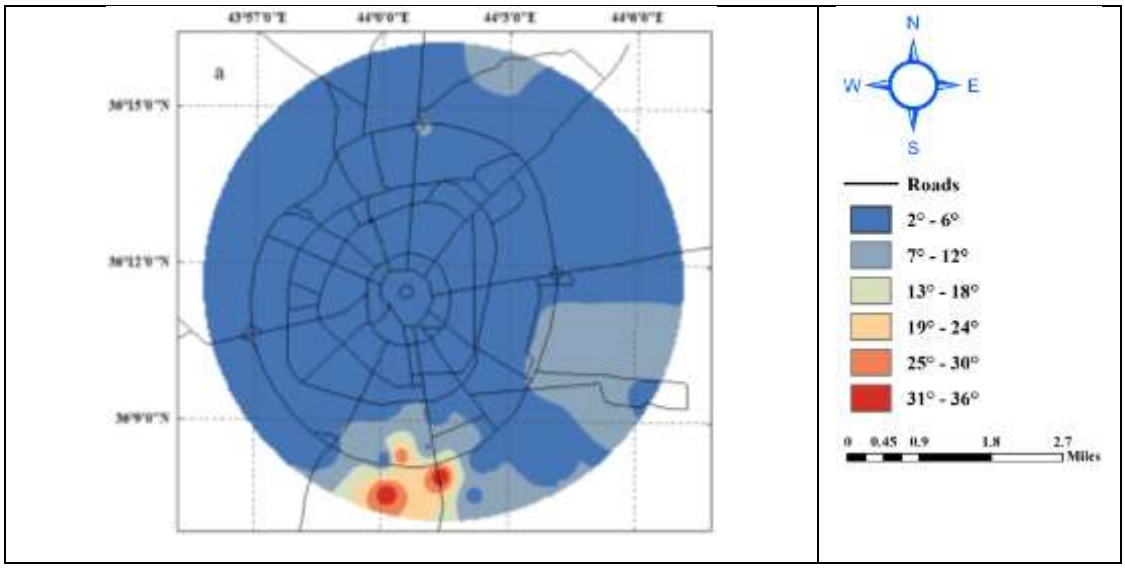


Figure 4.8-a Internal friction angle (degree) distribution model for soils at depth, 1.5-3.5m.

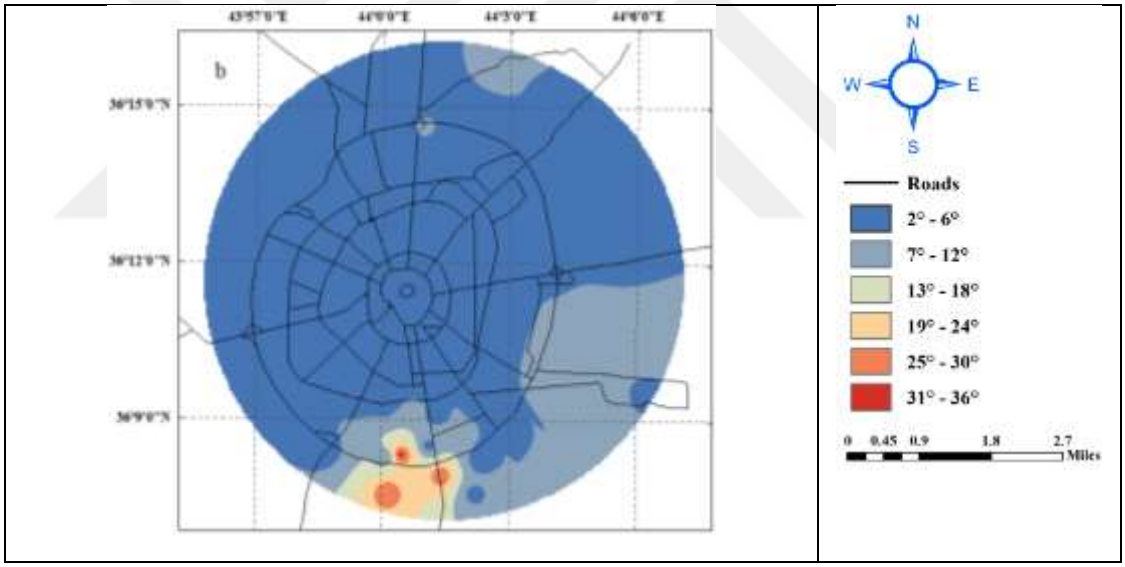


Figure 4.8-b Internal friction angle (degree) distribution model for soils at depth, 3.5-6.5m.

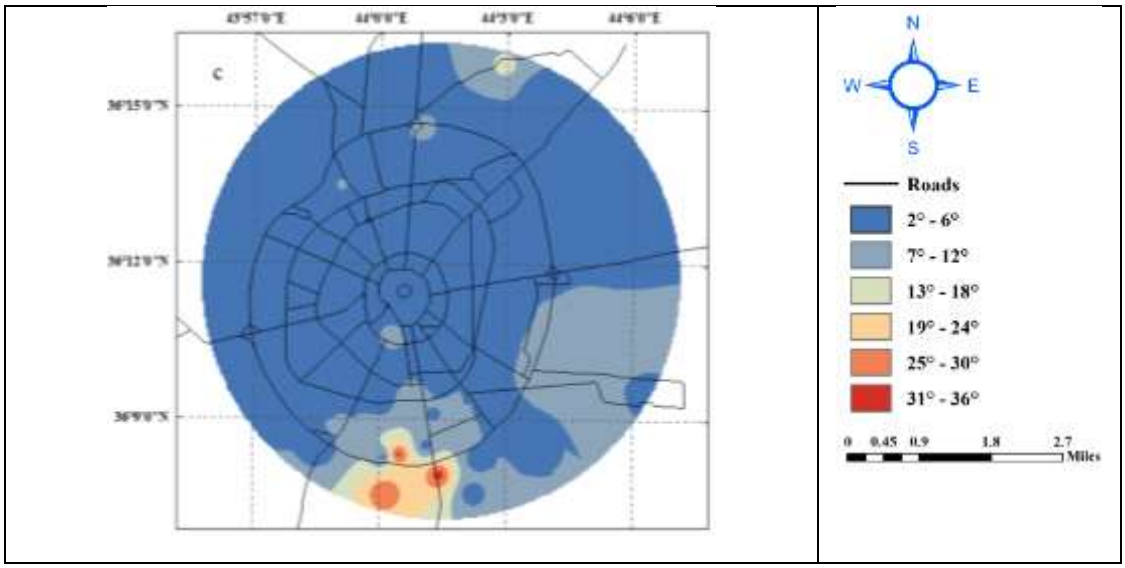


Figure 4.8-c Internal friction Angle (degree) distribution model for soils at depth, 6.5-9.5m.

4.2.6 Consolidation Parameters

The consolidation parameters, namely the compression index and swelling index, are critical factors that must be considered during the analysis and design of foundations on clayey soils. These parameters describe the behavior of soil under load and can have significant implications for the stability and performance of foundation systems. The compression index of a soil refers to its ability to undergo compression due to applied loads. It is a measure of the rate at which the soil consolidates or compacts under load. A high compression index indicates that the soil is susceptible to significant compression under load, which can lead to excessive settlement of foundations. Settlement can cause damage to structures and lead to costly repairs, so it is essential to ensure that the compression index of the soil is checked during foundation design. The swelling index of a soil is another important parameter to consider during foundation design. It refers to the amount of swelling that a soil undergoes due to changes in moisture content.

When the soil becomes saturated with water, it can swell significantly, and this can cause significant problems for foundations. For example, swelling of soil can cause uplift forces, leading to the heaving of foundation slabs or damage to foundation walls. Therefore, it is essential to check the swelling index of the soil and take steps to mitigate any potential problems. Both the compression index and swelling index are

determined from laboratory tests on soil samples (Powrie, 2018). The results of these tests are used to calculate the settlement of the foundation and to design the foundation system accordingly. The foundation system may include measures such as increasing the foundation size, using deeper foundations, or providing additional support to mitigate any potential problems due to soil consolidation and swelling (Gunduz and Arman, 2007).

This study focused on examining the distribution of the compression index and swelling index across the study area, as well as their variations with soil depth. Figure 4.9 illustrates that the compression index of soils in Erbil city center exhibited values ranging from 0.17 to 0.22, with lower values observed at greater depths. The compression index plays a significant role in determining soil compression and consolidation characteristics. The findings indicate that shallow soil layers in the study area possess a high potential for consolidation and settlement, while the settlement potential is expected to decrease with depth due to variations in compression indices.

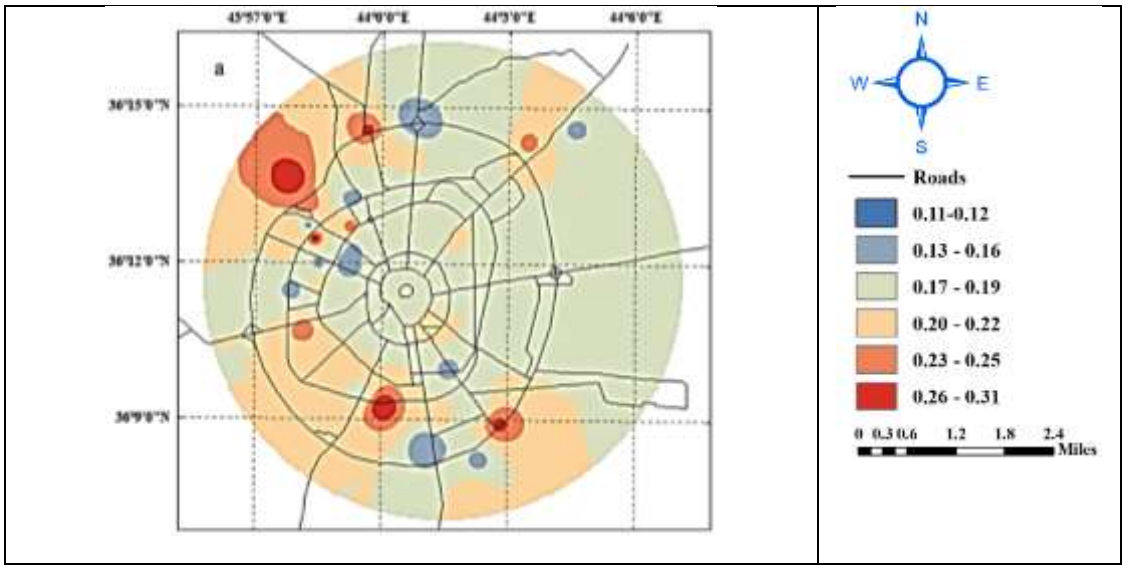


Figure 4.9-a Compression index for soil layer at depth, 1.5-3.5m.

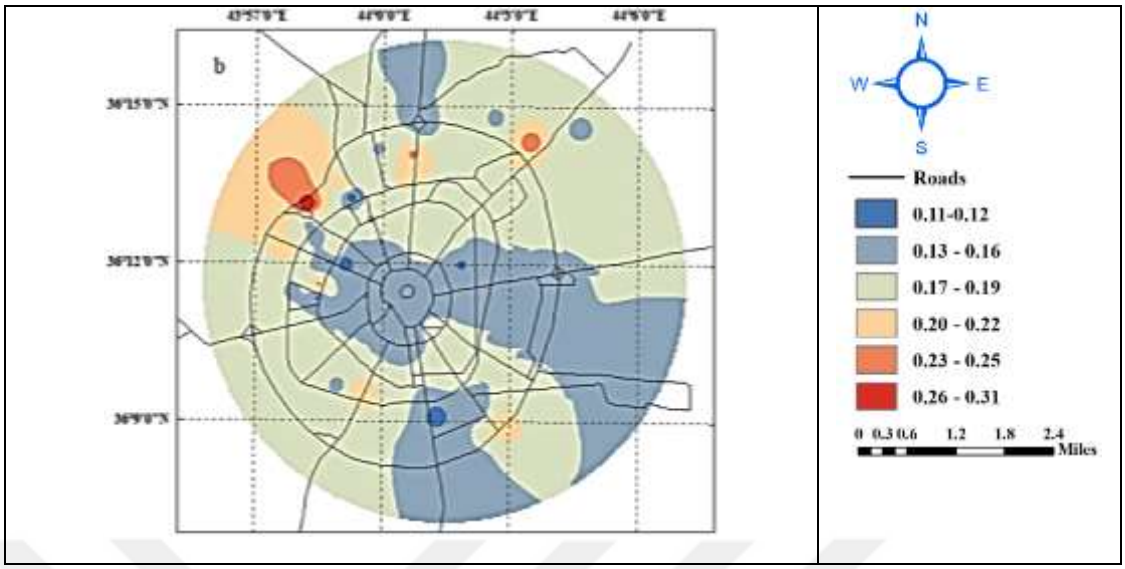


Figure 4.9-b Compression index for soil layer at depth, 3.5-3.5m.

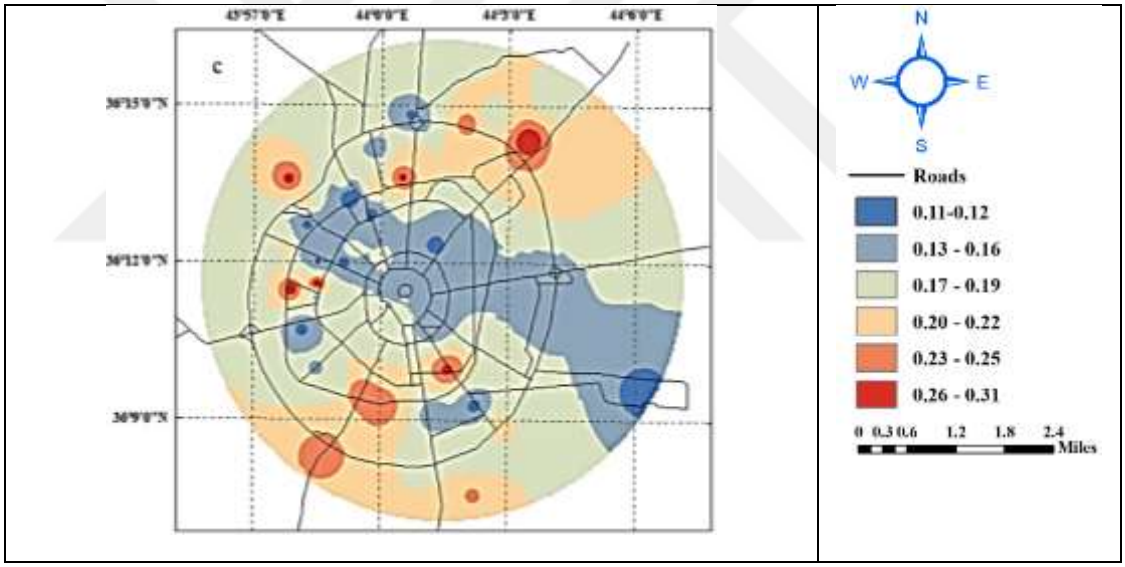


Figure 4.9-c Compression index for soil layer at depth, 6.5-9.5m.

Figure 4.10 provides insights into the rebound index, an important parameter in geotechnical engineering that indicates the soil's tendency to undergo expansion or contraction in response to changes in moisture content. A high rebound index value signifies increased susceptibility to expansion and contraction, while a low value indicates greater stability. The findings depicted in Figure 4.10 suggest that the soil in the study area exhibits moderate to low rebound index values, ranging from 0.015 to 0.078. This indicates that the soil is relatively stable and less prone to expansion or contraction in the presence of varying moisture content. Consequently, the study

concludes that there is no significant potential for soil swelling or shrinkage in the investigated area.

Figure 4.10 illustrates a consistent trend of minimum values across all levels within the study area. The highest swelling index values were observed in the northern region of Erbil at the first level, while in the southern area at the second and third levels. The majority of the examined area displayed moderate parameter values ranging from 0.015 to 0.078. These findings align with previous research studies conducted by Aldefae et al. (2020), Nareeman and Fattah (2007), and Qurtas (2018) regarding consolidation parameters. In summary, the consolidation parameters, including the compression index and swelling index, hold significant importance and should be thoroughly assessed during the analysis and design of foundations on clayey soils. These parameters can significantly impact the stability and performance of foundation systems. Therefore, appropriate measures must be implemented to ensure the safety and durability of the foundations.

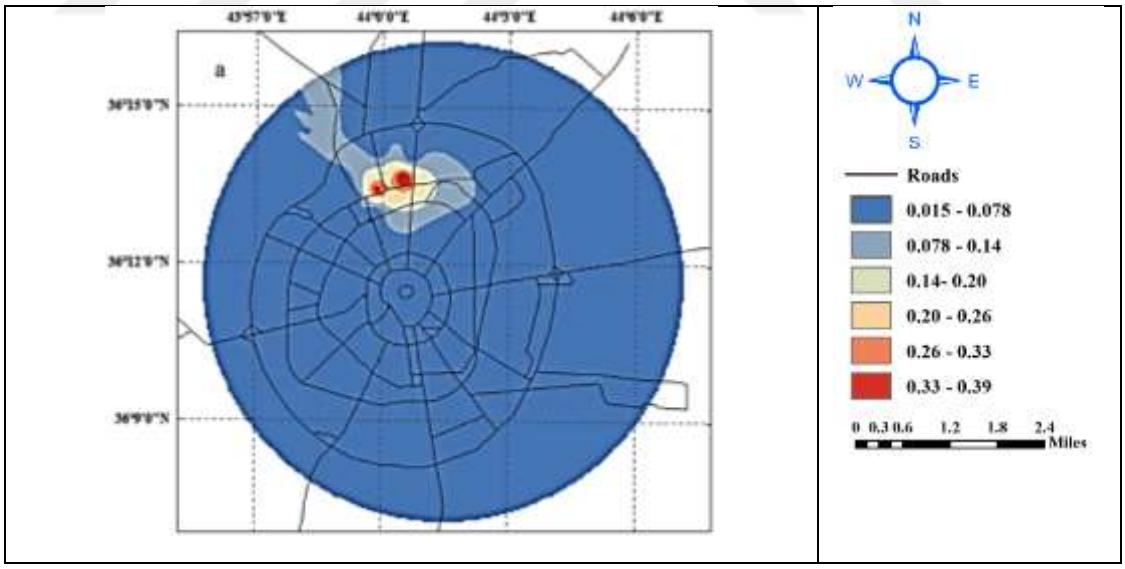


Figure 4.10-a Rebound index for soil layer at depth, 1.5-3.5m.

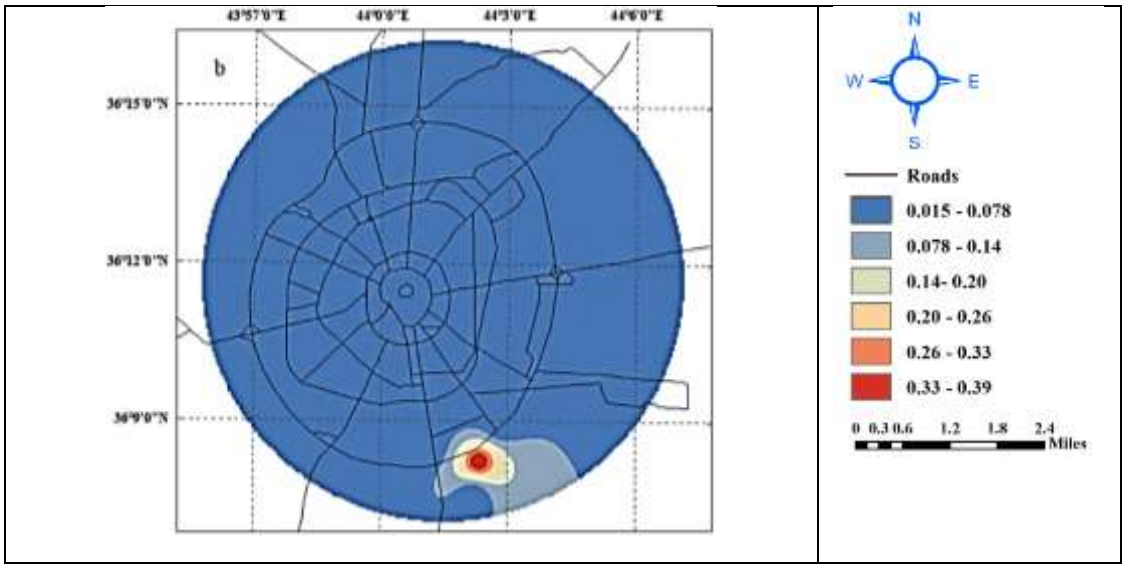


Figure 4.10-b Rebound index for soil layer at depth, 3.5-6.5m.

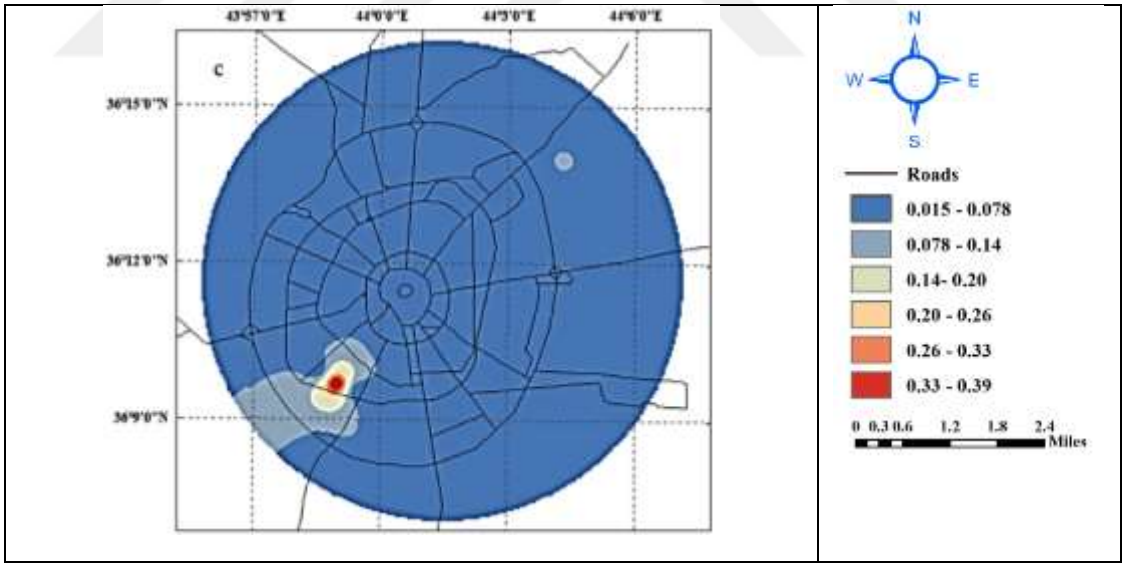


Figure 4.10-c Rebound index for soil layer at depth, 6.5-9.5m.

4.2.7 SPT-N value

SPT is widely employed as one of the commonly used in-situ testing methods to determine soil type, stratigraphy, and relative strength parameters during site investigations (Bowles, 1982; Kumar, 2016). However, in the eastern part of Erbil,

higher SPT values were observed, which can be attributed to the presence of stiffer and stronger soil layers, as well as the higher unit weight of soils, as depicted in Figure 4.11.

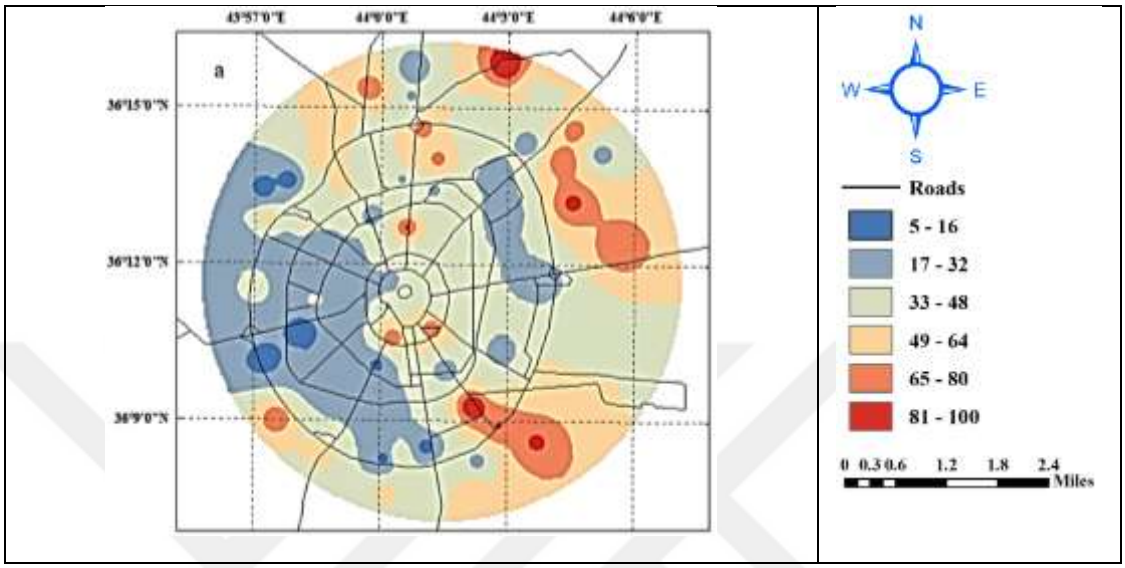


Figure 4.11-a SPT-N Value model for soil layer at depth, 1.5-3.5m.

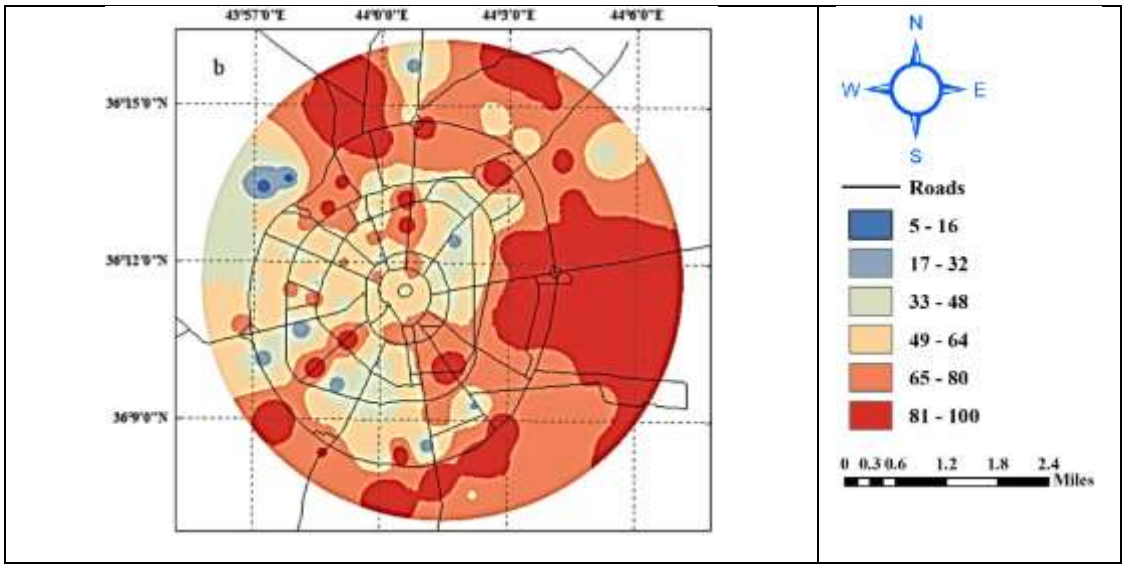


Figure 4.11-b SPT-N Value model for soil layer at depth, 3.5-3.5m.

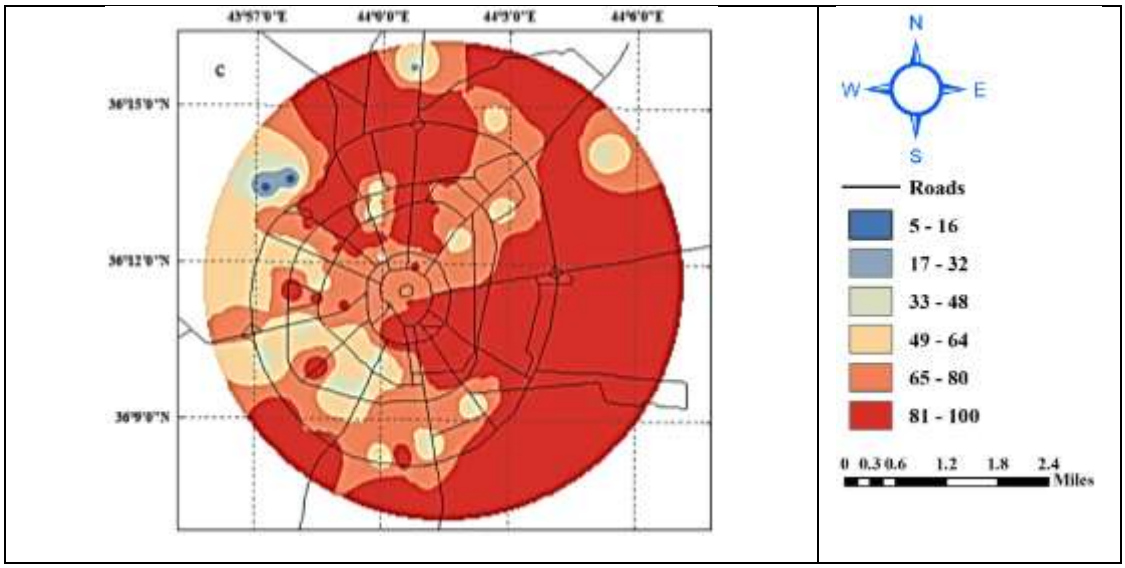


Figure 4.11-c SPT-N Value model for soil layer at depth, 6.5-9.5m.

At a depth of 6.5 m - 9.5 m, the SPT values of soils primarily ranged from 35 to 60, with an increasing trend from west to east in the study area. This increase in SPT values with depth can be influenced by various factors. Soil type plays a significant role, as different soil types possess distinct characteristics such as density, porosity, and strength, all of which impact the SPT results. Additionally, the unit weight, representing the weight per unit volume of soil, also contributes to the variation in SPT values, as higher unit weights tend to yield higher SPT values.

The increase in confining pressure, which refers to the pressure exerted on the soil by the surrounding materials, as depth increases, contributes to higher SPT values. These SPT values provide valuable insight into the soil's strength and its variations throughout the study area. To further establish the relationship between SPT values and shear strength parameters such as cohesion and angle of internal friction, data obtained from boreholes were analyzed. Figures 4.12 and 4.13 display the correlation between SPT values and shear strength parameters for the soils within the study area. The figures clearly demonstrate a strong correlation between SPT values, cohesion, and angle of internal friction. In general, most of the SPT-N values within the study area, from the center to the west of Erbil City, range from 17 to 48, while in the northeast and southeast regions, the values are higher than 50. These findings align with various studies (Hasan et al., 2020; Myslivec and Kysela, 2014) that indicate the soil in Erbil City is medium to very dense based on the SPT-N results.

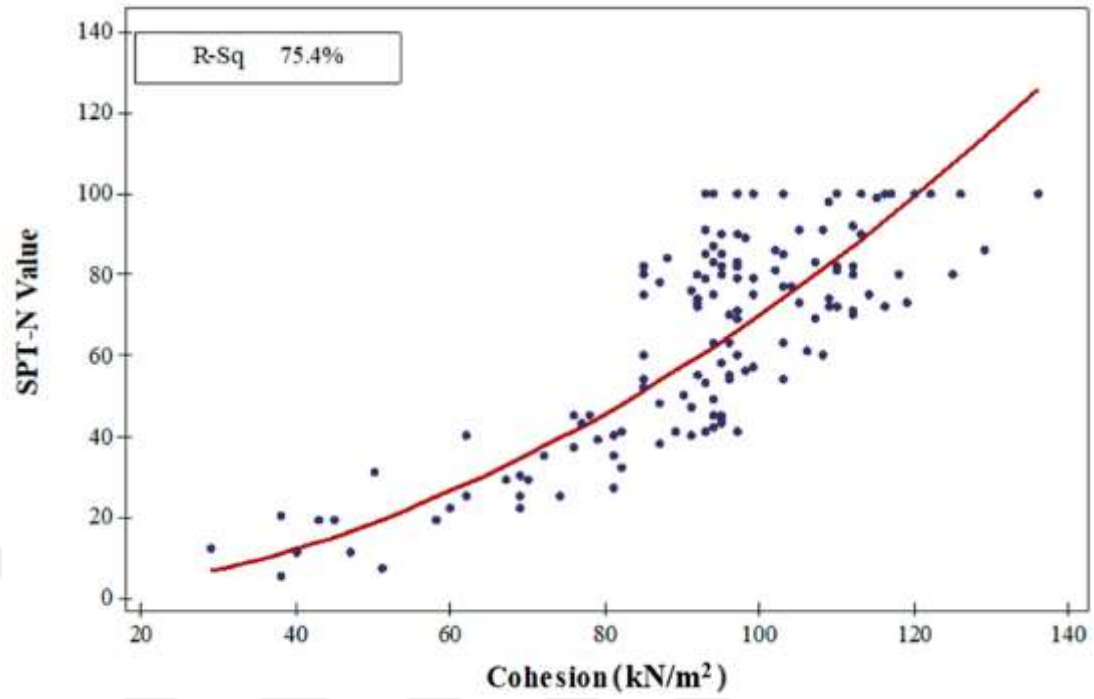


Figure 4.12 Correlation of SPT-N values with cohesion of soils in the study area.

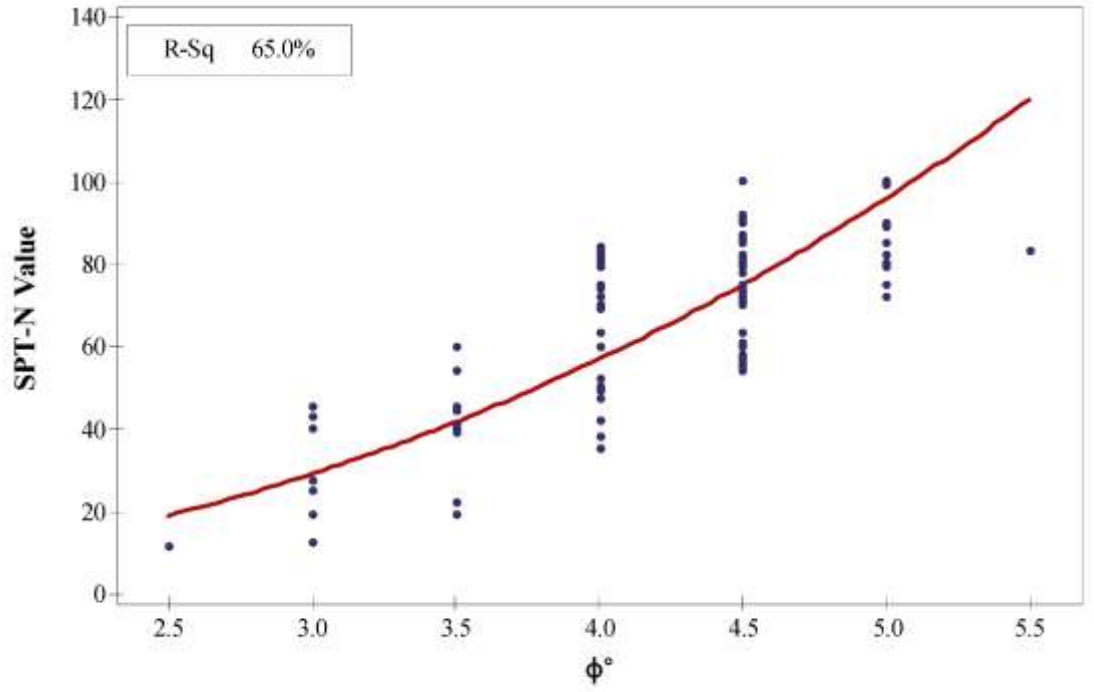


Figure 4.13 Correlation of SPT-N values with angle of internal friction (ϕ) of soils in the study.

4.2.8 Bearing Capacity

The bearing capacity of soil plays a crucial role in the design of footings. Various methods exist to estimate soil bearing capacity, taking into account factors such as soil shear strength, type of footing, and SPT (Standard Penetration Test) values (Dauji and Rafi, 2021). In this study, the ultimate bearing capacity of the soil layers was estimated using two approaches: one based on shear strength parameters using Meyerhof's equation and the other based on SPT-N values, as discussed in Chapter 3.The variation in the soil strata's ultimate bearing capacity, determined by Meyerhof's equation, is presented in Figure 4.14.

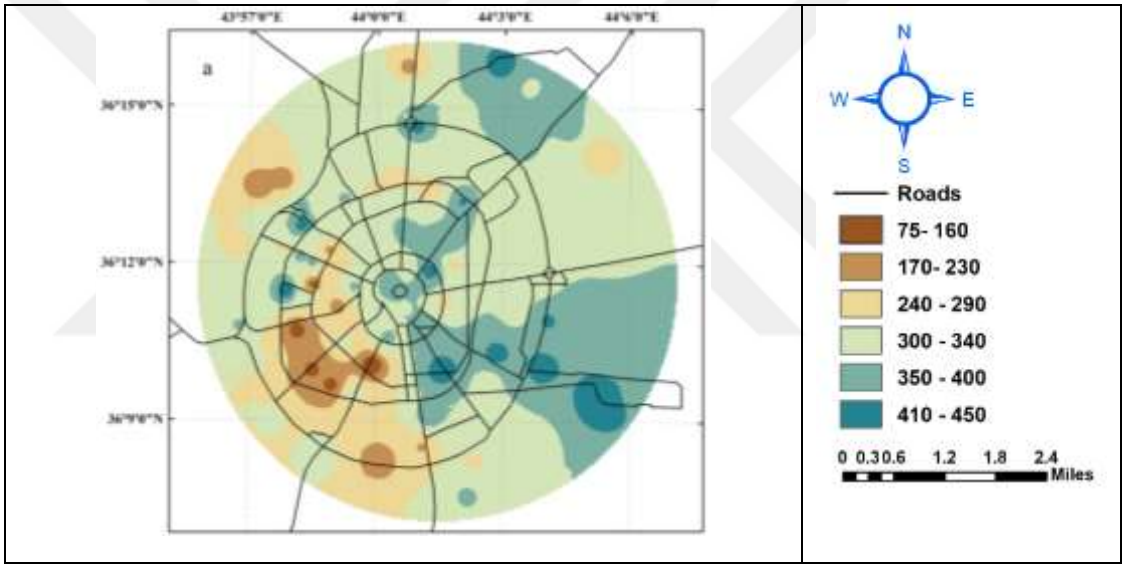


Figure 4.14-a Ultimate bearing capacity model (kN/m^2) for soil layer according to Meyerhof's equation at depth, 1.5-3.5m.

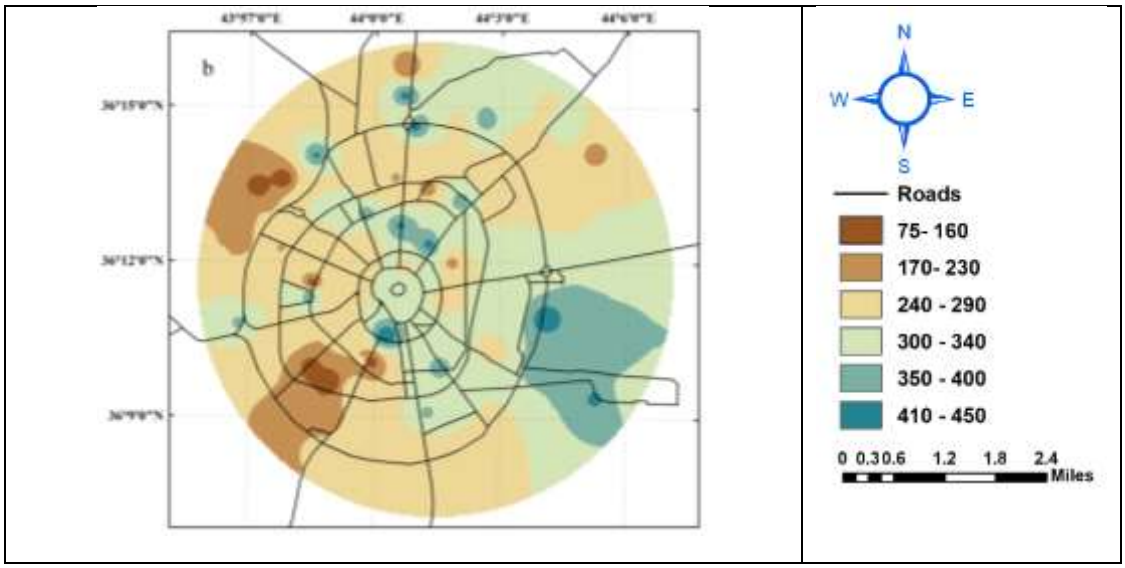


Figure 4.14-b Ultimate bearing capacity model (kN/m^2) for soil layer according to Meyerhof's equation at depth, 3.5-6.5m.

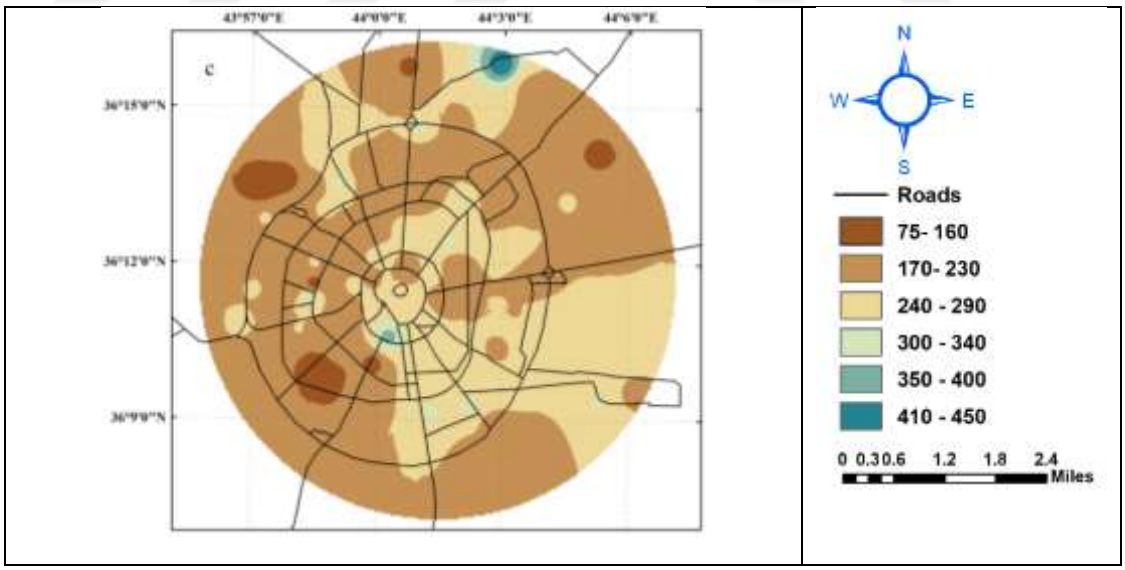


Figure 4.14-c Ultimate bearing capacity model (kN/m^2) for soil layer according to Meyerhof's equation at depth, 6.5-9.5m.

Figure 4.15 illustrates the ultimate bearing capacity of the soil strata at three different depths within the study area, estimated from the SPT values. The findings reveal variations in the ultimate bearing capacity across the study region.

The ultimate bearing capacity of soil layers within the examined region holds significant importance in the design of both shallow and deep foundations. Based on the results presented in Figure 4.14, the majority of the study area at shallow depths exhibited an ultimate bearing capacity ranging between 170 kPa and 940 kPa. However, smaller areas with lower ultimate bearing capacities were also observed. It is worth noting that the ultimate bearing capacity increased with greater depth, which can be attributed to the escalation in soil confining pressure and soil unit weight. These findings provide valuable insights for determining the design parameters and load-bearing capacity of foundations within the study area.

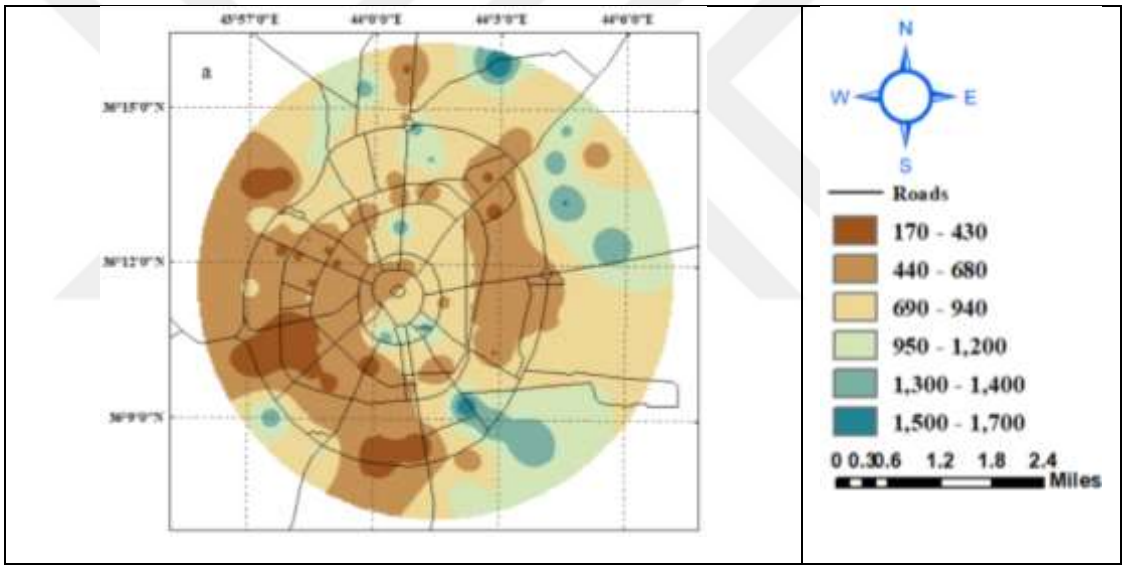


Figure 4.15-a Ultimate bearing capacity model (kN/m^2) from SPT-N value at depth, 1.5-3.5m.

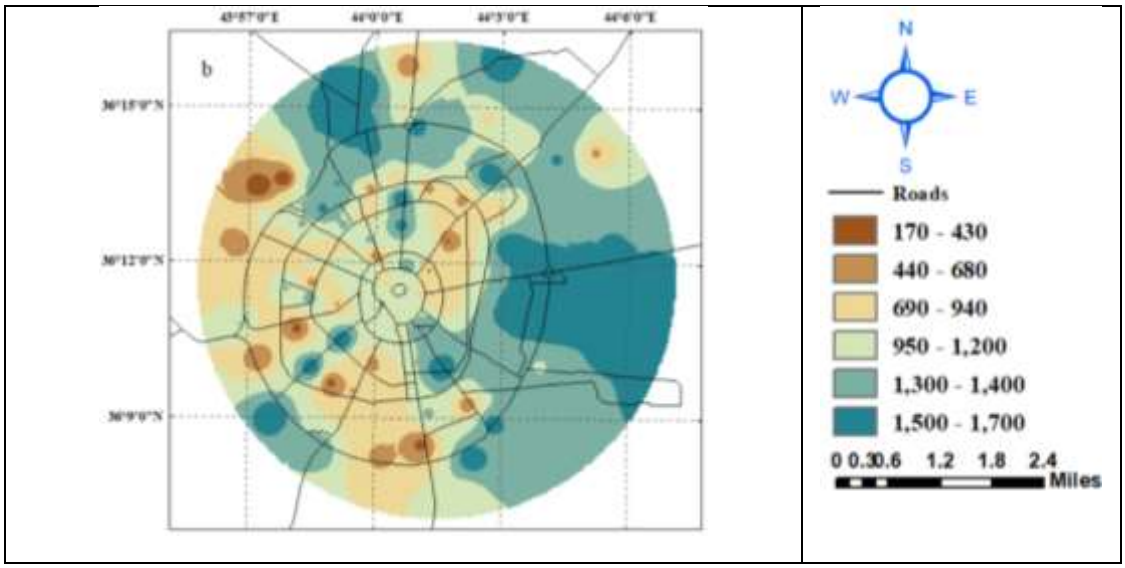


Figure 4.15-b Ultimate bearing capacity model (kN/m^2) from SPT-N value at depth, 3.5-6.5m.

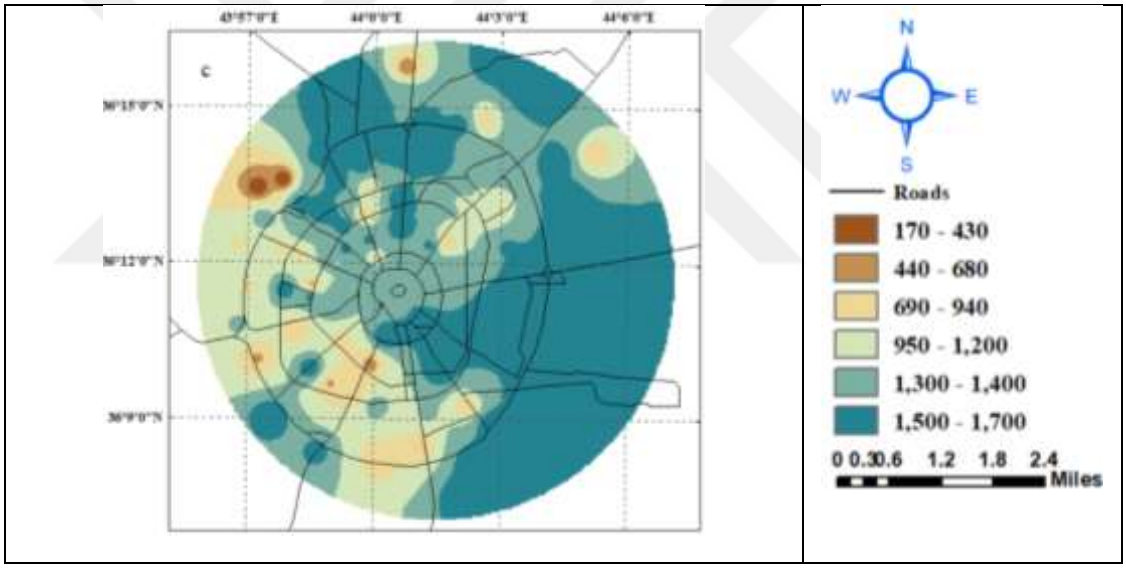


Figure 4.15-c Ultimate bearing capacity model (kN/m^2) from SPT-N value at depth, 3.5-6.5m.

Figure 4.16 depicts the correlation between the ultimate bearing capacity obtained from Meyerhof's equation and the SPT values of the soils in the study area. The figure demonstrates a strong correlation between the SPT values and the ultimate bearing capacity of the foundations. Furthermore, Figure 4.17 displays the correlation between the ultimate bearing capacity derived from the SPT values of the soil strata within the study area and the soil cohesion (shear strength parameter). Estimating the ultimate bearing capacity based on SPT values is a relatively straightforward approach

compared to other methods that involve more extensive experimental tests and complex equations based on shear strength parameters of the soil. This method relies on empirical correlations and has gained widespread use in the field of geotechnical engineering. Its advantage lies in its simplicity; however, it may not precisely represent the actual soil conditions, which can be influenced by factors such as soil type, stratigraphy, and loading conditions (Dauji and Rafi, 2021).

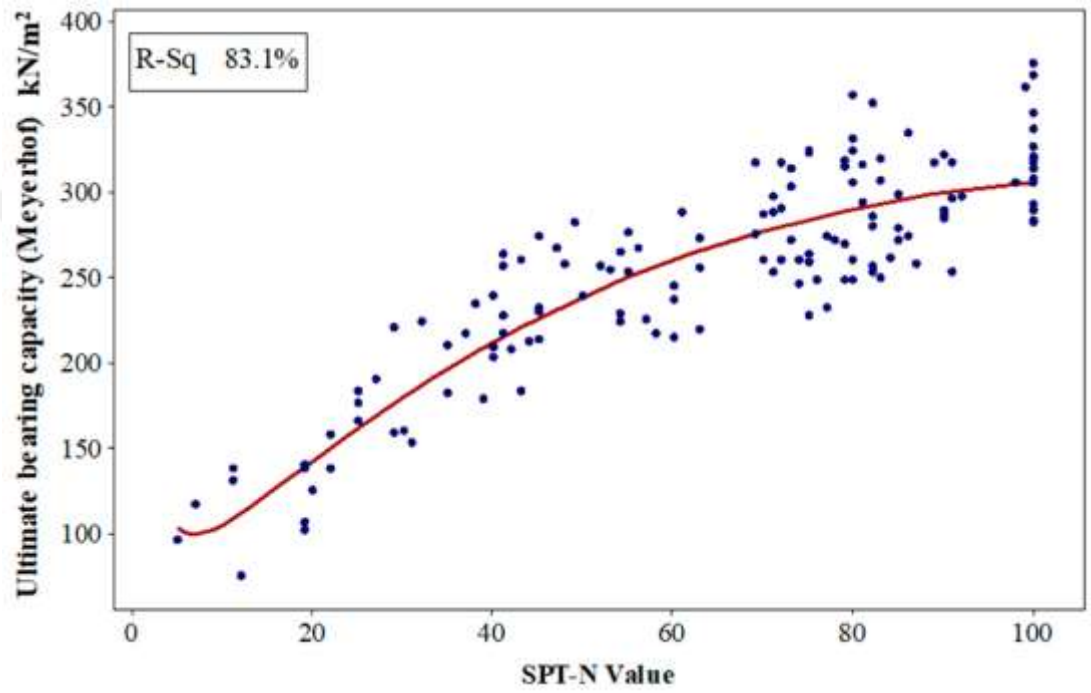


Figure 4.16 Correlation of ultimate bearing capacity (Meyerhof) with SPT-N values of soils in study area.

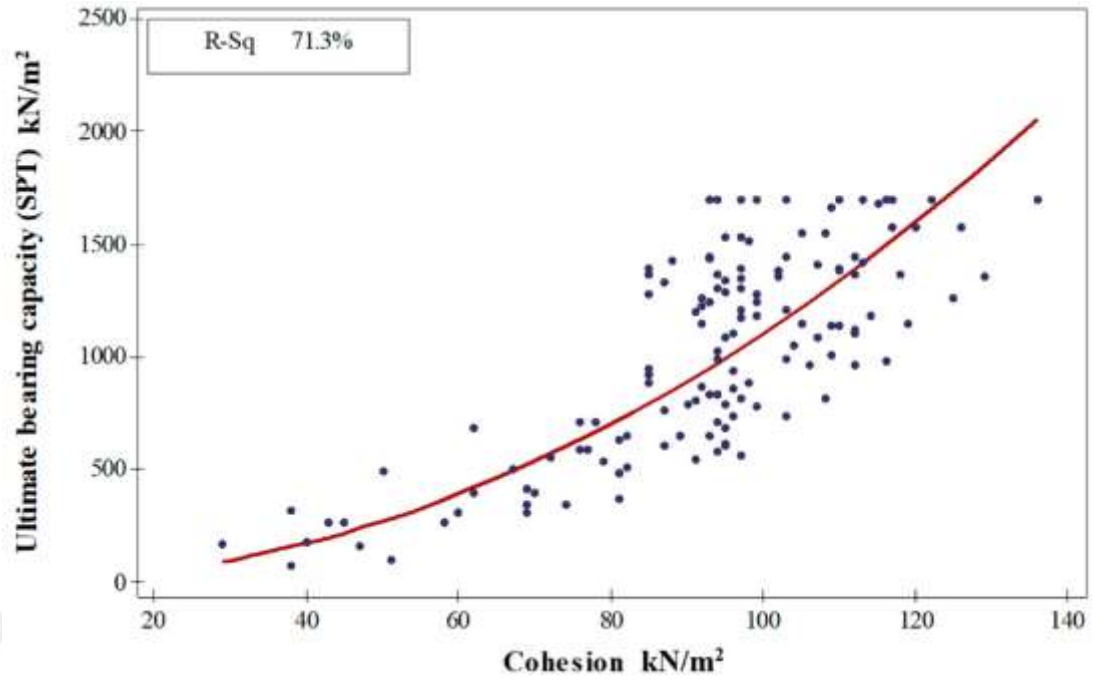


Figure 4.17 Correlation of ultimate bearing capacity (SPT-N) with soil cohesion of soils in study area.

4.3 Artificial Neural Network

Artificial Neural Network (ANN) models are commonly employed for regression and classification tasks, including prediction problems. These models comprise interconnected nodes, known as artificial neurons, which process and transmit information. The nodes are organized into layers, and the links between them can be adjusted during the training phase to minimize the discrepancy between the expected and observed outcomes.

ANN models have gained widespread acceptance in various fields due to their ability to handle complex relationships and provide accurate predictions. In several models, the relationship between the predicted original SPT values and bearing capacity was demonstrated using training and testing data. These models exhibit acceptable R^2 values, indicating a good fit to the data, and minimal error, demonstrating their efficacy in predicting the relationship between SPT values and bearing capacity. Once the input and output data were collected and organized, training and testing sets were created. The training set consisted of 70% of the borehole data, while 15% were used for testing, and another 15% were reserved for validation purposes. Prediction for SPT-N value from two models was enveloped (Souri et al., 2018).

In this study using a feed-forward back-propagation network model to predict SPT-N and Q-Ultimate with includes 306 data from three different level field works. Therefore, at the first phase SPT-N value were predicted from eight models with different parameters as consist of Atterberg limit values, water content, cohesion, internal of friction, fine content. In the second and third phases, the estimation of Q-Ultimate was carried out using various parameters, including Atterberg limit values, water content, cohesion, angle of internal friction, and fine content. Additionally, in the third phase, the SPT-N value was incorporated into the model to improve the estimation accuracy. By integrating these parameters, the model was able to estimate the Q-Ultimate values for the specific phases under consideration. In the supervised learning ANN algorithm, the learning ability of a neural network is influenced by its architecture and the training process algorithm, with the optimal value of the ANN determined by observing the correspondence between predicted and actual values. R^2 is one of the most important parameters used to assess this correspondence, with values ranging between 0 and +1. Chin (1998) categorized the accuracy level of R^2 as substantial, moderate, or weak, as shown in Table 4.1.

Table 4.1 Accuracy of coefficient determination (Chin, 1998)

R^2	Desired Value
0.67	Substantial
0.33	More Moderate
0.19	Weak

4.3.1 Prediction for SPT-N Value

Once the input and output data were collected and arranged, training and testing sets were created. Out of the total 306 data points from the boreholes, 70% (214 data points) were allocated for training the models, 15% (46 data points) were set aside for testing, and the remaining 15% were used for validation purposes. Eight models were developed to predict the SPT-N value, and their results were presented collectively. Specifically, the results for group-A are illustrated in Figures 4.18 to 4.25, showcasing the predictions generated by the Artificial Neural Network (ANN) models.

ANNs have been widely used in geotechnical engineering for predicting various soil properties, including SPT-N value. ANNs have the capability to learn complex

relationships and patterns from the input data and predict accurate outputs. In the case of SPT-N value prediction, ANNs can be trained using various input parameters such as soil composition, Atterberg limits, moisture content, cohesion, and internal friction angle.

The prediction of SPT-N values using ANNs has become a popular approach in geotechnical engineering due to their ability to handle complex relationships and make accurate predictions. In the study of (Erzin and Tuskan, 2016) mentioned, two ANN models were used to predict the SPT-N values based on different input variables, and both models showed good agreement between the predicted and measured values, with R^2 values of 0.92 and 0.90 for the training data, and 0.81 and 0.80 for the testing data, respectively.

The results of the ANN model for predicting the SPT-N values were presented in figures 4.18 to 4.25. Among these figures, figure 4.18 demonstrated a commendable level of correspondence between the predicted and measured SPT-N values. This indicates that the ANN model accurately predicted the SPT-N values based on the input variables used in the model. The strong correlation between the predicted and observed values indicates that the ANN model can serve as a dependable tool for predicting SPT-N values under comparable soil conditions. In Figure 4.18, the R^2 value was determined to be 0.92 for the training data and 0.81 for the testing data. The model employed Atterberg limit values, water content, cohesion, and angle of internal friction as input variables to predict the SPT value as its output. This indicates a strong correlation between the input variables and the predicted SPT values, with a high level of accuracy in both the training and testing datasets.

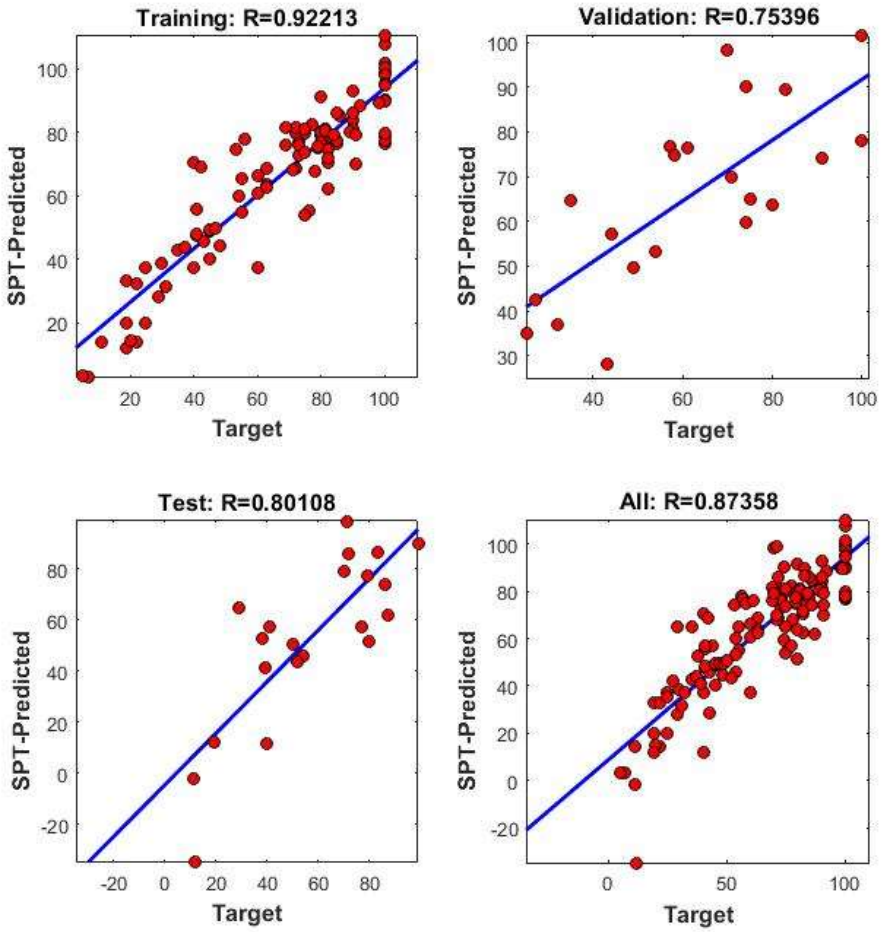


Figure 4.18 Model A relations between (LL, PL, PI, WC, c, ϕ, Fine cont) and SPT-N.

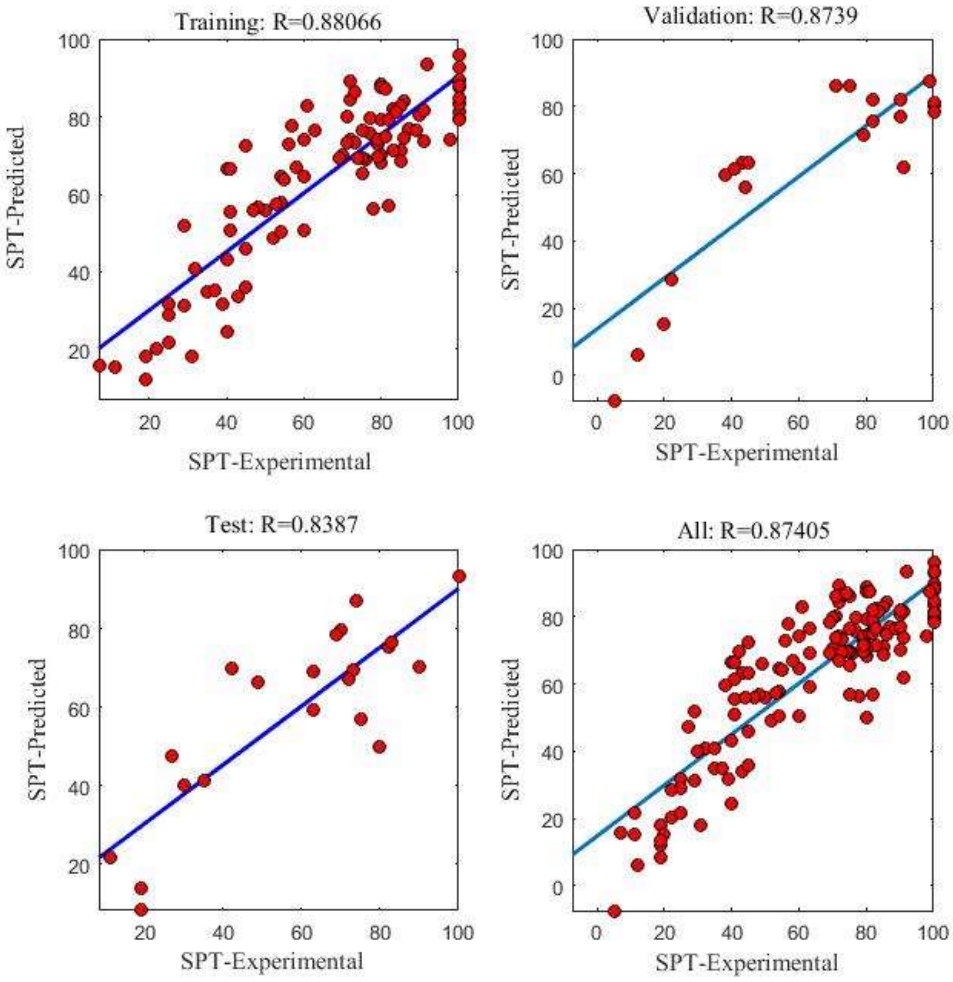


Figure 4.19 Model A1 relations between (LL, PL, PI, WC, c, ϕ) and SPT-N.

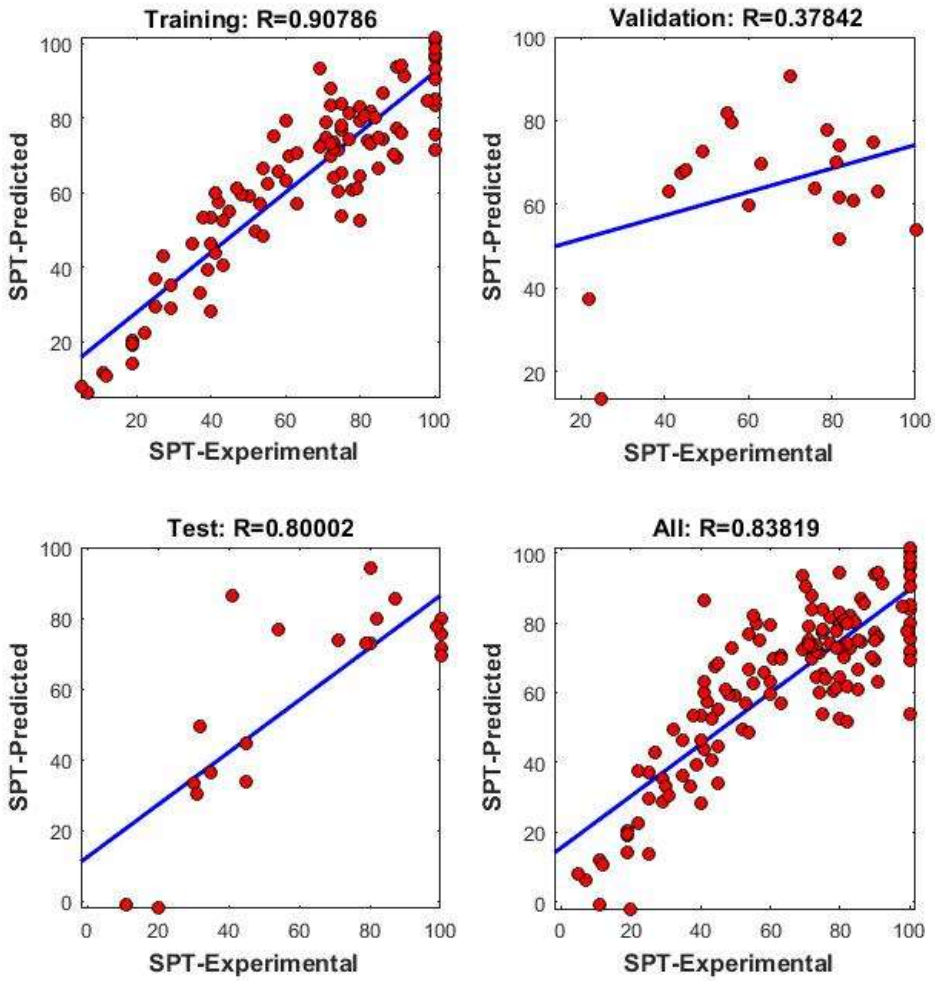


Figure 4.20 Model A2 relations between (LL, PL, PI, WC, ϕ) and SPT-N.

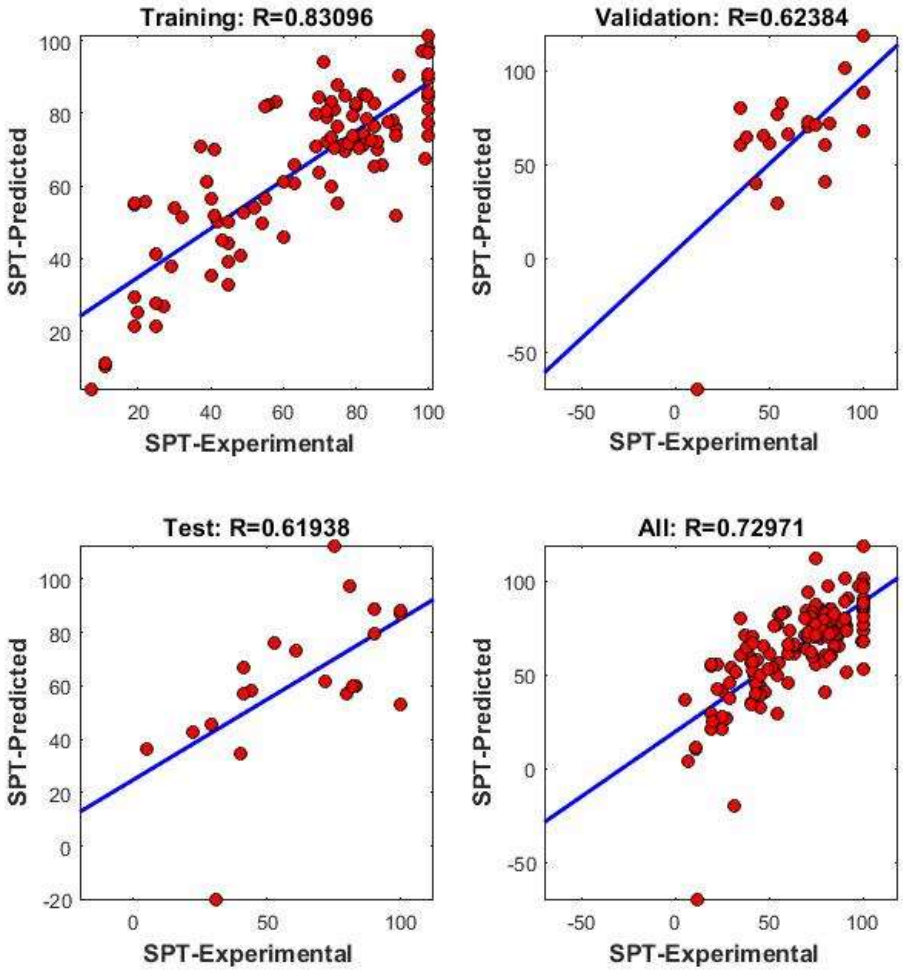


Figure 4.21 Model A3 relations between (LL, PL, PI, WC, c) and SPT-N.

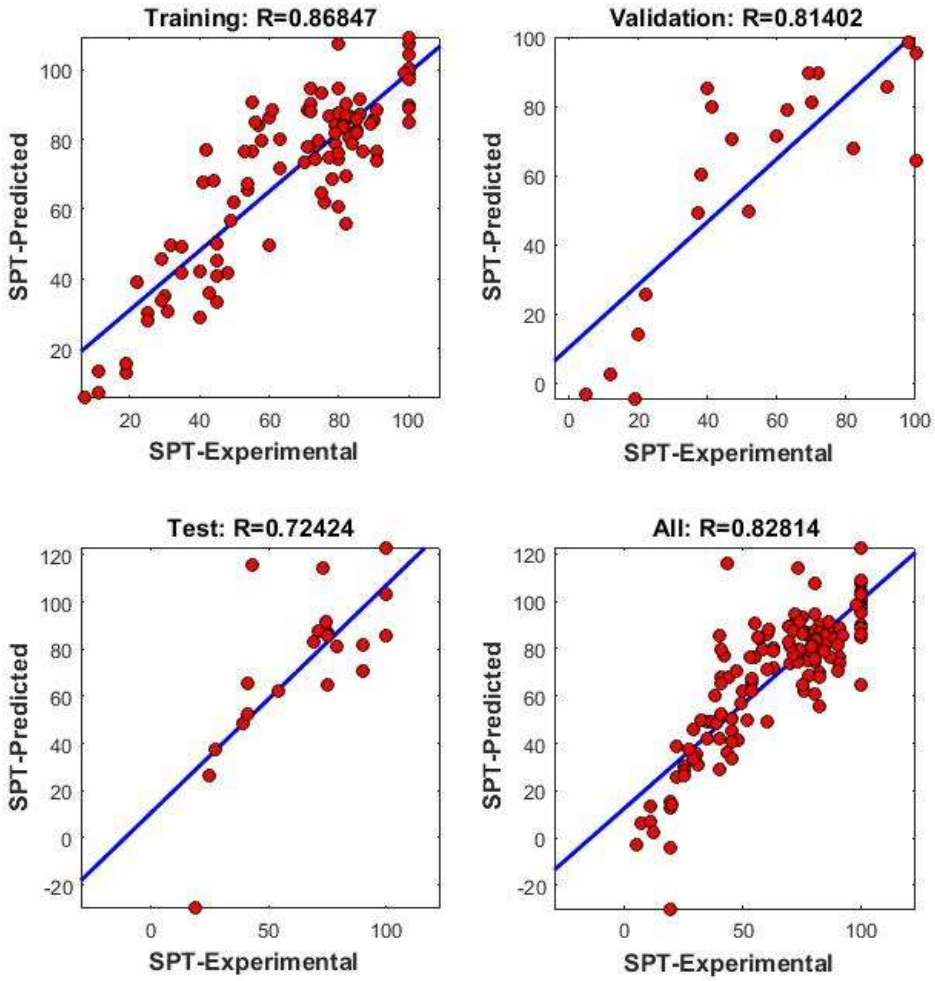


Figure 4.22 Model A4 relations between (LL, PL, PI, c, ϕ, Fine cont) and SPT-N.

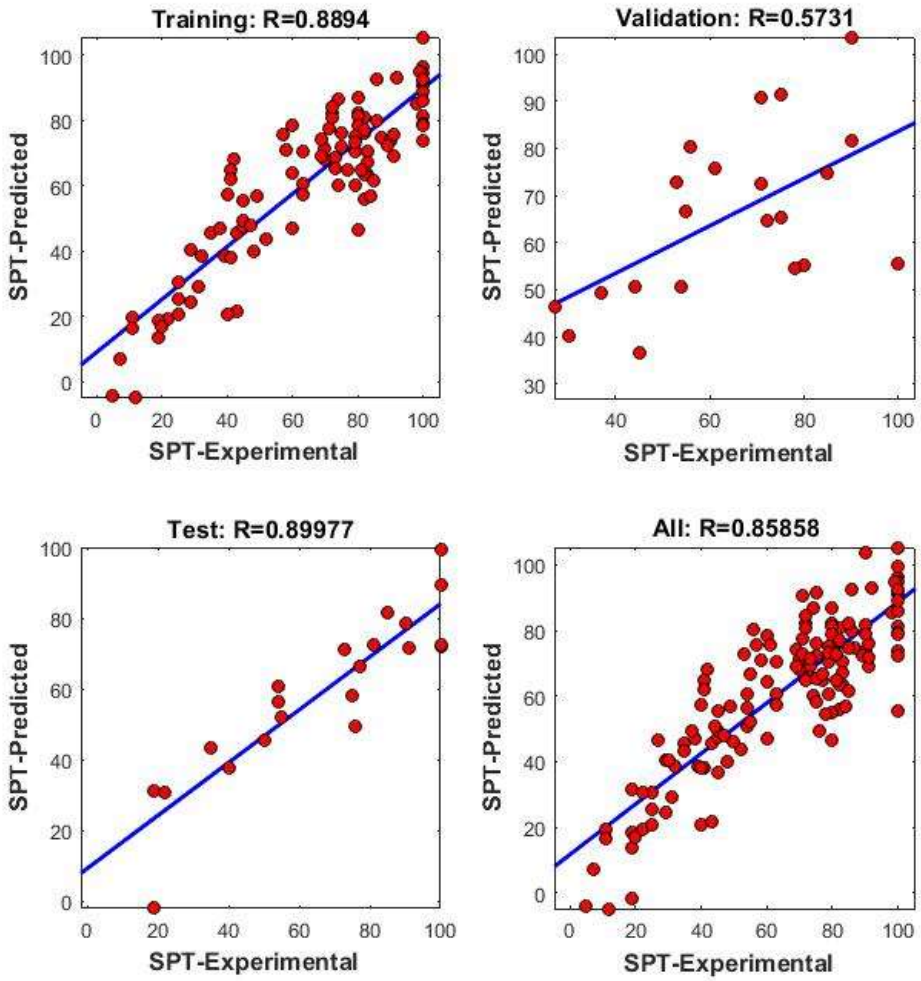


Figure 4.23 Model A5 relations between (LL, PL, WC, c, ϕ, Fine cont) and SPT-N.

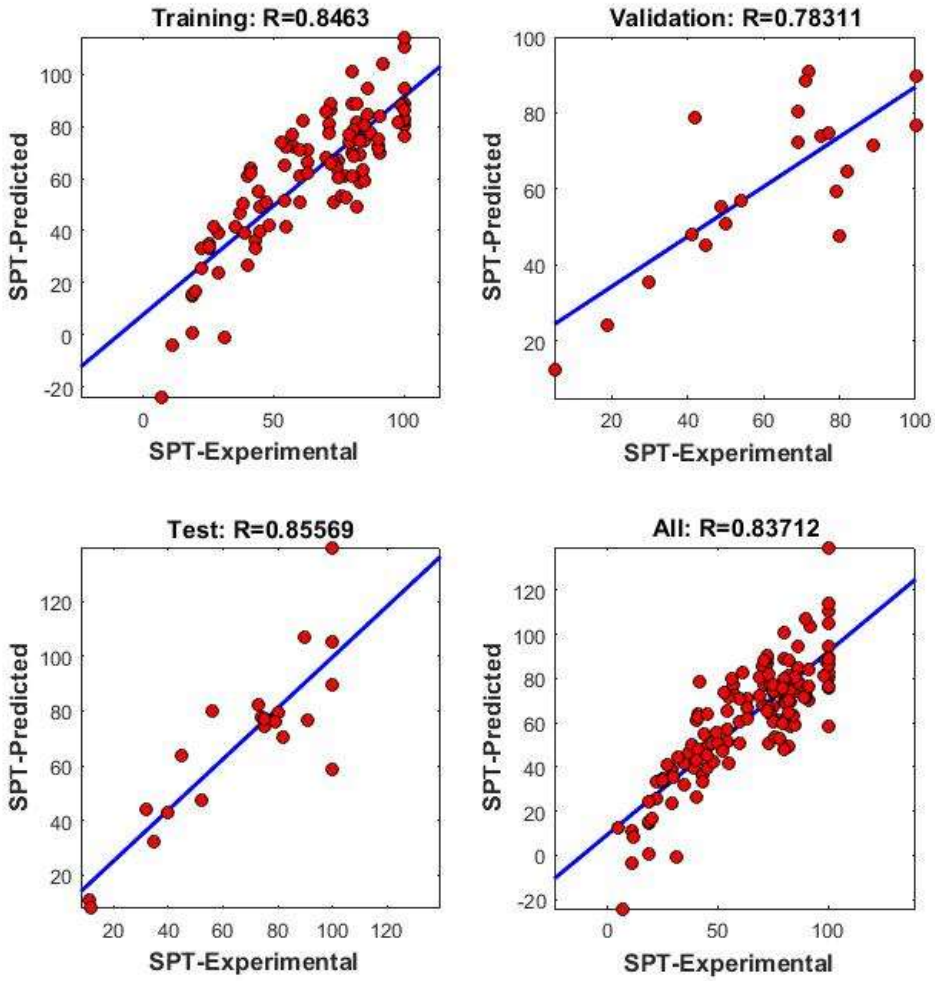


Figure 4.24 Model A6 relations between (LL, PI, WC, c, ϕ, Fine cont) and SPT-N.

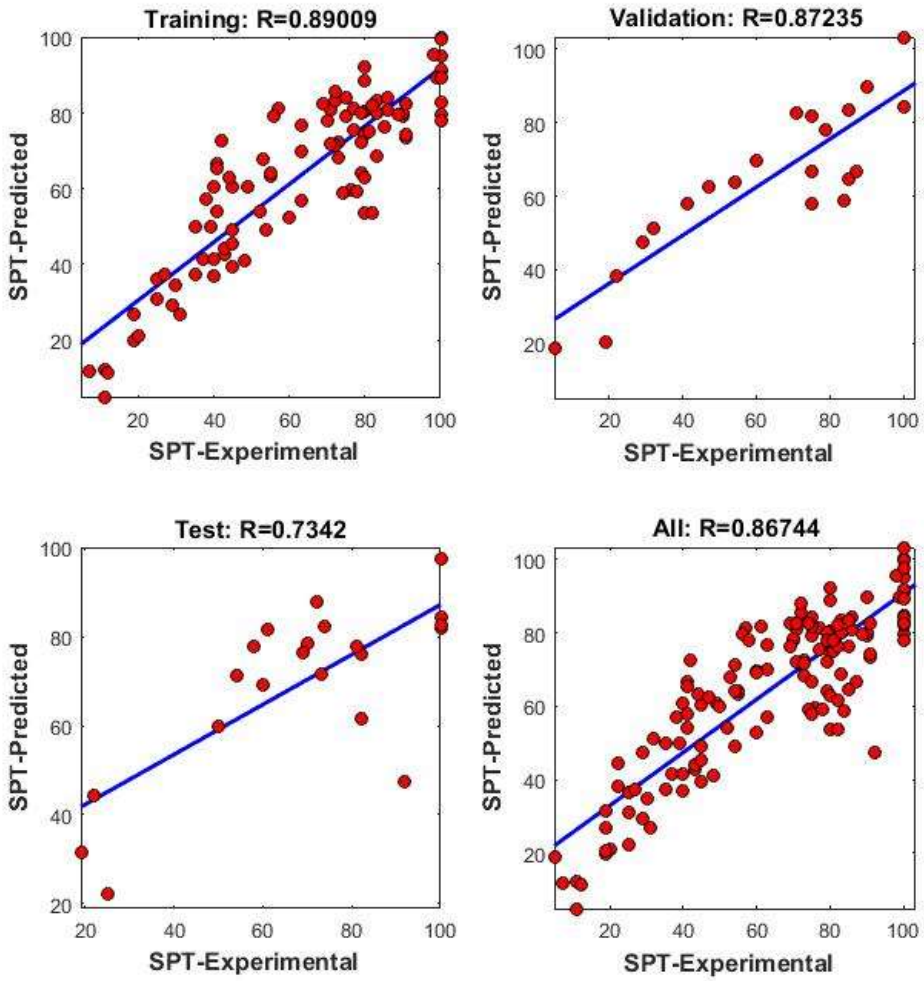


Figure 4.25 Model A7 relations between (PL, PI, WC, c, ϕ, Fine cont) and SPT-N.

Alternatively, by using input parameters such as LL%, PL%, PI%, WC, ϕ and fine content, the ANN models were able to predict the SPT N value as the output. The resulting R^2 values were determined to be 0.90 for the training dataset and 0.80 for the testing dataset. These values indicate a strong agreement between the predicted SPT values and the actual values. As mentioned in previous studies (Jasim et al., 2019), the R^2 values obtained in model (I) and model (II) demonstrate a significant level of agreement, highlighting the effectiveness of ANN modelling in geotechnical engineering. This modelling approach proves beneficial in the design of infrastructures by providing valuable insights and predictions for SPT values.

Similarly, in another study conducted by Fernando et al. (2021), ANNs were used to predict the SPT-N values. The study found that the ANN model showed R^2 values of 0.90 and 0.8 for the training and testing data, respectively. Overall, this demonstrates

the effectiveness of ANNs in predicting SPT-N values using various input parameters, highlighting the potential of ANNs in tables 4.2 and 4.3.

4.3.2 Prediction of Q-Ultimate Bearing Capacity

Using Artificial Neural Networks (ANNs) for predicting the ultimate bearing capacity of soil involves employing a machine learning technique. In this approach, a dataset comprising soil properties and corresponding ultimate bearing capacity values is used to train a neural network model. Once trained, this model can be utilized to forecast the ultimate bearing capacity of new soil samples based on their properties. The use of ANNs for prediction offers several advantages. Firstly, it allows for the handling of non-linear relationships between soil properties and ultimate bearing capacity, which may be challenging to capture using traditional analytical methods. Additionally, ANNs have the capability to incorporate complex relationships between soil properties and ultimate bearing capacity, allowing for a more accurate prediction. Furthermore, ANNs are well-suited for handling large datasets with numerous input variables, making them effective in analyzing and predicting the ultimate bearing capacity of soil based on a wide range of soil properties.

The outcomes of the bearing capacity prediction utilizing ANN modeling exhibit consistency with previous studies, as demonstrated in Jasim et al. (2019). Figures 4.26 to 4.33 depict the relationship between the predicted ultimate bearing capacity and the actual ultimate bearing capacity for both the training and testing datasets. These figures provide visual representations of the accuracy and effectiveness of the ANN model in predicting the ultimate bearing capacity.

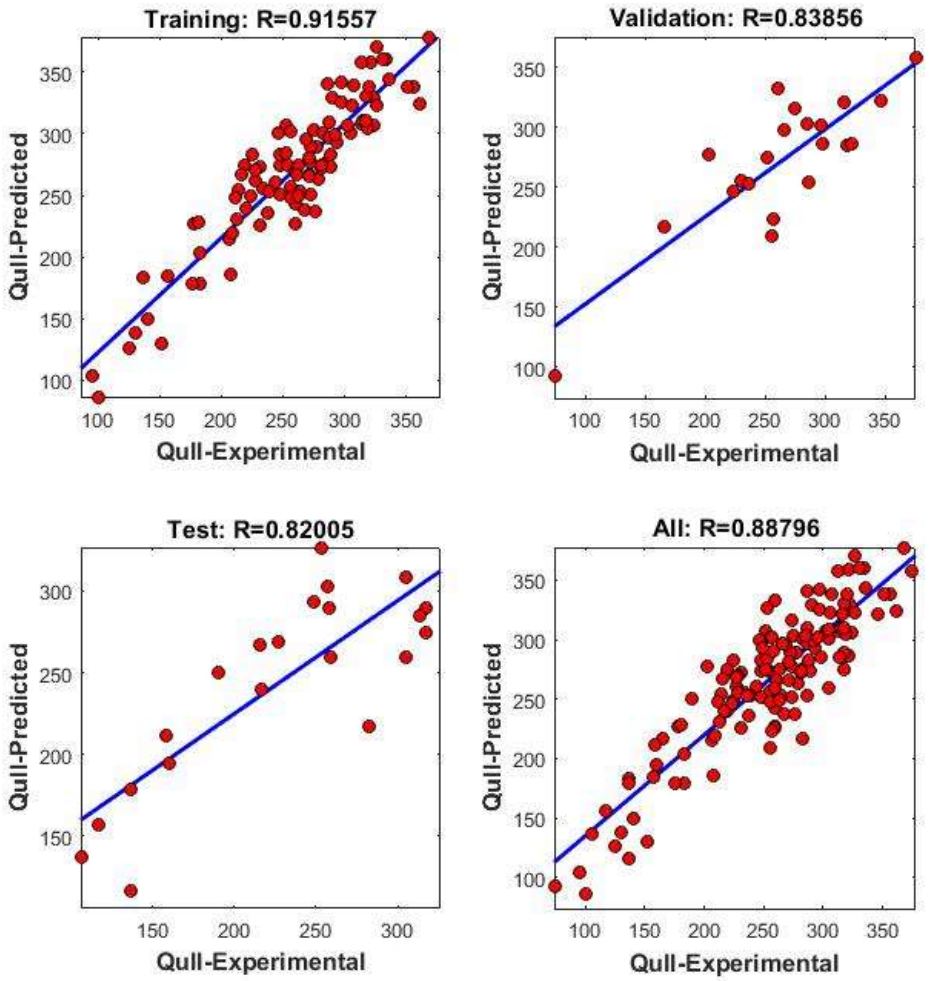


Figure 4.26 Model B relations between (LL, PL, PI, WC, c, ϕ, Fine cont) and Qultimate.

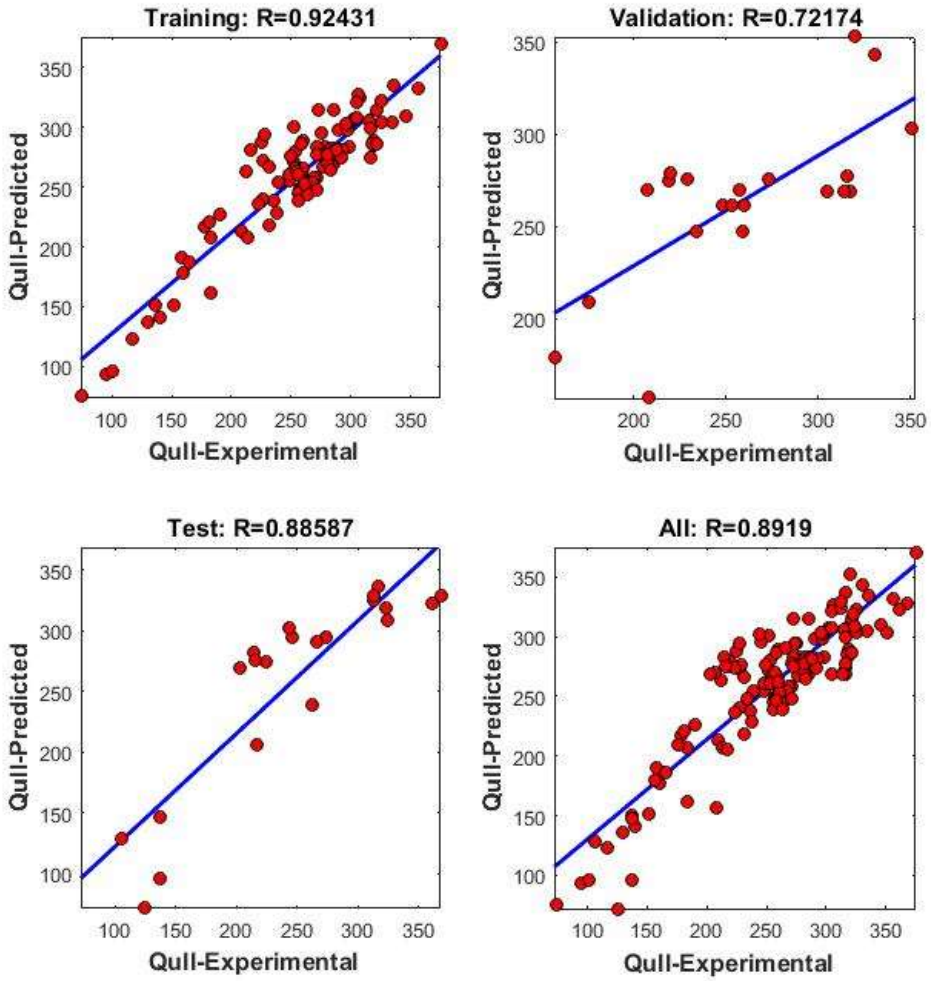


Figure 4.27 Model B1 relations between (LL, PL, PI, WC, c, ϕ) and Qultimate.

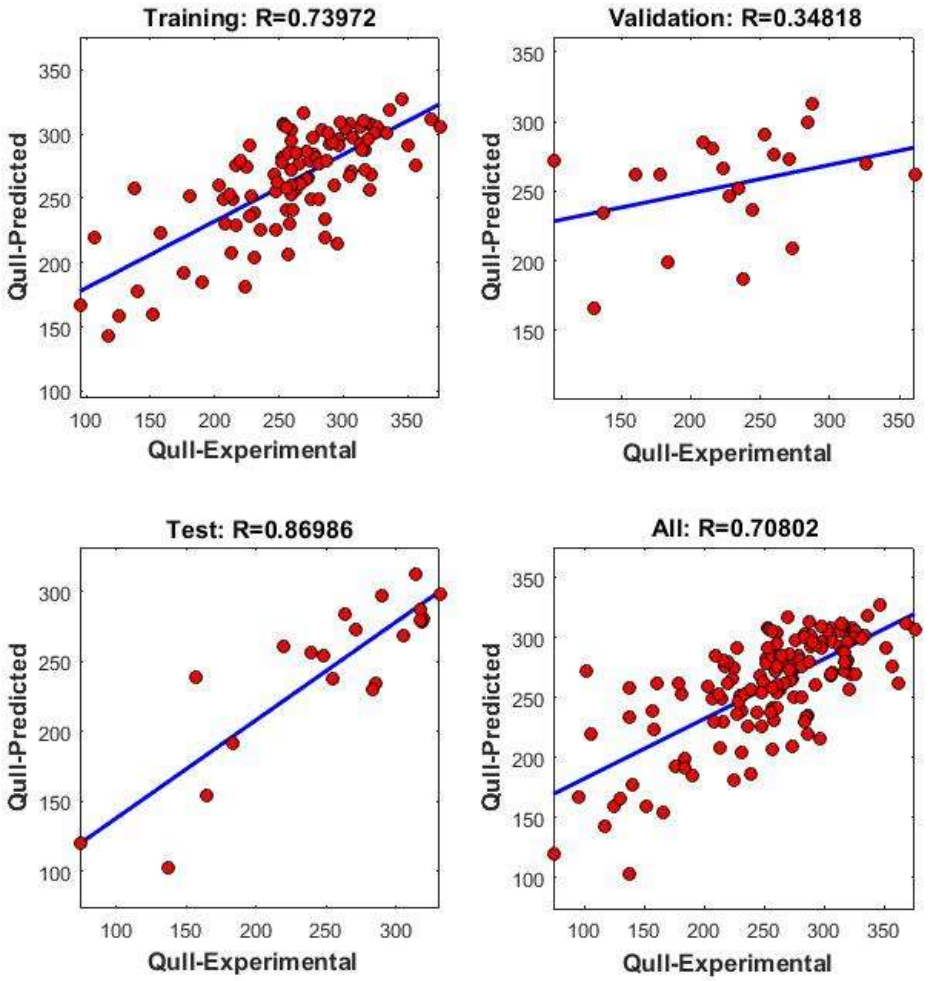


Figure 4.28 Model B2 relations between (LL, PL, PI, WC, ϕ) and Qultimate.

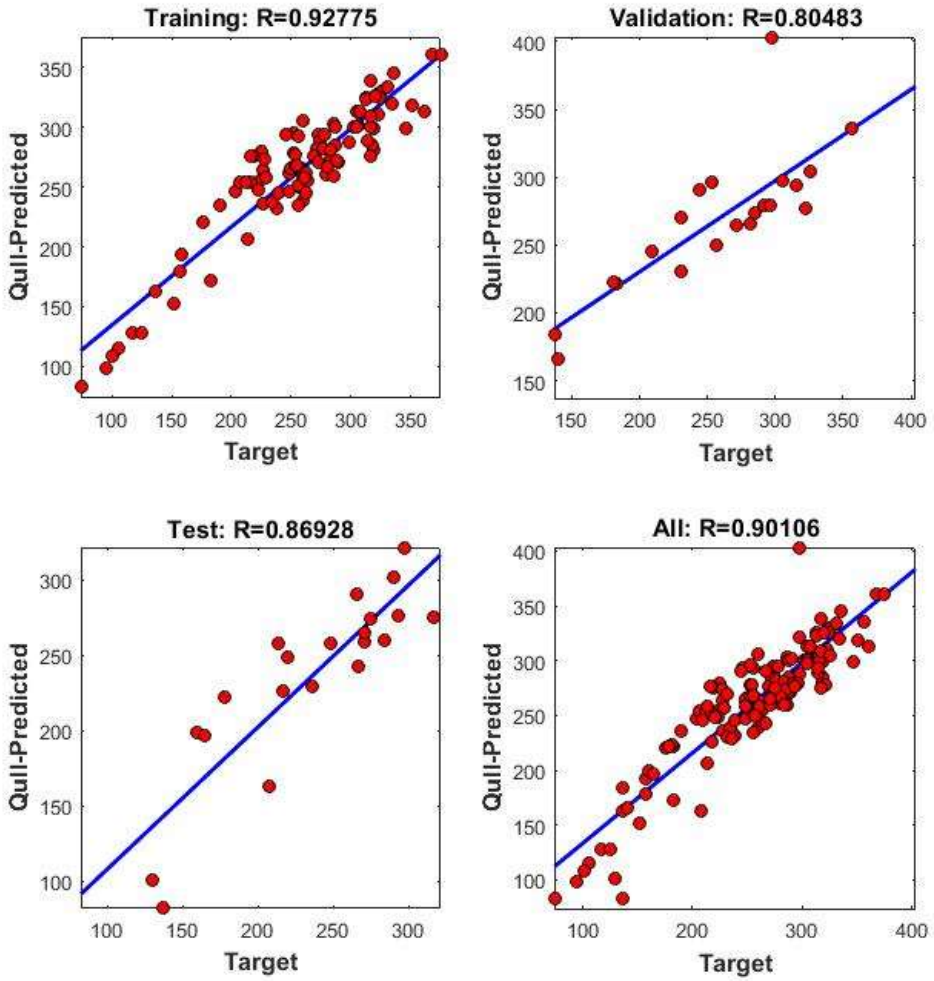


Figure 4.29 Model B3 relations between (LL, PL, PI, WC, c) and Qultimate.

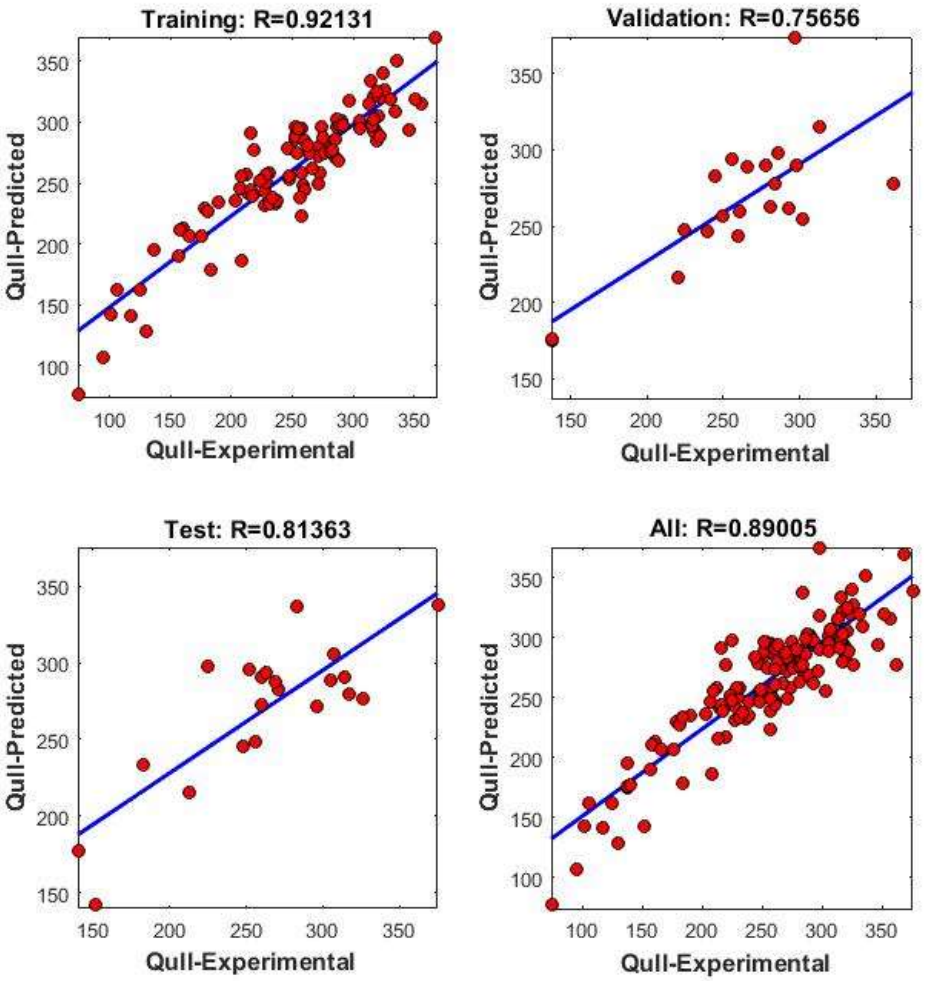


Figure 4.30 Model B4 relations between (LL, PL, PI, c, ϕ, Fine cont) and Qultimate.

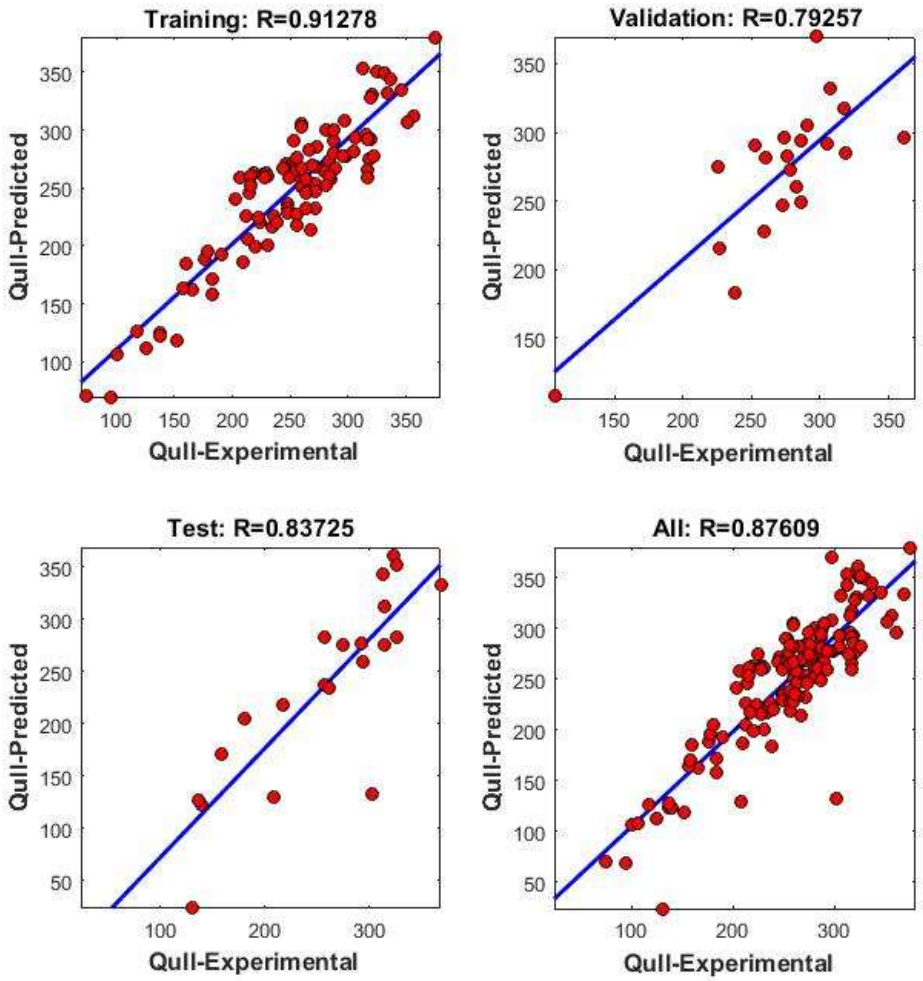


Figure 4.31 Model B5 relations between (LL, PL, WC, c, ϕ, Fine cont) and Qultimate.

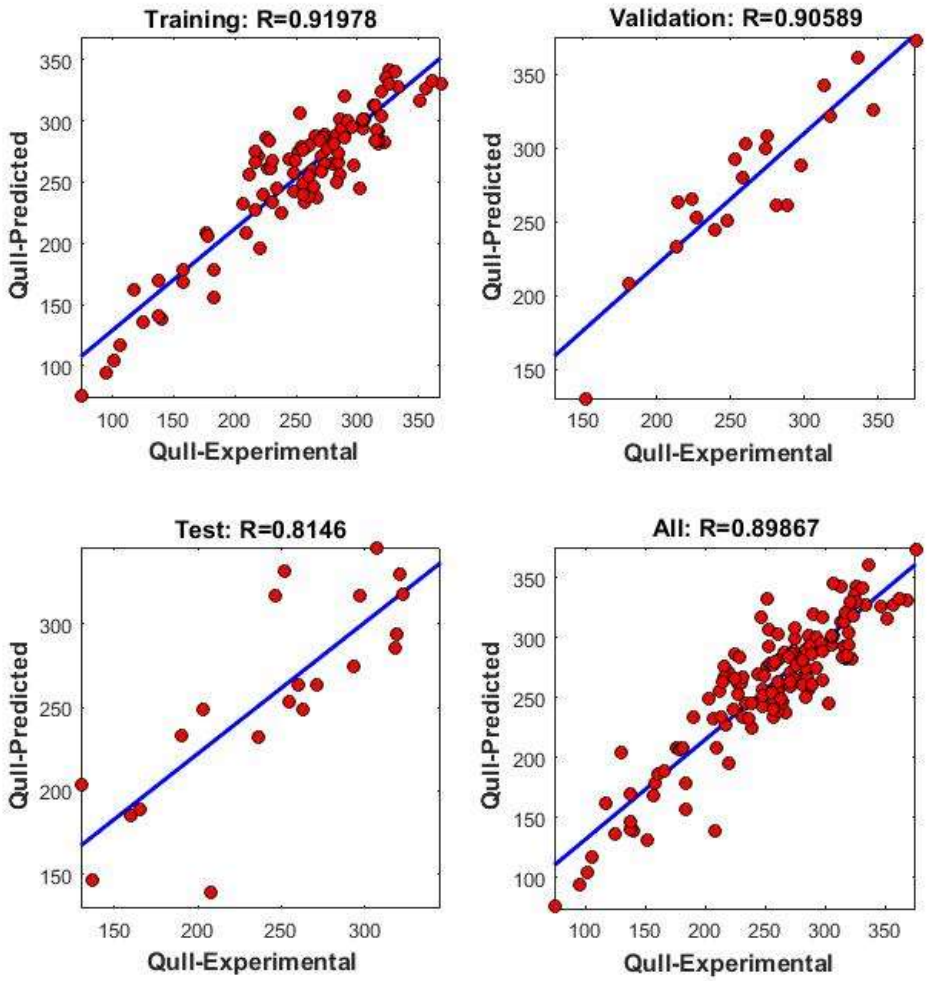


Figure 4.32 Model B6 relations between (LL, PI, WC, c, ϕ, Fine cont) and Qultimate.

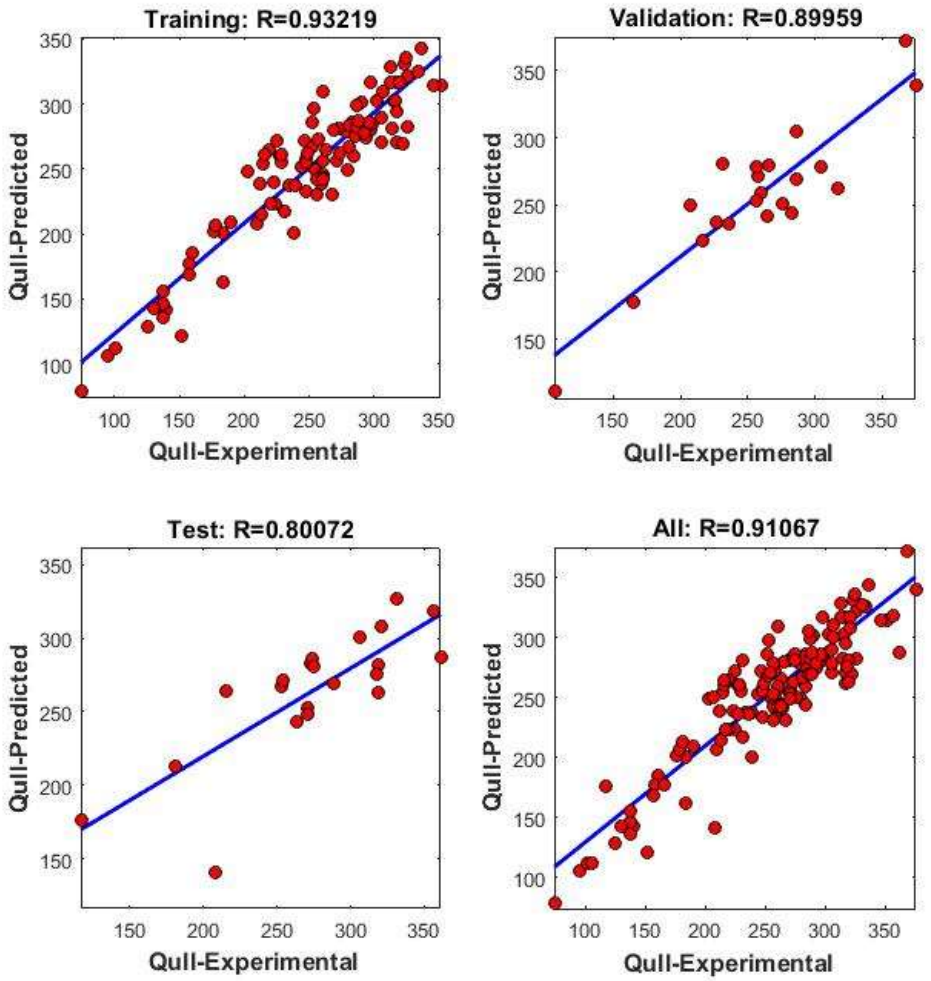


Figure 4.33 Model B7 relations between (PL, PI, WC, c, ϕ, Fine cont) and Qultimate.

Table 4.3 displays the R^2 values of the models, and Figure 4.33 illustrates a strong correlation between the predicted and actual values, along with low variance in the residuals. The model exhibits a good fit to the training data, as evidenced by an R^2 value of 0.93. Furthermore, its ability to generalize well is demonstrated by an R^2 value of 0.80 for the testing data. However, in Model 4.28, the exclusion of the cohesion value as an input variable has resulted in a decrease in the R^2 value. Cohesion plays a crucial role in influencing soil bearing capacity, and its omission from the input variables can reduce the accuracy of the model. This emphasizes the importance of incorporating all relevant variables into the model's input variables to enhance its accuracy and predictability.

To achieve the best prediction results for the ultimate bearing capacity, a total of eight models were employed. Table 4.2, 4.3, and 4.4 present the inputs and outputs of these

models, along with the corresponding R^2 values. R^2 is a statistical measure that evaluates the degree of agreement between the model and the data. It ranges from 0 to 1, with a higher R^2 value indicating a better fit between the model and the data. This R^2 value serves as an indicator to assess the accuracy of the ultimate bearing capacity predictions made by the model using the provided input parameters.

Table 4.2 ANN models for SPT-N prediction

No	Model No.		Input	Output	Training	Validation	Testing	Adjust R^2
1	GROUP A	Mod A	LL, PL, PI, WC, c, ϕ, Fine cont.	SPT-N	92.2	75.3	80.1	87.3
2		Mod A1	LL, PL, PI, WC, c, ϕ		88.06	87.39	83.87	87.4
3		Mod A2	LL, PL, PI, WC, ϕ , Fine cont		90.7	37.8	80	83.8
4		Mod A3	LL, PL, PI, WC, c, Fine cont		83.09	62.38	61.93	72.9
5		Mod A4	LL, PL, PI, c, ϕ , Fine cont		86.84	81.4	72.4	82.8
6		Mod A5	LL, PL, WC, c, ϕ , Fine cont		88.9	57.3	89.97	85.85
7		Mod A6	LL, PI, WC, c, ϕ , Fine cont		84.6	78.3	85.56	83.7
8		Mod A7	PL, PI, WC, c, ϕ , Fine cont		89	87.23	73.4	86.7

Table 4.3 ANN models for Q-Ultimate prediction

No	Model No.		Input	Output	Training	Validation	Testing	Adjust R^2
1	GROUP B	Model B	LL, PL, PI, WC, c, ϕ, Fine cont.	Q-Ultimate	91.5	83.8	82	88.79
2		Mod B1	LL, PL, PI, WC, c, ϕ		92.4	72.17	88.5	89.19
3		Mod B2	LL, PL, PI, WC, ϕ, Fine cont		73.97	34.8	86.98	70.8
4		Mod B3	LL, PL, PI, WC, c, Fine cont		92.7	80.48	86.9	90.1
5		Mod B4	LL, PL, PI, c, ϕ, Fine cont		92.13	75.65	81.36	89
6		Mod B5	LL, PL, WC, c, ϕ, Fine cont		91.27	79.25	83.72	87.6
7		Mod B6	LL, PI, WC, c, ϕ, Fine cont		91.97	90.58	81.46	89.86
8		Mod B7	PL, PI, WC, c, ϕ, Fine cont		93.2	89.95	80	91.06

Table 4.4 ANN models for Q-Ultimate II prediction

No	Model No.		Input	Output	Training	Validation	Testing	Adjust R^2
1	GROUP C	Model C	LL, PL, PI, WC, c, ϕ, Fine cont., SPT-N	Q-Ultimate II	93.37	94.53	92.4	94.54
2		Mod C1	LL, PL, PI, WC, c, ϕ, SPT-N		95.2	93.09	93.84	94.68
3		Mod C2	LL, PL, PI, WC, ϕ, Fine cont., SPT-N		94.45	72.12	91.95	90.38
4		Mod C3	LL, PL, PI, WC, c, Fine cont., SPT-N		94.57	89.49	96.93	94.52
5		Mod C4	LL, PL, PI, c, ϕ, Fine cont., SPT-N		98.47	80.23	90.5	93.74
6		Mod C5	LL, PL, WC, c, ϕ, Fine cont., SPT-N		95.55	81.33	90	91.27
7		Mod C6	LL, PI, WC, c, ϕ, Fine cont., SPT-N		96.84	92.07	92	94.84
8		Mod C7	SPT-N		90.42	88.05	90.6	90.18

Soil cohesion plays a crucial role in determining the shear strength of soil, which directly affects its capacity to bear loads. Extensive research in geotechnical engineering has consistently demonstrated that soil cohesion is the most significant factor in estimating soil bearing capacity. This is primarily because soil cohesion governs the soil's resistance to sliding or deformation under applied loads, thus ensuring the stability and integrity of structures constructed on the soil. Consequently, precise determination of soil cohesion is of utmost importance for the safe and effective design of geotechnical structures.

4.3.3 Prediction to Q-Ultimate Bearing Capacity II (included SPT-N)

In the third phase of estimating the Q-ultimate from SPT-N value, eight different models were developed with input parameters that included LL%, PL%, PI%, WC, c, ϕ, Fine content, and SPT-N. These models were demonstrated in figures 4.34 to 4.41. The training of these models was evaluated using R^2, a statistical measure that represents how well the model fits the data. Among these eight models, the one with the best training in terms of R^2 was indicated to be model C4.

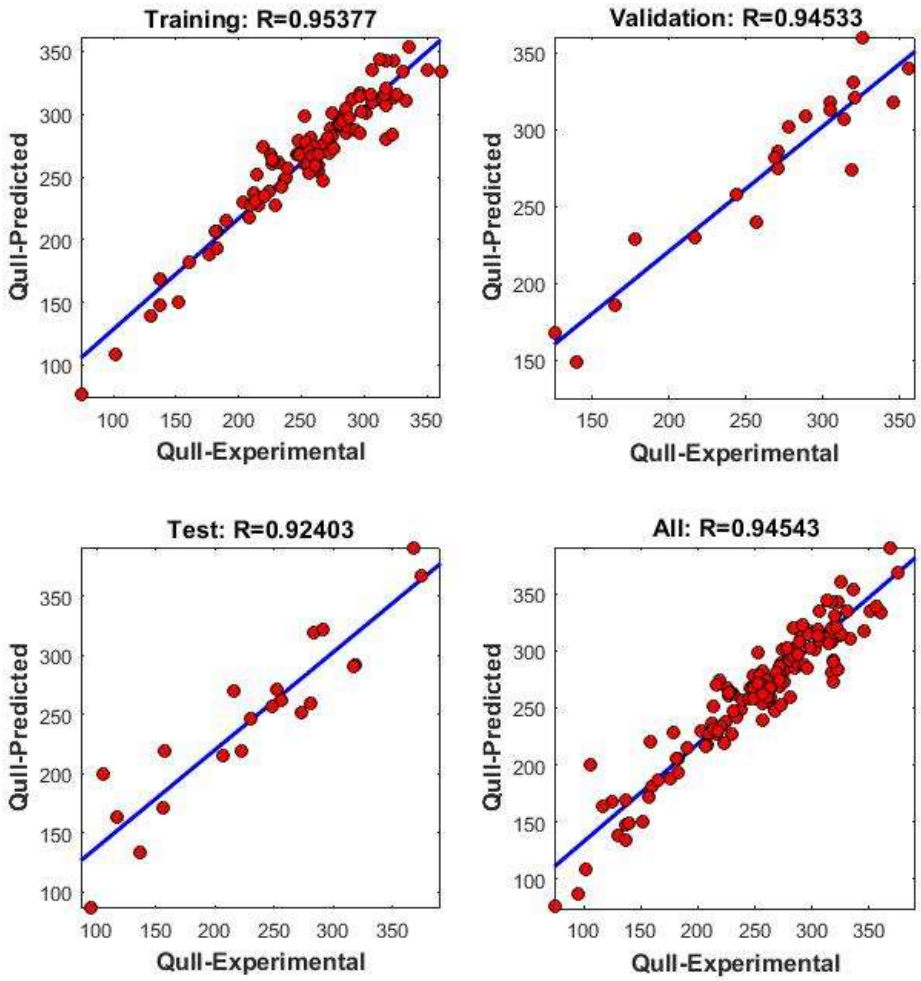


Figure 4.34 Model C relations between (LL, PL, PI, WC, c, ϕ, Fine cont., SPT-N) and Qultimate.

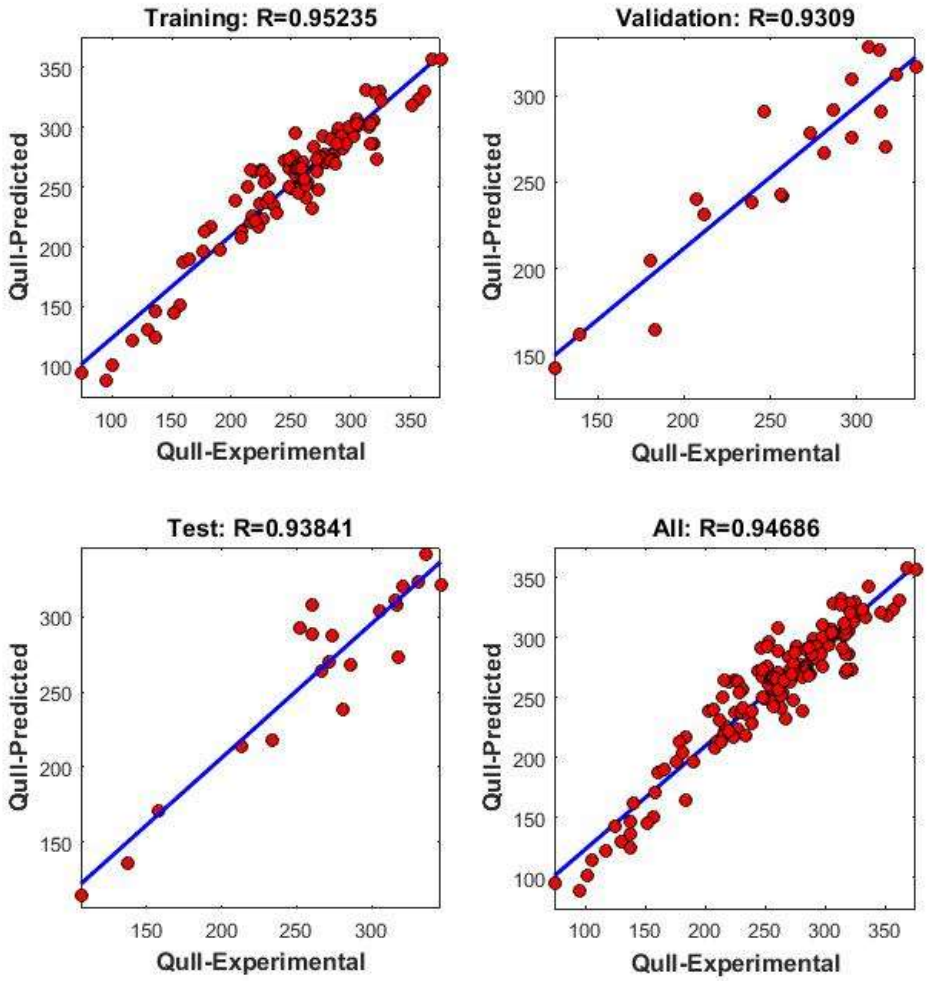


Figure 4.35 Model C1 relations between (LL, PL, PI, WC, c, ϕ, SPT-N) and Qultimate.

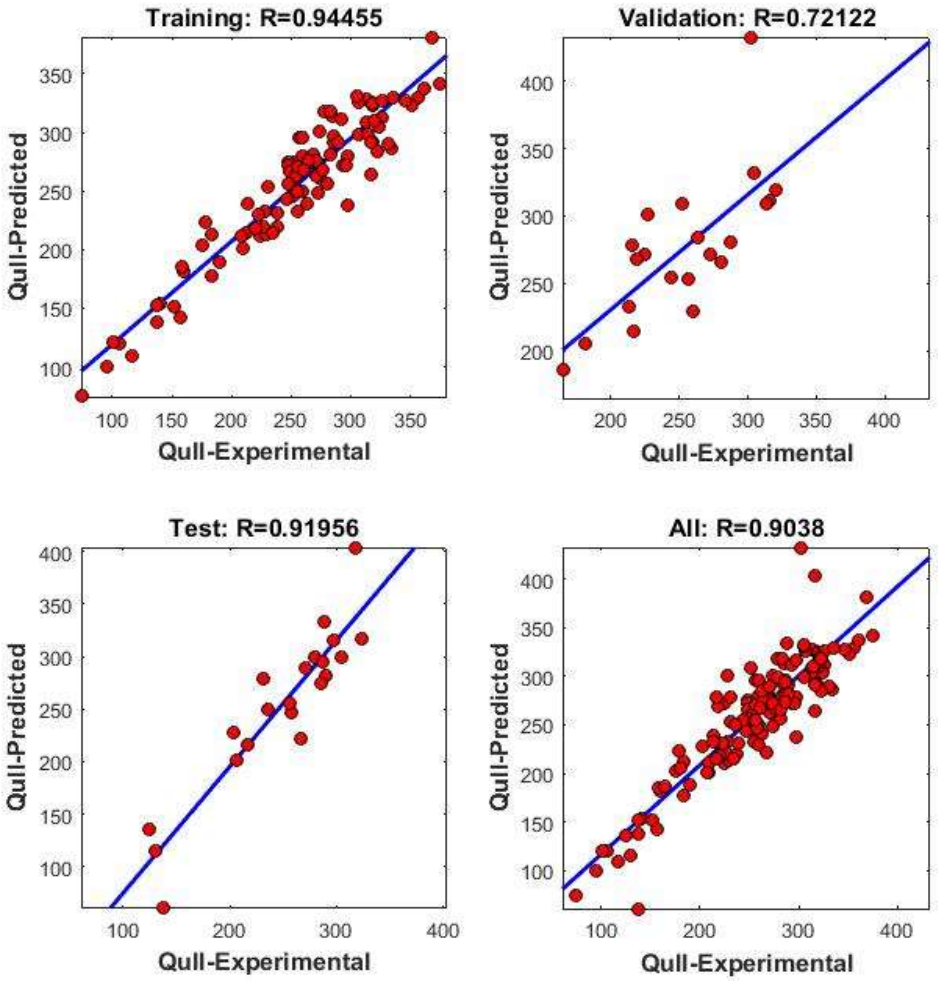


Figure 4.36 Model C2 relations between (LL, PL, PI, WC, ϕ, SPT-N) and Qultimate.

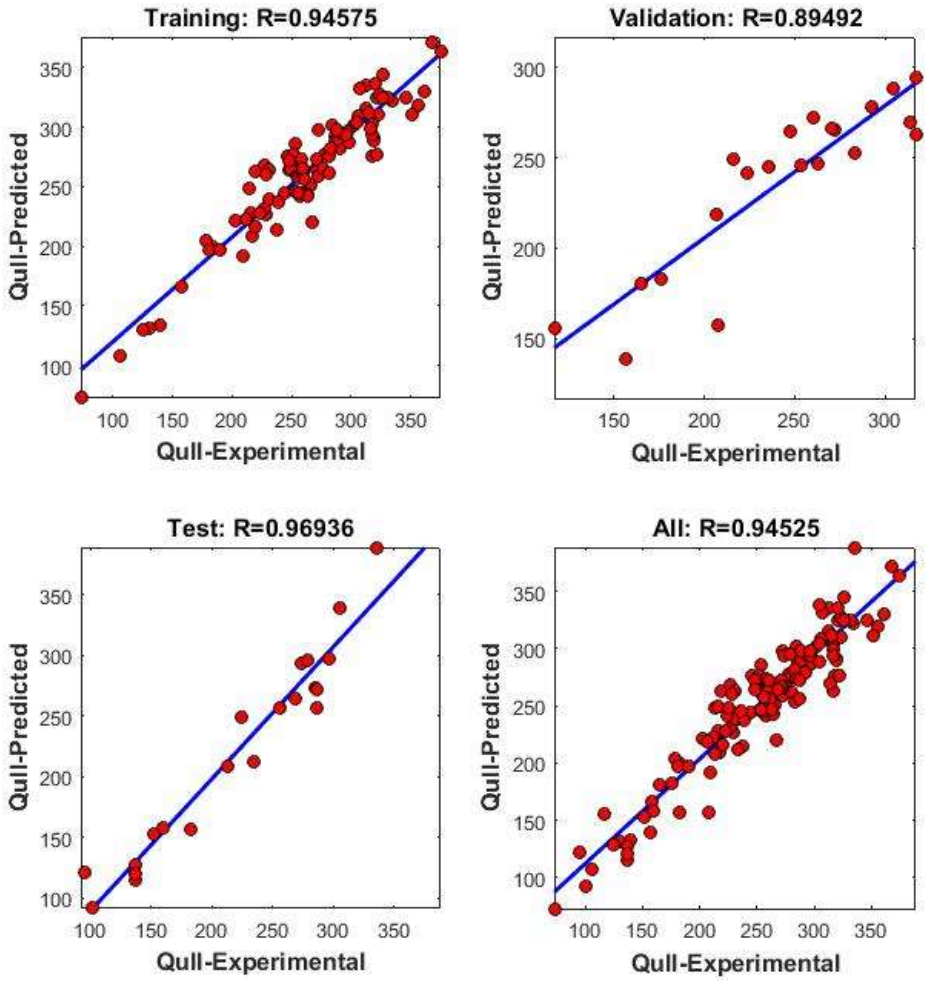


Figure 4.37 Model C3 relations between (LL, PL, PI, WC, c, SPT-N) and Qultimate.

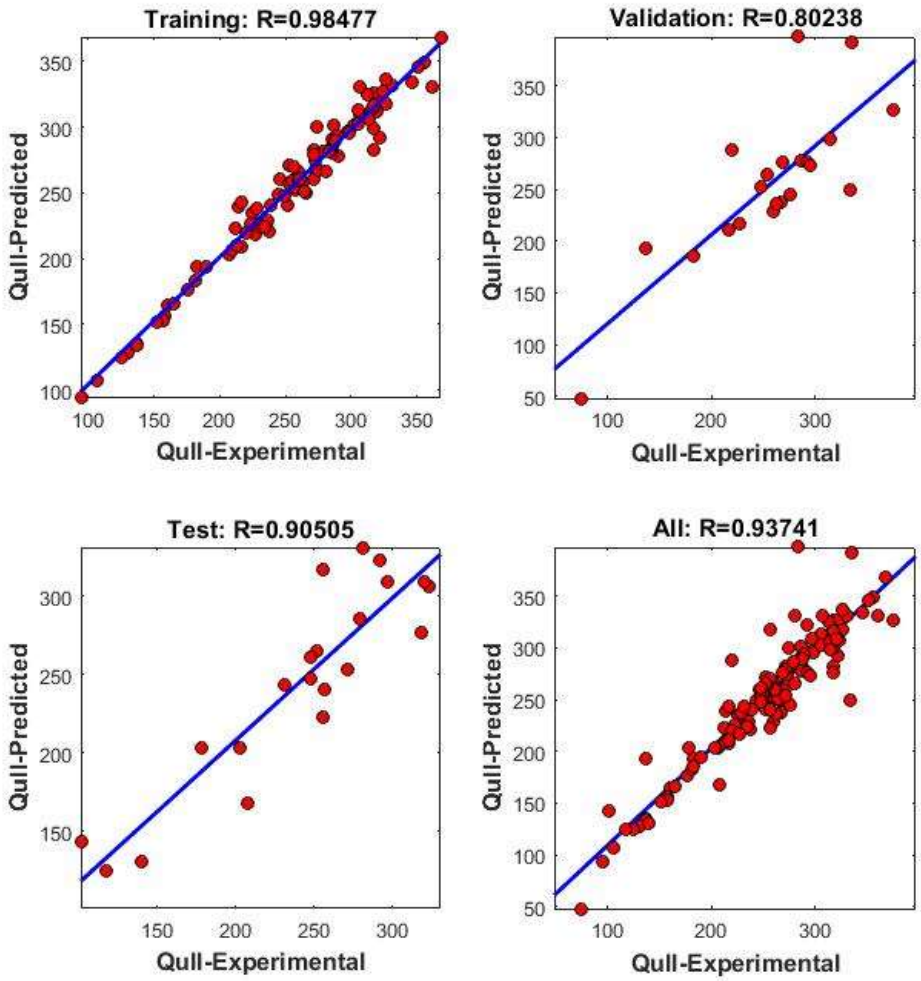


Figure 4.38 Model C4 relations between (LL, PL, PI, c, ϕ, Fine cont., SPT-N) and Qultimate.

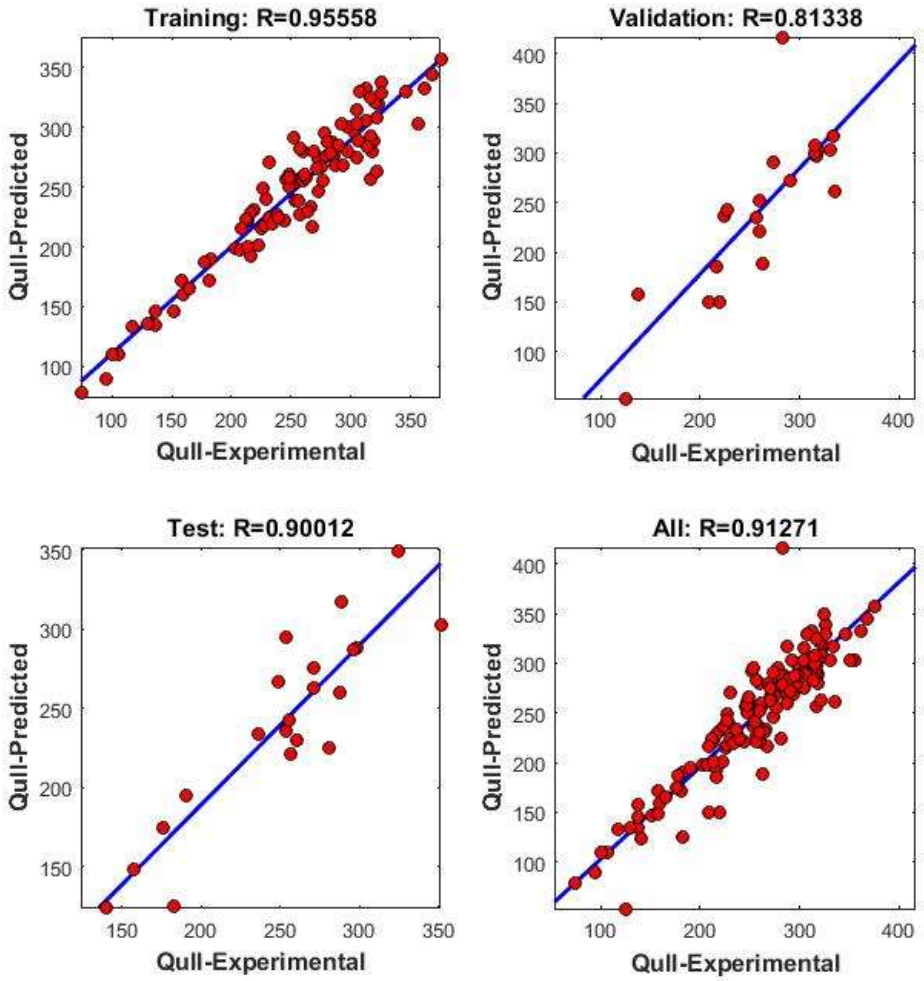


Figure 4.39 Model C5 relations between (LL, PL, WC, c, ϕ, Fine cont., SPT-N) and Qultimate.

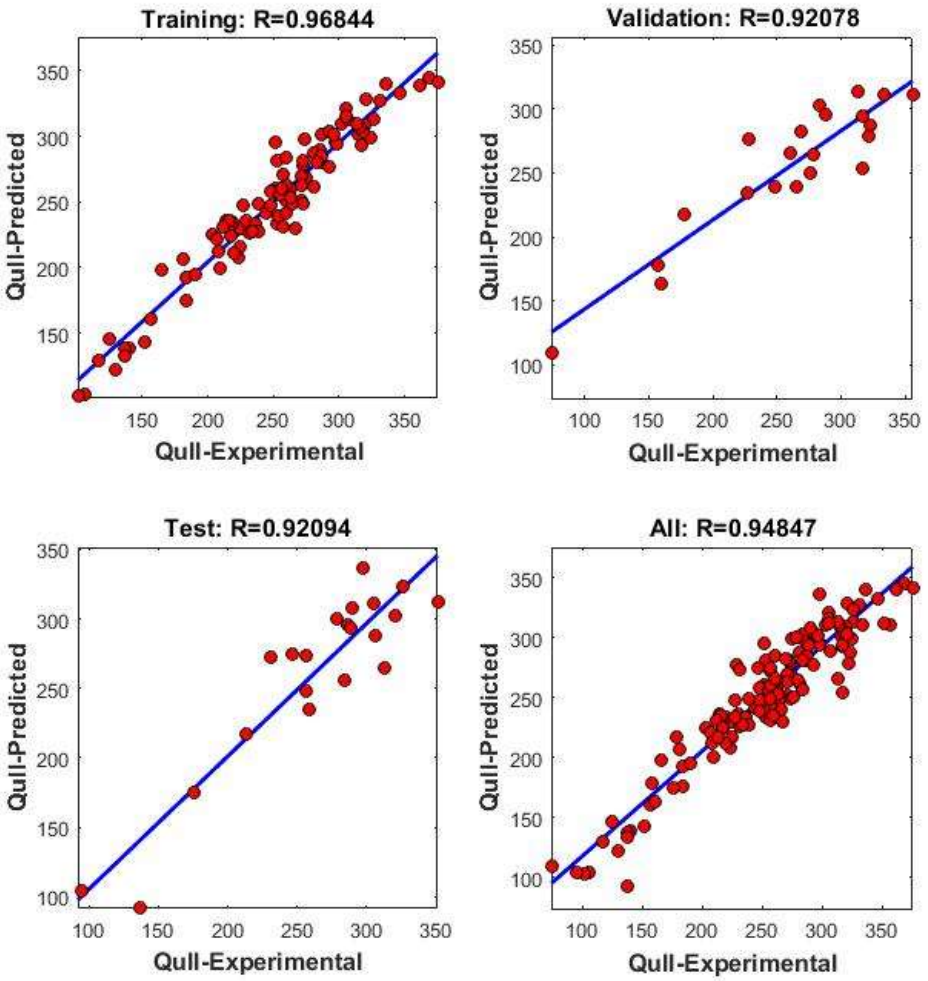


Figure 4.40 Model C6 relations between (LL, PI, WC, c, ϕ, Fine cont., SPT-N) and Qultimate.

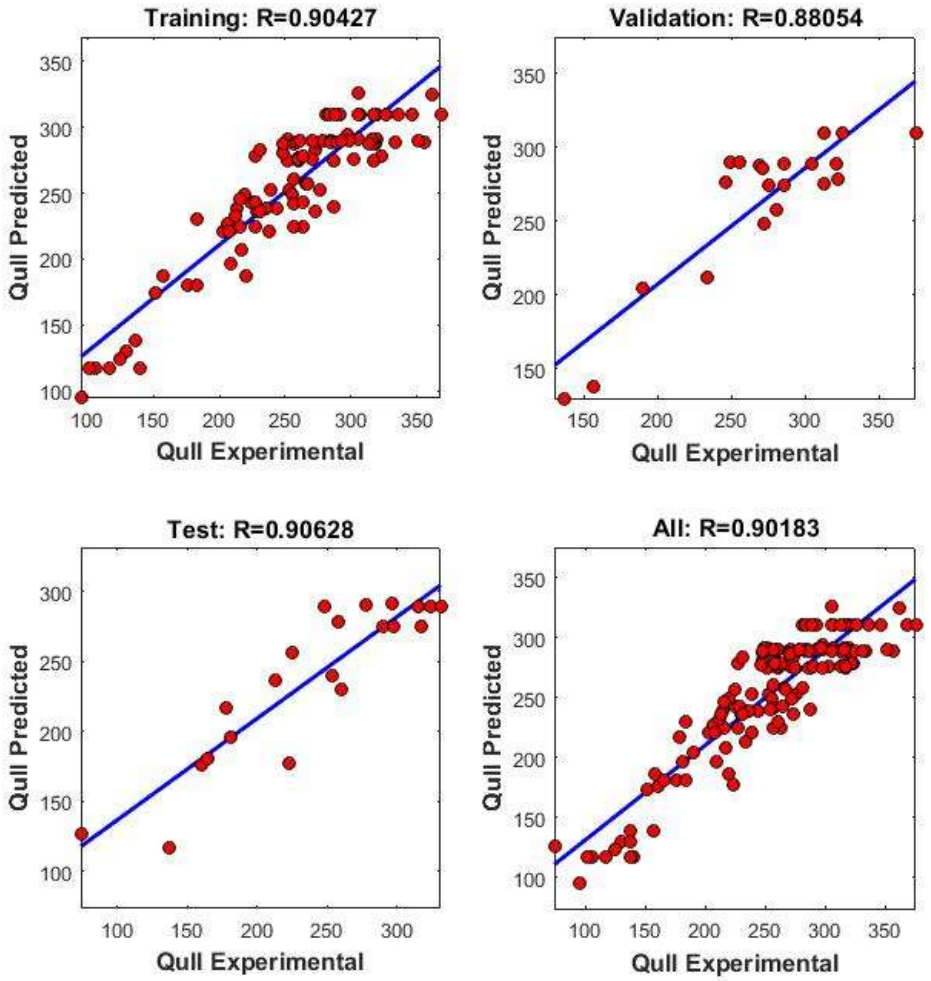


Figure 4.41 Model C7 relations between SPT-N and Qultimate.

Further evaluation of the accuracy of these models was conducted by comparing their R^2 values. Figures 4.42 to 4.44 show the comparison of R^2 for all models predicting Q-ultimate, including SPT-N value. The ANN model that used SPT-value as an input to predict Q-ultimate showed maximum accuracy compared to the model without SPT-N value. The R^2 value of the best model was found to be 0.9847, as demonstrated in figure 4.43. The use of SPT-N value as an input in predicting Q-ultimate is essential since it provides critical information about the soil's strength and stiffness. The SPT-N value is the number of blows required for a standard sampler to penetrate a certain depth under a standard hammer weight and fall. It is commonly used in geotechnical engineering to evaluate the properties of the soil.

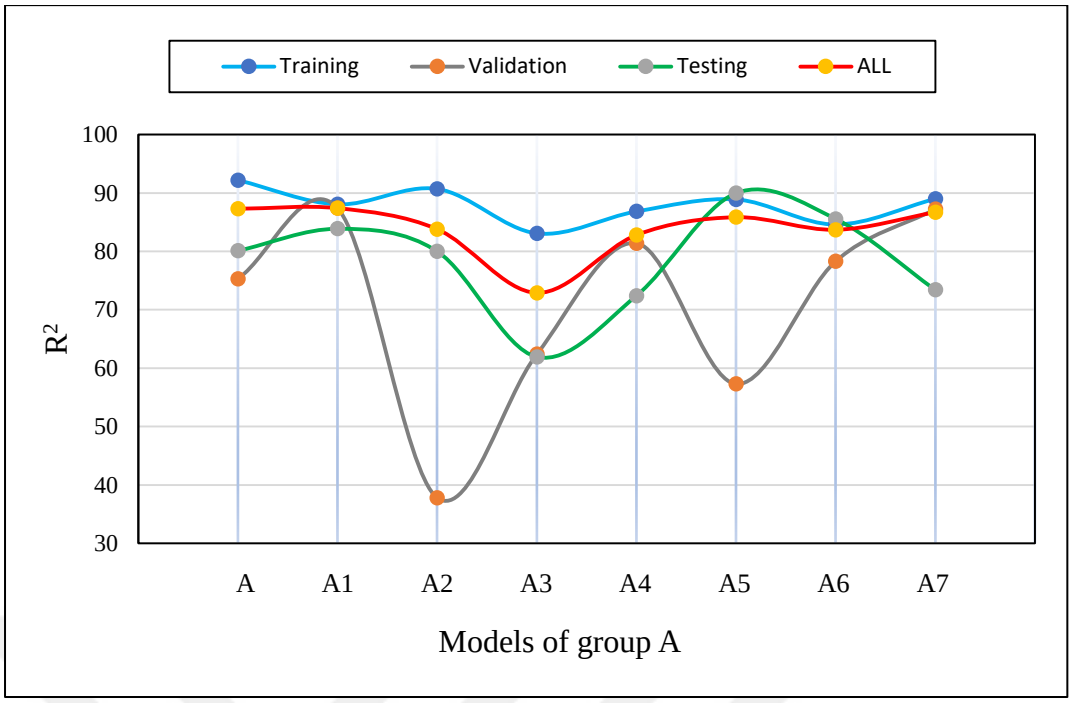


Figure 4.42 Comparison ANN models for predict SPT-N.

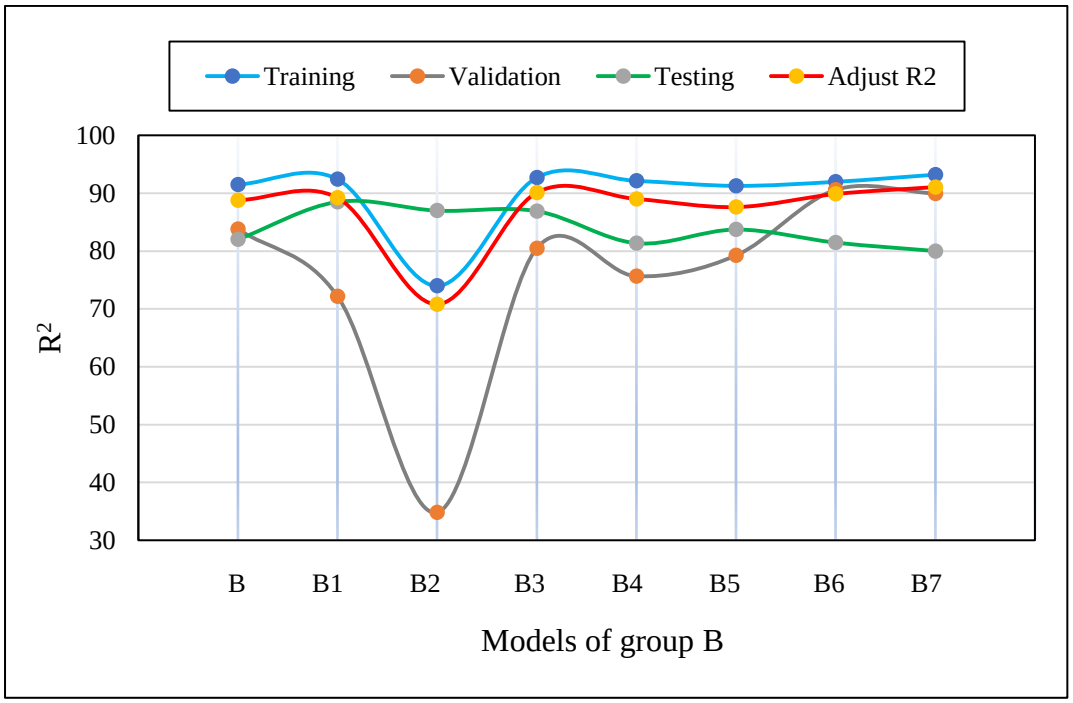


Figure 4.43 Comparison ANN models for predict Q-ultimate.

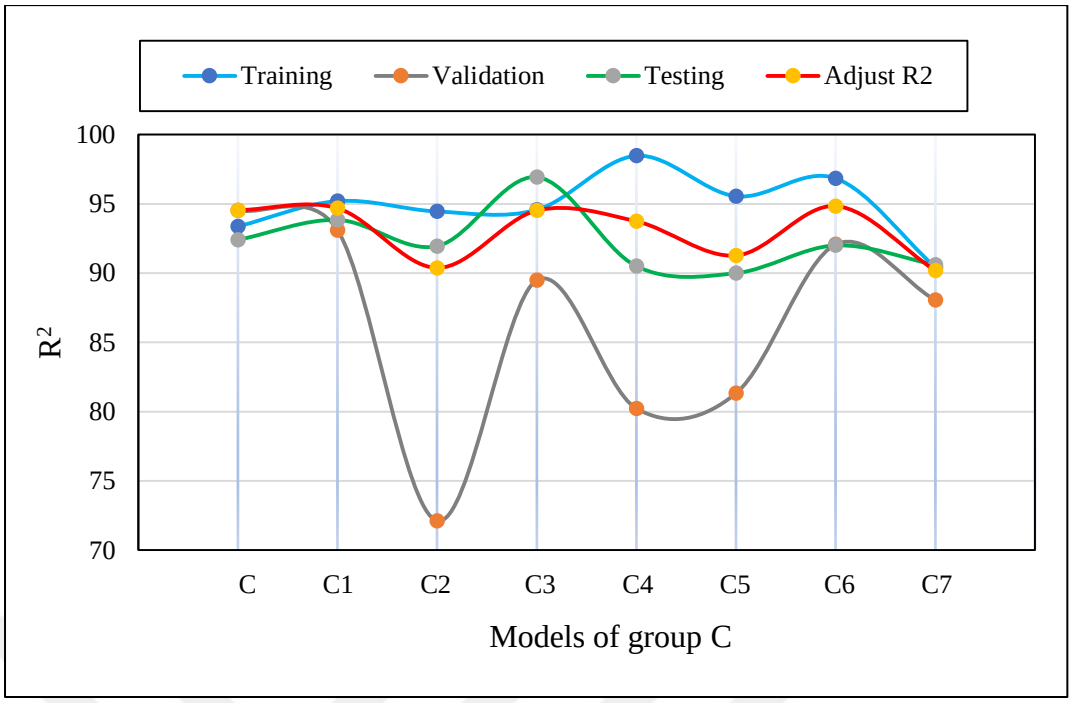


Figure 4.44 Comparison ANN models for predict Q-ultimate II.

The development of accurate models to estimate the Q-ultimate from SPT-N value can provide significant benefits in geotechnical engineering projects. The Q-ultimate is an essential parameter used to estimate the bearing capacity of the soil and predict the settlement of structures on the ground. Therefore, the accuracy of the Q-ultimate estimation is crucial for the safety and performance of the structures. The use of SPT-N value as an input parameter in predicting Q-ultimate has been demonstrated to improve the accuracy of the estimation. The ANN model with SPT-N value as an input has shown the highest accuracy, with an R^2 value of 0.9847, indicating that this model is the most reliable for predicting Q-ultimate in geotechnical engineering projects.

4.3.4 Percentage Error of ANNs Models

Figures 4.45 and 4.46 present the error percentage lines for the accuracy models' outcomes. The error percentage quantifies the deviation between predicted values and actual values, reflecting the accuracy of the model's predictions. A lower error percentage indicates higher precision, while a higher error percentage suggests lower precision. The acceptable error percentage in geotechnical engineering varies depending on the specific application and the acceptable level of error within that particular field. For instance, in the design of a building's foundation, a low error percentage of 1-2% may be considered acceptable to ensure the safety and stability of the structure. On the other hand, in soil classification tasks, a higher error percentage

might be deemed acceptable if the cost associated with reducing the error to a lower level is prohibitively high. Ultimately, the determination of an acceptable error percentage depends on the specific requirements and constraints of the geotechnical engineering project.

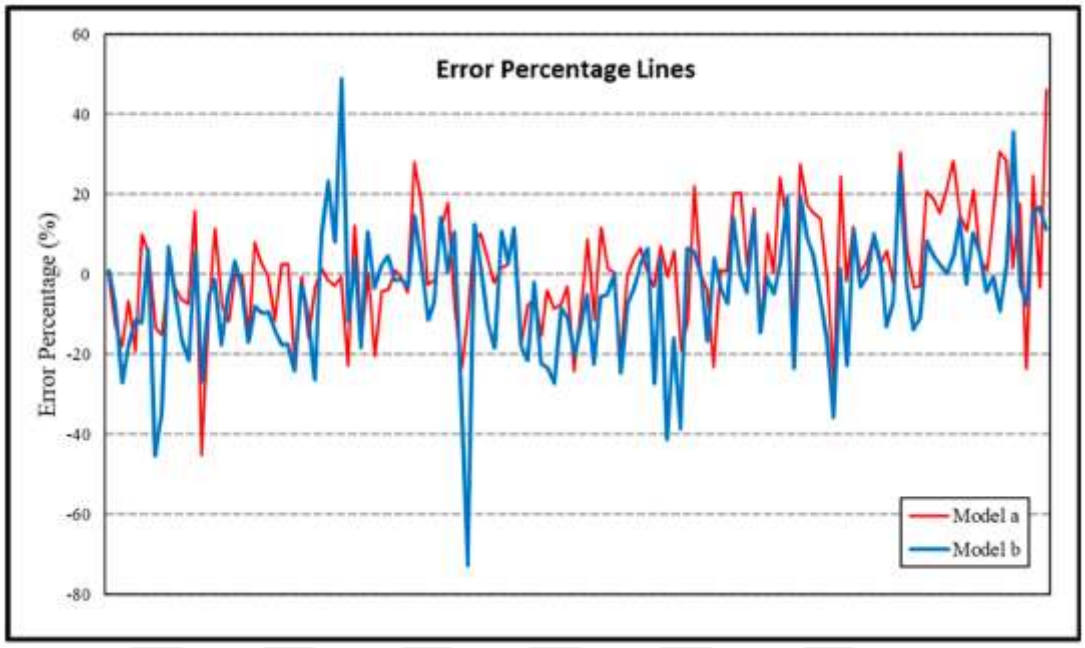


Figure 4.45 Error percentage lines of model (a) and (b) for prediction SPT-N value.

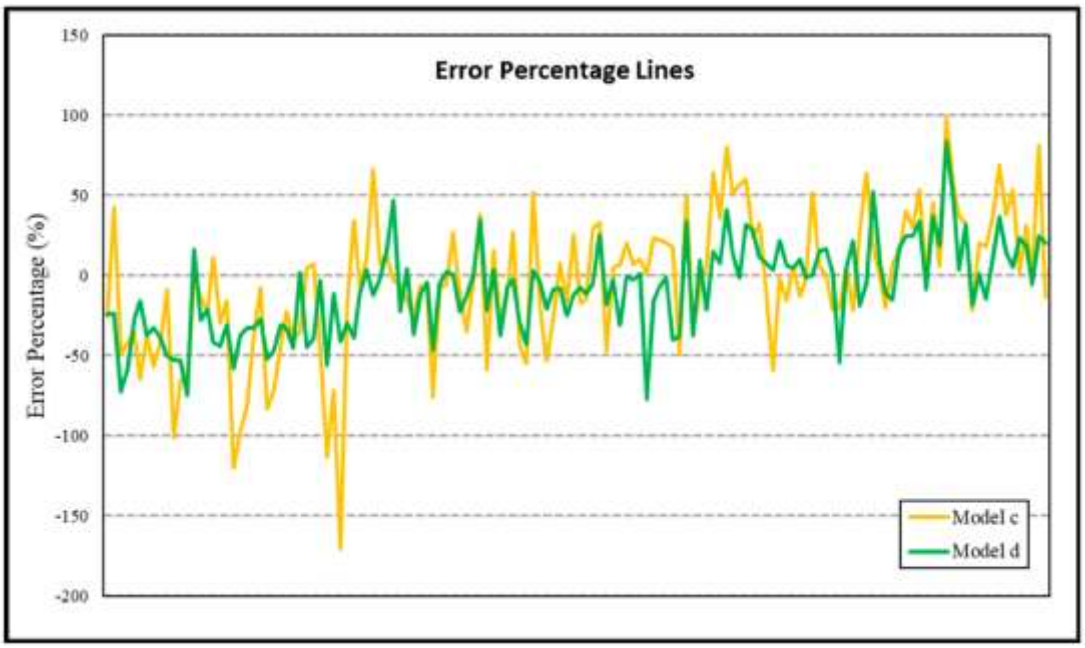


Figure 4.46 Error percentage lines of model (c) and (d) for prediction Q ultimate.

It is crucial to acknowledge that no model can achieve 100% accuracy, and there will always be some level of inherent error. The objective is to minimize the error to the greatest extent feasible while generating predictions that are meaningful and applicable. In addition, it is essential to validate the models by comparing their predictions with actual field measurements to ensure their reliability and accuracy. The application of machine learning techniques, specifically ANN, has demonstrated encouraging outcomes in forecasting soil properties and parameters. However, it is important to use caution when using these models since they can suffer from overfitting, where the model becomes too complex and is trained on noise instead of meaningful patterns in the data. Therefore, it is important to validate the models with independent datasets and use appropriate model selection techniques to avoid overfitting.

4.3.5 Analysis of Models

Sensitivity analysis plays a vital role in evaluating models by assessing the influence of individual parameters on the final results. The absence of a sensitivity analysis in the referenced study may limit the understanding of the model's behavior and the confidence in the obtained results. Particularly when employing analysis of variance (ANOVA) models, analyzing the parameters becomes essential as they can significantly impact the spatial structure of the data. Conducting a sensitivity analysis would enable researchers to assess the robustness of the model outcomes. It is suggested that a sensitivity analysis should be conducted to evaluate the effect of each model parameter, as depicted in Table 4.5, using semi-variograms.

Table 4.5. Analysis of models and effect each parameter on the output of prediction.

Model a			Model b			Model c			Model d		
Parameters	F-Value	*p*-Value	Parameters	F-Value	*p*-Value	Parameters	F-Value	*p*-Value	Parameters	F-Value	*p*-Value
LL%	1.63	0.204	LL%	0.03	0.862	LL%	0.17	0.677	LL%	2.02	0.157
PL%	1.07	0.303	PL%	0.51	0.477	PL%	0.07	0.792	PL%	2.19	0.142
PI%	0.46	0.497	PI%	0.27	0.607	PI%	1.01	0.316	PI%	0.24	0.627
WC	2.52	0.115	WC	2.36	0.126	WC	1.12	0.291	WC	5.95	0.016
c	157.85	0.000	φ	0.75	0.387	c	320.21	0.000	φ	0.03	0.873
φ	10.29	0.002	No.200	46.73	0.000	φ	28.47	0.000	No.200	68.38	0.000
No.200	1.81	0.180				No.200	0.04	0.843			

In hypothesis testing, a commonly used threshold for determining statistical significance is a p-value less than 0.05. In this context, when a specific model parameter yields a p-value less than 0.05, it indicates a statistically significant relationship between the parameter and the outcome variable being modelled. This suggests that the parameter has a significant impact on the outcome, providing evidence to support its inclusion in the model.

In the present study, a p-value less than 0.05 associated with a specific model parameter signifies its significant influence on the model results. Understanding the relationships inherent in the data can be invaluable for comprehending underlying patterns and aiding further analysis or interpretation of the outcomes. However, it is essential to consider additional factors like the sample size, data quality, and overall model fit to assess the reliability and robustness of the results. Relying solely on p-values may not provide a complete picture and must be considered in conjunction with other relevant factors to make informed conclusions.

CHAPTER 5
CONCLUSIONS

This study primarily focuses on two key aspects of investigations. Firstly, it aims to develop maps for soil geotechnical properties, which are widely used by geotechnical engineers for the design of foundations. The generated maps provide valuable information about the distribution and variability of important soil properties across the study area. Some important points that can be highlighted from this study include:

- Engineers can effectively apply GIS as a tool for analyzing preliminary geotechnical site investigations. In this study, information from 102 boreholes was collected and evaluated, considering the main geotechnical properties. This data was then utilized as input for GIS analysis, enabling engineers to gain valuable insights and make informed decisions regarding the geotechnical aspects of the site.
- The findings suggest that a significant portion of Erbil city is characterized by soil containing a substantial amount of fine-grained materials, such as clay and silt. The presence of a high fines content in the soil can have notable effects on its physical and engineering properties, including compressibility, permeability, and shear strength. Moreover, soils with high fines content are more prone to swelling and shrinkage, which can compromise the stability of structures constructed on or within the soil. However, it is worth noting that in the southeast region of the study area, smaller zones were identified with lower fine contents. These areas may possess different soil characteristics and offer potential sites for structures that require more stable soil conditions. These findings bear significance for the design and construction of infrastructure and buildings within the city, emphasizing the need to account for the varying soil characteristics and potential challenges associated with high fines content.
- The Atterberg limits measured in most areas of Erbil City ranged from 40% to 52% for the liquid limit and 19% to 30% for the plastic limit. These findings indicate a significant presence of low-plasticity clay and clayey silt in the city. The analysis results of the liquid limit and plastic limit values in the study area

- offer valuable information for engineers and urban planners working in Erbil City center. These findings emphasize the prevalence of low plastic clay in substantial proportions within the study area, as well as the importance of carefully assessing critical locations with high liquid limit and plastic limit values for future construction and development projects.
- Through digital mapping, the shear strength parameters of the soil in the study area were analyzed at three different depths. It was found that most soil layers had an internal friction angle ranging from 2° to 6°, while the cohesive strength varied from 76 kPa to 130 kPa. The cohesion values indicate that the soils at shallow depths in the study area possess moderate to high cohesion, with higher cohesion values observed in areas with a higher proportion of fine particles. On the other hand, the analysis of the angle of internal friction reveals that the soils in the study area generally exhibit moderate to low shear strength, with slightly higher shear strength values observed in the eastern and southern parts of the area. The implications of these findings are significant in assessing the soil's suitability for various types of structures and developing suitable designs and construction methods that align with the prevailing soil conditions in the area.
- The soil characteristics in the study area indicate a moderate level of compressibility and resilience, along with a moderate to low rebound capacity. As one goes deeper into the ground, the compression index decreases, suggesting that the soil becomes less prone to compression. The rebound index reveals that the soil has a moderate to low capacity for regaining its initial volume after being compressed. These findings are significant for the design of structures constructed on or within the soil in the study area, as they offer valuable insights into the soil's behavior and response to applied loads.
- The SPT values obtained in the study area reveal a moderate soil strength in the shallow soil layers, ranging from 17 to 48. However, as the depth increases, the SPT values progressively rise, covering a significant portion of the study area. This indicates an increase in soil strength with depth. The SPT test is a widely accepted in-situ measurement for assessing soil strength, and these findings offer valuable insights for designing foundations and other structures that rely on soil support. The higher SPT values observed at greater depths indicate enhanced soil strength characteristics, which can have implications for

load-bearing capacity and structural stability considerations during the design phase.

- Based on the findings, it can be concluded that the soil in Erbil City may not possess the inherent capacity to support heavy loads without the implementation of modification or specific design measures. The ultimate bearing capacity of the soil represents the maximum weight or load that it can sustain without failure. In cases where the value is below 170 kPa, it suggests that the soil may not be suitable for accommodating substantial structures like buildings and bridges without additional treatment or specialized foundation design. Enhancing the soil's properties, such as through compaction or stabilization techniques, and incorporating specialized footing designs like piles, can improve the soil's bearing capacity. These measures are essential for ensuring the stability and safety of structures constructed on the soil.
- During the preliminary design phase, the digital geotechnical maps provide valuable information for the designer. By utilizing the geotechnical parameters, consolidation characteristics, and SPT values displayed on these digital maps, the designer can effectively visualize the relevant data for the proposed region. This visual display simplifies the decision-making process by allowing the designer to assess the necessary information and make informed choices based on the displayed values.
- In the second phase of the study, a NN model was employed to estimate both the SPT-N value and the Q-ultimate bearing capacity. The findings revealed a significant correlation between the SPT values and shear strength parameters of the soil within the study area. To develop the ANN model, 150 SPT-N values were collected from 102 boreholes covering an area of 250 km2 in Erbil. The soil in this area mostly consisted of fine-grained deposits of silt and clay, with weathered gravel and sand. The input parameters used to develop the model included borehole location coordinates and soil type percentages.
- The optimal model in this study was obtained by using 2 nodes in the hidden layer, a momentum term of 0.75, a learning rate of 0.25, and the tanh transfer function in the hidden layer and the sigmoid transfer function in the output layer.
- The performance of the ANN model developed was evaluated by comparing the predicted SPT-N values and Q-ultimate bearing capacity with the measured

values obtained from field tests. The results indicated that the predicted values were in close agreement with the measured values. Additionally, several performance indices, including R^2, MAPE, and RMSE, were calculated to assess the prediction performance of the ANN model. The model exhibited good prediction performance based on these indices.

- Therefore, the ANN model developed in this study offers a valuable tool for predicting both the SPT-N value and the Q-ultimate bearing capacity by considering soil parameters and borehole coordinates. By utilizing the ANN model, it is possible to reduce the uncertainties typically encountered in geotechnical engineering projects. This highlights the potential of Artificial Neural Networks to introduce innovative techniques and approaches that mitigate potential inconsistencies in correlations. However, it is important to note that while ANN prediction is a valuable tool for estimating the ultimate bearing capacity of soil, it should be used in conjunction with other methods and validated using independent data to ensure accurate and reliable predictions.
- The ANN model's efficacy in reducing uncertainties in soil engineering projects has been demonstrated, highlighting its usefulness as a valuable tool. This advantage enables ANNs to surpass the limitations of conventional approaches. Furthermore, ANNs can continually improve their performance by incorporating fresh calibration data. Nonetheless, ANNs' drawback is that the association between input parameters and output is frequently intricate and difficult to articulate. Additionally, the success of ANNs in establishing this relationship is not assured. The effectiveness of the ANN model has further demonstrated the value of the neural network as a tool for reducing the uncertainties that can arise during soil engineering projects. Thus, utilizing artificial neural networks may offer fresh thoughts and procedures while minimizing the risk of inconsistent correlations.

REFERENCES

Abiodun, O. I., Jantan, A., Omolara, A. E., Dada, K. V., Mohamed, N. A., and Arshad, H. (2018). State-of-the-art in artificial neural network applications: A survey. *Heliyon*, ***4***(11), e00938.

Abraham, A. (2001). Neuro fuzzy systems: State-of-the-art modeling techniques. In *Connectionist Models of Neurons, Learning Processes, and Artificial Intelligence: 6th International Work-Conference on Artificial and Natural Neural Networks, IWANN 2001 Granada, Spain, June 13–15, 2001 Proceedings, Part 1 6* 269-276. Springer Berlin Heidelberg.

Afram, A., Janabi-Sharifi, F., Fung, A. S., and Raahemifar, K. (2017). Artificial neural network (ANN) based model predictive control (MPC) and optimization of HVAC systems: A state of the art review and case study of a residential HVAC system. *Energy and Buildings*, ***141***, 96-113.

Aggour, M. S., and Radding, W. R. (2001). Standard penetration test (SPT) correction. *Report No. MD02-007B48, Maryland State Highway Administration, Baltimore, 87*.

Ahmad, I., El Naggar, M. H., and Khan, A. N. (2007). Artificial neural network application to estimate kinematic soil pile interaction response parameters. *Soil Dynamics and Earthquake Engineering*, ***27***(9), 892-905.

Ahmed, C., Mohammed, A., and Saboonchi, A. (2022). ArcGIS mapping, characterisations and modelling the physical and mechanical properties of the Sulaimani City soils, Kurdistan Region, Iraq. *Geomechanics and Geoengineering*, ***17***(2), 384-397.

Aldefae, A. H., Mohammed, J., and Saleem, H. D. (2020). Digital maps of mechanical geotechnical parameters using GIS. *Cogent Engineering*, ***7***(1), 1779563.

Ali, M., Emch, M., Donnay, J. P., Yunus, M., and Sack, R. B. (2002). Identifying environmental risk factors for endemic cholera: a raster GIS approach. *Health and Place*, ***8***(3), 201-210.

Al-Sanjari, M. N., and Al-Tamimi, M. A. (2009). Interpretation of water quality parameters for Tigris River within Mosul City by using principal components analysis. *Tikrit Journal of Pure Science*, ***14***(2), 68-74.

Amine, A., Elberrichi, Z., Simonet, M., and Malki, M. (2008, November). Wordnet-based and n-grams-based document clustering: A comparative study. In *2008 Third International Conference on Broadband Communications, Information Technology and Biomedical Applications* (pp. 394-401). IEEE.

Arnous, M. O. (2013). Geotechnical site investigations for possible urban extensions at Suez City, Egypt using GIS. *Arabian Journal of Geosciences*, ***6***(5), 1349-1369.

ASTM (2019) Standard Test Method for Standard Penetration Test (SPT) and Split-Barrel Sampling of Soils, D1586/D1586M-18.

ASTM Committee D-18 on Soil and Rock. (2009). Standard test methods for particle-size distribution (gradation) of soils using sieve analysis: ASTM International

ASTM Committee D-18 on Soil and Rock. (2010). Standard test methods for liquid limit, plastic limit, and plasticity index of soils. ASTM international.

ASTM D1586/D1586M-18. (2018). Standard Test Method for Standard Penetration Test (SPT) and Split-Barrel Sampling of Soils, ASTM D1586/D1586M-18, West Conshohocken, PA.

ASTM D3441 (2016) Standard test method for mechanical cone penetration testing of soils.

ASTM, D. (1994). 3080-90: Standard test method for direct shear test of soils under consolidated drained conditions. Annual book of ASTM standards, 4, 290-5.

Avunduk, E., and Copur, H. (2018). Empirical modeling for predicting excavation performance of EPB TBM based on soil properties. *Tunnelling and Underground Space Technology*, *71*, 340-353.

Awodele, O., and Jegede, O. (2009). Neural networks and its application in engineering. *Sci IT*, 83-95.

Azad, D. K. (2009). GIS based urban transportation system for Allahabad city (*Doctoral dissertation*, Motilal Nehru National Institute of Technology Allahabad).

Bapeer, G. B. (2011). The study of infiltration rate and atterberg limits of soils in Koi Sanjaq City, Erbil Governorate, Kurdistan Region, North Iraq. *Iraqi Bull Geol Min*, ***7***(2), 41-55.

Barczewski, R., and Kania, M. (2004). Study of ground and buildings vibrations generated by vibratory rollers. *Proceedings of the Vibrations in Physical Systems, Poznan, Poland*, ***21***, 97-100.

Basheer, I. A., and Hajmeer, M. (2000). Artificial neural networks: fundamentals, computing, design, and application. *Journal of microbiological methods*, ***43***(1), 3-31.

Basma, A. A., and Kallas, N. (2004). Modeling soil collapse by artificial neural networks. *Geotechnical and Geological Engineering*, ***22***, 427-438.

Blasby, D., Davis, M., Kim, D., and Ramsey, P. (2003). GIS conflation using open source tools. *White paper, The Jump Project*.

Bogati, K., Ground Improvement by Jet Grouting Techniques. 2019.

Bolstad, P., and Manson, S. (2008). *GIS fundamentals: A first text on geographic information systems* (Vol. 620). White Bear Lake, MN: Eider Press.

Bowden, G. J., Maier, H. R., and Dandy, G. C. (2002). Optimal division of data for neural network models in water resources applications. *Water resources research*, *38*(2), 2-1.

Bowles, J., (1982). Foundation analysis and design ″ McGraw-Hill Book Company. New York, 816p.

Bowles, J.E., (1997). Foundation Analysis and Design, fifth ed. McGraw Hill, 1168 pp.

BS 1377: (1975). Laboratory Determination Methods of Engineering Soil Properties. British Standards Institution, London.

BS1377 (1990) Method of test for soils for civil engineering purposes. British Standards Institution, London.

Burke, L. I., and Ignizio, J. P. (1992). Neural networks and operations research: an overview. *Computers and operations research*, ***19***(3-4), 179-189.

Cai, S., Toral, H., Qiu, J., and Archer, J. S. (1994). Neural network based objective flow regime identification in air-water two phase flow. *The Canadian Journal of Chemical Engineering*, ***72***(3), 440-445.

Cal, Y. (1995). Soil classification by neural network. *Advances in Engineering software*, ***22***(2), 95-97.

Carter, M. and S. Bentley, (1991). Correlations of soil properties. Pentech press publishers.

Casagrande, A. (1958). Notes on the design of the liquid limit device. *Geotechnique*, ***8***(2), 84-91.

Chan, L. W., and Fallside, F. (1987). An adaptive training algorithm for back propagation networks. *Computer speech and language*, ***2***(3-4), 205-218.

Chandio, I. A., Matori, A. N. B., WanYusof, K. B., Talpur, M. A. H., Balogun, A. L., and Lawal, D. U. (2013). GIS-based analytic hierarchy process as a multicriteria decision analysis instrument: a review. *Arabian Journal of Geosciences*, ***6***, 3059-3066.

Chang, Y. S., and Park, H. D. (2004). Development of a web-based geographic information system for the management of borehole and geological data. *Computers and Geosciences*, ***30***(8), 887-897.

Chen, C. J., and Juang, C. H. (2000). Calibration of SPT-and CPT-based liquefaction evaluation methods. In *Innovations and applications in geotechnical site characterization* (pp. 49-64).

Chester, D. L. (1990). Why two hidden layers are better than one. In *Proc. IJCNN, Washington, DC* ***1***,265-268.

Cheung, C. K., and Shi, W. (2004). Estimation of the positional uncertainty in line simplification in GIS. *The Cartographic Journal*, ***41***(1), 37-45.

Cheung, S. O., Suen, H. C., and Cheung, K. K. (2004). PPMS: a web-based construction project performance monitoring system. *Automation in construction*, ***13***(3), 361-376.

Chin, W. W. (1998). Commentary: Issues and opinion on structural equation modeling. *MIS quarterly*, vii-xvi.

Chung, J. W., and Rogers, J. D. (2010). GIS-based virtual geotechnical database for the St. Louis metro area. *Environmental and Engineering Geoscience*, ***16***(2), 143-162.

Clayton, C. R., Matthews, M. C., and Simons, N. E. (1982). *Site investigation* (No. Monograph). London: Granada.

Clayton, C.R.I. (1995). The Standard Penetration Test (SPT): Methods and Use, Construction Industry Research and Information Association Report, CIRIA, London. 143.

Coduto, D. P. (2014). *Foundation design: principles and practices*. Pearson Education Limited.

Costa, A. N., Polivanov, H., Alves, M. G., and Ramos, D. P. (2011). Multicriterial analysis in the investigation of favorable areas for edifications with shallow and deep foundations in the Municipality of Campos dos Goytacazes—Rio de Janeiro, Brazil. *Engineering Geology*, ***123***(3), 149-165.

Coutinho, R. Q., and Mayne, P. W. (Eds.). (2012). *Geotechnical and geophysical site characterization 4*. CRC Press.

Daniel, C. R., Howie, J. A., and Sy, A. (2003). A method for correlating large penetration test (LPT) to standard penetration test (SPT) blow counts. *Canadian Geotechnical Journal*, ***40***(1), 66-77.

Das, B., *Advanced soil mechanics*. 5th Edn. ISBN-13: 9780815379133. 2019, CRC Press, Taylor and Francis, Florida, USA.

Das, B.M. and N. Sivakugan, *Fundamentals of geotechnical engineering*. 2016: Cengage Learning.

Das, B.M. and N. Sivakugan, *Principles of foundation engineering*. 2018: Cengage learning.

Das, S. K., and Basudhar, P. K. (2006). Undrained lateral load capacity of piles in clay using artificial neural network. *Computers and Geotechnics*, *33*(8), 454-459.

Dauji, S., and Rafi, A. (2021). Spatial interpolation of SPT with artificial neural network. *Engineering Journal*, *25*(2), 109-120.

Deaton, S. L. (2013). *Geotechnical Information Database-Phase II* (No. FHWA/LA. 12/498). Louisiana. Dept. of Transportation and Development.

Dindar, H., Dimililer, K., Özdağ, Ö. C., Atalar, C., Akgün, M., and Özyankı, A. (2017). Vulnerability index assessment using neural networks (Viann): A case study of Nicosia, Cyprus. *SPRS Annals of Photogrammetry, Remote Sensing and Spatial Information Sciences*, 14-15.

Duong, T. V., Tang, A. M., Cui, Y. J., Trinh, V. N., Dupla, J. C., Calon, N., ... and Robinet, A. (2013). Effects of fines and water contents on the mechanical behavior of interlayer soil in ancient railway sub-structure. *Soils and foundations*, ***53***(6), 868-878.

Ebrahimi, A. (2011). Behavior or fouled ballast. *Railway Track and Structures*, ***107***(8).

Erzin, Y., and Tuskan, Y. (2016). Prediction of Standard Penetration Test (SPT) Value in Izmir, Turkey using General Regression Neural Network. In *International Conference on Agricultural, Civil and Environmental Engineering (ACEE-16) April* (pp. 18-19).

Eslami, A., Moshfeghi, S., Molaabasi, H., and Eslami, M. M. (2019). *Piezocone and cone penetration test (CPTu and CPT) applications in foundation engineering*. Butterworth-Heinemann.

ESRI. Environmental Systems Research Institute. (2005). Available from: https://www.esri.com/ .

Fahlman, S. E., Lebiere, C., and Touretzky, D. (1990). Advances in neural information processing systems.

Fang, H. Y. (2013). *Foundation engineering handbook*. Springer Science and Business Media.

Faraway, J., ans Chatfield, C. (1998). Time series forecasting with neural networks: a comparative study using the air line data. *Journal of the Royal Statistical Society Series C: Applied Statistics*, ***47***(2), 231-250.

Fernando, H., Nugroho, S. A., Suryanita, R., and Kikumoto, M. (2021). Prediction of SPT value based on CPT data and soil properties using ANN with and without normalization. *International Journal of Artificial Intelligence Research*, ***5***(2), 123-131.

First, G. I. S., Second, G. I. S., and Third, G. I. S. (1996). *Geographic information systems as an integrating technology*: context, concepts, and definitions.

Flood, I., and Kartam, N. (1994). Neural networks in civil engineering. II: Systems and application. *Journal of Computing in Civil Engineering*, ***8***(2), 149-162.

Folguera, L., Zupan, J., Cicerone, D., and Magallanes, J. F. (2015). Self-organizing maps for imputation of missing data in incomplete data matrices. *Chemometrics and Intelligent Laboratory Systems*, ***143***, 146-151.

Fortin, V., Ouarda, T. B., and Bobée, B. (1997). Comment on "The use of artificial neural networks for the prediction of water quality parameters" by HR Maier and GC Dandy. *Water Resources Research*, ***33***(10), 2423-2424.

Gardner, C., et al., Soil water content. *Soil and environmental analysis*: Physical methods.(KA Smith and CE Mullins, Eds.)(Second Edi). 2000, New York: Marcel Dekker, Inc.

Garip, Z. Ş. (2011). *Yapay sinir ağları ile mevcut yapıların deprem riski açısından durum tespiti*. Açık Akademik Arşiv Sistemi.

GEOL 260 – GIS and Remote Sensing https://geol260.academic.wlu.edu (accessed October 8, 2021).

Geotechnical and Geoenvironmental Software Directory (GGSD). www.ggsd.com (accessed October 4, 2021).

Germaine, J. T., and Germaine, A. V. (2009). *Geotechnical laboratory measurements for engineers*. John Wiley and Sons.

Ghaleini, E. N., Koopialipoor, M., Momenzadeh, M., Sarafraz, M. E., Mohamad, E. T., and Gordan, B. (2019). A combination of artificial bee colony and neural network for approximating the safety factor of retaining walls. *Engineering with Computers*, ***35***(2), 647-658.

Gilbert, P. A. (1992). *Effect of sampling disturbance on laboratory-measured soil properties*. Army Engineer Waterways Experiment Station Vicksburg Ms Geotechnical Lab.

Globevnik, L., Holjevic, D., Petkovsek, G., and Rubinic, J. (2003). Applicability of the Gavrilovic method in erosion calculation using spatial data manipulation techniques. *International Association of Hydrological Sciences*, Publication, ***279***, 224-233.

GOH, A. C. (1994). Nonlinear modelling in geotechnical engineering using neural networks. Transactions of the Institution of Engineers, Australia. *Civil engineering*, ***36***(4), 293-297.

Graettinger, A. J., Ryals, Z. T., and Smith, R. K. (2011). A web-based geotechnical gis. *International Scholarly Research Notices*, 2011.

Günaydın, O. (2009). Estimation of soil compaction parameters by using statistical analyses and artificial neural networks. *Environmental Geology*, ***57***(1), 203.

Gunduz, Z., and Arman, H. (2007). Possible relationships between compression and recompression indices of a low-plasticity clayey soil. *Arabian Journal for Science and Engineering*, ***32***(2), 179.

Hajela, P., and Berke, L. (1991). Neurobiological computational models in structural analysis and design. *Computers and Structures*, ***41***(4), 657-667.

Hameed, H. (2013). *Water harvesting in Erbil Governorate*, Kurdistan region, Iraq: detection of suitable sites using geographic information system and remote sensing. Student thesis series INES.

Hammerstrom, D. (1993). Working with neural networks. *IEEE spectrum*, ***30***(7), 46-53.

Hanna, A. M., Morcous, G., and Helmy, M. (2004). Efficiency of pile groups installed in cohesionless soil using artificial neural networks. *Canadian Geotechnical Journal*, ***41***(6), 1241-1249.

Hasan, A. M., Mawlood, Y. I., Ahmed, A. A., And Ibrahim, H. H. (2020). Correlation Of Shear Wave Velocity With SPT-N For A Tower-Building Site at Erbil City. *Journal of Duhok University*, ***23***(2), 235-245.

Hassannejad, H., Pakbaz, M. S., and Mehdizadeh, R. (2015). Comparison and evaluation of artificial neural network (ANN) training algorithms in predicting soil type classification. *Pharmacology and Life Sciences Bull*. Env. Pharmacol. Life Sci, ***4***, 212-218.

Hassoun, M. H. (1995). *Fundamentals of artificial neural networks*. MIT press.

Hecht-Nielsen, R. (1989). On the algebraic structure of feedforward network weight spaces. *In Advanced Neural Computers*. 129-135. North-Holland.

Hellawell, E. E., Lamont-Black, J., Kemp, A. C., and Hughes, S. J. (2001). GIS as a tool in geotechnical engineering. *Proceedings of the Institution of Civil Engineers-Geotechnical Engineering*, ***149***(2), 85-93.

Hinton, G. E., Sejnowski, T. J., and Poggio, T. A. (1999). *Unsupervised learning: foundations of neural computation*. MIT press.

Hofmann-Wellenhof, B., Lichtenegger, H., and Collins, J. (2012). *Global positioning system: theory and practice*. Springer Science and Business Media.

Hopkins, T. C., Beckham, T. L., Sun, L., and Pfalzer, B. (2005). *Kentucky geotechnical database*.

Hore, R., Al-Mamun, S. and Ansary, M.A. (2018). SPT-CPT correlations for reclaimed areas of dhaka. *Journal of Engineering*, ***9***(1), pp.35-46

Hornik, K., Stinchcombe, M., and White, H. (1989). Multilayer feedforward networks are universal approximators. *Neural Networks*, ***2***(5), 359-366.

Hunt, R. E. (2005). *Geotechnical engineering investigation handbook*. Second Edition. New York: Taylor and Francis Group Crc Press.

Hurtado, J. E., Londono, J. M., and Meza, M. A. (2001). On the applicability of neural networks for soil dynamic amplification analysis. *Soil Dynamics and Earthquake Engineering*, ***21***(7), 579-591.

Ibrahim, R. I., Mushatat, S. A., and Abdelmonem, M. G. (2015). Erbil. *Cities*, ***49***, 14-25.

Inam, A., Ishikawa, T., and Miura, S. (2012). Effect of principal stress axis rotation on cyclic plastic deformation characteristics of unsaturated base course material. *Soils and Foundations*, ***52***(3), 465-480.

Innes, J. E., and Simpson, D. M. (1993). Implementing GIS for planning lessons from the history of technological innovation. *Journal of the American Planning Association*, ***59***(2), 230-236.

Jasim, M. M., Al-Khaddar, R. M., and Al-Rumaithi, A. (2019). Prediction of bearing capacity, angle of internal friction, cohesion, and plasticity index using ANN (case study of Baghdad, Iraq). *International Journal of Civil Engineering and Technology*, ***10***(1), 2670-2679.

Jassim, S. Z., and Goff, J. C. (Eds.). (2006). *Geology of Iraq*. DOLIN, sro, distributed by Geological Society of London.

Jeremiah, J. J., Abbey, S. J., Booth, C. A., and Kashyap, A. (2021). Results of Application of Artificial Neural Networks in Predicting Geo-Mechanical Properties of Stabilised Clays—A Review. *Geotechnics*, ***1***(1), 147-171.

Kalinski, M. E. (2011). *Soil mechanics*: lab manual (No. Ed. 2). John Wiley and Sons.

Kanta, A., Soupios, P., Barsukov, P., Kouli, M., and Vallianatos, F. (2013). Aquifer characterization using shallow geophysics in the Keritis Basin of Western Crete, Greece. *Environmental Earth Sciences*, ***70***(5), 2153-2165.

Karim, H. M. A. (2019). Production of lightweight thermal insulating clay bricks using papyrus. *Polytechnic Journal*, ***9***(1), 74-81.

Kavli, T. (1993). ASMO—Dan algorithm for adaptive spline modelling of observation data. *International Journal of Control*, ***58***(4), 947-967.

Kayen, R. E., Mitchell, J. K., Seed, R. B., Lodge, A., Nishio, S. Y., and Coutinho, R. (1992). Evaluation of SPT-, CPT-, and shear wave-based methods for liquefaction potential assessment using Loma Prieta data. In *Proceedings of the 4th Japan-US Workshop on Earthquake Resistant Design of Lifeline Facilities and Countermeasures for Soil Liquefaction, Hamada, M. and O'Rourke, TD, eds*.

Kaynar, O., Görmez, Y., Işık, Y. E., and Demirkoparan, F. (2016). Değişik Kümeleme Algoritmalarıyla Eğitilmiş Radyal Tabanlı Yapay Sinir Ağlarıyla Saldırı Tespiti. In *International Artificial Intelligence and Data Processing Symposium (IDAP'16)*.

Khan, M. S., Park, J., and Seo, J. (2021). Geotechnical property modeling and construction safety zoning based on GIS and BIM integration. *Applied Sciences*, ***11***(9), 4004.

Khudhur, S. M., and Khudhur, N. S. (2015). Soil pollution assessment from industrial area of Erbil City. *Journal of Zankoi Sulaimani*, ***17***(4), 225-238.

Kim, D., Sagong, M., and Lee, Y. (2005). Effects of fine aggregate content on the mechanical properties of the compacted decomposed granitic soils. *Construction and Building Materials*, ***19***(3), 189-196.

Koester, J. P. (1992). The influence of test procedure on correlation of Atterberg limits with liquefaction in fine-grained soils. *ASTM geotechnical testing journal*, ***15***(4), 352-361.

Kudrycki, T. P. (1988). *Neural network implementation of a medical diagnosis expert system*. Master's thesis, Coll. of Eng., Univ. of Cincinnati, Cincinnati, Ohio.

Kulga, B., Artun, E., and Ertekin, T. (2018). Characterization of tight-gas sand reservoirs from horizontal-well performance data using an inverse neural network. *Journal of Natural Gas Science and Engineering*, ***59***, 35-46.

Kumar, R., Bhargava, K., and Choudhury, D. (2016). Estimation of engineering properties of soils from field SPT using random number generation. *INAE Letters*, ***1***, 77-84.

Kunapo, J., Dasari, G. R., Phoon, K. K., and Tan, T. S. (2005). Development of a Web-GIS based geotechnical information system. *Journal of Computing in Civil Engineering*, ***19***(3), 323-327.

Lachtermacher, G., and Fuller, J. D. (1994). Backpropagation in hydrological time series forecasting. In Stochastic and Statistical Methods in Hydrology and Environmental Engineering: *Time Series Analysis in Hydrology and Environmental Engineering* (229-242). Dordrecht: Springer Netherlands.

Laslett, G. M., McBratney, A. B., Pahl, P., and Hutchinson, M. F. (1987). Comparison of several spatial prediction methods for soil pH. *Journal of Soil Science*, ***38***(2), 325-341.

Lee, S. J., Lee, S. R., and Kim, Y. S. (2003). An approach to estimate unsaturated shear strength using artificial neural network and hyperbolic formulation. *Computers and Geotechnics*, ***30***(6), 489-503.

Lendaris, G. G., Mathia, K., and Saeks, R. (1999). Linear Hopfield networks and constrained optimization. *IEEE Transactions on Systems*, Man, and Cybernetics, Part B (Cybernetics), ***29***(1), 114-118.

Lenz, J. A., and Baise, L. G. (2007). Spatial variability of liquefaction potential in regional mapping using CPT and SPT data. *Soil Dynamics and Earthquake Engineering*, ***27***(7), 690-702.

Lesik, S. A. (2018). *Applied statistical inference with MINITAB®*. Chapman and Hall/CRC.

Li, J., and Heap, A. D. (2008). A review of spatial interpolation methods for environmental scientists. *Geoscience Australia.*

Liber, K., Goodfellow, W., Den Besten, P., Clements, W., Galloway, T., Gerhardt, A., and Simpson, S. (2007). In situ-based effects measures: Considerations for improving methods and approaches. *Integrated Environmental Assessment and Management: An International Journal*, ***3***(2), 246-258.

Likos, W. J., Song, X., Xiao, M., Cerato, A., and Lu, N. (2019). Fundamental challenges in unsaturated soil mechanics. *Geotechnical fundamentals for addressing new world challenges*, 209-236.

Lippmann, R. (1987). An introduction to computing with neural nets. *IEEE Assp magazine*, ***4***(2), 4-22.

Liu, S., Chang, R., Zuo, J., Webber, R. J., Xiong, F., and Dong, N. (2021). Application of Artificial Neural Networks in Construction Management: *Current Status and Future Directions. Applied Sciences*, ***11***(20), 9616.

Lokesh, P., Balasubramanya, S., and Anuradha, M. (2014). Cost effective quantification of camptothecin and a comparative study of its content in Nothapodytes foetida and Ophiorrhiza mungos sourced from selected geographical locations. *Oriental Pharmacy and Experimental Medicine*, ***14***(2), 87-92.

Look, B. G. (2007). *Handbook of geotechnical investigation and design tables*. Taylor and Francis.

Lupiezowiec, M., (2013). The application of c-φ reduction method to estimate the bearing capacity of subsoil. *Architecture Civil Engineering Environment*, ***6***(4): p. 35-44

Maier, H. R., and Dandy, G. C. (2000). Neural networks for the prediction and forecasting of water resources variables: a review of modelling issues and applications. *Environmental Modelling and Software*, ***15***(1), 101-124.

Malczewski, J. (2004). GIS-based land-use suitability analysis: a critical overview. *Progress in planning*, ***62***(1), 3-65.

Manual, O. (2008). *Highway Design Manual* (HDM) | Caltrans.

Masters, T. (1993). *Practical neural network recipes in C++*. Academic Press Professional, Inc.

McPhail, J. D. (2001). *Electronic storage and interchange of geotechnical engineering data* (Doctoral dissertation).

Meyerhof, G. G. (1963). Some recent research on the bearing capacity of foundations. *Canadian Geotechnical Journal*, ***1***(1), 16-26.

Miljković, D. (2010, May). Review of novelty detection methods. In *The 33rd International Convention MIPRO*, 593-598. IEEE.

Minns, A. W., and Hall, M. J. (1996). Artificial neural networks as rainfall-runoff models. *Hydrological Sciences Journal*, ***41***(3), 399-417.

Mishra, M. V., Agarwal, S. M., and Puri, N. (2018). Comprehensive and Comparative Analysis of Neural Network. *International Journal of Computer Application*, ***2***(8), 126-137.

Mitchell, J. K., and Soga, K. (2005). *Fundamentals of soil behavior* (Vol. 3, p. USA). New York: John Wiley and Sons.

Monnet, J. (2015). *In situ tests in geotechnical engineering*. John Wiley and Sons.

Mwajuma, I.L. (2015). *In-Situ Penetration as Alternative to Extensive Boreholes and Lab Testing for Exploration in Sandy Soils*. MSc thesis, Stockholm.

Myslivec, A., and Kysela, Z. (2014). *The bearing capacity of building foundations*. Elsevier.

Najjar, Y. M., Ali, H. E., and Basheer, I. A. (1999). "On the use of neurons for simulating the stress-strain behavior of soils." Proc., 7th Int. Symposium on Numerical *Models in Geomechanics*, G. N. Pande, ed., Graz, Austria, NUMOG VII, September ***1-3***, 657-662.

Najjar, Y. M., Basheer, I. A., and Naouss, W. A. (1996). On the identification of compaction characteristics by neuronets. *Computers and Geotechnics*, ***18***(3), 167-187.

Nareeman, B. J., and Fattah, M. Y. (2012). Effect of soil reinforcement on shear strength and settlement of cohesive-frictional soil. *International Journal of GEOMATE*, ***3***(1), 308-313.

Nawari, N. O., Liang, R., and Nusairat, J. (1999). Artificial intelligence techniques for the design and analysis of deep foundations. *Electronic Journal of Geotechnical Engineering*, ***4***, 1-21.

Nemoto, T., Masumoto, S., Nanogaki, S., Raghavan, V., and Yonezawa, G. (2015). Development of a Distributed Database System for Borehole Dana using Free and Open Source Software. *International Journal of Geometrics*, ***11***(3).

NeuralWare, (1999) *NeuralWorks Professional II/Plus Supplement*, report, 72 pp., Pittsburgh, Pa.

Nilsson, N. J. (2009). *The quest for artificial intelligence*. Cambridge University Press.

Oberlender, G. D., and Trost, S. M. (2001). Predicting accuracy of early cost estimates based on estimate quality. *Journal of Construction Engineering and Management*, ***127***(3), 173-182.

Obianyo, I. I., Anosike-Francis, E. N., Ihekweme, G. O., Geng, Y., Jin, R., Onwualu, A. P., and Soboyejo, A. B. (2020). Multivariate regression models for predicting the compressive strength of bone ash stabilized lateritic soil for sustainable building. *Construction and Building Materials*, ***263***, 120677.

OGC, Open Geospatial Consortium E-learning (2021) e-learning 2.0.0 documentation. Open Geospatial Consortium. https://opengeospatial.github.io/e-learning/index.html.

Oloufa, A. A., and Ikeda, M. (1995). An automated environment for soils-and terrain-dependent applications. *Automation in Construction*, ***4***(2), 139-146.

Özbay, E. (2007). *Effects of mineral admixtures on the fresh and hardened properties of self-compacting concretes: binary, ternary and quaternary systems*. PhD thesis.

Ozturk, T. (2014). Artificial neural networks approach for earthquake deformation determination of geosynthetic reinforced retaining walls. *International Journal of Intelligent Systems and Applications in Engineering*, ***2***(1), 1-9.

Patel, A., (2019). *Geotechnical investigations and improvement of ground conditions*: Woodhead Publishing. 209

Payne, P., and Bell, A. (2021). Geotechnical Data Archiving and Risk Reduction. In Piling 2020: *Proceedings of the Piling 2020 Conference*, 555-559. ICE Publishing.

Qurtas, S. S. (2018). Using groundwater levels and Specific Yield to Estimate the Recharge, South of Erbil, Kurdistan Region, Iraq. *Academic Journal of Nawroz University*, ***7***(4), 191-196.

Radan, G. (2015). *Manual. Geophysical Survey Systems*. Inc.: Nashua, NH, USA.

Rafiq, M. Y., Bugmann, G., and Easterbrook, D. J. (2001). Neural network design for engineering applications. *Computers and Structures*, ***79***(17), 1541-1552.

Rahman, M. S., Wang, J., Deng, W., and Carter, J. P. (2001). A neural network model for the uplift capacity of suction caissons. *Computers and Geotechnics*, ***28***(4), 269-287.

Ranković, V., Novaković, A., Grujović, N., Divac, D., and Milivojević, N. (2014). Predicting piezometric water level in dams via artificial neural networks. *Neural Computing and Applications*, ***24***(5), 1115-1121.

Rashed, K. A., and Hussein, A. A. (2020). GIS as a tool for expansive soil detection at Sulaymaniyah City. *Journal of Engineering*, ***26***(6), 152-171.

Reale, C., Gavin, K., Librić, L., and Jurić-Kaćunić, D. (2018). Automatic classification of fine-grained soils using CPT measurements and Artificial Neural Networks. *Advanced Engineering Informatics*, ***36***, 207-215.

Reiffsteck, P., Benoît, J., Bourdeau, C., and Desanneaux, G. (2018). Enhancing geotechnical investigations using drilling parameters. Journal of Geotechnical and *Geoenvironmental Engineering*, ***144***(3), 04018006.

Robertson, P. K. (2016). Cone penetration test (CPT)-based soil behaviour type (SBT) classification system—an update. *Canadian Geotechnical Journal*, ***53***(12), 1910-1927.

Rowe, R. K. (Ed.). (2012). Geotechnical and geoenvironmental engineering handbook. Springer Science and Business Media.

Roy, S. and S.K. Bhalla. (2017). Role of geotechnical properties of soil on civil engineering structures. *Resources and Environment*. **7**(4): p. 103-109.

Sagiroglu, S., Besdok, E., and Erler, M. (2003). Artificial intelligence applications in Engineering I: artificial neural networks. *Ufuk Kitap Kirtasiye-Yayincilik, Kayseri, Turkey*.

Salchenberger, L. M., Cinar, E. M., and Lash, N. A. (1992). Neural networks: A new tool for predicting thrift failures. *Decision Sciences*, ***23***(4), 899-916.

Sancio, R. B., and Bray, J. D. (2005). An assessment of the effect of rod length on SPT energy calculations based on measured field data. *Geotechnical Testing Journal*, ***28***(1), 22-30.

Satyanayarana, R., Benoit, J., and Stetson, K. (2000). The national geotechnical experimentation sites database. *ASCE Geotechnical Special Publication*, 93.

Schnaid, F. (2005). Geocharacterisation and properties of natural soils by in situ tests. *In Proceedings of the International Conference on Soil Mechanics and Geotechnical Engineering*, ***16***, 1-3. Aa Balkema Publishers.

Schuster, G. T. (2017). *Seismic inversion*. Society of Exploration Geophysicists.

Shahin, M. A., and Jaksa, M. B. (2006). Pullout capacity of small ground anchors by direct cone penetration test methods and neural networks. *Canadian Geotechnical Journal*, ***43***(6), 626-637.

Shahin, M. A., and Jaksa, M. B. (2009). Intelligent computing for predicting axial capacity of drilled shafts. *In Contemporary Topics in In Situ Testing, Analysis, and Reliability of Foundations*, 26-33.

Shahin, M. A., Jaksa, M. B., and Maier, H. R. (2005). Neural network based stochastic design charts for settlement prediction. *Canadian Geotechnical Journal*, ***42***(1), 110-120.

Shahin, M. A., Jaksa, M. B., and Maier, H. R. (2008). State of the art of artificial neural networks in geotechnical engineering. *Electronic Journal of Geotechnical Engineering*, ***8***(1), 1-26.

Shahin, M., Jaksa, M., and Maier, H. (2004). Application of neural networks in foundation engineering. In Theme paper to the International e-Conference on Modern

Trends in Foundation Engineering: *Geotechnical Challenges and Solutions*, Theme (No. 5).

Shang, J. Q., Ding, W., Rowe, R. K., and Josic, L. (2004). Detecting heavy metal contamination in soil using complex permittivity and artificial neural networks. *Canadian Geotechnical Journal*, ***41***(6), 1054-1067.

Sitányiová, D., Vondráčková, T., Stopka, O., Myslivečková, M., and Muzik, J. (2015). GIS based methodology for the geotechnical evaluation of landslide areas. *Procedia Earth and Planetary Science*, ***15***, 389-394.

Sivakugan, N., Eckersley, J., and Li, H. (1998). Settlement predictions using neural networks. *Australian Civil Engineering Transactions*, ***40***, 49-52.

Skempton, A. (1984). Effective stress in soils, concrete and rocks. *Selected papers on soil mechanics*, ***1032***(3), 4-16.

Souri, M., Khosravifar, A., Dickenson, S. E., Schlechter, S., and McCullough, N. (2018). Inertial and liquefaction-induced kinematic demands on a pile-supported Wharf: Physical modeling. In *Geotechnical Earthquake Engineering and Soil Dynamics V: Numerical Modeling and Soil Structure Interaction* (pp. 388-397). Reston, VA: American Society of Civil Engineers.

Spagnoli, G., and Feinendegen, M. (2017). Relationship between measured plastic limit and plastic limit estimated from undrained shear strength, water content ratio and liquidity index. *Clay Minerals*, ***52***(4), 509-519.

Spiller, M., and Agudelo, C. (2011). Mapping diversity of urban metabolic functions: A planning approach for more resilient cities. In *Proceedings of the 5th AESOP Young Academics Network Meeting*, 126-139.

Stavrou, A., Lawrence, J. A., Mortimore, R. N., and Murphy, W. (2011). A geotechnical and GIS based method for evaluating risk exposition along coastal cliff environments: a case study of the chalk cliffs of southern England. *Natural Hazards and Earth System Sciences*, ***11***(11), 2997-3011.

Stojanovic, B., Milivojevic, M., Milivojevic, N., and Antonijevic, D. (2016). A self-tuning system for dam behavior modeling based on evolving artificial neural networks. *Advances in Engineering Software*, ***97***, 85-95.

Stokoe, K. H., Joh, S. H., and Woods, R. D. (2004). Some contributions of in situ geophysical measurements to solving geotechnical engineering problems. In Proceedings 97-132.

Su, S., Sherman, W., Harris, F., and Dye, M. (2006). TAVERNS: Visualization and manipulation of GIS data in 3D large screen immersive environments. *In 16th International Conference on Artificial Reality and Telexistence—Workshops*, 656-661. IEEE.

Sutton, R. S., and Barto, A. G. (2018). *Reinforcement learning: An introduction*. MIT press.

Taleb Bahmed, I., Harichane, K., Ghrici, M., Boukhatem, B., Rebouh, R., and Gadouri, H. (2019). Prediction of geotechnical properties of clayey soils stabilised with lime using artificial neural networks (ANNs). *International Journal of Geotechnical Engineering*, ***13***(2), 191-203.

Tarsauliya, A., Kala, R., Tiwari, R., and Shukla, A. (2011). Financial time series volatility forecast using evolutionary hybrid artificial neural network. In *Advances in Network Security and Applications: 4th International Conference, CNSA 2011, Chennai, India*, 463-471. Springer Berlin Heidelberg.

Teh, C. I., Wong, K. S., Goh, A. T. C., and Jaritngam, S. (1997). Prediction of pile capacity using neural networks. *Journal of Computing in Civil Engineering*, ***11***(2), 129-138.

Tenpe, A., and Kaur, S. (2015). Artificial neural network modeling for predicting compaction parameters based on index properties of soil. *International Journal of Science and Research*, 4-7.

Tokar, A. S., and Johnson, P. A. (1999). Rainfall-runoff modeling using artificial neural networks. *Journal of Hydrologic Engineering*, ***4***(3), 232-239.

Tsangaratos, P., Koumantakis, I., and Rozos, D. (2010). GIS-based application for geotechnical data managing. *Bulletin of the Geological Society of Greece*, ***43***(3), 1656-1666.

Twomey, J. M., and Smith, A. E. (1997). Validation and verification. Artificial neural networks for civil engineers: *Fundamentals and Applications*, 44-64.

Ural, D. N., and Saka, H. (1998). "Liquefaction assessment by neural networks." Electronic Journal of Geotechnical Engrg. http://geotech.civen.okstate.edu/ejge/ppr9803/index.html.

Uzielli, M. (2008). Statistical analysis of geotechnical data. *Geotechnical and Geophysical Site Characterization*, ***3***, 173-193.

Walker, R., Indraratna, B., and Rujikiatkamjorn, C. (2012). Vertical drain consolidation with non-Darcian flow and void-ratio-dependent compressibility and permeability. *Géotechnique*, ***62***(11), 985-997.

Wang, Q., Tang, A. M., Cui, Y. J., Delage, P., Barnichon, J. D., and Ye, W. M. (2013). The effects of technological voids on the hydro-mechanical behaviour of compacted bentonite–sand mixture. *Soils and Foundations*, ***53***(2), 232-245.

Wang, Y. Q. (2014). MeteoInfo: GIS software for meteorological data visualization and analysis. *Meteorological Applications*, ***21***(2), 360-368.

Wan-Mohamad, W. N. S., and Abdul-Ghani, A. N. (2011). The use of geographic information system (GIS) for geotechnical data processing and presentation. *Procedia Engineering*, ***20***, 397-406.

Wazoh, H. N., and Mallo, S. J. (2014). Standard Penetration Test in engineering geological site investigations–A review.

Whitman, R. V. (2000). Organizing and evaluating uncertainty in geotechnical engineering. *Journal of Geotechnical and Geoenvironmental Engineering*, ***126***(7), 583-593.

Winter, M. G., Smith, D. M., Eldred, P. J. L., and Toll, D. G. (Eds.). (2015). Geotechnical Engineering for Infrastructure and Development: XVI European Conference on Soil Mechanics and Geotechnical Engineering. ICE Publishing.

Wise, S. (2018). GIS fundamentals. 2nd Edition: Stephen Wise – Routledge. CRC Press.

Wu, W., Mhaimeed, A. S., Al-Shafie, W. M., Ziadat, F., Dhehibi, B., Nangia, V., and De Pauw, E. (2014). Mapping soil salinity changes using remote sensing in Central Iraq. *Geoderma Regional*, ***2***, 21-31.

Xie, M., Zhou, G., Li, D., and Gong, J. (2000). Design and Implementation of Attribute Database Management System in A GIS System: GeoStar. *Geographic Information Sciences*, ***6***(2), 170-180.

Yang, Y. J., and Zhang, Q. (1998). The application of neural networks to rock engineering systems (RES). *International Journal of Rock Mechanics and Mining Sciences*, ***35***(6), 727-745.

Yang, Y., and Rosenbaum, M. S. (2002). The artificial neural network as a tool for assessing geotechnical properties. *Geotechnical and Geological Engineering*, ***20***(2), 149-168.

Yegnanarayana, B. (2009). *Artificial neural networks*. PHI Learning Pvt. Ltd.

Yu, B., Zheng, H., and Zhan, M. (2005). Geotechnical use of WebGIS in digital library projects. *In International Conference on Asian Digital Libraries*, 467-468. Springer, Berlin, Heidelberg.

Yuanyou, X., Yanming, X., and Ruigeng, Z. (1997). An engineering geology evaluation method based on an artificial neural network and its application. *Engineering Geology*, ***47***(1-2), 149-156.

Zakaria, W. (2011). Bearing capacity based on SPT-computer interpolation. Diyala *Journal of Engineering Sciences*, ***4***(2), 118-129.

Zand, A. G. (2011). Enabling geotechnical data for broader use by the spatial data infrastructures. University of Southern California.

Zekić-Sušac, M., Šarlija, N., and Benšić, M. (2005). Selecting neural network architecture for investment profitability predictions. *Journal of Information and Organizational Sciences*, ***29***(2), 83-95.

Zhang, J., Wu, C., Wang, Y., Ma, Y., Wu, Y., and Mao, X. (2018). The BIM-enabled geotechnical information management of a construction project. *Computing*, ***100***(1), 47-63.

APPENDIX A

Table A1 The soil properties and SPT data were measured using hammer systems for BH (1-5)

BH ID	DEPTH	SPT- N VALUE	SOIL PROPERTISE
BH-1	1.5-3.5 m	5	Fill materials; Soft brownish gray mixture of Sandy lean Silty CLAY with a lot of broken brick fragments/pieces and black traces of organic matter together with white spots of soluble salts.
	3.5-6.5 m	18	Fill materials; Soft to medium brown to light brownish gray Sandy lean Silty CLAY mixture with black spots of organic matter & rusty traces of iron oxide compounds together with some broken brick pieces.
	6.5-9.5 m	12	Fill materials; Medium to stiff brown to brownish gray Sandy lean Silty CLAY with little tiny brick pieces & rusty traces of iron oxide compounds.
BH-2	1.5-3.5 m	53	Very stiff brown to dark brown lean Silty CLAY with black spots of organic matter and white pockets of calcareous materials, together with little fine Gravel at bottom.
	3.5-6.5 m	72	Very stiff to hard brown fat Silty CLAY with black spots of organic matter and white pockets of calcareous materials.
	6.5-9.5 m	83	
BH-3	1.5-3.5 m	41	Stiff to very stiff brown fat Silty CLAY with little fine-grained Gravel & black spots of organic matter.
	3.5-6.5 m	70	
	6.5-9.5 m	100	hard brown tolight brown lean silty claywith white spots calcareous materials
BH-4	1.5-3.5 m	65	Dense to very dense brown to grayish brown fine, medium to coarse grained Clayey Sandy GRAVEL with little white spots of carbonate compound.
	3.5-6.5 m	90	Very dense grayish brown fine, medium to coarse grained Silty Sandy GRAVEL.
	6.5-9.5 m	100	
BH-5	1.5-3.5 m	45	Stiff to very stiff brown lean Silty CLAY with little fine to medium grained Gravel & black spots of organic matter.
	3.5-6.5 m	73	Dense to very dense brown to light brown mixture of fine, medium to coarse grained Clayey GRAVEL.
	6.5-9.5 m	92	Very stiff brown fat Silty CLAY with white pockets of calcareous materials & black spots of organic matter together with little fine Gravel.

Table A2 The soil properties and SPT data were measured using hammer systems for BH (6-10)

BH ID	DEPTH	SPT- N VALUE	SOIL PROPERTISE
BH-6	1.5-3.5 m	57	Stiff to very stiff brown lean Silty CLAY with white spots of carbonate compounds and black spots of organic matter
	3.5-6.5 m	86	Very stiff to hard brown lean Silty CLAY with black spots of organic matter
	6.5-9.5 m	95	
BH-7	1.5-3.5 m	41	Very stiff brown Sandy lean Silty CLAY with fine grained Gravel and white pocket of carbonate compounds together with black traces of organic matter
	3.5-6.5 m	97	Very stiff to hard brown to light brown Gravelly lean Silty CLAY with little medium to coarse grained Sand and white spots of calcareous materials
	6.5-9.5 m	100	Hard brown lean Silty CLAY with little fine-grained Gravel and white spots of carbonate compounds together with black traces of organic matter
BH-8	1.5-3.5 m	33	Stiff to very stiff brown to dark brown lean Silty CLAY with white spots of carbonate compounds and black spots of organic matter
	3.5-6.5 m	78	Very stiff to hard brown lean Silty CLAY with white pockets of carbonate compounds and black spots of organic matter
	6.5-9.5 m	95	Hard brown fat Silty CLAY with white pockets of calcareous materials
BH-9	1.5-3.5 m	19	Backfill material consist of brown lean Silty CLAY with some garbage materials like woods & plastic pieces.
	3.5-6.5 m	92	Dense to very dense light brownish gray mixture of fine-grained Clayey Sandy GRAVEL with white spots/pockets of calcareous materials.
	6.5-9.5 m		
BH-10	1.5-3.5 m	40	Very stiff brown to light brown mixture of Gravelly fat Silty CLAY with white spots of carbonate compounds and black traces organic matter.
	3.5-6.5 m	91	Very stiff brown Gravelly fat Silty CLAY mixture with white spots of calcareous materials.
	6.5-9.5 m	100	Very stiff to hard brown Gravelly fat Silty CLAY with white spots of carbonate compounds and black traces of organic matter.

Table A3 The soil properties and SPT data were measured using hammer systems for BH (11-15)

BH ID	DEPTH	SPT- N VALUE	SOIL PROPERTISE
BH-11	1.5-3.5 m	21	Stiff to very stiff brown to light brown lean Silty CLAY with white spots of calcareous materials and black traces of organic matter.
	3.5-6.5 m	33	Very stiff brown to light reddish brown lean Silty CLAY with a lot of white traces of carbonate compounds/ calcareous materials and little black spots of organic matter.
	6.5-9.5 m	47	
BH-12	1.5-3.5 m	18	Stiff to very stiff brown to brownish gray lean Silty CLAY with white spots of calcareous materials and black traces of organic matter
	3.5-6.5 m	29	Very stiff brown to light brown lean Silty CLAY with white traces of calcareous materials and black spots of organic matter
	6.5-9.5 m	65	
BH-13	1.5-3.5 m	63	Very stiff brown fat Silty CLAY with little fine grained Sand at bottom and little white spots of calcareous materials together with black spots of organic matter.
	3.5-6.5 m	76	Very stiff to hard light brown to brown fat Silty CLAY with little fine grained Gravel in parts and white spots of calcareous materials.
	6.5-9.5 m	100	Very stiff to hard brown to light brown fat Silty CLAY with little white spots of calcareous materials.
BH-14	1.5-3.5 m	80	Very stiff to hard light brown to brown Sandy lean Silty CLAY with black traces of organic matter & white spots of calcareous materials .
	3.5-6.5 m	100	Very stiff to hard light brown to white Sandy lean Silty CLAY with fine to medium grained Gravel and white spots of carbonate compound.
	6.5-9.5 m	100	Very dense to hard light brown mixture of fine to medium grained Clayey Gravelly SAND.
BH-15	1.5-3.5 m	41	Very stiff to hard brown lean Silty CLAY with little black traces of organic matter and white spots of carbonate compounds.
	3.5-6.5 m	95	Hard brown to dark brown lean Silty CLAY with white traces of carbonate compounds.
	6.5-9.5 m	100	Hard brown Gravelly lean Silty CLAY with white pockets of calcareous materials & little black spots of organic matter.
	6.5-9.5 m		Very stiff dark brown fat Silty CLAY with white pockets of calcareous materials and black spots of organic matter.

Table A4 The soil properties and SPT data were measured using hammer systems for BH (16-20)

BH ID	DEPTH	SPT- N VALUE	SOIL PROPERTISE
BH-16	1.5-3.5 m	20	Fill materials consists of very stiff to stiff brown mixture of Gravelly lean Silty CLAY with a lot of fine grained Sand together with white spots of calcareous materials.
	3.5-6.5 m	50	
	6.5-9.5 m		Very stiff dark brown fat Silty CLAY with white pockets of calcareous materials and black spots of organic matter.
BH-17	1.5-3.5 m	50	Very stiff brown to light brown fat Silty CLAY with white pockets of calcareous materials and black spots of organic matter.
	3.5-6.5 m	47	
	6.5-9.5 m	78	Very stiff brownish gray to gray Sandy fat Silty CLAY with white pockets of calcareous materials and black spots of organic matter.
BH-18	1.5-3.5 m	43	Medium to dense gray to brownish gray mixture of fine grained Clayey Sandy GRAVEL with white spots of carbonate compounds .
	3.5-6.5 m	82	Stiff to very stiff brown to light brown Gravelly lean Silty CLAY with white spots of carbonate compounds
	6.5-9.5 m	100	Very dense gray to brownish light gray fine grained Clayey Sandy GRAVEL mixture with white spots of carbonate compounds
BH-19	1.5-3.5 m	71	Very dense gray to light gray fine to medium grained Clayey Sandy GRAVEL with little black traces of organic matter.
	3.5-6.5 m	68	Very stiff to hard gray to grayish light brown Gravelly lean Silty CLAY with black spots of organic matter.
	6.5-9.5 m	100	Very dense brown to light brownish gray fine to medium grained Clayey GRAVEL with little medium to coarse grained Sand.
BH-20	1.5-3.5 m	100	Dense to very dense brownish light gray to brownish gray fine to medium grained Clayey GRAVEL with little white spots of calcareous materials.
	3.5-6.5 m	100	Hard brown to light brown Gravelly lean Silty CLAY with fine to medium grained Sand and white spots of calcareous materials.
	6.5-9.5 m	100	Very dense brownish light gray to light gray fine to medium grained Clayey GRAVEL with little medium to coarse grained Sand in parts.

Table A5 The soil properties and SPT data were measured using hammer systems for BH (21-26)

BH ID	DEPTH	SPT- N VALUE	SOIL PROPERTISE
BH-21	1.5-3.5 m	31	Stiff to very stiff brown fat Silty CLAY with little fine grained Gravel & white spots of carbonate compound together with black traces of organic matter.
	3.5-6.5 m	39	
	6.5-9.5 m	45	
BH-22	1.5-3.5 m	57	Very stiff to hard brown to light brown lean Silty CLAY with a lot of fine grained Gravel and black spots of organic matter together with white pockets of calcareous materials.
	3.5-6.5 m	69	Very stiff brown to light brown mixture of Gravelly lean Silty CLAY with white pockets of calcareous materials.
	6.5-9.5 m	96	Hard brown to light brown Gravelly lean Silty CLAY with little black spots of organic matter and white pockets of calcareous materials.
BH-23	1.5-3.5 m	79	Very stiff to hard light brown to brownish light gray Gravelly lean Silty CLAY mixture with black spots of organic matter
	3.5-6.5 m	87	
	6.5-9.5 m	100	Hard brown to brownish gray fat Silty CLAY with little fine grained Gravel and black traces of organic matter
BH-24	1.5-3.5 m	18	Stiff to very stiff brown fat Silty CLAY with white pockets of carbonate compounds and black spots of organic matter .
	3.5-6.5 m	39	
	6.5-9.5 m	57	Very stiff brown to light brown fat Silty CLAY with white pockets of calcareous materials and black spots of organic matter .
BH-25	1.5-3.5 m	22	Back fill materials; consist of stiff to very stiff brown Gravelly lean Silty CLAY with some pebbles & boulders.
	3.5-6.5 m	45	Very stiff brown Sandy lean Silty CLAY with a lot of fine to medium grained Gravel and cobble, pebbles particles in parts.
	6.5-9.5 m	56	Very stiff brown to dark brown lean Silty CLAY with very little fine grained Gravel particles together with white spots of calcareous materials.
BH-26	1.5-3.5 m	23	Backfilled Soil; consist of brown to light brown lean Silty CLAY with white traces of carbonate compounds & little black spots of organic matter.
	3.5-6.5 m	44	Stiff to very stiff brown lean Silty CLAY with white traces of carbonate compounds and little black spots of organic matter.
	6.5-9.5 m	77	Very stiff to hard brown lean Silty CLAY with white traces of calcareous materials and little fine grained Gravel particles at bottom.

Table A6 The soil properties and SPT data were measured using hammer systems for BH (27-33)

BH ID	DEPTH	SPT- N VALUE	SOIL PROPERTISE
BH-27	1.5-3.5 m	19	Stiff brown to light brown lean Silty CLAY with white traces of carbonate compounds & little black spots of organic matter.
	3.5-6.5 m	44	Stiff to very stiff brown lean Silty CLAY with little fine grained Gravel and white traces of carbonate compounds.
	6.5-9.5 m	75	Very stiff to hard brown lean Silty CLAY with white traces of calcareous materials and little fine grained Gravel particles.
BH-28	1.5-3.5 m	22	Fill materials; consist of brown to light brown lean Silty CLAY with white traces of carbonate compounds and little black spots of organic matter .
	3.5-6.5 m	39	Stiff to very stiff brown fat Silty CLAY with little black traces of organic matter and white pockets of calcareous materials.
	6.5-9.5 m	79	
BH-29	1.5-3.5 m	41	Very stiff brown to dark brown lean Silty CLAY with white pockets of calcareous materials and black spots of organic matter.
	3.5-6.5 m	63	
	6.5-9.5 m	69	
BH-30	1.5-3.5 m	19	Very stiff to hard brown to light brown lean Silty CLAY with little white spots of calcareous materials & black traces of organic matter.
	3.5-6.5 m	70	Very stiff to hard light brown to brown lean Silty CLAY with little black traces of organic matter & white pockets of calcareous materials.
	6.5-9.5 m	63	
BH-31	1.5-3.5 m	29	Stiff to very stiff brown to dark brown lean Silty CLAY with black spots of organic matter and white pockets of carbonate compounds.
	3.5-6.5 m	40	Very stiff to hard brown lean Silty CLAY with white pockets of calcareous materials and little black traces of organic matter.
	6.5-9.5 m	90	Very stiff to hard brown to light brown fat Silty CLAY with little fine grained Gravel and white spots of carbonate compounds .
BH-32	1.5-3.5 m	39	Very stiff to hard brown fat Silty CLAY with white spots of calcareous materials and little black spots of organic matter.
	3.5-6.5 m	72	
	6.5-9.5 m	91	Hard brown fat Silty CLAY with little white spots of calcareous materials and black spots of organic matter together with very little fine Gravels in parts .
BH-33	1.5-3.5 m	22	Very stiff brown lean Silty CLAY with white spots of calcareous materials.
	3.5-6.5 m	41	Very stiff to hard brown fat Silty CLAY with white spots of calcareous materials and black spots of organic matter.
	6.5-9.5 m	72	

Table A7 The soil properties and SPT data were measured using hammer systems for BH (34-40)

BH ID	DEPTH	SPT- N VALUE	SOIL PROPERTISE
BH-34	1.5-3.5 m	20	Fill materials consists of medium brown fine to medium grained Silty Clayey GRAVEL with a lot of debris materials.
	3.5-6.5 m	52	Very stiff to hard brown fat Silty CLAY with white spots and/or pockets of calcareous materials and black spots of organic matter
	6.5-9.5 m	83	
BH-35	1.5-3.5 m	44	Very stiff brown Gravelly fat Silty CLAY with white spots of calcareous materials.
	3.5-6.5 m	63	Very stiff to hard brown to reddish brown fat Silty CLAY with a lot of white pockets of calcareous inaterials & black spots of organic matter together with little fine grained Gravel in parts.
	6.5-9.5 m	89	Very stiff to hard brown fat Silty CLAY with black spots of organic matter and a lot of white pockets of calcareous material and/or calcareous rock crushed pieces at bottom.
BH-36	1.5-3.5 m	23	Stiff to very stiff light grayish brown lean Silty CLAY with white pockets of calcareous materials.
	3.5-6.5 m	50	
	6.5-9.5 m	79	Very stiff to hard light brown to brown fat Silty CLAY with black spots of organic matter & white traces of calcareous materials.
BH-37	1.5-3.5 m	39	Stiff to very stiff brown to light brown fat Silty CLAY with white spots of carbonate compounds and black traces of organic matter.
	3.5-6.5 m	45	
	6.5-9.5 m	85	very stiff brown to light brown fat Silty CLAY with white spots of calcareous materials.
BH-38	1.5-3.5 m	21	Very stiff to hard brown to light brown lean Silty CLAY with large white pockets of calcareous materials and little black spots of organic matter.
	3.5-6.5 m	100	
	6.5-9.5 m	100	Hard brown lean Silty CLAY with little medium to coarse grained Sand and/or fine Gravel together with white pockets of calcareous materials.
BH-39	1.5-3.5 m	61	Dense light brownish gray mixture of sub base materials consist of fine, medium to coarse grained Sandy GRAVEL with little fine fraction of Silt/Clay.
	3.5-6.5 m	76	Dense to very dense brown to light brown fine, medium to coarse grained Clayey Sandy GRAVEL with white spots of carbonate compounds.
	6.5-9.5 m	100	Very dense to hard brown to light brown mixture of fine, medium to coarse grained Clayey Sandy GRAVEL.
BH-40	1.5-3.5 m	43	Dense to very dense brown to brownish gray mixture of Clayey GRAVEL with white spots of carbonate compounds & black traces of organic matter.
	3.5-6.5 m	92	Very stiff to hard mixture of Gravelly lean Silty CLAY with black spots of organic matter & white traces of calcareous materials.
	6.5-9.5 m	98	

Table A8 The soil properties and SPT data were measured using hammer systems for BH (41-47)

BH ID	DEPTH	SPT- N VALUE	SOIL PROPERTISE
BH-41	1.5-3.5 m	72	Very stiff to hard brown lean Silty CLAY with white pockets of calcareous materials and black spots of organic matter.
	3.5-6.5 m	95	
	6.5-9.5 m	100	Very stiff to hard brown fat Silty CLAY with little fine grained Sand and white pockets of calcareous materials together with black spots of organic matter.
BH-42	1.5-3.5 m	74	Very stiff brown to light brown Gravelly lean Silty CLAY with white pockets of calcareous materials & black spots of organic matter.
	3.5-6.5 m	69	Dense to very dense brown fine, medium to coarse grained Clayey Silty GRAVEL with fine to medium grained Sand and white pockets of calcareous materials.
	6.5-9.5 m	100	Very dense brown fine to medium grained Sandy GRAVEL with little fine fraction of Silty/Clay and white pockets of calcareous materials.
BH-43	1.5-3.5 m	23	Very stiff brown to light brown lean Silty CLAY with white pockets of calcareous materials and black spots of organic matter.
	3.5-6.5 m	30	Very dense brown fine to medium grained Clayey GRAVEL with white pockets of calcareous materials.
	6.5-9.5 m	87	Stiff to very stiff brown lean Silty CLAY with little fine grained Gravel and white pockets of calcareous materials together with black spots of organic matter.
BH-44	1.5-3.5 m	39	Very stiff brown to dark brown lean Silty CLAY with black spots of organic matter and white pockets of calcareous materials.
	3.5-6.5 m	74	Very stiff to hard brown to dark brown fat Silty CLAY with white pockets of calcareous materials & black spots of organic matter.
	6.5-9.5 m	81	
BH-45	1.5-3.5 m	8	Medium brownish light gray to grayish brown Sandy Clayey SILT with black spots of organic matter and white pockets of calcareous materials.
	3.5-6.5 m	30	Stiff light brown Gravelly lean Silty CLAY with white pockets of calcareous materials.
	6.5-9.5 m	50	Stiff to very stiff brownish light gray to grayish brown lean Silty CLAY with little black spots of organic matter and white pockets of calcareous materials.
BH-46	1.5-3.5 m	100	Fill materials; consist of grayish brown mixture of fine, medium to coarse grained Sandy GRAVEL with little fine fraction of Silt/Clay.
	3.5-6.5 m	35	Stiff to very stiff brown lean Silty CLAY with little fine grained Gravel & white spots of calcareous materials together with white Limestone fragments.
	6.5-9.5 m	47	
BH-47	1.5-3.5 m	81	very stiff to hard brown lean silty clay
	3.5-6.5 m	91	hard brown mixture of gravelly lean silty clay wit fine grain sand and black spots
	6.5-9.5 m	100	

Table A9 The soil properties and SPT data were measured using hammer systems for BH (48-53)

BH ID	DEPTH	SPT- N VALUE	SOIL PROPERTISE
BH-48	1.5-3.5 m	27	very stiff to brown lean silty clay with white pockets of calcareous material
	3.5-6.5 m	97	very stiff to hard brown lean silty clay
	6.5-9.5 m	93	very stiff to hard brown lean silty clay with a lot of white spots
BH-49	1.5-3.5 m	45	Dense to very dense brown to light brown fine, medium to coarse grained Gravelly Clayey SAND mixture with white traces of carbonate compounds and black spots of organic matter.
	3.5-6.5 m	100	Very dense light grayish brown fine to medium grained Clayey Silty SAND with white spots of carbonate compounds.
	6.5-9.5 m	80	Very dense light brown fine to medium grained Clayey Silty SAND with little fine grained Gravel.
BH-50	1.5-3.5 m	49	Stiff to very stiff brown to reddish light brown lean Silty CLAY with some fine grained Gravel and a lot of white pockets of calcareous materials together with black spots of organic matter.
	3.5-6.5 m	63	Very stiff to hard brown to dark brown Gravelly fat Silty CLAY with white pockets of calcareous materials and black spots of organic matter.
	6.5-9.5 m	100	Hard brown to reddish light brown Gravelly lean Silty CLAY with little fine grained Sand and white pockets of calcareous materials.
BH-51	1.5-3.5 m	22	Stiff to very stiff brown fat Silty CLAY with white spots of calcareous materials and black traces of organic matter.
	3.5-6.5 m	41	
	6.5-9.5 m	79	Very stiff brown fat Silty CLAY with white pockets of carbonate compounds and black spots of organic matter.
BH-52	1.5-3.5 m	33	Stiff to very stiff light brown to brown lean Silty CLAY with some fine grained Gravel in parts and white spots of calcareous materials together with black spots of organic matter.
	3.5-6.5 m	20	
	6.5-9.5 m	59	Stiff to very stiff brownish gray to brownish light gray fat Silty CLAY with white spots of calcareous materials and black spots of organic matter.
BH-53	1.5-3.5 m	18	Soft to medium brown to grayish brown Clayey SILT with a lot of white shiny spots of soluble salts and black traces of organic matter together with little fine grained Sand in parts.
	3.5-6.5 m	20	Medium to stiff brown Sandy lean Silty CLAY with white shiny crystal of soluble salts and black trace of organic matter together with rusty spots of iron oxide compounds.
	6.5-9.5 m	38	Stiff to very stiff brown Clayey SILT with white shiny crystal of soluble salts and rusty spots of iron oxide compounds together with black trace of organic matter .

Table A10 The soil properties and SPT data were measured using hammer systems for BH (54-60)

BH ID	DEPTH	SPT- N VALUE	SOIL PROPERTISE
BH-54	1.5-3.5 m	19	Stiff to very stiff brown lean Silty CLAY with white spots of carbonate compounds and black traces of organic matter.
	3.5-6.5 m	100	Very stiff brown to dark brown lean Silty CLAY with little fine grained Gravel and white spots of carbonate compounds.
	6.5-9.5 m	100	Very dense brown to light brown Clayey Sandy GRAVEL with white spots of carbonate compounds
BH-55	1.5-3.5 m	5	Fill materials consists of soft to medium light brown to brown lean Silty Clay with some fine to medium grained Sand & black spots of organic matter.
	3.5-6.5 m	20	Medium to stiff brown to dark brown Sandy lean Silty CLAY with little fine grained Gravel & white spots of calcareous materials.
	6.5-9.5 m	40	Medium to dense gray brownish gray fine medium to coarse grained Gravelly SAND with little fine fraction of Silt/Clay.
BH-56	1.5-3.5 m	39	Very stiff to hard brownish gray to gray lean Silty CLAY with black spots of organic matter and little fine grained Gravel.
	3.5-6.5 m	81	Very stiff to hard brown fat Silty CLAY with little fine-grained Gravel and a lot of white spots of calcareous materials together with little black traces of organic matter.
	6.5-9.5 m	89	
BH-57	1.5-3.5 m	19	Fill material; Medium dark brown to grayish brown Clayey SILT with a lot of fine grained Sand and black spots of organic matter together with brick broken pieces.
	3.5-6.5 m	31	Medium dark gray to dark grayish brown Sandy lean Silty CLAY with black spots of organic matter .
	6.5-9.5 m	38	Stiff to very stiff brown to light brown lean Silty CLAY with white spots of calcareous materials and little traces of organic matter.
BH-58	1.5-3.5 m	23	Very stiff brown lean Silty CLAY with white spots of calcareous materials and little black spots of organic matter.
	3.5-6.5 m	71	
	6.5-9.5 m	100	Very stiff to hard brown lean Silty CLAY with little black spots of organic matter.
BH-59	1.5-3.5 m	41	Stiff to very stiff light grayish brown lean Silty CLAY with a lot of white spots of calcareous materials.
	3.5-6.5 m	57	
	6.5-9.5 m	55	Very stiff to hard brownish light gray to grayish light brown lean Silty CLAY with black spots of organic matter and little white pockets of calcareous materials.
BH-60	1.5-3.5 m	54	Very stiff to hard brown lean Silty CLAY with white pockets of calcareous materials and black spots of organic matter.
	3.5-6.5 m	81	
	6.5-9.5 m	91	Very stiff to hard brown Sandy lean Silty CLAY with green pockets of Marly Clay and white spots of calcareous materials together with black traces of organic matter

Table A11 The soil properties and SPT data were measured using hammer systems for BH (61-66)

BH ID	DEPTH	SPT- N VALUE	SOIL PROPERTISE
BH-61	1.5-3.5 m	7	Fill materials; Medium to stiff brown to brownish gray Sandy lean Silty CLAY with little tiny brick pieces & rusty traces of iron oxide compounds.
	3.5-6.5 m	9	
	6.5-9.5 m	12	
BH-62	1.5-3.5 m	54	Very stiff to hard brownish light gray to grayish light brown lean Silty CLAY with black spots of organic matter and little white pockets of calcareous materials.
	3.5-6.5 m	60	
	6.5-9.5 m	80	Very stiff to hard brown lean Silty CLAY with white pockets of calcareous materials and black spots of organic matter.
BH-63	1.5-3.5 m	45	Stiff to very stiff light grayish brown lean Silty CLAY with a lot of white spots of calcareous materials.
	3.5-6.5 m	77	Very stiff to hard brown fat Silty CLAY with little fine-grained Gravel and a lot of white spots of calcareous materials together with little black traces of organic matter.
	6.5-9.5 m	82	
BH-64	1.5-3.5 m	63	Very stiff to hard brown to dark brown Gravelly fat Silty CLAY with white pockets of calcareous materials and black spots of organic matter.
	3.5-6.5 m	80	Very stiff to hard brown fat Silty CLAY with little fine-grained Gravel and a lot of white spots of calcareous materials together with little black traces of organic matter.
	6.5-9.5 m	82	
BH-65	1.5-3.5 m	60	Very stiff to hard brown to dark brown Gravelly fat Silty CLAY with white pockets of calcareous materials and black spots of organic matter.
	3.5-6.5 m	99	Very stiff to hard brown lean Silty CLAY with little black spots of organic matter.
	6.5-9.5 m	100	
BH-66	1.5-3.5 m	75	Very stiff brown lean Silty CLAY with white spots of calcareous materials and little black spots of organic matter.
	3.5-6.5 m	100	Very stiff to hard brown lean Silty CLAY with little black spots of organic matter.
	6.5-9.5 m	100	

Table A12 The soil properties and SPT data were measured using hammer systems for BH (67-72)

BH ID	DEPTH	SPT- N VALUE	SOIL PROPERTISE
BH-67	1.5-3.5 m	30	Medium dark gray to dark grayish brown Sandy lean Silty CLAY with black spots of organic matter .
	3.5-6.5 m	62	Very stiff to hard brown to dark brown Gravelly fat Silty CLAY with white pockets of calcareous materials and black spots of organic matter.
	6.5-9.5 m	85	Very stiff to hard brown to dark brown fat Silty CLAY with white pockets of calcareous materials & black spots of organic matter.
BH-68	1.5-3.5 m	42	Stiff to very stiff light grayish brown lean Silty CLAY with a lot of white spots of calcareous materials.
	3.5-6.5 m	89	Very stiff to hard brown Sandy lean Silty CLAY with green pockets of Marly Clay and white spots of calcareous materials together with black traces of organic matter
	6.5-9.5 m	90	
BH-69	1.5-3.5 m	29	Stiff to very stiff light brown to brown lean Silty CLAY with some fine-grained Gravel in parts and white spots of calcareous materials together with black spots of organic matter.
	3.5-6.5 m	35	
	6.5-9.5 m	78	Very stiff brown lean Silty CLAY with white spots of calcareous materials and little black spots of organic matter.
BH-70	1.5-3.5 m	99	Very stiff to hard brown lean Silty CLAY with little black spots of organic matter.
	3.5-6.5 m	79	Very stiff brown lean Silty CLAY with white spots of calcareous materials and little black spots of organic matter.
	6.5-9.5 m	70	
BH-71	1.5-3.5 m	19	Fill material; Medium dark brown to grayish brown Clayey SILT with a lot of fine grained Sand and black spots of organic matter together with brick broken pieces.
	3.5-6.5 m	100	Very stiff to hard brown lean Silty CLAY with little black spots of organic matter.
	6.5-9.5 m	72	Very stiff brown lean Silty CLAY with white spots of calcareous materials and little black spots of organic matter.
BH-72	1.5-3.5 m	17	Fill material; Medium dark brown to grayish brown Clayey SILT with a lot of fine grained Sand and black spots of organic matter together with brick broken pieces.
	3.5-6.5 m	43	Stiff to very stiff light grayish brown lean Silty CLAY with a lot of white spots of calcareous materials.
	6.5-9.5 m	55	

Table A13 The soil properties and SPT data were measured using hammer systems for BH (73-78).

BH ID	DEPTH	SPT- N VALUE	SOIL PROPERTISE
BH-73	1.5-3.5 m	45	Stiff to very stiff light grayish brown lean Silty CLAY with a lot of white spots of calcareous materials.
	3.5-6.5 m	83	Very stiff to hard brown to dark brown fat Silty CLAY with white pockets of calcareous materials & black spots of organic matter.
	6.5-9.5 m	100	Very stiff to hard brown lean Silty CLAY with little black spots of organic matter.
BH-74	1.5-3.5 m	85	Very stiff to hard brown fat Silty CLAY with little fine-grained Gravel and a lot of white spots of calcareous materials together with little black traces of organic matter.
	3.5-6.5 m	83	
	6.5-9.5 m	100	Very stiff to hard brown lean Silty CLAY with little black spots of organic matter.
BH-75	1.5-3.5 m	25	Medium to stiff brown to dark brown Sandy lean Silty CLAY with little fine grained Gravel & white spots of calcareous materials.
	3.5-6.5 m	32	
	6.5-9.5 m	54	Stiff to very stiff light grayish brown lean Silty CLAY with a lot of white spots of calcareous materials
BH-76	1.5-3.5 m	22	Stiff to very stiff brown fat Silty CLAY with white spots of calcareous materials and black traces of organic matter.
	3.5-6.5 m	38	
	6.5-9.5 m	83	Very stiff to hard brown fat Silty CLAY with little fine-grained Gravel and a lot of white spots of calcareous materials together with little black traces of organic matter.
BH-77	1.5-3.5 m	32	Medium to stiff brown to dark brown Sandy lean Silty CLAY with little fine grained Gravel & white spots of calcareous materials.
	3.5-6.5 m	63	Very stiff to hard brown to dark brown Gravelly fat Silty CLAY with white pockets of calcareous materials and black spots of organic matter.
	6.5-9.5 m	70	Very stiff brown lean Silty CLAY with white spots of calcareous materials and little black spots of organic matter.
BH-78	1.5-3.5 m	31	Stiff to very stiff light brown to brown lean Silty CLAY with some fine-grained Gravel in parts and white spots of calcareous materials together with black spots of organic matter.
	3.5-6.5 m	69	Very stiff brown lean Silty CLAY with white spots of calcareous materials and little black spots of organic matter.
	6.5-9.5 m	75	

Table A14 The soil properties and SPT data were measured using hammer systems for BH (79-84).

BH ID	DEPTH	SPT- N VALUE	SOIL PROPERTISE
BH-79	1.5-3.5 m	37	Stiff to very stiff brown fat Silty CLAY with white spots of calcareous materials and black traces of organic matter.
	3.5-6.5 m	73	Very stiff brown lean Silty CLAY with white spots of calcareous materials and little black spots of organic matter.
	6.5-9.5 m	89	Very stiff to hard brown Sandy lean Silty CLAY with green pockets of Marly Clay and white spots of calcareous materials together with black traces of organic matter
BH-80	1.5-3.5 m	82	Very stiff to hard brown fat Silty CLAY with little fine-grained Gravel and a lot of white spots of calcareous materials together with little black traces of organic matter.
	3.5-6.5 m	91	Very stiff to hard brown lean Silty CLAY with little black spots of organic matter.
	6.5-9.5 m	99	
BH-81	1.5-3.5 m	77	Very stiff to hard brown fat Silty CLAY with little fine-grained Gravel and a lot of white spots of calcareous materials together with little black traces of organic matter.
	3.5-6.5 m	86	
	6.5-9.5 m	100	Very stiff to hard brown lean Silty CLAY with little black spots of organic matter.
BH-82	1.5-3.5 m	32	Medium to stiff brown to dark brown Sandy lean Silty CLAY with little fine grained Gravel & white spots of calcareous materials.
	3.5-6.5 m	100	Very stiff to hard brown lean Silty CLAY with little black spots of organic matter.
	6.5-9.5 m	100	
BH-83	1.5-3.5 m	28	very stiff to brown lean silty clay with white pockets of calcareous material
	3.5-6.5 m	50	Stiff to very stiff brownish light gray to grayish brown lean Silty CLAY with little black spots of organic matter and white pockets of calcareous materials
	6.5-9.5 m	72	Very stiff brown lean Silty CLAY with white spots of calcareous materials and little black spots of organic matter.
BH-84	1.5-3.5 m	33	Medium to stiff brown to dark brown Sandy lean Silty CLAY with little fine grained Gravel & white spots of calcareous materials.
	3.5-6.5 m	79	Very stiff brown lean Silty CLAY with white spots of calcareous materials and little black spots of organic matter.
	6.5-9.5 m	81	

Table A15 The soil properties and SPT data were measured using hammer systems for BH (85-90).

BH ID	DEPTH	SPT- N VALUE	SOIL PROPERTISE
BH-85	1.5-3.5 m	39	Stiff to very stiff brown to light brown lean Silty CLAY with white spots of calcareous materials and little traces of organic matter.
	3.5-6.5 m	38	
	6.5-9.5 m	71	Very stiff brown lean Silty CLAY with white spots of calcareous materials and little black spots of organic matter.
BH-86	1.5-3.5 m	41	Stiff to very stiff brown to light brown lean Silty CLAY with white spots of calcareous materials and little traces of organic matter.
	3.5-6.5 m	36	
	6.5-9.5 m	69	Very stiff brown lean Silty CLAY with white spots of calcareous materials and little black spots of organic matter.
BH-87	1.5-3.5 m	35	Stiff to very stiff brown to light brown lean Silty CLAY with white spots of calcareous materials and little traces of organic matter.
	3.5-6.5 m	41	
	6.5-9.5 m	84	Very stiff to hard brown fat Silty CLAY with little fine-grained Gravel and a lot of white spots of calcareous materials together with little black traces of organic matter.
BH-88	1.5-3.5 m	31	Medium to stiff brown to dark brown Sandy lean Silty CLAY with little fine grained Gravel & white spots of calcareous materials.
	3.5-6.5 m	100	Very stiff to hard brown lean Silty CLAY with little black spots of organic matter.
	6.5-9.5 m	87	Very stiff to hard brown Sandy lean Silty CLAY with green pockets of Marly Clay and white spots of calcareous materials together with black traces of organic matter
BH-89	1.5-3.5 m	34	Stiff to very stiff brown to light brown lean Silty CLAY with white spots of calcareous materials and little traces of organic matter.
	3.5-6.5 m	100	Very stiff to hard brown lean Silty CLAY with little black spots of organic matter.
	6.5-9.5 m	100	
BH-90	1.5-3.5 m	37	Stiff to very stiff brown to light brown lean Silty CLAY with white spots of calcareous materials and little traces of organic matter.
	3.5-6.5 m	90	Very stiff to hard brown Sandy lean Silty CLAY with green pockets of Marly Clay and white spots of calcareous materials together with black traces of organic matter
	6.5-9.5 m	100	Very stiff to hard brown lean Silty CLAY with little black spots of organic matter.

Table A16 The soil properties and SPT data were measured using hammer systems for BH (90-96).

BH ID	DEPTH	SPT- N VALUE	SOIL PROPERTISE
BH-91	1.5-3.5 m	50	Stiff to very stiff brownish light gray to grayish brown lean Silty CLAY with little black spots of organic matter and white pockets of calcareous materials
	3.5-6.5 m	68	Very stiff brown lean Silty CLAY with white spots of calcareous materials and little black spots of organic matter.
	6.5-9.5 m	100	Very stiff to hard brown lean Silty CLAY with little black spots of organic matter.
BH-92	1.5-3.5 m	20	Medium to stiff brown to dark brown Sandy lean Silty CLAY with little fine grained Gravel & white spots of calcareous materials.
	3.5-6.5 m	80	Very stiff to hard brown fat Silty CLAY with little fine-grained Gravel and a lot of white spots of calcareous materials together with little black traces of organic matter.
	6.5-9.5 m	100	Very stiff to hard brown lean Silty CLAY with little black spots of organic matter.
BH-93	1.5-3.5 m	44	Stiff to very stiff light grayish brown lean Silty CLAY with a lot of white spots of calcareous materials.
	3.5-6.5 m	73	Very stiff brown lean Silty CLAY with white spots of calcareous materials and little black spots of organic matter.
	6.5-9.5 m	79	
BH-94	1.5-3.5 m	11	Fill materials; Medium to stiff brown to brownish gray Sandy lean Silty CLAY with little tiny brick pieces & rusty traces of iron oxide compounds.
	3.5-6.5 m	37	Stiff to very stiff brown to light brown lean Silty CLAY with white spots of calcareous materials and little traces of organic matter.
	6.5-9.5 m	45	
BH-95	1.5-3.5 m	83	Very stiff to hard brown fat Silty CLAY with little fine-grained Gravel and a lot of white spots of calcareous materials together with little black traces of organic matter.
	3.5-6.5 m	100	Very stiff to hard brown lean Silty CLAY with little black spots of organic matter.
	6.5-9.5 m	100	
BH-96	1.5-3.5 m	47	Stiff to very stiff brown to light brown lean Silty CLAY with white spots of calcareous materials and little traces of organic matter.
	3.5-6.5 m	100	Very stiff to hard brown lean Silty CLAY with little black spots of organic matter.
	6.5-9.5 m	100	

Table A17 The soil properties and SPT data were measured using hammer systems for BH (97-102).

BH ID	DEPTH	SPT- N VALUE	SOIL PROPERTISE
BH-97	1.5-3.5 m	53	Stiff to very stiff brownish light gray to grayish brown lean Silty CLAY with little black spots of organic matter and white pockets of calcareous materials
	3.5-6.5 m	100	Very stiff to hard brown lean Silty CLAY with little black spots of organic matter
	6.5-9.5 m	100	
BH-98	1.5-3.5 m	29	Stiff to very stiff brown to light brown lean Silty CLAY with white spots of calcareous materials and little traces of organic matter.
	3.5-6.5 m	48	
	6.5-9.5 m	49	
BH-99	1.5-3.5 m	18	Fill materials; Medium to stiff brown to brownish gray Sandy lean Silty CLAY with little tiny brick pieces & rusty traces of iron oxide compounds
	3.5-6.5 m	29	Stiff to very stiff brown to light brown lean Silty CLAY with white spots of calcareous materials and little traces of organic matter.
	6.5-9.5 m	33	
BH-100	1.5-3.5 m	7	Fill materials; Medium to stiff brown to brownish gray Sandy lean Silty CLAY with little tiny brick pieces & rusty traces of iron oxide compounds.
	3.5-6.5 m	26	Stiff to very stiff brown fat Silty CLAY with little fine grained Gravel & white spots of carbonate compound together with black traces of organic matter.
	6.5-9.5 m	38	
BH-101	1.5-3.5 m	75	Very stiff brown lean Silty CLAY with white spots of calcareous materials and little black spots of organic matter.
	3.5-6.5 m	100	Very stiff to hard brown lean Silty CLAY with little black spots of organic matter
	6.5-9.5 m	100	
BH-102	1.5-3.5 m	65	Very stiff brown lean Silty CLAY with white spots of calcareous materials and little black spots of organic matter.
	3.5-6.5 m	90	Very stiff to hard brown Sandy lean Silty CLAY with green pockets of Marly Clay and white spots of calcareous materials together with black traces of organic matter
	6.5-9.5 m	100	Very stiff to hard brown lean Silty CLAY with little black spots of organic matter

APPENDIX B

Table B1. Full data of all boreholes of study area.

BH	DEPTH	X	Y	LL%	PL%	PI%	WC%	c (kN/m^2)	Φ (°)	Fine Content	SPT-N Value (kN/m^2)
1	1.5–3.5	406,851.5	4,009,570	46	22	24	28.3	51	4	62.1	7
2	1.5–3.5	405,972.9	4,009,284.2	40	22	18	15	96	3	94.1	54
3	1.5–3.5	407,487.6	4,007,947.1	47	25	22	18	99	5	91.5	57
4	1.5–3.5	406,121.1	4,008,204.7	40	22	18	15.0	96	3	94.1	54
5	1.5–3.5	407,443.2	4,008,702.7	50	27	23	20.8	109	5	92.9	41
6	1.5–3.5	407,941.4	4,009,347.7	50	28	22	13.9	108	4	91.8	45
7	1.5–3.5	408,217.9	4,008,512.23	35	20	19	20.0	96	4	96	41
8	1.5–3.5	408,997.4	4,008,917.8	39	21	18	16.3	109	5	89.4	45
9	1.5–3.5	408,743.4	4,009,398.1	47	25	22	18.0	99	5	91.5	57
10	1.5–3.5	408,026.1	4,010,406	45	24	21	16.6	96	5	95.5	63
11	1.5–3.5	409,617.8	4,011,321.6	46	27	19	20.2	99	5	90.7	41
12	1.5–3.5	408,588.1	4,011,780.2	45	25	20	19.0	97	4	91.6	60
13	1.5–3.5	409,762.1	4,012,805.4	48	26	22	19.7	94	5	81.3	75
14	1.5–3.5	411,184.2	4,011,787.2	49	23	26	19.6	108	4	96.3	33
15	1.5–3.5	411,184.3	4,012,540.7	47	25	22	15.6	105	5	97.4	30
16	1.5–3.5	411,247.7	4,013,522.9	48	26	22	18.4	58	3	92.7	19
17	1.5–3.5	409,969.9	4,010,643.8	58	31	27	20.5	91	4	88.9	40
18	1.5–3.5	409,662.9	4,009,977	56	30	26	18.8	94	4	69.1	42
19	1.5–3.5	409,915.1	4,009,232.2	45	24	21	13.6	77	3	95.9	29
20	1.5–3.5	410,862.1	4,009,607.35	44	25	19	18.3	69	5	94.5	30
21	1.5–3.5	411,994.6	4,009,216.9	42	23	19	19.2	70	4	98.2	29
22	1.5–3.5	411,166.1	4,010,438.9	50	26	24	17.9	95	5	92.2	58
23	1.5–3.5	412,126.9	4,010,308.3	51	29	29	19.8	95	5	96.2	70
24	1.5–3.5	411,550.5	4,011,441.2	44	23	21	14.8	95	7	100	80
25	1.5–3.5	413,143.3	4,011,488.9	44	25	19	20.5	97	4	93.5	41
26	1.5–3.5	414,064.7	4,011,692.8	41	23	18	17.4	110	4	53.6	37
27	1.5–3.5	415,317.3	4,010,885.4	50	26	24	15.9	116	5	68.5	23
28	1.5–3.5	414,149.3	4,009,671.4	51	27	24	19.1	94	4	87.3	19
29	1.5–3.5	414,362.5	4,008,450.6	52	24	28	19.7	90	4	86.4	17
30	1.5–3.5	416,171.1	4,012,249.6	45	24	21	15.3	98	6	79.8	43
31	1.5–3.5	415,609.8	4,012,761.8	38	21	17	16.0	95	5	70.6	45
32	1.5–3.5	414,549.1	4,013,637	38	21	17		70	12	97	100
33	1.5–3.5	417,922.5	4,010,462	53	27	26	21.6	69	3	92.6	25
34	1.5–3.5	416,961.1	4,011,319.3	49	23	26	15.1	112	5	86.7	71
35	1.5–3.5	416,542.1	4,010,233.5	43	23	20	17.8	91	3	89.3	79
36	1.5–3.5	416,909.4	4,008,754	44	24	20	14.8	92	4	66.2	85

Table B1. *Cont.*

BH	DEPTH	X	Y	LL %	PL%	PI%	WC%	c (kN/m^2)	Φ (°)	Fine Content	SPT-N Value (kN/m^2)
37	1.5–3.5	406,775.3	4,007,107.5	50	26	24	18.3	82	4	92.1	18
38	1.5–3.5	405,227.4	4,007,274.3	53	27	26	17.3	74	3	96.4	25
39	1.5–3.5	407,403.9	4,006,885.3	40	22	18	13.6	105	5	63.8	19
40	1.5–3.5	407,715.1	4,007,488.5	43	22	21	19.1	90	4	93.2	20
41	1.5–3.5	408,445.4	4,007,069.4	45	24	21	15.8	58	5	95.9	19
42	1.5–3.5	408,736.7	4,005,101.9	44	25	19	17.6	60	4	95.5	22
43	1.5–3.5	408,248.5	4,006,694.7	43	24	19	19.9	69	4	92.1	22
44	1.5–3.5	407,872.4	4,006,657.22	56	25	31	15.6	116	5	95.5	28
45	1.5–3.5	409,311.9	4,005,786	46	24	22	17.7	112	4	97.4	32
46	1.5–3.5	408,775.59	4,006,631.24	46	22	24	21.1	85	4	95.8	19
47	1.5–3.5	409,973.4	4,006,133	53	25	28	20.9	87	5	93.6	31
48	1.5–3.5	409,048.64	4,007,069.39	46	24	22	16.6	89	4	96.2	29
49	1.5–3.5	409,874.19	4,007,406.1	46	24	22	17.7	92	5	94.1	37
50	1.5–3.5	408,985.14	4,007,907.6	54	26	28	15.3	99	4	94.1	39
51	1.5–3.5	411,015.2	4,007,902.7	55	24	31	15.3	112	5	95.2	82
52	1.5–3.5	418,521.8	4,007,163.4	57	25	32	19.6	104	4	92.9	77
53	1.5–3.5	409,785.25	4,008,333.1	48	22	26	14.4	97	4	95.5	22
54	1.5–3.5	410,998.6	4,008,878.3	49	26	23	18.8	105	4	92.2	32
55	1.5–3.5	410,109.1	4,006,834.44	41	19	22	16.8	101	4	87.3	41
56	1.5–3.5	410,419.8	4,006,001	45	21	24	16.3	123	5	52.3	28
57	1.5–3.5	412,049.02	4,007,215.97	52	24	28	21.8	109	5	51.8	44
58	1.5–3.5	411,263	4,006,447.5	51	27	24	19.4	96	4	94.2	33
59	1.5–3.5	412,664.18	4,007,328.4	49	25	24	19.4	124	4	92.6	38
60	1.5–3.5	411,990	4,006,315.2	44	25	19	21.7	136	5	95.7	39
61	1.5–3.5	413,164.9	4,008,779	43	23	20	18.9	119	5	96.6	41
62	1.5–3.5	412,846.74	4,006,559.81	49	26	23	17.4	79	4	93.5	39
63	1.5–3.5	412,536.5	4,005,174.2	48	27	21	18.0	81	4	93.5	35
64	1.5–3.5	415,747.4	4,005,960.69	48	23	25	16.8	96	4	96.4	21
65	1.5–3.5	414,814.8	4,007,156.9	40	21	19	17.9	97	5	39.7	31
66	1.5–3.5	415,071.9	4,004,866.9	47	24	23	19.0	95	5	90.8	34
67	1.5–3.5	417,971.23	4,001,685.01	48	27	21	17.4	88	8	30	61
68	1.5–3.5	418,519	4,003,222.9	0	0	0	17.7	85	10	18	37
69	1.5–3.5	415,926	4,002,878	0	0	0	19.0	83	9	14	50
70	1.5–3.5	416,167	4,004,572.3	0	0	0	11.0	80	8	15	36
71	1.5–3.5	419,289	4,001,977.6	0	0	0	18.6	114	5	25	40
72	1.5–3.5	411,924.27	4,004,297.59	57	25	32	16.4	116	5	94.7	72
73	1.5–3.5	410,482.29	4,003,953.63	48	23	25	13.4	109	5	91.4	74
74	1.5–3.5	412,426.98	4,002,802.69	45	21	24	12.1	144	4	95.6	23

Table B1. *Cont.*

BH	DEPTH	X	Y	LL %	PL%	PI%	WC%	c (kN/m²)	Φ (°)	Fine Content	SPT-N Value (kN/m²)
81	1.5–3.5	414,253.79	4,000,845.76	47	22	25	17.5	86	5	91.7	81
82	1.5–3.5	415,598.5	4,000,259	45	22	24	20.1	89	3	93.5	83
83	1.5–3.5	413,510.13	3,999,595.57	47	25	22	20.5	81	3	95.6	27
84	1.5–3.5	412,160.93	3,999,051.88	41	22	19	12.7	12	36	100	45
85	1.5–3.5	410,732.9	3,999,785	40	21	19	10.8	15	30	33	47
86	1.5–3.5	410,253	3,998,445	43	23	20	5.7	19	35	42	53
87	1.5–3.5	413,309	3,998,392.5	41	21	20	12.3	108	5	81.6	60
88	1.5–3.5	410,136.16	4,001,490.72	55	26	29	17.3	81	3	96.2	22
89	1.5–3.5	409,296.11	4,002,026.51	46	24	22	22.1	96	5	96.8	31
90	1.5–3.5	408,932.6	4,003,851.9	50	24	26	14.8	90	3	97.3	29
91	1.5–3.5	408,515.58	4,002,310.93	44	30	14	31.1	25	2	90.1	18
92	1.5–3.5	409,939	4,003,009.6	44	28	16	29.2	29	3	89.2	12
93	1.5–3.5	407,821.05	4,002,866.56	42	21	21	23.2	45	4	91.6	19
94	1.5–3.5	407,298.5	4,004,255.62	49	26	23	16.7	38	3	89.8	5
95	1.5–3.5	405,937	4,003,224	43	23	20	13.3	90	4	93.3	7
96	1.5–3.5	407,774.75	4,005,380.1	38	21	17	16.9	98	4	96.6	39
97	1.5–3.5	407,844.33	4,005,870.11	39	22	17	18.9	43	4	56.7	19
98	1.5–3.5	406,914.85	4,005,671.15	45	23	22	14.5	121	6	94.6	23
99	1.5–3.5	405,242	4,004,431.7	46	25	21	15.6	110	4	98.1	25
100	1.5–3.5	405,684.54	4,005,717.45	43	21	22	14.8	95	4	94.3	41
101	1.5–3.5	408,025.12	3,999,907.5	46	24	22	15.7	103	4	96.2	54
102	1.5–3.5	406,400.4	4,001,124	42	26	16	15.5	94	4	96.1	75
103	3.5–6.5	406,851.5	4,009,570	49	23	26	29.4	40	4	83.5	11
104	3.5–6.5	405,972.9	4,009,284.2	48	23	25	29.1	45	5	87	9
105	3.5–6.5	407,487.6	4,007,947.1	50	24	26	19.2	109	5	95.1	72
106	3.5–6.5	406,121.1	4,008,204.7	46	26	20	19.4	85	4	97.9	60
107	3.5–6.5	407,443.2	4,008,702.7	52	26	26	23.2	112	4	94.9	70
108	3.5–6.5	407,941.4	4,009,347.7	52	29	23	14.8	103	4	93.7	77
109	3.5–6.5	408,217.9	4,008,512.23	40	22	18	20.5	113	5	100	90
110	3.5–6.5	408,997.4	4,008,917.8	36	23	13		105	5	98.4	73
111	3.5–6.5	408,743.4	4,009,398.1	44	24	20	19.3	102	5	95.1	86
112	3.5–6.5	408,026.1	4,010,406	42	23	19	15.5	102	6	94.1	80
113	3.5–6.5	409,617.8	4,011,321.6	64	33	31	19.5	89	4	80.5	97
114	3.5–6.5	408,588.1	4,011,780.2	48	25	23	20.1	93	5	89.1	99
115	3.5–6.5	409,762.1	4,012,805.4	46	25	21	17.2	98	5	72.5	100
116	3.5–6.5	411,184.2	4,011,787.2	45	24	21	14.3	104	4	95.7	50
117	3.5–6.5	411,184.3	4,012,540.7	49	28	21	18.2	132	6	92.9	62
118	3.5–6.5	411,247.7	4,013,522.9	45	27	18	19.0	62	4	100	25
119	3.5–6.5	409,969.9	4,010,643.8	51	27	24	18.7	93	5	94.3	91
120	3.5–6.5	409,662.9	4,009,977	54	29	25	19.3	95	5	94.2	89
121	3.5–6.5	409,915.1	4,009,232.2	47	23	24	17.5	87	5	94.6	33
122	3.5–6.5	410,862.1	4,009,607.35	46	22	24	20.7	82	4	98.2	41
123	3.5–6.5	411,994.6	4,009,216.9	45	21	23	17.0	72	5	97.5	35

Table B1. *Cont.*

BH	DEPTH	X	Y	LL %	PL%	PI%	WC%	c (kN/m^2)	Φ (°)	Fine Content	SPT-N Value (kN/m^2)
124	3.5–6.5	411,166.1	4,010,438.9	54	25	29	18.6	91	4	97.8	76
125	3.5–6.5	412,126.9	4,010,308.3	55	26	29	19.3	93	4	92.1	79
126	3.5–6.5	411,550.5	4,011,441.2	46	22	24	14.8	97	8	100	100
127	3.5–6.5	413,143.3	4,011,488.9	46	25	21	21.1	99	4	95.2	75
128	3.5–6.5	414,064.7	4,011,692.8	60	32	28	21.2	147	5	86.6	50
129	3.5–6.5	415,317.3	4,010,885.4	50	28	22	20.2	98	5	91.9	56
130	3.5–6.5	414,149.3	4,009,671.4	42	23	19	19.4	95	5	41.6	100
131	3.5–6.5	414,362.5	4,008,450.6	71	36	35	19.7	95	5	59.7	43
132	3.5–6.5	416,171.1	4,012,249.6	38	21	17	16.8	95	5	82.6	82
133	3.5–6.5	415,609.8	4,012,761.8	44	25	19	16.1	97	6	85.8	83
134	3.5–6.5	414,549.1	4,013,637	42	23	19	10.4	75	11	100	100
135	3.5–6.5	417,922.5	4,010,462	48	26	22	20.2	76	5	96.1	37
136	3.5–6.5	416,961.1	4,011,319.3	48	23	25		114	5	69.1	75
137	3.5–6.5	416,542.1	4,010,233.5	45	26	19	21.6	94	5	94.9	87
138	3.5–6.5	416,909.4	4,008,754	54	32	22	19.6	94	4	89.4	83
139	3.5–6.5	406,775.3	4,007,107.5	53	28	25	19.3	78	3	97.9	45
140	3.5–6.5	405,227.4	4,007,274.3	54	28	26	16.8	82	4	98.6	32
141	3.5–6.5	407,403.9	4,006,885.3	38	21	17	17.3	98	5	92.5	39
142	3.5–6.5	407,715.1	4,007,488.5	47	23	24	21.5	92	5	96.1	55
143	3.5–6.5	408,445.4	4,007,069.4	44	23	21	19.3	81	3	96.3	40
144	3.5–6.5	408,736.7	4,005,101.9	46	23	23	19.2	87	4	93.8	38
145	3.5–6.5	408,248.5	4,006,694.7	52	26	26	22.3	93	5	94.6	53
146	3.5–6.5	407,872.4	4,006,657.22	57	26	31	18.7	106	5	95.6	61
147	3.5–6.5	409,311.9	4,005,786	55	26	29	17.6	103	4	96.9	63
148	3.5–6.5	408,775.59	4,006,631.24	47	23	25	15.8	96	5	92.2	70
149	3.5–6.5	409,973.4	4,006,133	43	21	22	20.5	107	4	87.9	69
150	3.5–6.5	409,048.64	4,007,069.39	46	23	23	17.3	90	4	94.6	50
151	3.5–6.5	409,874.19	4,007,406.1	45	22	23	17.5	92	5	94	73
152	3.5–6.5	408,985.14	4,007,907.6	56	30	26	18.2	110	5	93.3	72
153	3.5–6.5	411,015.2	4,007,902.7	63	28	35	21.8	102	6	94	91
154	3.5–6.5	418,521.8	4,007,163.4	56	24	32	16.6	129	5	96.1	86
155	3.5–6.5	409,785.25	4,008,333.1	51	27	24	18.2	118	6	96.4	40
156	3.5–6.5	410,998.6	4,008,878.3	49	26	23	18.7	99	5	96.3	100
157	3.5–6.5	410,109.1	4,006,834.44	46	19	27	17.2	98	5	90.3	30
158	3.5–6.5	410,419.8	4,006,001	48	20	28	18.2	126	5	87.2	50
159	3.5–6.5	412,049.02	4,007,215.97	54	28	26	17.8	134	6	96.4	63
160	3.5–6.5	411,263	4,006,447.5	55	24	31	19.5	99	5	94.2	79
161	3.5–6.5	412,664.18	4,007,328.4	46	26	20	17.2	118	4	96.6	22
162	3.5–6.5	411,990	4,006,315.2	46	25	21	17.1	121	5	96.5	38
163	3.5–6.5	413,164.9	4,008,779	47	23	24	16.3	115	6	69.1	36
164	3.5–6.5	412,846.74	4,006,559.81	45	24	21	23.8	76	4	94.7	45
165	3.5–6.5	412,536.5	4,005,174.2	47	26	21	18.9	89	5	98.1	41
166	3.5–6.5	415,747.4	4,005,960.69	45	21	24	20.4	126	5	98.4	100
167	3.5–6.5	414,814.8	4,007,156.9	44	22	22	20.4	120	5	96.4	100

Table B1. *Cont.*

BH	DEPTH	X	Y	LL %	PL%	PI%	WC%	c (kN/m^2)	Φ (°)	Fine Content	SPT-N Value (kN/m^2)
168	3.5–6.5	415,071.9	4,004,866.9	46	23	23	18.9	117	5	90.8	100
169	3.5–6.5	417,971.23	4,001,685.01	45	25	20	17.4	91	9	39	76
170	3.5–6.5	418,519	4,003,222.9	45	24	21	17.7	95	11	64	90
171	3.5–6.5	415,926	4,002,878	41	23	19	19.0	89	11	39	68
172	3.5–6.5	416,167	4,004,572.3	40	20	24	18.0	76	9	55	99
173	3.5–6.5	419,289	4,001,977.6	0	0	0	18.6	112	5	78.8	92
174	3.5–6.5	411,924.27	4,004,297.59	62	26	36	16.6	125	5	68.3	80
175	3.5–6.5	410,482.29	4,003,953.63	49	23	26	16.6	115	6	17.6	69
176	3.5–6.5	412,426.98	4,002,802.69	48	25	23	18.1	140	5	39.9	100
177	3.5–6.5	414,365	4,003,408	39	21	18	17.5	92	4	98.1	80
178	3.5–6.5	411,975.73	4,001,202.95	61	26	35	16.9	137	5	97.2	72
179	3.5–6.5	414,022.9	4,002,387	53	26	27	16.6	119	5	63.6	73
180	3.5–6.5	411,697.91	4,000,107.57	44	23	21	20.3	98	5	50.4	20
181	3.5–6.5	410,200	3,999,706	37	25	12	17.8	60	6	94.2	37
182	3.5–6.5	413,372.73	4,001,528.38	42	21	21	16.3	94	6	87.5	29
183	3.5–6.5	414,253.79	4,000,845.76	46	22	24	20.1	92	4	76.5	91
184	3.5–6.5	408,932.6	4,000,259	48	23	25	19.2	94	4	94.7	100
185	3.5–6.5	413,510.13	3,999,595.57	48	24	24	17.4	85	3	88.6	97
186	3.5–6.5	412,160.93	3,999,051.88	39	21	18	14.1	38	29	100	100
187	3.5–6.5	410,732.9	3,999,785	38	20	18	10.8	8	32	41	100
188	3.5–6.5	410,253	3,998,445	41	20	21	8.7	13	29	44	100
189	3.5–6.5	413,309	3,998,392.5	46	24	22	13.4	94	5	61.1	63
190	3.5–6.5	410,136.16	4,001,490.72	58	27	31	18.4	93	5	99.1	41
191	3.5–6.5	409,296.11	4,002,026.51	50	26	24	21.0	108	4	93.5	39
192	3.5–6.5	409,707	4,003,851.9	51	28	23	15.0	87	3	96	48
193	3.5–6.5	408,515.58	4,002,310.93	50	28	22	28.2	38	4	95.3	20
194	3.5–6.5	409,939	4,003,009.6	41	24	17	25.4	40	5	78.4	29
195	3.5–6.5	407,821.05	4,002,866.56	45	26	19	24.7	51	4	87.9	100
196	3.5–6.5	407,298.5	4,004,255.62	45	23	22	12.2	102	5	93.4	20
197	3.5–6.5	405,937	4,003,224	41	23	18	15.0	87	3	89.8	26
198	3.5–6.5	407,774.75	4,005,380.1	48	23	25	19.9	128	6	91.4	81
199	3.5–6.5	407,844.33	4,005,870.11	38	26	12	23.7	50	4	66.7	31
200	3.5–6.5	406,914.85	4,005,671.15	55	26	29	17.4	112	5	98.7	71
201	3.5–6.5	405,242	4,004,431.7	48	23	25	17.2	125	5	93.8	70
202	3.5–6.5	405,684.54	4,005,717.45	50	27	23	16.2	94	3	98.1	45
203	3.5–6.5	408,025.12	3,999,907.5	48	26	22	17.7	81	3	99.1	81
204	3.5–6.5	406,400.4	4,001,124	49	26	23	21	85	4	98.8	100
205	6.5–9.5	406,851.5	4,009,570	47	23	24	26.9	41	3	83.5	10
206	6.5–9.5	405,972.9	4,009,284.2	51	24	27	30.4	51	3.5	93.8	12
207	6.5–9.5	407,487.6	4,007,947.1	56	30	26	19.1	107	4	93.5	83
208	6.5–9.5	406,121.1	4,008,204.7	54	28	26	16.4	112	5	95.7	80
209	6.5–9.5	407,443.2	4,008,702.7	49	27	22	13.6	105	4.5	94.8	96
210	6.5–9.5	407,941.4	4,009,347.7	55	26	29	21.7	97	4	97.5	82
211	6.5–9.5	408,217.9	4,008,512.23	42	28	0	18.3	117	5	100	100

Table B1. *Cont.*

BH	DEPTH	X	Y	LL %	PL%	PI%	WC%	c (kN/m^2)	Φ (°)	Fine Content	SPT-N Value (kN/m^2)
212	6.5–9.5	408,997.4	4,008,917.8	54	26	28	18.5	110	5	98.4	82
213	6.5–9.5	408,743.4	4,009,398.1	42	23	19	17.4	108	6.5	97.3	95
214	6.5–9.5	408,026.1	4,010,406	41	28	13	17.4	110	5.5	91.7	82
215	6.5–9.5	409,617.8	4,011,321.6	46	25	21	18.4	122	5.5	52.1	100
216	6.5–9.5	408,588.1	4,011,780.2	42	25	17	19.1	103	5.5	86.3	100
217	6.5–9.5	409,762.1	4,012,805.4	47	26	21	21.4	99	5	90.9	100
218	6.5–9.5	411,184.2	4,011,787.2	47	26	21	21.9	118	4.5	91.7	80
219	6.5–9.5	411,184.3	4,012,540.7	53	25	28	18.3	103	4.5	90	85
220	6.5–9.5	411,247.7	4,013,522.9	47	28	0	19.7	67	4.5	100	29
221	6.5–9.5	409,969.9	4,010,643.8	56	30	26	18.8	93	4	90.7	85
222	6.5–9.5	409,662.9	4,009,977	39	21	18	18.2	95	4.5	82.4	90
223	6.5–9.5	409,915.1	4,009,232.2	44	22	22	16.2	91	4	91.3	47
224	6.5–9.5	410,862.1	4,009,607.35	55	28	27	17.4	85	4	96.1	80
225	6.5–9.5	411,994.6	4,009,216.9	48	23	25	16.1	87	4.5	98.5	78
226	6.5–9.5	411,166.1	4,010,438.9	53	25	28	21.7	92	4.5	90.1	100
227	6.5–9.5	412,126.9	4,010,308.3	56	26	30	12.9	91	4	96.6	99
228	6.5–9.5	411,550.5	4,011,441.2	47	21	26	15.6	108	8.5	100	100
229	6.5–9.5	413,143.3	4,011,488.9	41	21	20	21.7	95	3.5	76.9	90
230	6.5–9.5	414,064.7	4,011,692.8	59	28	31	16.6	130	5	93.8	47
231	6.5–9.5	415,317.3	4,010,885.4	64	33	31	18.7	92	4	64.2	74
232	6.5–9.5	414,149.3	4,009,671.4	56	33	23	18.1	92	4	73.4	72
233	6.5–9.5	414,362.5	4,008,450.6	66	29	37	18.2	96	4.5	61.6	55
234	6.5–9.5	416,171.1	4,012,249.6	32	15	17	16.1	94	4.5	52.4	100
235	6.5–9.5	415,609.8	4,012,761.8	36	20	16	18.2	93	4.5	42.3	100
236	6.5–9.5	414,549.1	4,013,637	44	21	23	11.3	78	14	100	100
237	6.5–9.5	417,922.5	4,010,462	43	25	18	17.1	62	3.5	94.9	40
238	6.5–9.5	416,961.1	4,011,319.3	46	22	24	17.2	110	4.5	74.3	81
239	6.5–9.5	416,542.1	4,010,233.5	55	31	24	20.7	116	4	88.7	100
240	6.5–9.5	416,909.4	4,008,754	48	24	24	22.7	110	5	86.2	100
241	6.5–9.5	406,775.3	4,007,107.5	52	27	25	17.8	85	4	98.4	52
242	6.5–9.5	405,227.4	4,007,274.3	51	26	25	18.2	85	4.5	94.3	54
243	6.5–9.5	407,403.9	4,006,885.3	45	25	20	20.5	103	4	94.4	45
244	6.5–9.5	407,715.1	4,007,488.5	49	26	23	20.1	97	4.5	96.1	71
245	6.5–9.5	408,445.4	4,007,069.4	48	26	22	20.7	85	4	93.1	82
246	6.5–9.5	408,736.7	4,005,101.9	54	25	29	16.6	83	3.5	94.1	83
247	6.5–9.5	408,248.5	4,006,694.7	50	27	23	19.2	97	5	93	79
248	6.5–9.5	407,872.4	4,006,657.22	51	25	26	19.4	138	4	93.3	60
249	6.5–9.5	409,311.9	4,005,786	49	26	23	18.2	130	4.5	97.5	70
250	6.5–9.5	408,775.59	4,006,631.24	48	23	25	17.6	97	5	94.9	69
251	6.5–9.5	409,973.4	4,006,133	44	24	20	17.7	99	5	92.2	75
252	6.5–9.5	409,048.64	4,007,069.39	48	24	24	18.4	97	4.5	90.4	90
253	6.5–9.5	409,874.19	4,007,406.1	46	23	23	15.8	98	5	93.3	89
254	6.5–9.5	408,985.14	4,007,907.6	56	25	31	18.8	108	4.5	96.7	91

Table B1. *Cont.*

BH	DEPTH	X	Y	LL%	PL%	PI%	WC%	c (kN/m^2)	Φ (°)	Fine Content	SPT-N Value (kN/m^2)
257	6.5–9.5	409,785.25	4,008,333.1	46	24	22	18.8	95	3.5	94	43
258	6.5–9.5	410,998.6	4,008,878.3	49	27	22	18.6	103	4.5	92.9	100
259	6.5–9.5	410,109.1	4,006,834.44	42	28	14	17.2	108	5.5	92.1	59
260	6.5–9.5	410,419.8	4,006,001	55	23	32	17.1	120	4.5	91.2	72
261	6.5–9.5	412,049.02	4,007,215.97	55	24	31	15.4	130	5	82.3	89
262	6.5–9.5	411,263	4,006,447.5	55	26	29	18.4	102	4	92.7	81
263	6.5–9.5	412,664.18	4,007,328.4	48	25	23	16.4	133	5.5	96.1	43
264	6.5–9.5	411,990	4,006,315.2	49	26	23	16.5	120	5	89.7	71
265	6.5–9.5	413,164.9	4,008,779	45	27	18	20.2	123	5.5	86	69
266	6.5–9.5	412,846.74	4,006,559.81	45	24	21	19.6	85	4.5	94.7	75
267	6.5–9.5	412,536.5	4,005,174.2	37	18	19	20.2	88	4	98.0	84
268	6.5–9.5	415,747.4	4,005,960.69	46	22	24	18.4	89	4	91.2	100
269	6.5–9.5	414,814.8	4,007,156.9	43	22	21	16.3	128	5	42.3	87
270	6.5–9.5	415,071.9	4,004,866.9	38	21	17	16.3	122	4	45	100
271	6.5–9.5	417,971.23	4,001,685.01	47	25	22	17.2	97	9.5	42	100
272	6.5–9.5	418,519	4,003,222.9	37	21	16	16.8	90	9.5	36	100
273	6.5–9.5	415,926	4,002,878	44	23	21	17.0	93	10	42	100
274	6.5–9.5	416,167	4,004,572.3	43	23	20	20.1	80	9	60	100
275	6.5–9.5	419,289	4,001,977.6	44	24	20	17.7	109	4	81.4	98
276	6.5–9.5	411,924.27	4,004,297.59	56	25	31	14.4	142	5	96.3	100
277	6.5–9.5	410,482.29	4,003,953.63	0	0	0	15.6	131	7	18.1	100
278	6.5–9.5	412,426.98	4,002,802.69	43	23	20	20.5	136	4.5	93.1	100
279	6.5–9.5	414,365	4,003,408	58	32	26	17.2	97	5	93.7	100
280	6.5–9.5	411,975.73	4,001,202.95	51	24	27	18.1	129	5.5	97.6	72
281	6.5–9.5	414,022.9	4,002,387	81	26	55	15.3	140	5	95.1	79
282	6.5–9.5	411,697.91	4,000,107.57	51	28	23	17.5	131	4.5	94.2	40
283	6.5–9.5	410,200	3,999,706	48	28	22	16.8	103	5	61.4	45
284	6.5–9.5	413,372.73	4,001,528.38	45	21	24	17.2	99	6	93.7	42
285	6.5–9.5	414,253.79	4,000,845.76	49	26	23	18.6	96	4.5	82	100
286	6.5–9.5	415,598.5	4,000,259	41	23	18	21.0	89	4	76.5	100
287	6.5–9.5	413,510.13	3,999,595.57	43	23	20	13.9	87	3.5	26.6	93
288	6.5–9.5	412,160.93	3,999,051.88	36	17	19	13.2	6	32	100	80
289	6.5–9.5	410,732.9	3,999,785	43	21	22	17.0	16	31	45	100
290	6.5–9.5	410,253	3,998,445	42	22	20	9.0	7	30	41	100
291	6.5–9.5	413,309	3,998,392.5	59	26	33	15.7	94	3.5	70.8	100
292	6.5–9.5	410,136.16	4,001,490.72	55	26	29	21.8	97	5	95.9	79
293	6.5–9.5	409,296.11	4,002,026.51	53	25	28	19.2	115	4.5	95.2	42
294	6.5–9.5	408,932.6	4,003,851.9	50	28	22	17.5	94	4	96.8	49
295	6.5–9.5	408,515.58	4,002,310.93	45	28	17	25.9	33	4.5	87.9	38
296	6.5–9.5	409,939	4,003,009.6	43	28	15	26.4	55	4.5	93	33
297	6.5–9.5	407,821.05	4,002,866.56	0	0	0	19.7	52	3.5	25.8	100
298	6.5–9.5	407,298.5	4,004,255.62	41	23	18	15.2	119	4.5	94.7	40
299	6.5–9.5	405,937	4,003,224	46	24	22	19.3	93	4.5	63.7	38
300	6.5–9.5	407,774.75	4,005,380.1	43	21	22	20.5	130	6	94.2	89

Table B1. *Cont.*

BH	DEPTH	X	Y	LL%	PL%	PI%	WC%	c (kN/m^2)	Φ (°)	Fine Content	SPT-N Value (kN/m^2)
301	6.5–9.5	407,844.33	4,005,870.11	43	23	20	19.8	49	3.5	98.9	38
302	6.5–9.5	406,914.85	4,005,671.15	48	23	25	18.7	99	4.5	94.8	100
303	6.5–9.5	405,242	4,004,431.7	50	26	24	15.5	115	5	96	73
304	6.5–9.5	405,684.54	4,005,717.45	48	23	25	18.7	99	5	94.8	100
305	6.5–9.5	408,025.12	3,999,907.5	45	25	20	22.8	105	4	92.6	91
306	6.5–9.5	406,400.4	4,001,124	48	25	23	22.1	97	5	69.7	100

CURRICULUM VITAE

PERSONAL INFORMATION

Name and surname: Zhvan Baqi Qader

EDUCATION

PhD degree in civil engineering, engineering college, Gaziantep University-

Turkey, 2023

MSc degree in civil engineering, engineering college, Gaziantep University -

Turkey, 2016

BSc degree in civil engineering, engineering college, Erbil Polytechnic University- Iraq, 2013

WORK EXPERIENCE

2013-2016 worked in private sector

LANGUAGE SKILLS

Kurdish

English

Arabic

Turkish